P-224

224 P.

Mechanics and Materials Center
TEXAS A&M UNIVERSITY
College Station, Texas

(175)

INTEGRATED RESEARCH IN CONSTITUTIVE MODELLING AT ELEVATED TEMPERATURES

FINAL REPORT

by

W.E. Haisler
and
D.H. Allen

Part 2

MM 4998-86-13

June 1986

AN EXPERIMENTAL COMPARISON OF CURRENT VISCOPLASTIC CONSTITUTIVE MODELS AT ELEVATED TEMPERATURE

A Thesis

by

GEORGE H. JAMES III

Submitted to the Graduate College of
Texas A&M University
in partial fulfillment of the requirements for the degree of
MASTER OF SCIENCE

August 1986

Major Subject: Aerospace Engineeing

ABSTRACT

Four current viscoplastic models are compared experimentally with Inconel 718 at 1100°F. This material system responds with apparent negative strain rate sensitivity, undergoes cyclic work softening, and is susceptible to low cycle fatique. The models used include Bodner's anisotropic model, Krieg, Swearengen, and Rhode's model, Schmidt and Miller's model, and Walker's exponential model. Schmidt and Miller's model and Walker's model correct for negative strain rate sensitivity response. A correction similar to Schmidt's is applied to the models of Bodner and Krieg, et al.

A series of tests have been performed to create a sufficient data base from which to evaluate material constants. A method to evaluate the constants is developed which draws on common assumptions for this type of material, recent advances by other researchers, and iterative techniques. A complex history test, not used in calculating the constants, is then used to compare to the predictive capabilities of the models.

The combination of exponentially based inelastic strain rate equations and dynamic recovery is shown to model this material system with the greatest success. The method of constant calculation developed in this work was successfully applied to the complex material response encountered and suggestions for improvement are provided. Back-stress measuring tests were found to be invaluable and warrant further development.

LIST OF TABLES

1. Test Programs 37

2. Inconel 718 Composition 49

3. Example Iterations 61

4. Computer Iteration Summary of Krieg, Swearengen, and Rhode's Model 65

5. Constants for Krieg, Swearengen, and Rhode's Model 68

6. Computer Iteration Summary of Bodner's Anisotropic Model 73

7. Constants for Bodner's Anisotropic Model 74

8. Computer Iteration Summary of Schmidt and Miller's Model 79

9. Constants for Schmidt and Miller's Model 80

10. Computer Iteration Summary of Walker's Exponential Model 85

11. Constants for Walker's Exponential Model 86

12. Complex History Test Input 100

List of Figures

1	A Strain Transient Test	29
2	A Stress Transient Test	30
3	Cyclic Hysteresis Loop with Hold Times	33
4	Creep Hold Response	34
5	Stress Relaxation Hold Response	35
6	Final Creep Frame Configuration	40
7	MTS Configuration	44
8	Furnace and Extensometer for MTS	45
9	Method of Thermocouple Attachment for MTS	47
10	Creep Frame Sample Configuration	50
11	MTS Sample Configuration	52
12	Test 65 Back Stress Determination Data	54
13	Model Response as Compared to Test 70	88
14	Model Response as Compared to Test 71	89
15	Stress-Strain Response at +.8% for Cycle 1	91
16	Stress-Strain Response at -.8% for Cycle 1	92
17	Stress-Strain Response at +.8% Saturated Cycle	93
18	10th Cycle Hysteresis Loops for Test 86	95
19	Test 86 +.8% Response at Each Cycle	96
20	Test 80 +.8% Response at Each Cycle	97
21	Test 72 +.8% Response at Each Cycle	98
22	Back Stress Plot	99
23	Complex History-Bodner's Uncorrected Model	101
24	Complex History-Bodner's Corrected Model	102

List of Figures Continued

25 Complex History-Uncorrected Model of Krieg, et al. 103

26 Complex History-Corrected Model of Krieg, et al. 104

27 Complex History-Schmidt and Miller's Model 105

28 Complex History-Walker's Model 106

TABLE OF CONTENTS

INTRODUCTION 1

LITERATURE REVIEW 4

Historical Review 4

Classical plasticity 4
Microphenominological based plasticity 5
Nonlinear viscoelasticity 5
Internal state variables 6

Selected Models For Further Comparison 7

Bodner's model 7
Krieg, Swearengen, and Rhode's model 8
Miller's model 9
Walker's model 11

Other Current Models 11

Krempl, et. al.'s model 11
Robinson's model 12
Hart, et. al.'s model 12
Cescotto and Leckie's model 12

Previous Comparative Studies 12

OVERVIEW OF MODELS 15

Thermodynamic Framework 15
General Viscoplastic Framework 18
Bodner's Anisotropic Model 20
Krieg, Swearengen, and Rhode's Model 21
Miller's Model 22
Walker's Exponential Model 23

EXPERIMENTAL REQUIREMENTS AND PROGRAM 25

Creep Tests 25
Stress Relaxation Tests 26
Monotonic Strain Rate Tests 26
Fully Reversed Cyclic Tests 27
Transient Tests During Monotonic Loading 27
Transient Tests During Cyclic Loading 31
Experimental Program 36

EXPERIMENTAL APPARATUS AND PROCEDURES 38

Creep Frame Set-up 38
Table of Contents Continued

Load frame 38
Data acquisition 39
Temperature measurement and control 41
Test procedures 42

Computer Controlled Test Set-up 43

Load Frame 43
Data acquisition 43
Temperature measurement and control 43
Test procedures 46
Basic materials characteristics 48

Sample Configurations 49

Heat treatment 51

Back Stress Measuring Tests 51

CALCULATION OF MATERIAL CONSTANTS 56

Generic Summary Of Constant Calculation Methods 57

Generic viscoplastic model 57
Initial assumptions 57
Computer iteration 59

Krieg, Swearengen, and Rhode's Model 61

Initial calculations 62
Computer iterations 64

Bodner's Anisotropic Model 67

Initial calculations 68
Computer iterations 72

Miller's Model 73

Initial calculations 74
Computer iterations 77

Walker's Exponential Model 78

Initial calculations 78
Computer iterations 84

MODEL RESULTS 87
Table of Contents Continued

Reproduction Of Test Data 87
Predictive Capabilities 100

CONCLUSIONS AND RECOMMENDATIONS 108

Conclusions and Recommendations Based On Models 108
Conclusions and Recommendations Based On Calculation of Constants 109
Conclusions and Recommendations Based On The Experimental Work 113

REFERENCES 115

APPENDIX A - DATA SET 125

APPENDIX B - PROPOSED INITIAL CALCULATION METHODS 136

Generic Summary Of Constant Calculation Methods 136

Generic viscoplastic model 136
Initial assumptions 137
Initial calculations 137

Krieg, Swearengen, And Rhode's Model 138
Bodner's Anisotropic Model 142
Miller's Model 143
Walker's Exponential Model 146

APPENDIX C - AUXILIARY MODEL RESULTS 149

APPENDIX D - EXPERIMENTAL COMPUTER PROGRAMS 175

INTRODUCTION

This thesis experimentally compares four current viscoplastic models at elevated temperature. The primary objective of this work is to uncover the mathematical forms which model reality most successfully and to develop basic understanding of the models. A secondary objective is to develop methods of constant calculation which are systematic and repeatable. A final objective is to develop experimental tests and test software to support viscoplastic modeling.

Current technological applications such as jet engines, rocket engines, and nuclear reactors operate at high temperature. The components of these mechanisms are also subjected to complex loading and temperature histories. Similar conditions will be found in future technologies such as the skins and engines of hypersonic transports, laser technologies, and alternative energy conversion systems. Hypersonic technology holds promise for revolutionizing intercontinental and orbital transportation. The proposed anti-ballistic missile shield may use laser technologies. Alternative energy conversion systems such as nuclear fusion reactors and solar energy conversion devices will be necessary to continue the advancement of modern civilization through the 21st century.

The materials considered for the technologies listed above have a thermoviscoplastic thermomechanical constitution. Thermomechanical constitution describes the relation between the load applied to the

material (measured as stress), the change in the size of the material (measured as strain), and the temperature. Thermoviscoplastic mechanical response is dependent on time, temperature, and loading history. The constitutive behavior of the material must be modelled before any of the devices mentioned above can be designed or built. This is especially critical in such expensive and potentially dangerous applications. Thermoviscoplastic models are mathematical representations which allow engineers to predict the behavior of these materials. Major improvements are needed in these current models, as will be demonstrated in this thesis.

Further development and evaluation of these models requires that the models be compared to the real response of a sample of material at elevated temperature and subjected to a complex loading history. Several problems must be overcome in order to carry out such a comparison. The models to be considered must be studied to determine the types of inputs needed to use each model. These inputs are material parameters which are unique to each model and must be determined from specialized tests on the material being studied. The hardware and software for these specialized tests must be collected or developed. These tests must be perfomed and methods developed to calculate the material parameters for each model being considered in the comparison. Tests with a very general loading history must be performed for comparison, so that the actual material response observed in these general tests can be compared to the response predicted by the models.

This research produces many positive results. First, the aspects of

each model which need further development are uncovered. Also, the most accurate mathematical forms of the models are determined. Third, basic understanding of the models is generated. Such understanding is necessary for actual engineering application of the models and for expanding the capabilities of the models. Fourth, systematic methods of material parameter evaluation are developed which draw on advances by all the modelers. Systematic constant calculation methods make the models much easier to use by researchers and engineers in the field and advance the technology toward automation and standardization. Finally, experimental techniques and needs are developed or reported which can either lead or support theoretical advances.

This thesis will begin with a review of the pertinent literature. An overview of the selected models will follow. Separate chapters dealing with experimental requirements, and experimental procedures will be presented in that order. The methods used to calculate material constants will be presented next. A chapter detailing model results will follow. Conclusions of the current research and recommendations for future research will conclude this thesis.

The intent of this thesis is to provide the interested reader with the necessary information to repeat and improve on the work presented. Four appendices are provided to support this intent. The first appendix provides necessary experimental data to recalculate the material constants. The second appendix presents proposed upgrades to the constant calculation procedures. A complete set of experimental and model results is contained in the next appendix. The final appendix

provides listings of the computer programs developed to perform the experimental and data reduction portions of this work.

LITERATURE REVIEW

The following literature review begins with the historical development of viscoplastic modelling. The next section traces the development of specific models chosen for comparison in this work. Current literature pertaining to the use, expected improvements, and attempted transient temperature extensions of the chosen models are also reviewed. Sections listing other current viscoplastic models and previous comparative studies are also provided.

Historical Review

Three primary areas of research motivate current viscoplastic models. The first area is rate-independent classical plasticity. This is a macrophenomenologically based theory which attempts modelling by observing the locally averaged response of the material. The second area of research is microphenomenological modelling. This area attempts to predict general mechanical response by studying microphysical response. The third area is nonlinear viscoelasticity. This study is inherently rate-dependent and draws heavily on thermodynamics. Thermodynamic considerations provide a framework for any constitutive model which can limit its functional forms.

Classical Plasticity. Tresca stated a possible means of predicting the onset of yield in 1864 and thus began the study of inelastic behavior [1]. Levy in 1870 [2] and Von Mises in 1913 [3] formed the basis of classical plasticity by independently forming the Levy-Mises equations. Von Mises also proposed his own yield criterion in the same paper. Hencky [4], Prandtl [5], and Reuss [6] also made important

advances in rate-independent plasticity. Prager [7], Ziegler [8], and Drucker[9] made advances which allowed classical plasticity to model work-hardening materials more accurately.

Bingham [10] and Hohenemser and Prager [11] made initial attempts to add rate-dependency to plasticity in 1922 and 1932. Freudenthal [12], Malvern [13,14], Lubliner [15], Perzyna [16-20], Cristescu [21], and Naghdi and Murch [22] attempted to model rate-dependent plasticity. Howeve, these models did not unify rate-dependent and rate-independent plasticity. Zienkiewicz and Cormeau [23] presented a classical plasticity based model which was unified and drew heavily on viscoelasticity. Bodner [24] and Robinson [25] proposed models which are still actively under development. Allen and Haisler [26] proposed a model which attempts to model transient temperature effects.

Microphenomenologically Based Plasticity. Coble [27], Nabarro [28], and Herring [29] produced early works on diffusion controlled creep. Sherby, et al. [30-32], Garofalo [33], Weertman [34], Alden [35], Mukherjee, Bird, and Dorn [36], Gibbs [37], Argon [38], Kocks [39], and Hart [40] are some other important contributers to the foundations of microphenomenologically based theory. Hart [40], Krieg, et al. [41], and Miller [42] have produced models which are still under development.

Nonlinear Viscoelasticity. Biot [43] produced a linear viscoelastic model in 1954 which was later expanded by Shapery to model nonlinearity [44]. A reduced time scale was used by Shapery to model nonlinear behavior. Valanis later used the same reduced time technique

to model plasticity [45,46]. Some other viscoelasticity based theories with thermodynamic considerations include Green and Rivlin [47], Coleman and Noll [48,49], and Green and Naghdi [50]. The models of Krempl [51] and Walker [52] are viscoelasticity based models which are still under development.

Internal State Variables. Rational thermodynamics has its basis in the work of Truesdell and Toupin [53]. Other works in the area include Coleman and Noll [49], Muller [54,55], Green and Naghdi [50], Green and Law [56], Day [57], and Kratochvil and Dillon [58,59]. The application of thermodynamics to constitutive modelling of history-dependent materials can be accomplished by a functional approach as shown by Coleman [60] or by internal state variables as shown by Coleman and Gurtin [61]. These two methods were shown to be equivalent in most cases by Lubliner [62].

The internal state variable approach is used extensively in current literature [63] and will be discussed further in the next chapter. An internal state variable maintains a material's memory by integrating an associated growth law or evolution equation through the history of the loading. The evolution equations for internal state variables usually follow a standard pattern of competing hardening and softening terms as proposed by Bailey [64] and Orowan [65].

Inelastic strain can be considered to be an internal state variable. In addition, several micro-structural phenomena may be represented by internal state variables. Dislocation arrangement, back stress, equilibrium stress, or kinematic hardening may be considered to

be an internal state variable. Dislocation density, drag stress, or isotropic hardening is another example. Damage mechanisms may also be represented as internal state variables [66].

Selected Models for Further Comparison

Four current viscoplastic models have been chosen for experimental comparison in this research. A review of these models follows. The models chosen are those of Bodner [67], Krieg, et al., [41], Miller [42], and Walker [52]. These models have been chosen because they are under active development, they have been put in a common thermodynamic framework [68], methods of determination of constants has been reported [41,42,52,69,70], the models have been studied in the past [68-73], and some attempt has been made or is being made to expand them to transient temperature modelling [69,72,74].

Bodner's Model. Bodner first proposed his model in 1975 [24]. The model assumed isotropic and isothermal conditions and required no yield function. One internal state variable was utilized to model isotropic hardening [75]. The model was later expanded to account for anisotropy and hence kinematic hardening [76-78]. A damage parameter has also been added [78,79]. The forms of the internal state variable growth laws are based on the earlier work of Onat [67,80,81].

Bodner's model is a unified phenomenologically based model which has a scalar variable for isotropic hardening and a symmetric second order tensor variable for anisotropic hardening. An effective scalar variable is produced from the anisotropic variable and added to the isotropic variable to produce a single hardness variable [78].

Transient temperature modelling has been attempted with Hastelloy X [74]. A coupled heat conduction equation has been produced which can be used in conjunction with the model [82].

The isotropic form of the model has been used to predict the response of Rene 95 at 650^0 F [83], Inconel 100 at 732^0 C [84], and Inconel 718 at 650^0 C [85,86,87]. Methods for the determination of material constants have also been reported [84,87,88]. The anisotropic form of the model has been used to predict the response of Hastelloy X at room temperature [89]. A method for the determination of the material constants for the anisotropic form has been reported [90]. Material constants for several other materials have also been reported [67].

Krieg, Swearengen, and Rhode's Model. Krieg, Swearengen, and Rhode presented a microphenomenologically based model in 1978 [41]. The model is equipped with an internal state variable for isotropic hardening and one for kinematic hardening. The hardening functions are given as constants. Krieg has suggested a modification for the hardening functions which has not been incorporated into this model [91,92]. The recovery terms in the internal state variable growth law follow the work of Friedel [92].

A method for the determination of the constants has been presented for the case where the isotropic hardening variable is constant. This method makes extensive use of a stress drop or strain transient dip test [41]. The authors have engaged in subsequent work to further develop this test for constitutive modelling [93,94]. The kinematic form of the

model has been used to model aluminum at room temperature [41] and Inconel 100 at 1350^0 F [71]. Walker has provided a method for evaluating the constants and has modelled Hastelloy X at several temperatures [72]. Transient temperature modelling has been attempted with Hastelloy X [72].

Miller's Model. Miller first proposed his microphenomenologically based model in 1976 [42]. The model relies heavily on microphysical considerations. Both a kinematic hardening internal state variable and an isotropic hardening variable are provided. Annealing is simulated, but recovery terms in the growth laws depend only on temperature. The hardening functions in the growth laws are given as constants [42].

A simplified form of the model was presented in 1977 [95]. This form has eliminated the kinematic hardening back stress variable and allows only isotropic hardening to be modelled. Initial attempts were made to model solute strengthening in the drag stress variable. The hardening function in the back stress growth law was altered in 1978 to produce a more realistic transition from elastic to inelastic behavior [96]. The form of this improvement was first proposed by Krieg [91].

Schmidt and Miller further improved the capability to model solute strengthening [97,98]. These modifications were designed to allow the model to be operated over a broader range of stress and temperature when solute effects can be expected. Kagawa and Asada cast Miller's model in multiaxial form in 1983 [99]. Miller has developed a new form of the model with four structurally based internal state variables for modelling long range back stresses, short range back stresses, long

range drag stresses, and short range drag stresses. This form of the model holds promise for predicting transient temperature effects [69,100] and work softening phenomena.

Miller has also presented a series of papers devoted solely to microstructural topics which give rise to various functions found in his models. Sherby and Miller explained in 1979 the form of the inelastic strain rate equation and its basis in steady state creep. They also explained the initial attempts to model deformation strengthening [101]. Miller and Ziaai-Moayyed pointed out and confirmed with further experimental work several results of Miller's model pertaining to steady state back stress, strain softening, and peak back stress [102]. Ruano, Miller, and Sherby emphasized the need to properly take into account diffusional properties in modelling creep at various stress levels [103]. Schmidt and Miller presented a paper dealing with the effect solutes have on material behavior [104]. Miller, Kasner, Rubin, and Sherby produced work correlating isotropic hardening transients to dislocation strengthening [105,106].

Miller first presented a method for calculating the constants for his model in 1976 [42]. This method used steady state creep, cyclic tests, and tensile tests. Miller presented a method for calculating the constants in his simplified model in 1977 [95]. This method used steady state creep tests and tensile tests. Schmidt presented a method of constant evaluation for the model incorporating solute strengthening effects in 1979 [97,98]. This method used microstructural data, creep tests, tensile tests, and cyclic tests. Walker presented a method of

constant evaluation for Miller's model based solely on cyclic tests in 1980 [72]. Miller's model has been used at several temperatures to model stainless steel 304 [42], aluminum [95], stainless steel 316 [97,98] and Hastelloy X. Transient temperature modelling has been attempted with Miller's model for Hastelloy X [72]. The newest form of the model is intended to have transient temperature capability [69,100].

Walker's Model. Walker proposed his theory in 1980 [52]. It is a viscoelasticity based model with microphenomenological considerations. Two microstructural internal state variables, back stress and drag stress, are provided. The model has been proposed with a term in the back stress growth law to allow for nonisothermal elastic excursions [72]. The model was presented in a different form and coupled with a damage internal state variable in 1984 [107].

Walker has provided a method of determination of constants for a kinematically hardening material (drag stress constant). The method relies totally on cyclic testing [52]. Walker's model has been used to model Hastelloy X at several constant as well as transient temperatures [72]. The latest form of the model has been used to model Inconel 718 at 650^0 C [107].

Other Current Models.

Krempl, et al.'s Model. Krempl's model is a viscoelasticity based model in which an equilibrium stress is subtracted from the applied stress. This fills the function of the back stress in a phenomenological model. A drag stress parameter is not utilized in the most recent presentation of the model. Recovery is not provided. The

equilibrium stress hardening term is dependent on total strain rather than inelastic strain [51,108-113].

Robinson's Model. Robinson's model is a classical plasticity based model with microphenomenological considerations and draws on work by Onat, Lagneborg, and Rice. Auxiliary equations are provided to better model separate material points [25,114-118]. It has been modified to model anisotropic behavior [119]. The model has also been used to model nonisothermal conditions [69,114-118,120-122]. Robinson has presented a series of papers outlining development of his model [123-130]. The constants are determined in torsion [131].

Hart, et al.'s Model. Hart presented his microphenomenologically based model in 1976. It includes a microstructural internal state variable for back stress, a constant for drag stress, and an internal state variable called hardness which affects the back stress growth law [40]. A method for the calculation of constants has been given [132]. The latest form of the model has four internal state variables. Two back stress and two hardness internal state variables are used [69,133].

Cescotto and Leckie's Model. Cescotto and Leckie presented a microphenomenologically based model in 1983 [134]. The model includes an internal state variable for back stress and one for drag stress. The evolution equations for these variables are not given in a specific form. They must be evaluated after a series of appropriate tests.

Previous Comparative Studies

Delph performed a comparative study between Robinson's [25] and Hart's [40] models in 1980 [115]. This was a quantitative study based

on constants derived from 2 1/4 Cr - 1 Mo steel at 1050 F. Cernocky produced a study in 1981 comparing the models of Bodner and Partom [24], Cernocky and Krempl [51,135] and two versions of a viscoelasticity based model by Wu and Yip [136,137]. This was an analytical and numerical study [73]. Walker completed a study in 1981 [72] which included a qualitative examination of several viscoplastic models. The study also performed an experimental comparison of Walker's theory [52], Miller's theory [42], and Krieg, Swearengen, and Rhode's theory [41]. This study utilized Hastelloy X at several temperatures and included extensions to thermomechanical testing.

Milly and Allen reviewed Bodner and Partom's theory [24], Krieg, et al.'s theory [41], Walker's theory [52], Krempl, et al.'s theory [135], and Zienkiewicz and Cormeau's theory [23]. A comparison of Bodner and Partom's model and Krieg, et al.'s model for Inconel 100 at 1350 F was also performed [71]. Beek, Allen, and Milly did a comparative study in 1983 of all the listed in the previous section plus the models of Valanis [45,46] and Allen and Haisler [26,138]. These models were all put in a common internal state variable framework to allow easier comparison [68]. Lindholm, et al. produced a review of several viscoplastic constitutive theories in 1984 [69]. The models covered included those of Walker [72], Bodner and Partom [75,78], Miller [42,97,98], Krieg, et al. [41], Chaboche [139], Robinson [25], Hart [40,133], Bodner's anisotropic model [67], Lee and Zaverl [140], and Ghosh [141]. Follow-up research to this project will utilize the models of Walker and Bodner's anisotropic form for thermomechanical testing.

Beek [142] used aluminum 5086 at room temperature to compare the models of Krieg, et al. [41], Bodner's isotropic model [75], and Miller's simplified model [95].

OVERVIEW OF MODELS

A brief description of the thermodynamic framework ofinternal state variables will open this chapter. The general form of current viscoplastic models will be discussed next. Individual sections will follow which deal with the specific forms of the models selected for this work.

Thermodynamic Framework

The material in this section is an abbreviated form of discussions found elsewhere [68,143]. A state variable is a parameter whose magnitude can be determined by looking at the current time only. The following state variables are necessary to fully characterize the thermomechanical state of a body at all points x_j and at all times t, while undergoing infinitesimal deformations:

1) The displacement field $u_i = u_i(x_k,t)$ (1)

2) the stress tensor $\sigma_{ij} = \sigma_{ij}(x_k,t)$ (2)

3) the body force per unit mass $f_i = f_i(x_k,t)$ (3)

4) the internal energy per unit mass $u = u(x_k,t)$ (4)

5) the heat supply per unit mass $r = r(x_k,t)$ (5)

6) the entropy per unit mass $s = s(x_k,t)$ (6)

7) the absolute temperature $T = T(x_k,t)$ (7)

8) the heat flux vector $q_i = q_i(x_k,t)$ (8)

and

9) $\alpha^m_{ij} = \alpha^m_{ij}(x_k,t)$, $m = 1, 2, \ldots n$ (9)

where α^m_{ij} are internal state variables (ISV) which are necessary to account for the nonlinear effects of rate, history, and temperature. ISV are not necessarily limited to second rank tensors.

The variables u_i (displacements) and T(temperature) are hypothesized to be specifiable variables. The following variables are then defined from the spatial derivatives of u_i and T:

$\varepsilon_{ij} \equiv \frac{1}{2} (u_{i,j} + u_{j,i})$; the strain (10)

$g_m = T_{,m}$;the spatial temperature gradient (11)

The following constitutive equations of state are then postulated:

$\sigma_{ij}(x_k,t) = \sigma_{ij}[\varepsilon_{mn}(x_k,t), T(x_k,t), g_m(x_k,t), \alpha^p_{mn}(x_k,t)]$ (12)

$$u\ (x_k,t) = u\ [\ \varepsilon_{mn}(x_k,t),\ T\ (x_k,t),\ g_m(x_k,t),\ \alpha^p_{mn}(x_k,t)\ ] \qquad (13)$$

$$s\ (x_k,t) = s\ [\ \varepsilon_{mn}(x_k,t),\ T\ (x_k,t),\ g_m(x_k,t),\ \alpha^p_{mn}(x_k,t)\ ] \qquad (14)$$

$$q_i(x_k,t) = q_i[\ \varepsilon_{mn}(x_k,t),\ T\ (x_k,t),\ g_m(x_k,t),\ \alpha^p_{mn}(x_k,t)\ ] \qquad (15)$$

The quantities σ_{ij} , u, s, and q_i are called observable state variables because they can be determined from the constitutive equations of state by observing at the current position(x_k) and current time(t) only. The magnitudes of ε_{mn} , T,g_m, and α^p_{mn} and the relationships between these independent variables will give the magnitudes of the dependent variables. The current magnitudes of the ISV α^p_{mn} are arrived at through growth laws or evolution equations of the form:

$$\dot{\alpha}^k_{ij}(x_m,t) \equiv \Omega^{\ k}_{ij}(\varepsilon_{mn},\ T,\ g_m,\ \alpha^l_{mn}) \qquad (16)$$

Equations (16) must be integrated through all time to arrive at the current magnitudes of the ISV:

$$\alpha^k_{ij} = \int_{\infty}^{t} \Omega^k_{ij}(x_m,t')\ dt' \qquad (17)$$

Where t' is a dummy variable of integration. The magnitudes cannot be determined by looking at the current time only and these quantities are

therefore called hidden or internal state variables. The distribution of f_i(body force) and r(heat supply) may be determined by the method of Coleman and Noll [49] with equations (12) through (16), conservation of linear momentum, and conservation of energy. Analysis of the mechanical response of materials will require that the precise forms of equations (12) and (16) be produced. A simplification is performed here in which the temperature gradient is assumed to be zero in the body of interest and in equations (12) and (16). This leaves the independent variables of strain (ε_{mn}) and temperature (T). These conditions are those needed to model thermoviscoplastic response. The mechanical equations of state for viscoplastic materials take the following form when T is assumed to be constant in time and space:

$$\sigma_{ij}(x_k,t) = \sigma_{ij}[\ \varepsilon_{mn}(x_k,t),\ \alpha^p_{mn}(x_k,t)\ ] \tag{18}$$

$$\dot{\alpha}^p_{ij}(x_k,t) = \Omega^p_{ij}(\ \varepsilon_{mn},\alpha^1_{mn}) \tag{19}$$

General Viscoplastic Framework

This research deals only with uniaxial response and the specific models will be presented in uniaxial form only. A general outline will be presented which defines the various parts of a typical, unified, internal state variable, viscoplastic model. The notation used will be that of Imbrie, et al. [70]. The general form of equation (18) for the uniaxial case is as follows:

$$\sigma = E\ (\varepsilon - \varepsilon^I). \tag{20}$$

where E is given to be Young's modulus, ε is the total strain, and ε^I is the inelastic strain. The thermodynamic framework presented in the preceding section requires that ε^I be an ISV. Labelling inelastic strain as the first ISV is a controversial issue and the reader is referred elsewhere for clarification [66].

A growth law for the inelastic strain, also called the flow law or inelastic strain rate equation, must be presented to fulfill equations (19):

$$\dot{\varepsilon}^I = f\ (\ \varepsilon,\ \varepsilon^I,\ B,\ D,\ldots\alpha^m) \tag{21}$$

where B (α^2) and D (α^3) are the second and third ISV, and α^m are other internal state variables not used in the specific model forms presented here. Equation (21) commonly takes the following form:

$$\dot{\varepsilon}^I = f_1\left(\frac{\sigma - B}{D}\right) \tag{22}$$

where $\sigma = E\ (\ \varepsilon - \varepsilon^I)$. The function f_1 can take several forms including exponential, power law, and hyperbolic functions. B is called back stress or equilibrium stress and is an ISV responsible for kinematic or directional hardening, the Bauschinger effect, or lower re-yield in compression. B may be thought of as a measure of the arrangement of dislocations in the crystalline lattice. D is called drag

stress and is responsible for isotropic work hardening, such as cyclic hardening or softening. Physically, this variable measures dislocation density. α^m are variables which may be used to account for the effects of damage, solution strengthening, short range dislocation effects, or temperature [79,97,98,100].

The growth laws for B and D commonly take the following forms:

$$\dot{B} = h_B(\dot{M}) - r_B^d(\dot{M}, B) - r_B^s(B) \tag{23}$$

$$\dot{D} = h_D(\dot{M}) - r_D^d(\dot{M}, D) - r_D^s(D) \tag{24}$$

where h are the hardening functions, r^d are dynamic recovery terms, and r^s are static thermal recovery terms. Various models may not have both recovery terms [42,41]. M is the measure of work hardening and is commonly inelastic strain (ε^I), total strain (ε), or plastic work (W_p). Equations (20-23) are specific forms of equations (18) and (19). Individual models will now be presented.

Bodner's Anisotropic Model

This model has the following form [67]:

$$\dot{\varepsilon}^I = \frac{2}{\sqrt{3}} D_0 \exp\{ - \frac{1}{2} [\frac{Z}{\sigma}]^{2n}\} \operatorname{sgn} \sigma \tag{25}$$

$$Z = Z^I + Z^A = Z^I + B \operatorname{sgn} \sigma \tag{26}$$

$$\dot{Z}^I = m_1[Z_1 - Z^I] \dot{W}_p - A_1 Z_1 [\frac{Z^I - Z_2}{Z^1}]^{r_1} \tag{27}$$

$$\dot{B} = m_2[\ Z_3 \operatorname{sgn} \sigma - Z^A]\ \dot{W}_p - A_2 Z_1 [\frac{|B|}{Z_1}]^{r_2} \operatorname{sgn} Z^A \qquad (28)$$

where D_0, n, m_1, Z_1, Z_2, A_1, r_1, m_2, Z_3, A_2, and r_2 are material constants.

The function f required for the flow law is exponentially based in equation (25). The model gives a limiting strain rate in shear of D_0 [70]. The term $-m_1 Z^I \dot{W}_p$ is a dynamic recovery term for Z^A in the isotropic growth law (27) and $- A_1 Z_1 [(\ Z - Z_2)\ Z_1^{-1}]^{r_1}$ is a static thermal recovery term. B is a uniaxial representation of a second order tensor in the multiaxial state which handles directional or anisotropic hardening. B is assumed to act as an isotropic variable on an incremental basis [78]. The growth law for B (28) has the same components as the growth law for D (27).

Bodner's model is seen to use the rate of plastic work instead of inelastic strain rate as the measure of work hardening (27,28). This is designed to allow for better modelling of strain rate jump tests [67].

Krieg, Swearengen, and Rhode's Model

Krieg, et al.'s growth laws have the following form [70]:

$$\dot{\varepsilon}^I = C\ (\frac{\sigma - B}{D})^n \operatorname{sgn} \sigma \qquad (29)$$

$$\dot{B} = A_1 \dot{\varepsilon}^I - A_2 B^2 [\ e^{(A_3 B^2)} - 1\ ] \operatorname{sgn} B \qquad (30)$$

$$\dot{D} = A_4 \dot{\varepsilon}^I - A_5 (\ D - D_0)^n \qquad (31)$$

where C, n, A_1, A_2, A_3, A_4, and A_5 are material constants.

Krieg, et al.'s flow law is seen to be a power law based equation. The back stress and drag stress growth laws (30,31) contain static thermal recovery terms but no dynamic recovery terms. The recovery term in (30) is based on a dislocation climb model by Friedel. The recovery term in (31) is based on a special case of the same climb recovery model used in (30) [41,92].

Miller's Model

Miller's growth laws have the following form [42].

$$\dot{\varepsilon}^I = B'\{ \sinh(\frac{\sigma - B}{D})^{1.5}\}^n \operatorname{sgn}(\sigma - B) \tag{32}$$

$$\dot{B} = H_1\dot{\varepsilon}^I - H_1B'\{ \sinh(A_1|B|) \}^n \operatorname{sgn}(B) \tag{33}$$

$$\dot{D} = H_2|\dot{\varepsilon}^I|(C_2 + |B| - \frac{A_2}{A_1} D^3) - H_2C_2B'\{ \sinh(A_2D^3) \}^n \tag{34}$$

where B', n, H_1, A_1, H_2, C_2, and A_2 are material constants.

Miller's flow law has the form of a hyperbolic sine. This form was chosen to model creep response better [42]. This same form is found in the static thermal recovery terms of the back stress and drag stress growth laws (33,34). The drag stress hardening term contains a hardening term, a dynamic recovery term, and a term which couples drag stress hardening to back stress magnitude. These three terms provide the proper cyclic, hardening, softening and saturation behavior [42].

Walker's Exponential Model

Walker's growth laws have the following form [90,107]:

$$\dot{\varepsilon}^I = \frac{\exp\left(\frac{\sigma - B}{D}\right) - 1}{\beta} \operatorname{sgn}(\sigma - B) \tag{35}$$

$$\dot{B} = n_2 - B\left\{\left[n_3 + n_4 \exp\left(-n_5 \left| \log\left(\frac{|\dot{R}|}{\dot{R}_0}\right)\right|\right)\right]\dot{R} + n_6\right\} \tag{36}$$

$$D = D_1 + D_2 \exp(-n_7 R) \tag{37}$$

$$\dot{R} = |\dot{\varepsilon}^I| \tag{38}$$

where β, n_2, n_3, n_4, n_5, $\dot{R}_0$, n_6, D_1, D_2, and n_7 are material constants.

This version of Walker's flow law (35) is based on an exponential function. The term $n_2\dot{\varepsilon}^I$ is seen to be a work hardening term in the back stress growth law. The term $B\left[n_3 + n_4 \exp(-n_5 |\log(|\dot{R}|/\dot{R}_0)|)\right]\dot{R}$ is a dynamic recovery term. Negative strain rate sensitivity effects can be modelled with the term $n_4 \exp(-n_5 |\log(|\dot{R}|/\dot{R}_0)|)$. Back stress thermal recovery is handled by the $B\, n_6$ term. Drag stress hardening is modelled through the $D_2 \exp(-n_7 R)$ term. No provision is made for drag stress recovery in this model.

EXPERIMENTAL REQUIREMENTS AND PROGRAM

This chapter contains sections covering the tests used as input to calculate material constants for viscoplastic models. These standard tests include creep tests, stress relaxation tests, monotonic strain rate tests, fully reversed cyclic tests, transient tests during monotonic loading, and transient tests during cyclic loading. These sections cover the input and expected output for each test, the information sought from each test, and the experimental requirements for each test. The final section covers the experimental program actually perfomed for this thesis.

Creep Tests

These tests are load controlled tests in which a constant stress, usually simulated by a constant load, is applied to a material sample. The resulting strain versus time response is monitored. The information sought in this test is the linear slope during secondary or steady-state creep. This region of material response is characterized by a stable and saturated microstructure [41,42]. A saturated microstructure in this case is a condition where the back stress and drag stress are unchanging due to a balance between the work hardening and the static thermal recovery terms. The saturated back stress is commonly assumed to have a linear relationship to applied stress [42]. Miller assumes the saturated drag stress values have a power law relation to applied stress [42,95]. Some model evaluation methods utilize points on the primary or transient creep curve [41].

The requirements for this test include a constant stress or a

constant load with small changes in cross-sectional area. A stable temperature over a long period of time and good control over initial load-up are also necessary. The time required for initial load-up should be short enough to eliminate thermal recovery effects and long enough to eliminate dynamic effects. The usual test length requires long term stability of the extensometry or strain measuring equipment. The strain rates encountered may be slow and good resolution is needed with the extensometry. Creep tests are usually run at several initial loads to arrive at a table of initial load versus steady state strain rate results. These are simple tests to run. However, they are prone to give scattered results [131].

Stress Relaxation Tests

These tests are strain controlled tests in which a constant strain is applied to a material sample. The resulting stress (or load) versus time response is monitored. The information sought in this test is the constant stress achieved following a hold at constant strain. The requirements for this test include a constant strain and a constant temperature [131].

Monotonic Strain Rate Tests

These tests are strain controlled tests in which a constant strain rate is applied to the sample. The stress versus strain response is then monitored. The information sought in this test includes the yield point or onset of substantial inelastic strain, the initial elastic modulus, the final saturated stress or final constant stress rate, and the strain rate sensitivity of the material. These tests are generally

run rapidly enough to neglect static thermal recovery terms and therefore provide data on work hardening and dynamic recovery constants [67]. This type of test requires the ability to input a constant strain rate and tests using several different strain rates are run.

Fully Reversed Cyclic Tests

These tests are strain controlled tests which ramp between the same value of strain in tension and compression. The resulting stress versus strain response is monitored. The data sought in this test include the yield point, initial elastic modulus, the cyclic hardening or softening characteristics, and the final saturated hysteresis loop. The drag stress usually changes in magnitude with each cycle until saturation to control the cyclic hardening, softening, and saturation characteristics [42]. This saturated state is often used as a reference condition from which transient tests are run [52,131]. Tests of this type are usually run at several different strain rates and strain limits [42,52]. The most difficult requirement for this test is usually machine alignment,since samples with straight gauge sections are prone to buckling when loaded compressively.

Transient Tests During Monotonic Loading

The purpose of these tests is to arrive at magnitudes for back stresses. The strain transient test, also called the stress drop test, during secondary creep and the stress transient test during saturated monotonic strain rate loading are the two tests mentioned here. These tests require the independent or controlled variable (stress for creep and strain for monotonic strain rate) to be reduced to a lower value and

held constant. The dependent variable (strain for creep or stress for monotonic strain rate) is then monitored versus time. The direction and magnitude of the change in the dependent variable for different reductions in the independent variable is sought. The stress on the sample is equal to the back stress whenever the dependent variable remains at a constant value following a drop [144]. Figure 1 shows the typical stress-time and strain-time response of a strain transient or stress drop test. Figure 2 shows the typical strain-time and stress-time response of a stress transient test. Several transient tests are usually run with one sample when the independent variable is returned to the reference condition before each drop.

These tests are both highly controversial. However, the strain transient test is generally better accepted. The stress transient test allows the microstructure to change (back stress magnitude changes) during the transient period [144]. The strain transient test during creep requires a great deal of understanding to properly interpret the results. The following paragraph will present a brief review of pertinent literature concerning the strain transient test.

Some of the earliest reports on strain transient testing were by Ahlquist and Nix [145-146]. They reported some early techniques and results. Poirier presented a paper in 1977 which gave the expected results of strain transient tests and possible means of analysis [147]. Gibeling, Nix, and Fuchs explained the resulting transient in terms of the microstructure [148-149]. These papers also discussed the

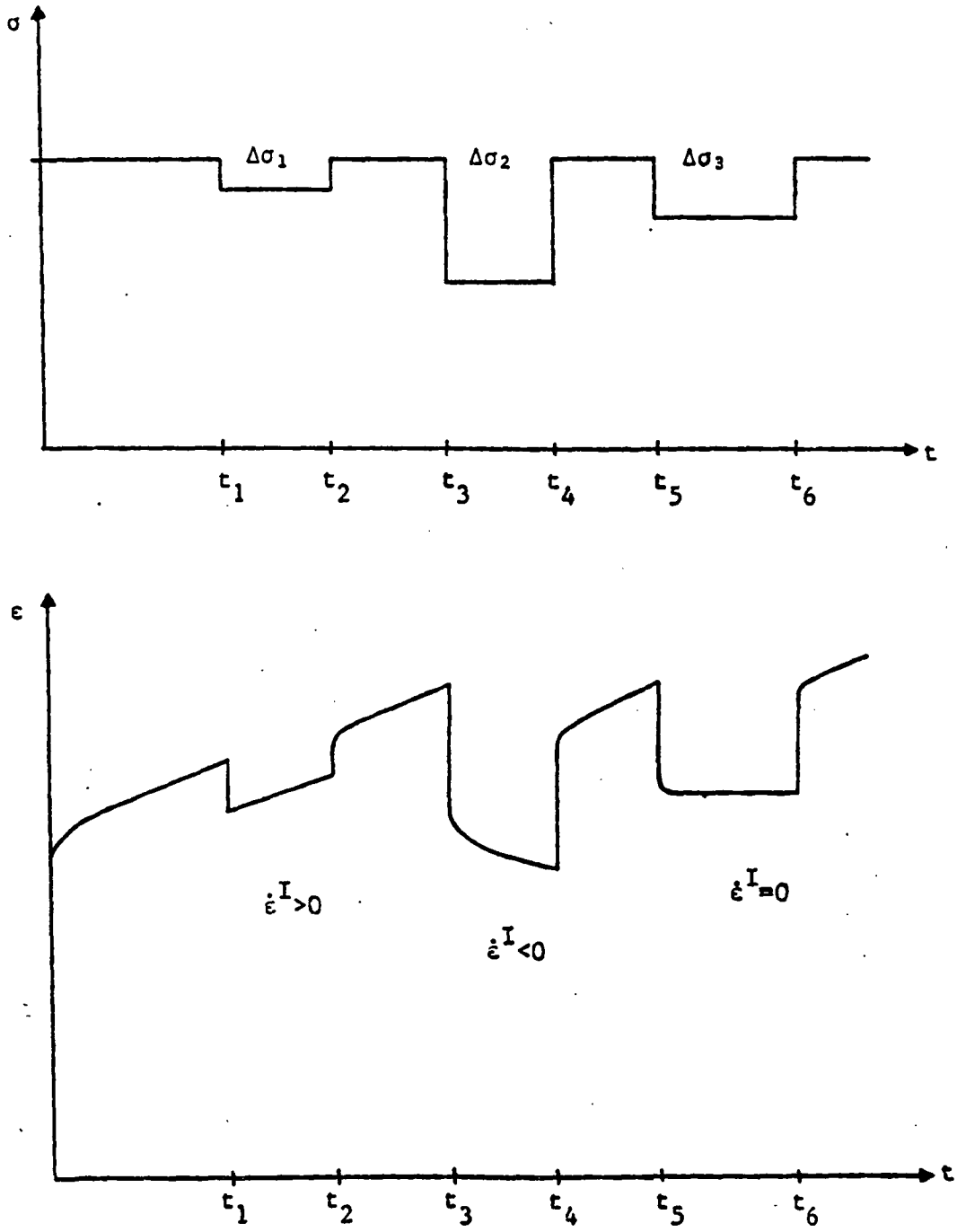

Figure 1 - A Strain Transient Test

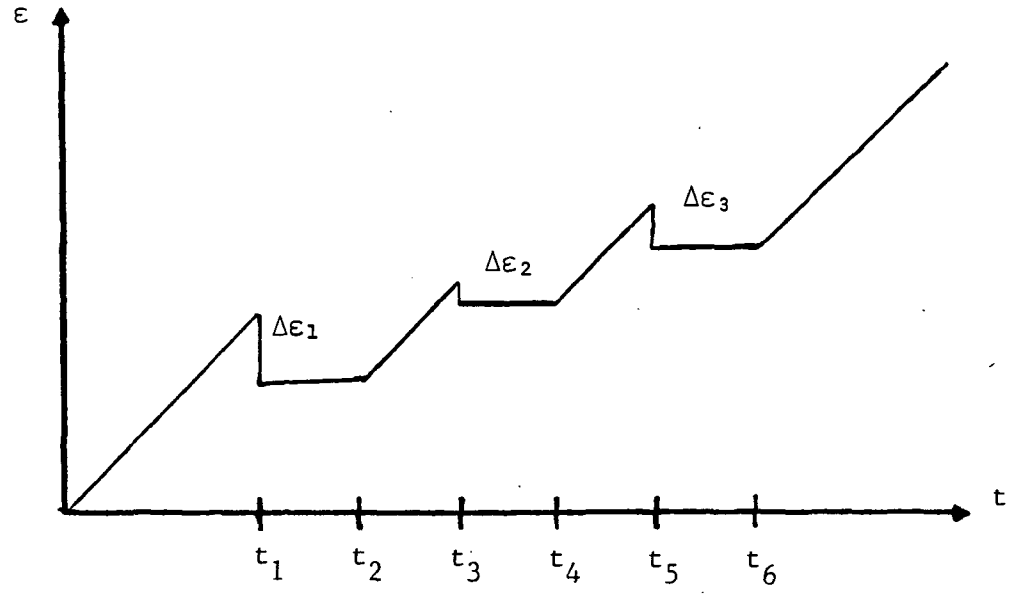

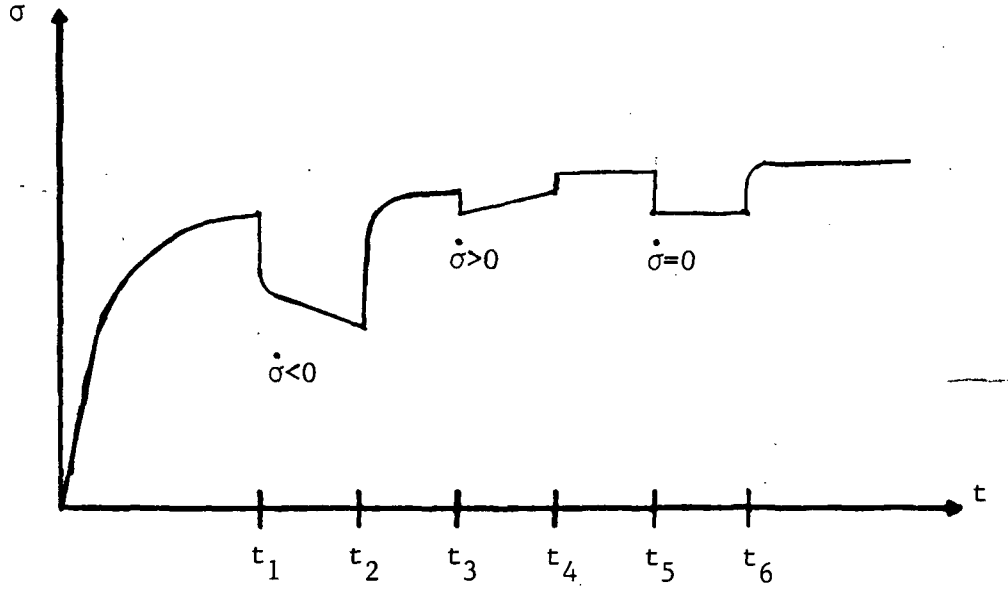

Figure 2 - A Stress Transient Test

physical nature of the back stress and when it was microphysically appropriate to include a back stress variable in a constitutive equation. It was also mentioned that hand smoothing of the data was usually necessary. Jones, Rhode, and Swearengen presented a machine for use in strain transient testing [93]. The typical method of analyzing strain transient data is to produce a zero strain rate following a stress drop. Blum and Finkel proposed an alternate means of analyzing strain transient data. This technique involves measuring initial and maximum changes in strain following a stress drop. Plotting these changes against the stress decrement allows the back stress to be calculated. This method assumes the ratio of back stress to applied stress is constant and independent of stress [150].

Strain transient tests during creep require varying amounts of stress to be quickly removed and reapplied. The strain must be measured with a resolution of a few microstrain for an indefinite amount of time. The data acquisition system must be able to take in data slowly during the creep portion of the test and rapidly during the transient portion of the test. These requirements make this a difficult test to carry out.

Transient Tests During Cyclic Loading

The purpose of these tests is to determine values of back stress for cyclically saturated conditions. A cyclically saturated condition is characterized by each successive cycle repeating the previous cycle when subjected to the same maximum and minimum strain limits. The creep test or the stress relaxation test is used during constant strain rate

cyclic conditions to produce these tests. The general assumption behind these tests is that the back stress changes only with inelastic strain. This assumption requires that elastic unload take place rapidly enough to ignore static thermal recovery [52].

These tests are performed by cycling a material until saturated conditions are reached. Hold times are then inserted at various points in the unloading region as shown in Figure 3. The stress value is greater than the back stress value if positive creep (strain increasing) or negative strain relaxation (stress decreasing) is observed. The stress value is less than the back stress value if negative creep (strain decreasing) or positive stress relaxation (stress increasing) is observed. The applied stress value equals the back stress value when no creep or stress relaxation is observed immediately following a hold. Figure 4 summarizes this typical response if creep tests are used and Figure 5 shows the typical response if stress relaxation tests are used. The material is cycled between each hold time to return the material to saturated conditions [52,131].

The requirements for these types of tests include the ability to cycle the material into compression, measure strain from 10^{-3} to microstrain, and to hold the test at various points. Creep transients also require the ability to switch between load and strain control. Ellis and Robinson have described an extensometer and associated calibration fixture for carrying out these transient tests [131]. They also report the merits of carrying out such tests under conditions of torsional cycling while using stress relaxation response.

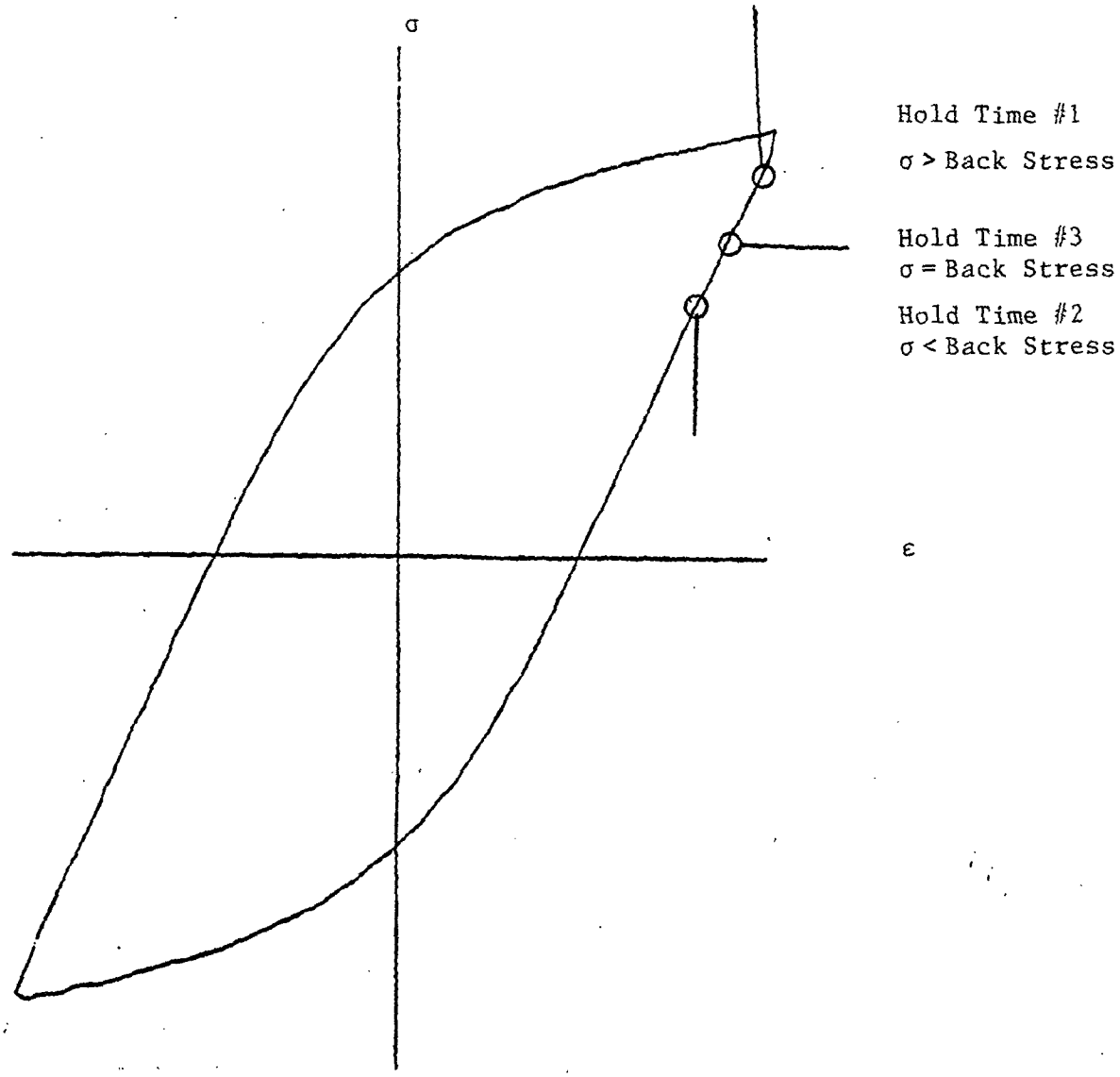

Figure 3 - Cyclic Hysteresis Loop With Hold Times

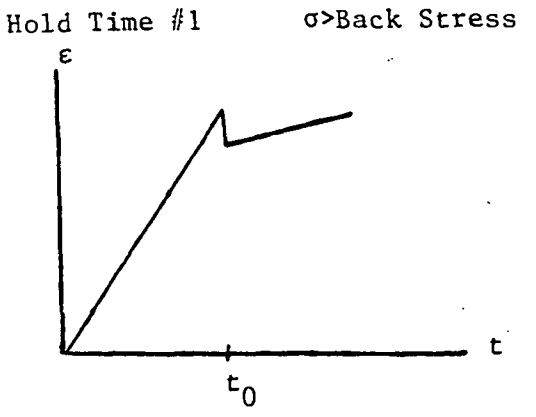

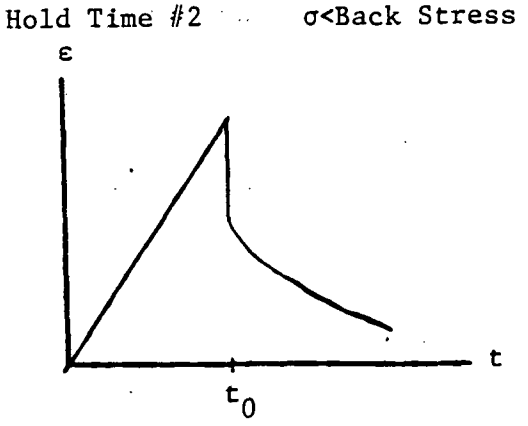

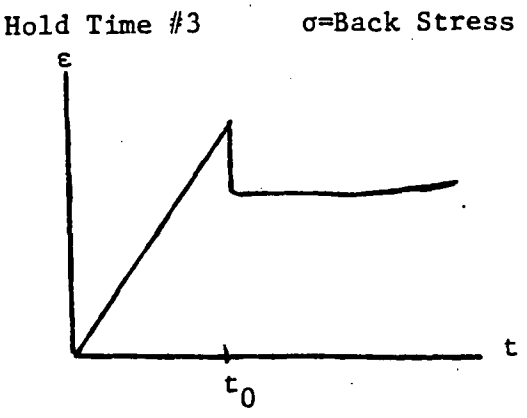

Figure 4 - Creep Hold Response

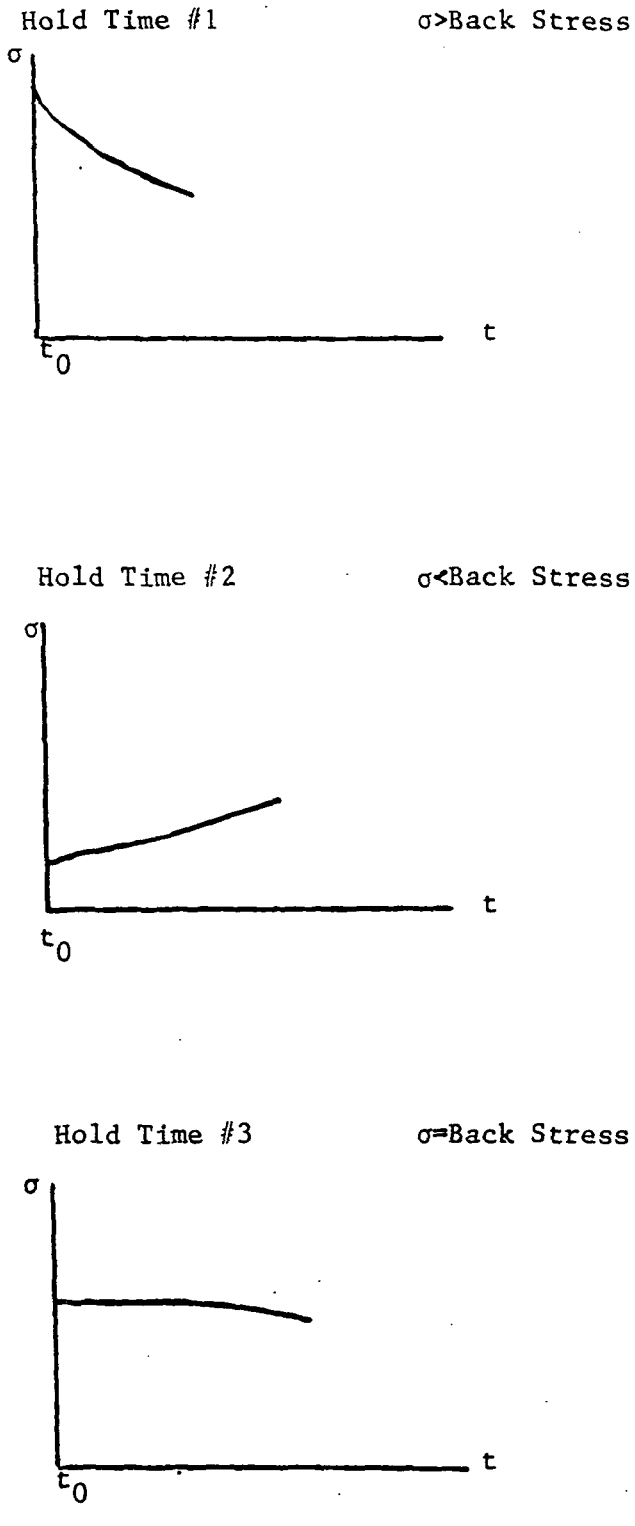

Figure 5 - Stress Relaxation Hold Response

Experimental Program

The basic experimental program consisted of the following tests:

(1) 2 monotonic tension tests to 1.5% strain (strain rates of $3.15X10^{-3}$ sec^{-1} and $7.25X10^{-6}$ sec^{-1});

(2) 5 fully reversed cyclic tests to $\pm$ .8% strain (strain rates between $1.00X10^{-3}$ sec^{-1} and $7.63X10^{-6}$ sec^{-1});

(3) 5 constant load creep tests (applied stresses between 119 ksi and 139 ksi);

(4) 4 back stress measuring tests during cyclic loading and 4 during secondary creep; and

(5) 1 complex history test. An auxiliary set of data was generated from a second series of material and was utilized only in specific instances when a broader data base was necessary. The second series was presumably from a different lot or heat treatment. The primary series of material was denoted as D2, whereas the auxiliary series was denoted as D8. The auxiliary data included the following:

(1) 8 monotonic tension tests (strain limits of 1.2% to 4% and strain rates between $9.25X10^{-4}$ sec^{-1} and $7.03X10^{-6}$ sec^{-1});

(2) 5 constant load creep tests (applied stresses between 110 ksi and 125 ksi); and

(3) 1 additional complex history test from the D2 series.

Table 1 provides more specific information on the test program. Column 1 provides the test number and column 2 provides the material series. The type of test is given in column 3. The strain rate and strain limits are given in columns 4 and 5. The applied stresses for

the creep tests are given in column 6. A complete data set in tabular form is provided in Appendix A.

Table 1 - Test Program

Test	Series	Type	$\dot{\varepsilon}_{app_1}$ sec^{-1}	ε_{lim}	σ_{app} ksi
70	D2	tension	3.151E-3	1.5%	
71	D2	tension	7.253E-6	1.5%	
86	D2	cyclic	1.002E-3	+/-.8%	
56	D2	cyclic	9.966E-4	+/-.8%	
65	D2	cyclic	3.127E-4	+/-.8%	
83	D2	cyclic	9.926E-5	+/-.8%	
80	D2	cyclic	3.054E-5	+/-.8%	
72	D2	cyclic	7.626E-6	+/-.8%	
64	D2	creep			138.8
63	D2	creep			133.9
62	D2	creep			127.0
61	D2	creep			124.0
60	D2	creep			119.0
84	D2	back	2.812E-3	+/-.8%	
88	D2	back	9.272E-4	+/-.8%	
81	D2	back	8.635E-4	+/-.8%	
65	D2	back	3.127E-4	+/-.8%	
63	D2	back			133.9
62	D2	back			127.0
61	D2	back			124.0
60	D2	back			119.0
89	D2	complex			
35	D8	tension	9.253E-4	4.0%	
37	D8	tension	6.048E-4	1.2%	
39	D8	tension	1.793E-4	1.2%	
34	D8	tension	7.637E-5	2.4%	
36	D8	tension	5.703E-5	1.2%	
42	D8	tension	1.914E-5	3.5%	
38	D8	tension	1.410E-5	1.2%	
40	D8	tension	7.029E-6	1.2%	
19	D8	creep			125.0
11	D8	creep			120.0
17	D8	creep			120.0
12	D8	creep			115.0
10	D8	creep			110.0
85	D2	complex			

EXPERIMENTAL APPARATUS AND PROCEDURES

This chapter will describe the test equipment used to carry out the tests described in the previous chapter. The first section will describe the test set-up used for the creep and strain transient tests based on a dead weight creep frame. Topics to be covered include the load frame, data acquisition, temperature measurement and control, and test procedures. The next section will describe the test set-up used for the monotonic strain rate, fully reversed cyclic tests, and transient tests during cyclic loading as well as creep and strain transient tests based on a computer controlled test set-up. The same topics will be covered. The next section covers material considerations of this work. Topics to be covered include basic material characteristics, sample configuration, and heat treatment. The final section will be devoted to a discussion of the procedures used to perform back-stress measuring tests on the automated load frame.

Creep Frame Test Set-up

Load Frame. The load frame utilized in this thesis was a creep frame produced at Texas A&M University. The initial configuration included a constant load cam and a constant stress cam as described by Garofalo, et al. [151]. The lift for the pan was provided by an ATS (Applied Test Systems) 2081 cyclic load module. Several modifications were made to this set-up. The constant stress cam was removed and a second constant load cam installed. This increased the maximum weight limit from 400 lbs. to 800 lbs. This also increased the stability of the load-pan during load-up and provided a seven to one load magnification.

The load pan was increased in size and supports were added to further aid stability during load-up. The cyclic load table was removed and replaced with a Century-Fox model CF-59 5 ton capacity hydraulic jack. This provided more lift capacity and gave more room for machine deflection during load-up. The final configuration of the machine is shown in Figure 6.

Further improvements needed include a more advanced load pan which would provide automated removal and replacement of portions of the load. Jones, et al. [93] have described such an apparatus. Similar modifications are needed to improve the results of the strain transient tests. Another improvement needed is a more advanced method of load-up. An apparatus such as an electric or pneumatic jack which could provide a calculable and repeatable load-up rate is needed.

Data Acquisition. The load was measured with a Strainsert TLN20-256K Tension Link driven by a Hewlett Packard 8805A Carrier Preamp. The strain was measured with an ATS model 4112 LVDT (Linear Variable Displacement Transducer) and extensometer driven by an ATS model 6974 signal conditioner. Two Hewlett Packard 8803A Low Level Preamps and two low pass filters were necessary to achieve the necessary resolution. Load and strain measurements were recorded on a Hewlett Packard series 7700 strip chart recorder. These components can be seen in Figure 6 also.

This data acquisition system was very prone to drift, noise, and non-linearity. All strain amplification, filtration, and data

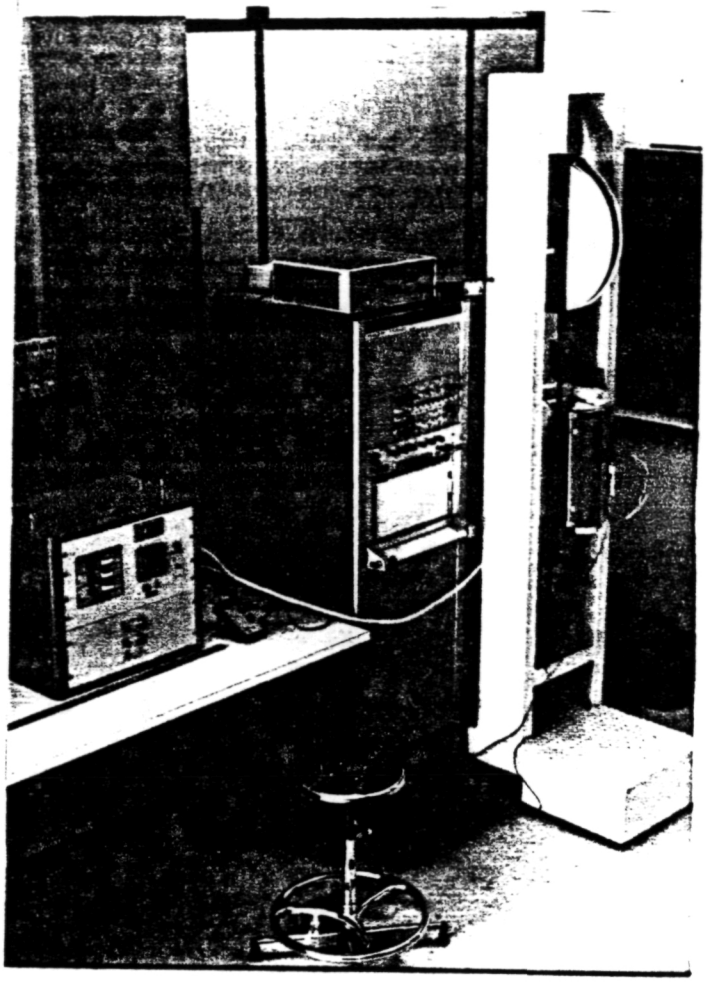

Figure 6 - Final Creep Frame Configuration

acquisition equipment were eventually replaced with a Kiethly model 197 logging digital multimeter. This set-up proved much more stable. However, it lacked the ability to take in a large number of data points. Much improvement is needed in strain data acquisition to produce a system which is stable, can take in large numbers of points and has sufficient resolution.

Temperature Measurement and Control. An ATS 2961 Clamshell oven and an LFE series 230 temperature controller were used for temperature control. Temperature measurement was handled by two 20 gauge K-type thermocouples. These were placed in contact with the sample in the middle of the gauge section on diametrically opposing sides. One thermocouple was used as input to the temperature controller. The other thermocouple was input to a Fluke 2176A digital thermometer for readout. The oven, controller, and digital thermometer can be seen in Figure 6 also.

Improvements in this system would include the ability to monitor the temperature at several points simultaneously along the gauge section. The temperature should also be input to a data acquisition system. The method of thermocouple attachment should also be upgraded. The optimum method of thermocouple attachment would be individual welding of the leads to the sample surface. This is described in the ASTM Thermocouple Handbook [152]. Such a procedure was attempted with 20 gauge thermocouple wire and a Duracom thermocouple welder. The samples tended to fail prematurely at the thermocouple welds and this method of thermocouple attachment was abandoned. Another

possible method using smaller 28 gauge thermocouples was used with the computer-controlled set-up and will be discussed in that section.

Test Procedures. The initial step was to measure the gauge length and gauge diameter. The gauge diameter was measured at the top, middle, and bottom of the gauge section. These measurements were averaged and an area calculated. The weight needed to produce the desired stress was calculated and loaded on the load pan. The weight of the pan alone was 45 lbs. and the load magnification of the frame was seven to one. The sample was then loaded in the extensometer and load train.

The sample temperature was stabilized at 1100^0 F using small changes in set point and zone power. This usually took 45 minutes to one hour. Zeroing and calibration of the LVDT followed a warm-up period of 30 minutes. A micrometer was provided on the extensometer for calibration. The LVDT was calibrated between 0 and 5 volts (.25 inch displacement). The digital voltmeter was set to take in one point every minute for the first 100 minutes and one point every 10 minutes for the remainder of the test. The weight was applied to the sample by releasing the pressure in the jack over a period of about 30 seconds.

Stress drop tests were carried out after three to six hours of creep testing. The digital voltmeter was set to take in a point every second and an increment of load was removed. The load was reapplied one to 15 minutes later after a creep rate was determined. The sample was allowed to creep at least 30 minutes before the next stress drop test.

Following a creep test the stress change during the test could be approximated by assuming a Poisson's ratio of 1/2 throughout the test.

This gave an upper limit as to the expected stress variation during the test.

Computer Controlled Test Set-up

Load Frame. The load frame utilized in these tests was an MTS (Materials Test System) model 880 electrohydraulic testing machine shown in Figure 7. MTS 652.01 Water-cooled hydraulic grips allowed fully reversed cyclic tests to be carried out at high temperature. The frame was controlled by a Digital Micro PDP-11 computer. Computer programs were written to run monotonic tension tests, cyclic tests, cyclic tests with hold times, creep tests, and creep stress drop tests. These programs are presented in Appendix D.

Data Acquisition. The Micro PDP-11 also handled data acquisition functions. An MTS 661.21A-02 10 kip load cell was the load transducer. An MTS 632.41B-02 axial extensometer was the strain transducer. This device had quartz extension rods which contacted the sample at two 120^0 punch holes. The extensometer can be seen in Figure 8. All data were stored on 5.25 inch floppy diskettes and could be retrieved in hard copy or graphical form.

Temperature Measurement and Control. An MTS 652 three-zone clamshell furnace and three Research Incorporated 63911 Process Temperature and Power Controllers were used for temperature control. The furnace is shown in Figure 8. Temperature Measurement was handled by six 28 gauge K-type thermocouples. These were placed in contact with the sample. Three thermocouples were fed into a Fluke 2176A Digital Thermometer for readout. These were placed with one each at the top,

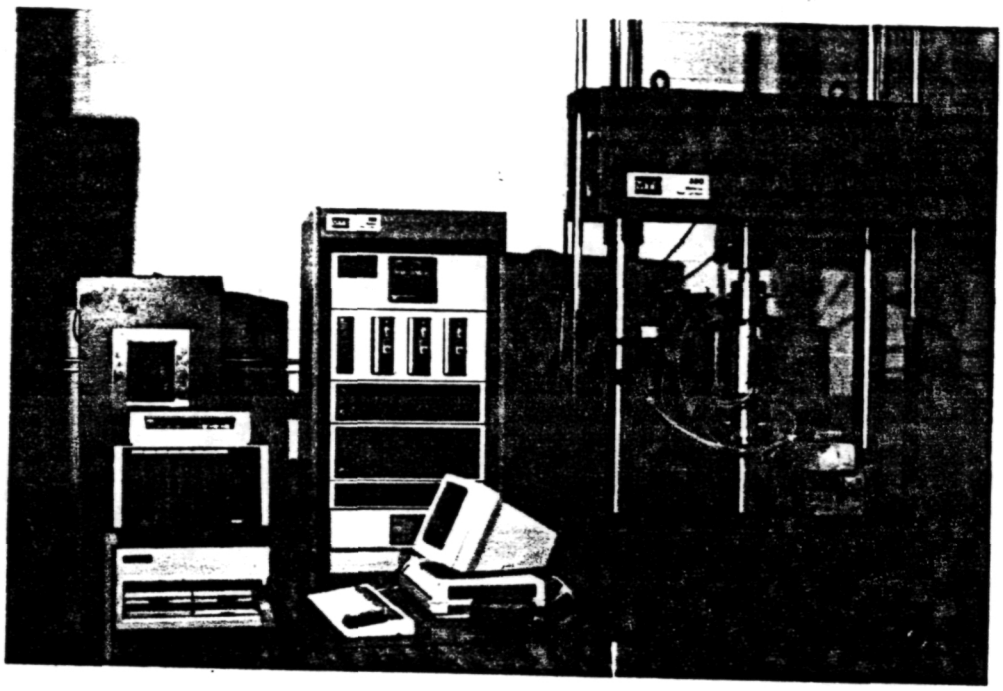

Figure 7 - MTS Configuration

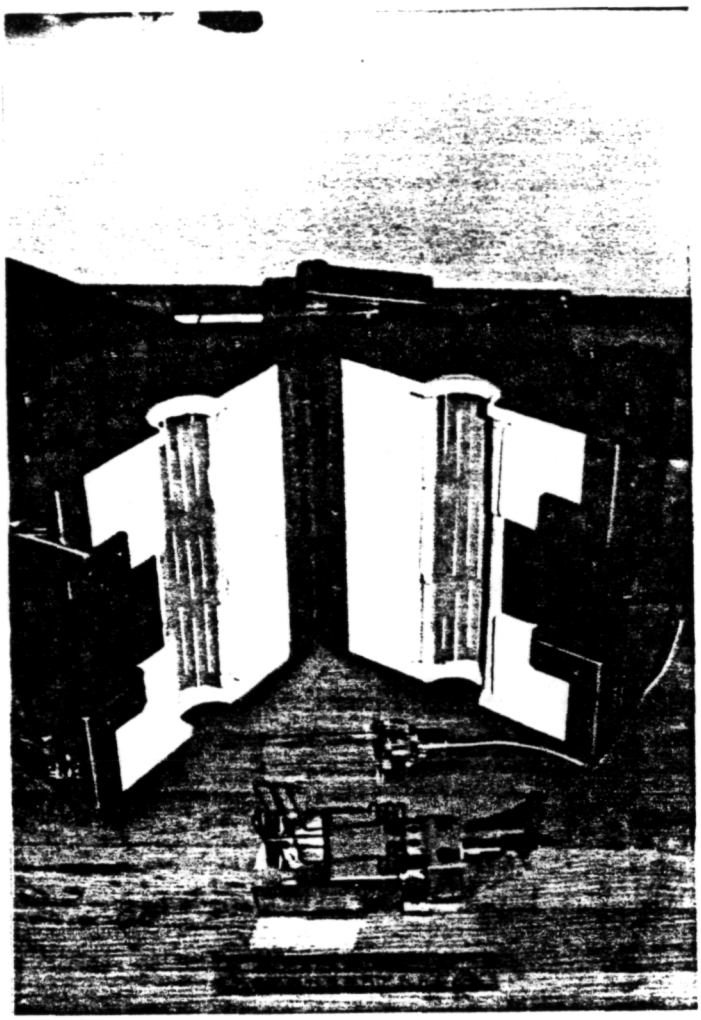

Figure 8 - Furnace and Extensometer for MTS

middle, and bottom of the gauge section. The other three thermocouples were fed into the temperature controllers. These were placed in the center of the furnace zone each was to sense. One thermocouple was placed in the center of the gauge section and one on each grip.

The thermocouples were fastened to the grips by fiberglass thread attached to the sample by self-supporting means. The thermocouples at the top and bottom of the gauge section were wound around the sample. The thermocouples used in the center of the gauge section were brought into the oven from different directions and tied to each other. These thermocouples were then wound around the sample for contact. This arrangement is shown in Figure 9. Welding the thermocouples to the sample would have produced harder contacts with more reliable temperature measurement. However, as mentioned earlier, premature failure occurred at the welds.

Test Procedures. The sample gauge length and gauge diameter were measured as mentioned earlier. The sample was then installed in the grip inserts using Nikal Nickel Special anti-seize lubricating compound to prevent freeze-up to the grips from high-temperatures. The sample was installed in the bottom grip and then the top grip. The hydraulic pressure was applied to the grips. Thermocouples, furnace, and extensometer were then mounted, respectively. The water and air for cooling of the grips and extensometer were then turned on, followed by the furnace. The machine was left on low pressure and in load control to compensate for thermal expansion. The temperature and temperature gradient were then stabilized using the set points of the temperature

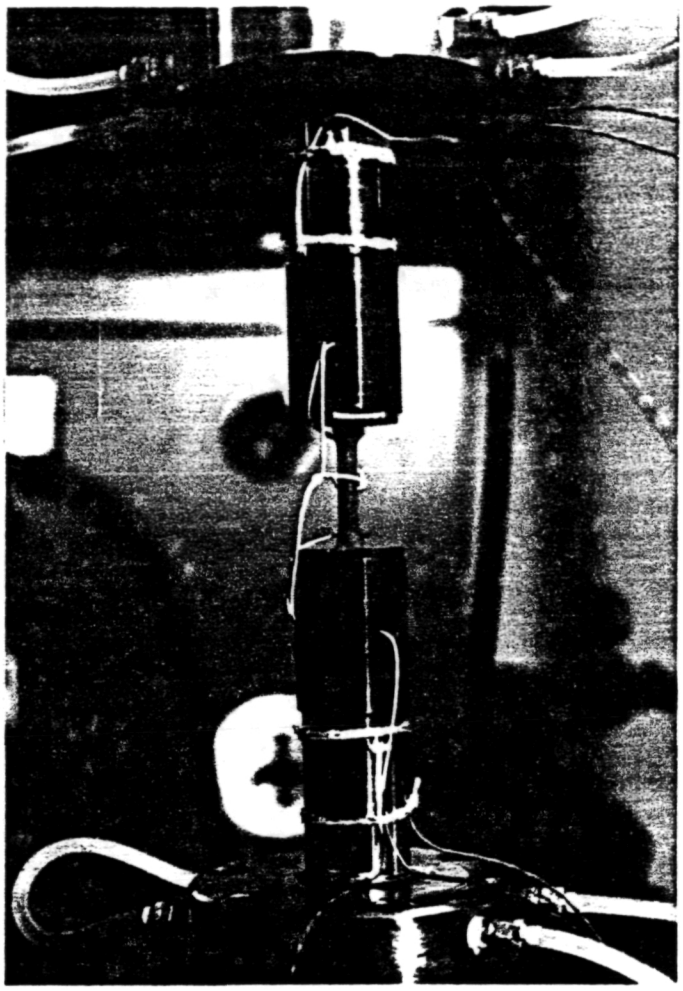

Figure 9 - Method of Thermocouple Attachment
for MTS

controllers. This usually took two to three hours to achieve an acceptable temperature gradient. The most efficient method was to gradually work the temperature up to the desired level.

Calibration of the extensometer was carried out with a Del-tron calibrater approximately every 5 tests. Grip alignment was checked with an Ames 212.5 .0001 inch dial gauge. The dial gauge was attached to the lower grip and the entire grip and fixture were rotated. A dial gauge reading of the relative displacement of the upper grip was taken at four places. Adjustments were made until the relative displacement was less than .0015 inches. Alignment was carried out as needed.

Material Considerations

Basic Material Characteristics. The material used in this work was Inconel 718 and was provided by NASA Lewis Research Center in Cleveland, Ohio. The temperature used was 593^0 C. (1100^0 F.). The typical chemical composition as reported by Thakker and Cowles [153] is shown in Table 2. The alloy is precipitation-hardenable and maintains high strength and creep resistance to 700^0 C. [153,154]. The material is used extensively in the aerospace and nuclear industries [154]. Young's modulus at 593^0 C. is reported by Korth and Smolik to be 24,230 ksi [154] and the average value produced in this work was 24,658 ksi. The same researchers report .2% yield stress values between 128 ksi and 140 ksi, ultimate tensile strengths between 147 ksi and 174 ksi, and a mean coefficient of thermal expansion of $14.56X10^6\ ^0C^{-1}$ [154]. The material used in this work produced .2% yield stress values between 115 and 131 ksi. Inconel 718 is reported to cyclically work soften by several

authors [153-158]. Such response was also experienced during this research.

Table 2 - Chemical Composition of Inconel 718

Chemical Component	Required Weight Percent
Ni	50.0-55.0
Cr	17.0-21.0
Fe	15.0-21.0
Cb+Ta	4.75-5.50
Mo	2.80-3.30
Ti	0.75-1.15
Co	1.0 Max
Al	0.3-0.7
Mn	0.35 Max
Si	0.35 Max
Cu	0.30 Max
C	0.02-0.08
P	0.015 Max
S	0.015 Max
B	0.006 Max

The material underwent strain aging and therefore responded with apparent negative strain rate sensitivity between the strain rates of $1X10^{-5}$ sec^{-1} and $1X10^{-3}$ sec^{-1}. A fatigue life of 5 to 30 cycles resulted specimens were cycled at strain limits over $\pm$1% strain. Lower strain rates and the inclusion of creep hold times also adversly affected the fatigue life. These observations are supported by several other researchers in the field [153-158].

Sample Configurations. Sample design for the creep frame was driven by machine requirements. Figure 10 shows the creep frame sample configuration. The shoulder grooves were necessary to maintain seating by the extensometer knives. The gauge diameter was reduced to .20 inches to bring the applied load values into the range of the load

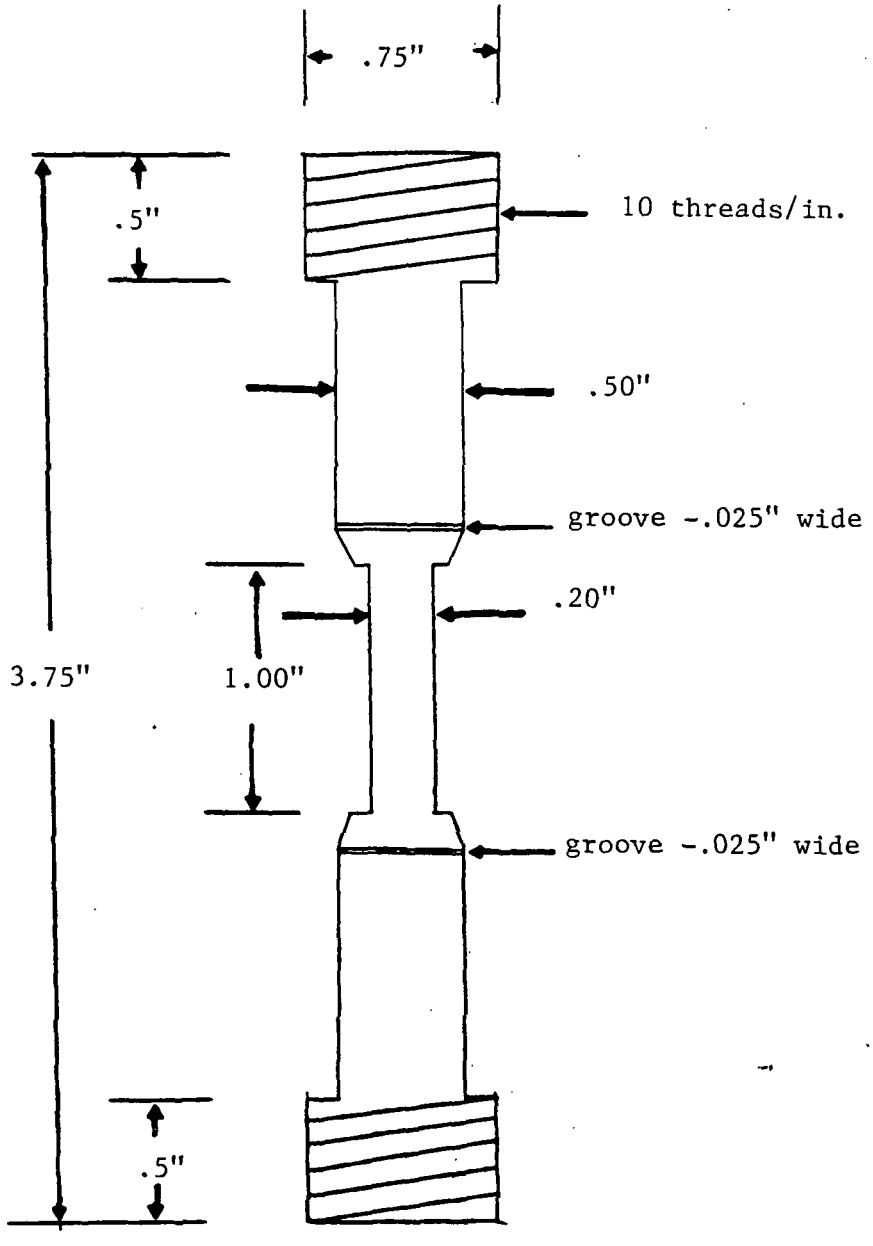

Figure 10 - Creep Sample Configuration

frame. The MTS 880 samples designed to ASTM E606-77T specifications for low cycle fatigue specimens. The sample configuration is shown in Figure 11.

Heat Treatment. All samples were subjected to the same heat treatment prior to being tested. The heat treatment used was given by the Metals Handbook [159]. The material was annealed at 954^0 C. for one hour followed by oil quench. Ageing at 718^0 C. for eight hours was next with a furnace cool. The furnace used was a Hevi Duty Electric Co. type 66-P. Temperature was monitored with a Keithly 871 Digital Thermometer. The resulting material state was found to be the easiest to machine. Therefore, the heat treatment was carried out before machining and again before testing.

Back Stress Measuring Tests

The values for back stress values reported in this work are at best estimates of the true values of and should be treated as such. Three reasons exist for this uncertainty. First, the transient tests during cyclic loading require saturated conditions. However, the fatigue lifetime problems for this material mentioned earlier did not permit complete saturation of the microstructure for fear of sample fracture. The criterion used to define saturation in this work was a cycle to cycle variation of the maximum stress of less than one ksi. These conditions were met after 10 to 15 cycles for this material. Second, the resulting strain measurements following a cyclic hold time or a creep stress drop were on the order of the digital resolution of the data aquisition system ($\approx 5.0X10^{-5}$in). This problem was lessened by

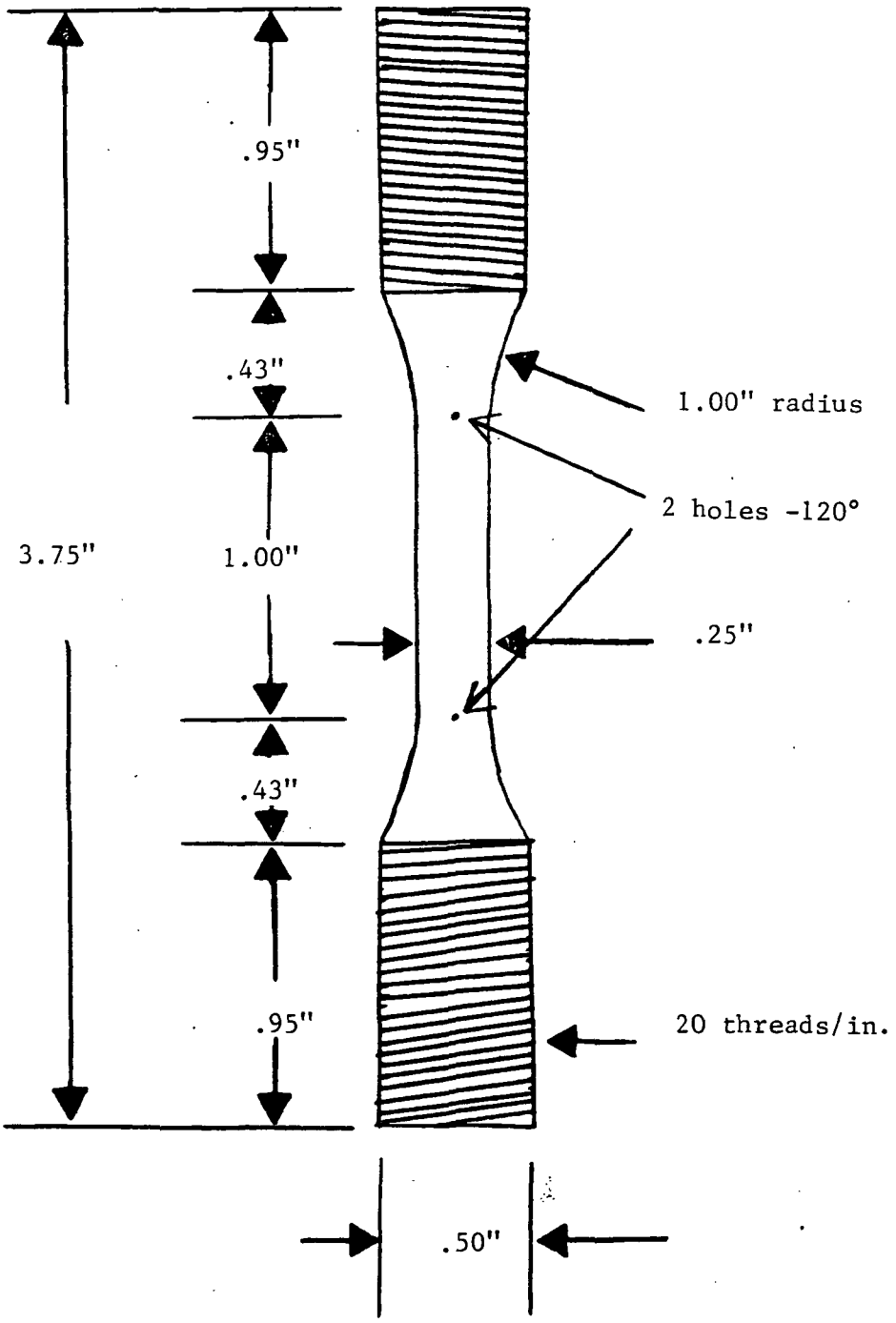

Figure 11 - MTS Sample Configuration

taking in large numbers of data points and using least squares regression analysis to calculate strain rates. Third, the determination of when recovery effects became significant following a cyclic hold time or creep stress drop was a very subjective decision. Each transient test had to be individually scrutinized to decide how many points to consider in the regression analysis.

The cyclic back stress numbers were obtained by holding a cyclic test at various points on the unloading curve, switching to load control and monitoring the strain rate following the hold. The material was recycled and a hold time at another stress value was carried out. A linear least squares fit to the strain versus time data provided a strain rate at each hold time. Another linear least squares fit to the strain rate versus hold stress data provided stress at which a zero strain rate would have been expected. The back stress was assumed to be equal to the stress at this point.

Figure 12 shows the data obtained from test 65 cyclic hold times. Test 65 was a cyclic test run at a strain rate of $3.127X10^{-4}$ sec^{-1} with strain limits of $\pm$ .8% strain. The x axis provides values of the strain rate calculated with the least squares regression after each cycle. The y axis provides the associated value of the stress at the hold time. The average maximum applied stress over the range of these tests was 108 ksi. A bilinear relationship can be seen in the data. A linear least squares fit to the data of the lower slope provided the back stress value used in this work of 48 ksi. It was assumed that the upper slope represented a breakdown in the linear assumption and was not

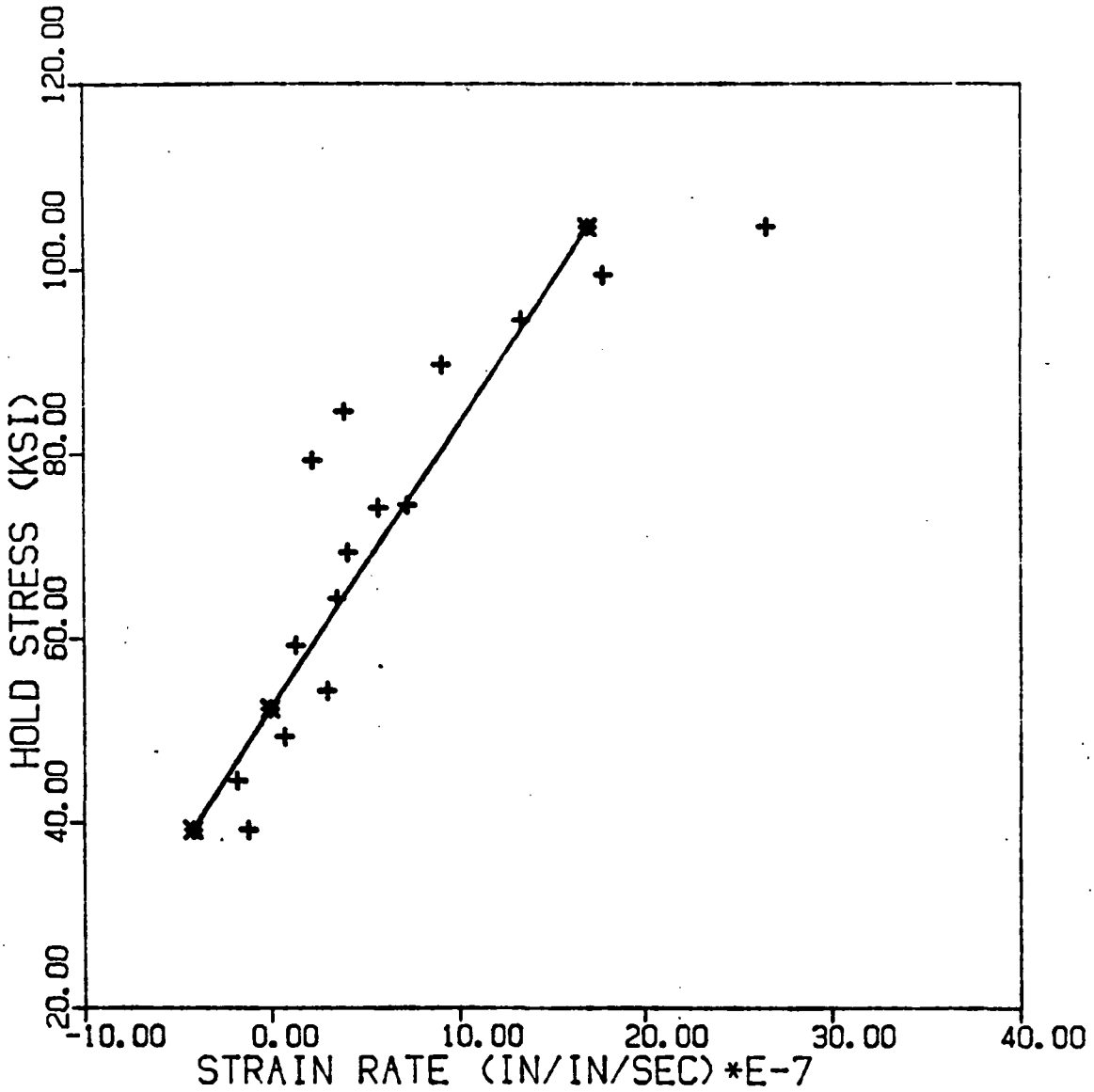

Figure 12 - Test 65 Back Stress Determination Data

considered. This analysis should be reconsidered. The upper slope may actually be considered and a back stress value of 80 ksi reported. Poirier [147] presents some models which would support a zero strain rate for a cyclic hold or stress drop which is below the back stress. The lower slope could be a viewed as a region of approximately zero strain rate and the associated stress values would be below the back stress value.

The back stress numbers were invaluable in estimating some material constants as will be seen in the next chapter. The results were also promising enough to warrant further study. The procedures used here could be greatly enhanced by equipment with greater resolution such as used by Jones, et al. [93] and less subjective methods of data reduction such as the method of Blum and Finkel [150]. Other techniques such as torsional cycling could also be considered [131]. The stress transient test [144] might also provide information for a material such a Inconel 718 which suffers from a short fatigue life when cycled. It should also be noted that cyclic hold times were attempted with stress relaxation holds rather than creep holds. The machine was found to be less stable in strain control. A smaller load frame might allow stress relaxation holds to be more stable and eliminate the need to switch between load and strain control. The back stress data presented graphically in Figure 12 are presented in tabular form in Appendix A as well as data from the other back stress measuring tests.

CALCULATION OF MATERIAL CONSTANTS

The complex response of Inconel 718 at 1100^0 F prompted flexible methods of constant calculation to be developed. The method for calculating constants for the models began by making a series of judicious assumptions which allowed commonly used constant calculation schemes to produce initial estimates of the constants. Some nonlinearity was avoided in this step and was reintroduced by a series of repeatable iterations to the final constants. The iterative step numerically integrated the models to predict the stress-strain response at a certain point. One material constant was then changed to match the prediction to the experimental value at this point. Another material constant was then changed to match another material point.

Physical insight, familiarity with the uncertainty in the data set, and engineering intuition guided the organization of the calculation process. However, the actual process was carried out as systematically as possible. The eventual creation of systematic and automatable methods to calculate constants has been a major driver in this phase of the work. This chapter is organized to allow an interested reader to recalculate the constants and to improve on the process used here. Table 1 should be consulted throughout this chapter as tests will be referred to by number. Appendix A presents all experimental data needed to repeat these calculations. Appendix B provides proposed upgrades to these procedures based on experience developed in this work.

The method used to calculate the material constants will be summarized using a generic viscoplastic model in the first section of this chapter. This is presented to make the actual calculations more understandable to the reader. The generic model used as an example will be presented first followed by a subsection outlining the general method of initial calculations and a subsection outlining the iterative step. Individual sections covering the four models used in this work will follow. Each section will contain one subsection describing the initial calculations and one describing the computer iterations.

Generic Summary of Constant Calculation Methods

Generic viscoplastic model. The growth laws for the example model are presented below:

$$\dot{\varepsilon}^I = \left(\frac{\sigma - B}{D}\right)^n \tag{39}$$

$$\dot{B} = C_1 \dot{\varepsilon}^I + C_2 B \, \dot{\varepsilon}^I + C_3 B \tag{40}$$

$$\dot{D} = C_4 |\dot{\varepsilon}^I| + C_5 D \tag{41}$$

n is a constant measuring strain rate sensitivity. C_1 is a constant measuring back stress hardening. C_2 is handling back stress dynamic recovery and C_3 measures back stress thermal recovery. C_4 produces drag stress hardening and C_5 models drag stress recovery.

Initial assumptions. The following initial assumptions were made in this work:

(1) back stress was assumed responsible for hardening in monotonic tension;

(2) drag stress was assumed responsible for cyclic softening;

(3) thermal recovery was assumed negligible for rapid tests ($\dot{\varepsilon}^I \geq 1.0X10^{-4} sec^{-1}$) ;

(4) drag stress thermal recovery was present in low strain rate saturated cyclic tests; and

(5) back stress thermal recovery was present in creep tests.

These assumptions allowed the constants for the inelastic strain rate equations, back stress hardening, drag stress hardening, drag stress recovery, and back stress recovery to be calculated in that general order. These assumptions also allowed much of the constant calculation schemes reported in the literature to be utilized with this material [41,42,52,70,72,90,97,142]. A new set of initial assumptions was found to be more appropriate upon completion of this work and proposed methods based on these new assumptions can be found in Appendix B.

The first step was to estimate the constants in the back stress growth law assuming thermal recovery was negligible. The back stress growth law took on the following form:

$$\dot{B} = [C_1 + B\ C_2]\ \dot{\varepsilon}^I \qquad (42)$$

Differential techniques for calculating work hardening such as seen in Chan's gamma and theta plot concepts [90] were useful. Experimental estimations of back stress values such as used by Krieg, et al. [41] and

Walker [52] were usually necessary. Relationships between saturated stresses and saturated back stresses as used by Miller [42] have also been used.

The next step was to calculate the strain rate sensitivity constant n and the initial value of drag stress denoted by D_0. Rewriting the inelastic strain rate equation in the following form was useful:

$$\ln(\sigma - B) = \frac{1}{n} \ln(\dot{\varepsilon}^I) + \ln(D_0) \qquad (43)$$

A linear fit to several data points typically provided 1/n as the slope and $\ln(D_0)$ as the intercept. This is a technique commonly used with Bodner's model [84]. The ability to estimate saturated stresses and back stresses using techniques such as the gamma or theta plot [90] and relations between saturated stress and back stress are useful [42,90].

Initial determination of the drag stress parameter C_4 was carried out by assuming that thermal recovery could be neglected for rapid tests. The cumulative inelastic strain was calculated to a point on the cyclic curve where B and D could be estimated. The drag stress recovery parameter C_5 was then calculated by assuming the drag stress growth law was equal to zero for the saturated cycle of a low strain rate test. The back stress recovery parameter C_3 was calculated by assuming the back stress growth law was equal to zero for creep tests.

Computer iterations. The computer iterations began by pairing each material constant with an experimental stress-strain point which the constant should intuitively have the greatest effect in predicting in a

sequential fashion. The constants in the generic model were paired in the following fashion for this work:

(1) D_0 was paired with a stress-strain point at .8% strain on test 70 ($\dot{\varepsilon} = 3.151X10^{-3}$ sec^{-1});

(2) C_2 was paired with a stress-strain point at 1.3% strain on test 70;

(3) C_1 was used to assure that the theoretical back stress values were in the same range expected from experimental values;

(4) n was paired with a stress-strain point at .8% strain on test 71 ($\dot{\varepsilon} = 7.253X10^{-6}$ sec^{-1});

(5) C_3 was paired with a point at 1.3% strain on test 71;

(6) C_4 was paired with a point at .8% on the 10th cycle of test 86 ($\dot{\varepsilon} = 1.002X10^{-3}$ sec^{-1});

(7) C_5 was paired with a point at .8% ot the 4th cycle of test 72 ($\dot{\varepsilon} = 7.626X10^{-6}$ sec^{-1});

The iterative procedure then progressed by numerically integrating the model to predict the experimental stress-strain value for a specific constant. The constant was altered to match this point while the others were held constant. Then another constant was altered to produce the proper prediction at its paired experimental point. The expected order with which these steps were to be carried out is shown in Table 3. The x marks indicate which constant is being altered during the step indicated in column 1. Steps 1 through 5 are setting the back stress hardening characteristics. Steps 6 through 9 are setting the strain rate sensitivity of the model. Steps 10 through 12 are setting the drag

stress hardening constant. The back stress recovery constants are being set in steps 13 through 15. Drag stress recovery is set in steps 16 through 18.

Table 3 - An Example Set of Iterations

Step	D_0	C_2	C_1	n	C_4	C_3	C_5
1	x						
2		x					
3			x				
4	x						
5		x					
6				x			
7	x						
8		x					
9				x			
10					x		
11		x					
12					x		
13						x	
14		x					
15						x	
16							x
17						x	
18							x

This method allows the entire process to be recorded. Automation of such a method is also possible if the initial calculations produce values which are close to the final constants. A systematic set of iterations may also allow a standard method for calculating constants to be produced. The lack of correction for strain aging effects in the initial calculations caused problems in implementing this iterative scheme. Appendix B provides some suggestions to avoid this.

Krieg, Swearengen and Rhode's Model

The growth laws for the model of Krieg, et al. are repeated below for completeness:

$$\dot{\varepsilon}^I = C\left(\frac{\sigma - B}{D}\right)^n \operatorname{sgn}(\sigma - B) \tag{44}$$

$$\dot{B} = A_1\dot{\varepsilon}^I - A_2B^2\left[e^{(A_3B^2)} - 1 \right] \operatorname{sgn}(B) \tag{45}$$

$$\dot{D} = A_4\left|\dot{\varepsilon}^I\right| - A_5(D - D_0)^n \tag{46}$$

Initial calculations. The initial calculations began by rewriting the inelastic strain rate equation in the following form:

$$\ln(\dot{\varepsilon}^I) = \ln\left(\frac{C}{D_0^n}\right) + n\cdot\ln(\sigma - B) \tag{47}$$

Assuming a constant D a linear fit between $\ln(\sigma - B)$ and $\ln(\dot{\varepsilon}^I)$ produces a slope of n and intercept $\ln(C/D^n)$. Experimental values of σ, B, and $\dot{\varepsilon}^I$ from tests 60, 61, 63, 65, 81, 84, and 88 produced an n value of 4.41257. Using a D_0 value of 1.00, C is estimated at $3.177\text{X}10^{-11}$ sec^{-1}. Now, assuming monotonic hardening is due to back stress, no thermal recovery is present, and the initial value of back stress is zero, then back stress is written as:

$$B = A_1\varepsilon^I \tag{48}$$

The constant A_1 is calculated from the following:

$$A_1 = \frac{\sigma - (\dot{\varepsilon}^I / C)^{1/n}}{\varepsilon^I}$$

Experimental values of σ, ε^I, and $\dot{\varepsilon}^I$ at .8% total strain from tests 70, 86, 56 provide an average value of A_1 = 20,533.82 ksi.

The constant A_4 is calculated by assuming that B and D grow without recovery for the first three half cycles. The following formula then provides an estimate of A_4 :

$$A_4 = \frac{[\sigma - A_1(\varepsilon_1^I + \varepsilon_2^I + \varepsilon_3^I)](\frac{\dot{\varepsilon}^I}{C})^{-1/n} - D_0}{|\varepsilon_1^I| + |\varepsilon_2^I| + |\varepsilon_3^I|} \qquad (49)$$

where ε_1^I, ε_2^I, and ε_3^I are the values of inelastic strain produced during each half cycle. Using values of σ, ε_1^I, ε_2^I, ε_3^I, and $\dot{\varepsilon}^I$ from tests 86 and 56, the average estimate of A_4 = -8.784 ksi was produced.

Cyclic saturation is assumed to be a balance between drag stress growth and recovery. Rewriting the drag stress growth law provides the following equation:

$$A_5 = A_4|\dot{\varepsilon}^I| \cdot |(\sigma - B) \cdot (\frac{\dot{\varepsilon}^I}{C})^{-1/n} - D_0|^{-n} \qquad (50)$$

Test 84 provides experimental values of σ, B, ε^I and produces A_5 = -13.8768 ksi sec^{-1}. D_0 has been set to 1.000.

Creep saturation is assumed to rely heavily on directional recovery. The back stress growth law is written as follows:

$$A_1\dot{\varepsilon}^I = A_2 B^2 [e^{(A_3 B^2)} - 1] \tag{51}$$

Using two tests, the following equation results for A_3 :

$$A_3 - \{ \ln[K(e^{(A_3 B_2^2)} - 1) + 1]\} B_1^{-2} = 0 \tag{52}$$

$$\text{where } K = \frac{\dot{\varepsilon}_1^I B_2^2}{\dot{\varepsilon}_2^I B_1^2}$$

All possible combinations of tests 60, 61, and 63 provided experimental values of $\dot{\varepsilon}_1^I$, B_1, $\dot{\varepsilon}_2^I$, and B_2 . The above equation was solved iteratively for A_3 and the resulting estimates averaged to produce $A_3 = 1.134X10^{-3}$ ksi^{-2}. The following equation then produced values for A_2:

$$A_2 = A_1\dot{\varepsilon}^I B^{-2} [e^{(A_3 B^2)} - 1]^{-1} \tag{53}$$

Averaging the values produced by tests 60, 61, and 63 provided $A_2 = 1.452X10^{-14}$ ksi sec^{-1}.

Computer Iterations. Table 4 summarizes the computer iterations carried out to obtain the final constants. The first column lists the step number of these sequential iterations. Each step consisted of changes in the constant provided in column two. The model was integrated at the same strain rate as the experimental test given in column three to match the experimental point at the total strain value

Table 4 - Computer Iteration Summary of Krieg, Swearengen, and Rhode's Model

Step	Const.	Test	Strain(%)	Cycle	Old Value	New Value
1	A1	70	1.28	1	20,533	5,000
2	C	70	.8	1	3E-11	3E-12
3	A1	70	1.28	1	5,000	3,000
4	C	70	.8	1	3E-12	2E-12
5	A1	70	1.28	1	3,000	2,500
6	C	86	.8	1	2E-12	9E-13
7	A4	86	.8	10	-8.78	-3.0
8	A5	86	.8	10	-13.876	-6.0
9	A1	70	1.28	1	2,500	750
10	C	70	.8	1	9E-13	1.75E-12
11	A1	70	1.28	1	750	1,000
12	C	86	.8	1	1.75E-12	7E-13
13	A4	86	.8	10	-3.0	-3.5
14	C	71	.8	1	7E-13	3.7E-15
15	A2	71	1.28	1	1.45E-14	1E-4
16	C	70	.8	1	3.7E-15	1.75E-12
17	A1	70	1.28	1	1,000	1,200
18	C	86	.8	1	1.75E-12	7E-13
19	C	71	.8	1	7E-13	3.7E-15
20	C	72	.8	1	3.7E-15	3.7E-15
21	C	65	.8	1	3.7E-15	1.8E-13
22	C	83	.8	1	1.8E-13	5E-14
23	C	80	.8	1	1.8E-13	1.375E-14
24	C					1
25	DO	86	.8	1	1	568.34
26	A4	86	.8	10	-3.5	-500
27	A5	86	.8	10	-6.0	1-E-19
28	β					2.1549
29	J					7E-6
30	F					1402.9
31	β	70	.8	1	2.15	2
32	J	70	.8	1	7E-6	1E-1
33	F	70	.8	1	14,029	1,500
34	β	71	.8	1	2	5
35	J	71	.8	1	1E-7	1E-9
36	F	71	.8	1	1,500	3,000
37	β	70	.8	1	5	1.5
38	J	70	.8	1	1E-9	7E-6
39	F	70	.8	1	3,000	1,300
40	DO	71	.8	1	568.34	475
41	n	70	.8	1	4.41257	15
42	DO	70	.8	1	475	100
43	C	70	.8	1	1	2E-4
44	A1	70	.8	1	1,200	1,000
45	β	70	.8	1	1.5	3.5
46	J	70	.8	1	7E-6	1E-9

Table 4 continued

Step	Const.	Test	Strain(%)	Cycle	Old Value	New Value
47	F	70	.8	1	1,300	100
48	β	71	.8	1	3.5	4.0
49	F	71	.8	1	100	120
50	A1	70	1.28	1	1,000	1,400

given in columns four and five. The old value of the constant is given in column six and the new value is given in column seven. Several iterations were required within each step to arrive at the proper new value. The steps were carried out sequentially. The constant being changed was chosen as the one which could be expected to have the greatest influence on the stress-strain point considered.

Steps 1 through 17 of Table 4 are tuning constants A_1, A_2, A_4, A_5. The true impact of the negative strain rate sensitivity material response showed itself at this point. The model could not match both tests 70 ($3.015X10^{-3}$ sec^{-1}) and test 71 ($7.626X10^{-6}$ sec^{-1}) in the form presented here. Steps 18 through 23 were used to locate individual values of the constant C to fit each strain rate. The values were then used to calculate a correction for the negative strain rate sensitivity problem. The modification used in this work came from Schmidt and Miller's non-interactive solute stregthening correction [98]. The inelastic strain rate equation is written in the following form:

$$\dot{\varepsilon}^I = C\left(\frac{\sigma - B}{D + F_{sol}}\right) \operatorname{sgn}(\sigma - B) \tag{54}$$

$$F_{sol} = F \cdot \exp\{ -\left(\frac{[\log(|\dot{\varepsilon}^I|) - \log(|J|)]}{\beta}\right)^2 \} \qquad (55)$$

Steps 24 through 27 of Table 4 show iterations in which all scaling is transferred from the C constant to the D variable. An initial assumption was that the maximum effect of the solutes was at $\dot{\varepsilon}^I = 7.000X10^{-6} sec^{-1}$. The effect was assumed to be non-existent for $\dot{\varepsilon}^I = 1.000X10^{-3} sec^{-1}$. The constant F is the maximum value of the solute stregthening. This constant was set by differencing D_0 values for tests 71 and 86 needed to provide proper scaling. The constant J is the strain rate at the peak effect and was set at $7.000X10^{-6}$ sec^{-1}. The constant β is the width of the correction and was set by the following equation:

$$\beta = \log(|\dot{\varepsilon}^I|) - \log(J) \qquad (56)$$

$\dot{\varepsilon}^I$ was set at $1.000X10^{-3}$ sec^{-1} and $\beta = 2.1549$ resulted.

Steps 31 through 40 tuned these constants. The correction was still not adequate. Steps 41 through 50 increased the constant n to lessen the strain rate sensitivity of the basic model. Table 5 shows the values of the constants after the initial calculations and the values after the computer iterations.

Bodner's Anisotropic Model

The growth laws for Bodner's anisotropic model are repeated below

for completeness:

$$\dot{\varepsilon}^I = \frac{2}{\sqrt{3}} D_0 \exp\left[-\left(\frac{Z}{\sigma}\right)^{2n}\right] \operatorname{sgn} \sigma \tag{57}$$

$$Z = Z^I + Z^A = Z^I + B \operatorname{sgn} \sigma \tag{58}$$

$$\dot{Z}^I = m_1 (Z_1 - Z^I) \dot{W}_p - A_1 Z_1 \left(\frac{Z^I - Z_2}{Z_1}\right)^{r_1} \tag{59}$$

$$\dot{B} = m_2 (Z_3 \operatorname{sgn} \sigma - Z^A) \dot{W}_p - A_2 Z_1 \left(\frac{|Z^A|}{Z_1}\right)^{r_2} \operatorname{sgn} Z^A \tag{60}$$

$$\dot{W}_p = \sigma \dot{\varepsilon}^I \tag{61}$$

Table 5 - Constants for Krieg, Swerengen, and Rhode's Model

Constant	Hand Calculations	Computer Iterations
n	4.412	15.00
C	3.176E-11	2.000E-4
A1	20,530	1,400
A2	1.451E-14	0.000
A3	1.133E-3	1.133E-3
A4	-8.784	-500.0
A5	-13.88	-1.000E-19
B0	0	0.00
D0	1.000	100.0
F		55
β		1,000
J		7.000E-6

Initial calculations. The initial calculations began by rewriting the inelastic strain rate equation in the following form:

$$\ln\left[\, 2\cdot\ln\left(\frac{2}{\sqrt{3}}\,\frac{D_o}{\dot{\varepsilon}^I}\right)\right] = -2n\cdot\ln(\sigma) + 2n\cdot\ln(Z) = \ln(S) \qquad (62)$$

A linear fit of $\ln(\sigma)$ versus $\ln(S)$ gave $-2n$ as the slope and $2n[\ln(Z)]$ as the intercept for stationary values of Z. n = .81316 was calculated in this fashion using tests 60, 61, 62, 63, 64, 71, 72, 80, 40, 38, 42, 36, and 34. These tests were low strain rate tests ($\dot{\varepsilon}^I \leq 1.0X10^{-4} sec^{-1}$) and exhibited positive strain rate sensitivity. The values of σ from tests 60, 61, 62, 63, and 64 were applied stresses and $\dot{\varepsilon}^I$ the strain rates during secondary creep. The σ values for the remaining tests were saturated stresses from the gamma plot and the $\dot{\varepsilon}^I$ values were values of applied strain rate. The gamma plot will be discussed later in this section. The value for D_0 was set at $1.000X10^4$ sec^{-1}.

At this point it is assumed that $Z_2 = Z_0$ at this point and Z_0 was estimated. The value of Z_0 is given by the following equation:

$$Z_0 = \sigma_0\left[\, 2\cdot\ln\left(\frac{2}{\sqrt{3}}\cdot\frac{D_o}{\dot{\varepsilon}_0^I}\right)\right]^{1/2n} \qquad (63)$$

The values of σ_0 were the values of stress at the onset of visible plastic flow. $\dot{\varepsilon}_0{}^I$ was the associated plastic strain rate and was typically $1X10^{-6}$ sec^{-1}. Test 72 produced a Z_0 value of 1063.23 ksi.

The gamma plot as described by Chan in reference [90] is a proposed method of analyzing the work hardening characteristics of a monotonic test assuming dynamic recovery and a measure of work hardening based on plastic work. The following assumptions are also made:

(1) Only values of σ and ε^I after .2% offset will be used;

(2) $\dot{\varepsilon}^I$ is constant and approximately equal to applied strain rate; and

(3) thermal recovery is negligible.

The assumption that Z^I is constant during a monotonic cycle was also made for this material system. The following equation is derived:

$$\gamma = \frac{d\sigma}{dW_p} = \left[-2 \cdot \ln\left(\frac{\sqrt{3}}{2} \cdot \frac{\dot{\varepsilon}^I}{D_0}\right)\right]^{-1/2n} m_2(Z_3 + Z_0) - m_2\sigma \qquad (64)$$

Values of γ were calculated by differentiating a polynomial curve fit of a stress-inelastic strain curve and dividing by the stress value at each point. A linear fit to the first ten points of a σ versus γ plot provided a slope of $-m_2$ and an x intercept of saturated stress. Saturated stress is defined to be the stress at which the internal state variables are unchanging. Values of Z_3 were calculated from the saturated stress using the following formula:

$$Z_3 = \sigma\left[2 \cdot \ln\left(\frac{\sqrt{3}}{2} \cdot \frac{D_0}{\dot{\varepsilon}^I}\right)\right]^{1/2n} - Z_0 \qquad (65)$$

The Z_0 values used in this step were individual values for each test and not the single value reported earlier. Averaging tests 71, 72, 80, 65, 56, 86, and 70 the following values were obtained:

Z_3 = 317.01 ksi

m_2 = 3.3068 ksi^{-1}

An initial estimate of Z_1 is obtained by assuming the gamma plot

works analogously for the positive side of the saturated cycle (assumed to be the tenth cycle). The value of Z_0 has changed to Z_1 at this cycle and the following equation results from the x intercept:

$$Z_1 = \sigma[\ 2 \cdot \ln(\frac{\sqrt{3}}{2} \cdot \frac{D_0}{\dot{\varepsilon}^I})]^{1/2n} - Z_3 \qquad (66)$$

Tests 65, 56, and 86 were averaged to produce the following value for Z_1:

Z_1 = 724.35 ksi

The gamma plot was used to obtain values of Z^I and W_p for every half cycle of 10 cycle cyclic tests. Z^I is calculated as Z_1 had been calculated above. W_p was calculated by integrating the polynomial producing γ. These values are then combined in the following equation to produce an estimate for m_1:

$$\ln(\ Z^I - Z_1) = -m_1 W_p + \ln(Z_0 - Z_1) \qquad (67)$$

Tests 86 and 56 produced an average value of m_1 = .4850 ksi^{-1}.

Calculation of the constants A_1 and r_1 required assuming that recovery of B was negligible and the gamma plot was still operative at the saturated cyclic loops of low strain rate tests. Values of Z^I were calculated as above and $\dot{W}_p$ values were calculated from the last two data points of each positive 10th cycle load-up. The following equation then allowed a linear fit to produce values for A_1 and r_1:

$$\ln\{ m_1[Z^I - Z_1] \dot{W}_p\} = r_1 \ln[\frac{|Z^I - Z_2|}{Z_1}] + \ln(-A_1 Z_1) \qquad (68)$$

Tests 72 ($\dot{W}_p = 8.454X10^{-4}$ ksi/sec) 80 ($\dot{W}_p = 3.138X10^{-3}$ ksi/sec), 83 ($\dot{W}_p = 1.014X10^{-2}$ ksi/sec), and 65 ($\dot{W}_p = 3.044X10^{-2}$ ksi/sec), produced the following values:

$A_1 = -.001 \text{ sec}^{-1}$

$r_1 = .49258$

Creep tests were used to determine values for A_2 and r_2. The assumption that $Z^I = Z_0$ was used at this point. Values of B were calculated from the inelastic strain rate equation. $\dot{W}_p$ values were also calculated from $\sigma \dot{\varepsilon}^I$. The following equation then provided r_2 and A_2 after a linear fit:

$$\ln[m_2(Z_3 - B) \dot{W}_p] = r_2 \ln[\frac{|B|}{Z_1}] + \ln(-A_2 Z_1) \qquad (69)$$

Tests 60, 61, 62, 63, and 64 provided the following values:

$A_2 = -6.9935 \text{ sec}^{-1}$

$r_2 = 21.9558$

Computer iterations. Table 6 summarizes the computer iterations carried out to obtain the final constants for Bodner's model. It should be interpreted in the same manner as in the section describing the model of Krieg, et al. Step 1 removes the directional recovery term from consideration. Steps 2 through 7 are setting the constants Z_0 and m_2 for test 70. Steps 8, 9, and 10 are setting the cyclic response through

the constants Z_1 and A_1. A correction for solute strengthening was found to be necessary for this model also. The model response was determined as a function of Z_0 in steps 11 through 15. This information was used to determine a solute strengthening correction. Schmidt and Miller's correction was again used to produce an inelastic strain rate equation of the following form:

$$\dot{\varepsilon}^I = \frac{2}{\sqrt{3}} D_0 \exp\left[-\frac{1}{2}\left(\frac{Z + F_{sol}}{\sigma}\right)^{2n}\right] \operatorname{sgn} \sigma \tag{70}$$

$$F_{sol} = F \cdot \exp\left\{ -\left[\frac{\log(|\dot{\varepsilon}^I|) - \log(J)}{\beta}\right]^2 \right\} \tag{71}$$

Table 6 - Computer Iteration Summary for Bodner's Anisotropic Model

Step	Const.	Test	Strain(%)	Cycle	Old Value	New Value
1	A2	70	.8	1	-6.99	0.0
2	Z0/Z2	70	.8	1	1062.23	825
3	M2	70	1.25	1	3.3068	.5
4	Z0/Z2	70	.8	1	825	1050
5	M1	70	1.25	1	.485	.05
6	Z0/Z2	70	.8	1	1050	975
7	M2	70	1.25	1	.5	.4
8	Z1	86	.8	10	72435	600
9	A1	71	.8	1	-.001	-.0001
10	Z1	86	.8	10	600	700
11	Z0/Z2	71	.8	1	975	1240
12	Z0/Z2	72	.8	1	975	1250
13	Z0/Z2	65	.8	1	975	1050
14	Z0/Z2	83	.8	1	975	1150
15	Z0/Z2	80	.8	1	975	1225
16	F					350
17	β					3
18	J					7E-6
19	Z0/Z2	70	.8	1		975
20	J	70	.8	1	7E-6	1E-6
21	Z0/Z2	71	.8	1	975	900

The constants F, β, and J, were calculated in the same manner as with the model of Krieg, et al. These parameters were introduced and tuned in steps 16 through 21. Table 7 compares the constants before and after the computer iteration process.

Miller's Model

The growth laws for Miller's model are repeated below for completeness:

$$\dot{\varepsilon}^I = B'\{ \sinh[(\frac{\sigma - B}{D})^{1.5}]^n \operatorname{sgn}(\sigma - B) \tag{72}$$

$$\dot{B} = H_1\dot{\varepsilon}^I - H_1B' \sinh(A_1|B|)^n \operatorname{sgn}(B) \tag{73}$$

$$\dot{D} = H_2| \dot{\varepsilon}^I|(C_2 + |B| - \frac{A_2}{A_1} D^3) - H_2C_2B' \sinh(A_2D^{1.5})^n \tag{74}$$

Table 7 - Constants for Bodner's Anisotropic Model

Constant	Hand Caluculations	Computer Iterations
n	.8132	.8132
A1	-.0010	-.0010
A2	-6.994	0.000
M1	.4850	.0500
M2	3.307	.4000
r1	.4926	.4926
r2	21.958	.4926
Z0	1063.23	900.0
Z1	724.35	700.0
Z2	1063.23	900.0
Z3	317.01	317.0
F		-350.0
β		3.0
J		1E-6

Initial Calculations. The first step in the calculation of Miller's constants is to write an auxiliary equation based on the inelastic strain rate equation in the following form:

$$\ln(\dot{\varepsilon}^{I}_{ss}) = n \ln[\sinh(A\,\sigma_{ss})] + \ln(B') \tag{75}$$

$\dot{\varepsilon}^{I}_{ss}$ and σ_{ss} are values of inelastic strain rate during secondary creep and the associated applied stress. The constant A is to be determined from the following equation:

$$\left|\frac{\ln(\dot{\varepsilon}^{I}_{2}) - \ln(\dot{\varepsilon}^{I}_{1})}{\ln(\dot{\varepsilon}^{I}_{3}) - \ln(\dot{\varepsilon}^{I}_{1})}\right| = \left|\frac{\ln[\sinh(A\,\sigma_{2})] - \ln[\sinh(A\,\sigma_{1})]}{\ln[\sinh(A\,\sigma_{3})] - \ln[\sinh(A\,\sigma_{1})]}\right| \tag{76}$$

The $\dot{\varepsilon}^{I}$ and σ values are again secondary creep rate and applied stress from 3 separate tests. This equation was solved iteratively for various combinations of tests 60, 61, 62, 63, and 64. The results were averaged for an A value of .0917092 ksi^{-1}. The same tests were then applied to the previous linear equations to produce n and B' through a linear fit. The following values were produced:

$n = 1.813$

$B' = 2.206X10^{-16}\ sec^{-1}$

D_0 was calculated from the following equation assuming B = 0.000:

$$D_0 = \sigma_0\{\sinh^{-1}[(\frac{\dot{\varepsilon}^{I}}{B'})^{1/n}]\}^{-2/3} \tag{77}$$

σ_0 and $\dot{\varepsilon}^{I}$ were the values at the appearance of plastic deformation. A

D_0 value of 16.264 ksi was produced by averaging the results of tests 71, 72, 80, 83, 65, 56, 86, and 70.

The constant H_1 was calculated from the following equation assuming drag stress had not grown and recovery was negligible:

$$H_1 = \left(\sigma - D_0\left\{ \sinh^{-1}\left[\left(\frac{\dot{\varepsilon}^I}{B'}\right)^{1/n}\right] \right\}^{2/3}\right)(\varepsilon^I)^{-1} \tag{78}$$

Utilizing points at .8% total strain the average of tests 70, 86, and 56 was H_1 = 4128.4085 ksi.

Estimates of A_1 and A_2 will be obtained from the following equations:

$$A_1 = A\,\frac{\sigma_{ss}}{B_{ss}} \tag{79}$$

$$A_2 = \left\{ A\left[\, 1 - \frac{\sigma_{ss}}{B_{ss}} \,\right]^{-1} \right\}^3 \tag{80}$$

Values of σ_{ss} and B_{ss} from tests 65, 81, 84, and 88 were used to calculate the following values:

A_1 = .170673 ksi^{-1}

A_2 = .0095544 ksi^{-3}

An estimate of C_2 was obtained from fast saturated cyclic tests with back stress recovery assumed negligible, drag stress saturated, and back stress value known. The following formulation results if such conditions can be met:

$$C_2 = \left(\frac{A_2}{A_1} D^3 - B\right)\left(1 - \left[B'\{ \sinh(A_2 D^3)\}^n\right](\dot{\varepsilon}^I)^{-1}\right)^{-1} \quad (81)$$

$$D = (\sigma - B)\{ \sinh^{-1}\left[\left(\frac{\dot{\varepsilon}^I}{B'}\right)^{1/n}\right\}^{-2/3} \quad (82)$$

The results of tests 65, 81, 84, and 88 are averaged to produce C_2 = $-5.335X10^{-2}$ ksi.

The constant H_2 was estimated from a fast cyclic test assuming no back stress recovery and no drag stress recovery. Back stress is estimated by calculating the cumulative inelastic strain for each of the first three half cycles. The following equation is written for H_2:

$$H_2 = (C_2\varepsilon^I)^{-1}(\sigma - B)\ \{\sinh^{-1}\left[\left(\frac{\dot{\varepsilon}^I}{B'}\right)^{1/n}\right]\ \}^{-2/3} \quad (83)$$

where $\varepsilon^I = |\varepsilon_1^I| + |\varepsilon_2^I| + |\varepsilon_3^I|$

The values ε_1^I, ε_2^I, and ε_3^I are the maximum inelastic strains from the first three half cycles. Tests 56,86, and 65 produced an average value of H_2 = -20189.385.

Computer iterations. Experience with the models of Bodner and Krieg, et al. prompted a change at this point to an upgraded version of this model which accounted for solute strengthening. The inelastic strain rate equation of the Schmidt and Miller model is as follows:

$$\dot{\varepsilon}^I = B'\{ \sinh\left[\left(\frac{\sigma/E - B}{D + F_{sol}}\right)^{1.5}\right]^n \}\ \mathrm{sgn}(\sigma/E - B) \quad (84)$$

$$F_{sol} = F \{ \exp(- [\frac{\log(|\dot{\varepsilon}^I|) - \log(J)}{\beta}]^2) \} \quad (85)$$

The noninteractive solute strengthening parameter was the only one used in this work (interactive solute strengthening modifies the growth of the drag stress). This allowed a more meaningful comparison to the other models since they were all corrected in a similar fashion. The calculation of the material constants was also simplified since only one parameter was utilized. The scale factor of Young's modulus in the inelastic strain rate equation should also be noted.

Table 8 summarizes the computer iterations carried out. Steps 1 through 14 have no order other than the intuitive guesses of the user. These iterations were correcting major deficiencies of the initial calculations. The solute strengthening parameters were set in steps 15 through 19. The basic strain rate sensitivity of the model is still too positive and steps 20 through 30 were increasing n to eliminate this problem. The solute strengthening parameters were being tuned in steps 31 through 36. The work hardening parameters were being set in steps 37 through 50. The constants after initial calculations and after computer iterations are shown in Table 9.

Walker's Exponential Model

The growth laws for Walker's model are repeated below for completeness:

$$\dot{\varepsilon}^I = \frac{\exp(\frac{\sigma - B}{D}) - 1}{C} \quad (86)$$

Table 8 - Computer Iteration Summary of Schmidt and Miller's Model

Step	Const.	Test	Strain(%)	Cycle	Old Value	New Value
1	H2	86	.8	1	-20189	.053353
2	C2	86	.8	1	-.053353	20189
3	DO	86	.8	1	16.264	10.0
4	H1	86	.8	1	4128.41	12000
5	A1	86	.8	1	.17087	.183445
6	A2	86	.8	1	.0095544	.0061674
7	A2	86	.8	10	.0001879	.02
8	C2	86	.8	10	20189	40
9	A1	86	.8	1	.183445	.2714418
10	DO	86	.8	1	0.0	11.0
11	C2	86	.8	1	40	1E-11
12	H2	86	.8	1	.053353	2.5E-1
13	A1	86	.8	1	.2714418	.3
14	A2	86	.8	1	.02	.027
15	F					.001
16	β					5
17	J					1E-6
18	A2	70	.8	1	.027	.023
19	B'	70	.8	1	2.206E-16	1.0E6
20	C2				1.0E-11	0
21	DO					1.0
22	H1					0
23	H2					0
24	n	70	.8	1	1.81	2.5
25	n	71	.8	1	2.5	5.0
26	DO	71	.8	1	1.0	.01
27	n	70	.8	1	5.0	6.0
28	DO	70	.8	1	.01	.001
29	n	71	.8	1	6.0	7.0
30	B'	70	.8	1	1.0E6	1.0E7
31	J	71	.8	1	1.0E-6	7.0E-6
32	F	71	.8	1	.001	.002
33	β	70	.8	1	5	3
34	J	71	.8	1	7.0E-6	1.0E-9
35	F	71	.8	1	.002	.005
36	F	71	.8	1	3.0	4.0
37	H1	70	.8	1	0	1.0E-5
38	C2	86	.8	1	0	-1,000
39	H2	86	.8	1	0	1.0E-7
40	H1	70	.8	1	1.0E-5	.15
41	H1	71	.8	1	.15	.1
42	F	70	.8	1	.005	.007
43	β	70	.8	1	4.0	3.5
44	B'	70	.8	1	1.0E-7	3.0E6
45	H1	70	.8	1	.1	.07
46	B'	71	.8	1	3.0E6	1.5E6
47	C2	86	.8	10	-1,000	-3.0E4

Table 8 Continued

Step	Const.	Test	Strain(%)	Cycle	Old Value	New Value
48	A2	72	.8	1	.023	10,000
49	A1	72	.8	1	.001	1
50	A1	86	.8	1	1	.001

Table 9 - Constants for Schmidt and Miller's Model

Constant	Hand Calculations	Computer Iterations
n	1.813	7.0
A1	.1707	.001
A2	.0096	10.000
B'	2.206E-16	1.5E6
C2	-5.335E-2	-3E4
D0	16.26	.001
H1	4128	.07
H2	-20190	1E-7
F		.007
β		3.5
J		1E-9

$$\dot{B} = n_2\dot{\varepsilon}^I - B\left\{\left[n_3 + n_4\exp\left(-n_5\left|\log\left(\frac{\dot{R}}{\dot{R}_0}\right)\right|\right)\right]\dot{R} + n_6\right\} \tag{87}$$

$$D = D_1 + D_2\exp(-n_7 R) \tag{88}$$

$$\dot{R} = \left|\dot{\varepsilon}^I\right| \tag{89}$$

Initial calculations. The initial step in evaluating Walker's constants was to calculate provisional values of C and D from experimental back stress measuring tests. The inelastic strain rate equation was rewritten in the following form:

$$\sigma - B = D \ln(\dot{\varepsilon}^I) + D \ln(C) \tag{90}$$

A linear fit to the data from tests 84, 88, 81, 65, 63, 61, and 60 produced the following values:

$D' = 4.372$ ksi

$C' = 7.211 \times 10^7$

The constant $\dot{R}_0$ was set at the strain rate at which the strain rate sensitivity switched sign. The value used here was 3.05×10^{-5} sec^{-1}. Chan [90] has proposed a method similar to the gamma plot for analyzing the work hardening characteristics of a back stress type model with dynamic recovery. The growth law for the back stress is first rewritten in a form similar to Bodner's model:

$$\dot{B} = (n_2 - B \cdot N)\, \dot{\varepsilon}^I \tag{91}$$

$$N = n_3 + n_4 f \tag{92}$$

$$f = \exp\left(-n_5 \left| \log\left[\left| \frac{\dot{\varepsilon}^I}{\dot{R}_0} \right| \right] \right| \right) \tag{93}$$

The same assumptions are made as with the gamma plot: only values of σ and ε^I past .2% offset will be used, $\dot{\varepsilon}^I$ is approximately constant and equal to applied strain rate, $\exp(\frac{\sigma - B}{D})$ 1.00 , D is constant during the monotonic portions of a cyclic test, and thermal recovery is negligible. The following equation results:

$$\theta = \frac{d\sigma}{d\varepsilon^I} = -N\,\sigma + [\, n_2 + N\,D\,\ln(\,C\,\dot{\varepsilon}^I)\,] \tag{94}$$

A linear fit to the first ten points produced a line of slope -N and an x intercept of saturated stress. A saturated stress condition would produce the following relationship:

$$B = \frac{n_2}{N} \tag{95}$$

This is also reported in [90]. The following equation was then used to produce the constant n_2:

$$n_2 = N_s[\,\sigma - D'\,\ln(\,\dot{\varepsilon}^I C' + 1\,)\,] \tag{96}$$

The values of N_s and σ are the slope and x intercept, respectively, of the theta plot for a specific test. $\dot{\varepsilon}^I$ is the total strain rate for the test if saturated conditions are assumed. The results of tests 70, 86, 56, and 65 produced an average n_2 of 22,523 ksi. The strain rate sensitivity appeared to be returning to positive after $1.0X10^{-3}$ sec^{-1}. The assumption that $N = n_3$ was made for tests 70, 86, 56, and the above equation produced values of n_3. Averaging the results of these tests gave $n_3 = 324.897$.

The constant n_5 was chosen by setting the f function equal to a small number (.1) for $\dot{\varepsilon}^I = 1.0X10^{-3}$. The following equation resulted:

$$n_5 = \frac{-\ln(\,.1\,)}{\ln[\,|\,\dot{\varepsilon}^I(\,\dot{R}_0)^{-1}\,|\,]} = .6566 \tag{97}$$

This equation was incorrect since the ln function in the denominator was supposed to be a log function.

The theta plot for test 80 was analyzed assuming $N = n_3 + n_4$. This produced the following value for n_4:

$$n_4 = -116.67$$

N is rewritten in the following form if recovery is present:

$$N = n_3 + n_4 f + \frac{n_6}{\dot{\varepsilon}^I} \tag{98}$$

The following equation then results for n_6:

$$n_6 = \dot{\varepsilon}^I \{ \frac{n_2}{B} - [n_3 + n_4 \exp(-n_5 | \log(\frac{\dot{\varepsilon}^I}{\dot{R}_0}) |)] \} \tag{99}$$

where $B = \sigma - D' \ln(\dot{\varepsilon}^I C' + 1)$

The x intercept of the theta plots for tests 71 and 72 produced an average value of $n_6 = -5.081X10-4$.

The next step was to calculate a new value for C to replace the provisional value. New values for $B_{lim} = n_2/N$ (where $N = n_3 + n_4 f + n_6/ \dot{\varepsilon}^I$) were calculated. Theta plots for the third half cycle then produced values of σ_{lim} for the following equation:

$$\sigma - B = D \ln(\dot{\varepsilon}^I) + D \ln(C) \tag{100}$$

Tests 86, 56, 65, 83, 80, and 72 produced a linear fit with C =

$1.132X10^8$ sec value produced.

The next step was to calculate the drag stress growth law constants. Theta plots from the positive half cycles 3, 5, and 7 produced values of σ_{lim} for tests 86, 56, 65, 83, 80, and 72. Values of $B_{lim} = n_2/N$ were calculated for each test. Equation (100) and the saturated values just calculated were used to calculate a value for D at each half cycle. The cumulative inelastic strain was estimated for each half cycle based on the stress values at .8% total strain. The following formula was used for this purpose:

$$R_j = \sum_{i=1}^{j} | \varepsilon_i^I | \; ; \; j = 3, 5, 7 \qquad (101)$$

where σ_i is the stress value at $\pm$.8% strain for each cycle. Three equations in three unknowns could then be written in the following form:

$$D_j = D_1 + D_2 \exp(-n_7 R_j) \; ; \; j = 3, 5, 7 \qquad (102)$$

where D_j and R_j were calculated above and D_2, D_1, and n_7 were the constants to be determined. These equations were solved iteratively to produce the following values:

$D_1 = 2.794$ ksi

$D_2 = 8.150$ ksi

$n_7 = 1.688$

Computer iterations. Table 10 summarizes steps used to finalize the constants for Walker's model. The immediate realization with

Table 10 - Computer Iteration Summary of Walker's Exponential Model

Step	Const.	Test	Strain(%)	Cycle	Old Value	New Value
1	D2					0
2	n4					0
3	n2					0
4	n3					0
5	D1					11.0
6	β	70	.8	1	1.13E8	1.0E6
7	n2					22523.623
8	n3	70	.8	1	0	1,000
9	n2	70	.8	1	22,523	41,000
10	n3	71	.8	1	1,000	325
11	n3	80	.8	1	325	95
12	n3					1,000
13	n4	70	.8	1	0	-900
14	n5	70	.8	1	.6566	1.7
15	n2					0
16	n4					0
17	n3					0
18	D1					1.0
19	C	70	.8	1	1.0E6	1.0E40
20	n2	71	.8	1	0	1,000
21	n2	70	.8	1	1,000	31,000
22	n3	70	.8	1	0	700
23	n3	80	.8	1	700	450
24	n3	71	.8	1	450	700
25	n3	86	.8	1	700	750
26	n5					.66
27	n4	70	.8	1	0	-300
28	n5	86	.8	1	.66	2.5
29	n3	70	.8	1	750	775
30	n4	80	.8	1	-300	-350
31	n5	71	.8	1	2.5	1.7
32	n4	71	.8	1	-350	-250
33	n3	71	.8	1	775	700
34	n5	70	.8	1	1.7	.66
35	n3	70	.8	1	700	750
36	n2	71	1.26	1	31,000	35,000
37	n2	70	1.28	1	35,000	33,000
38	n6	71	1.28	1	0	2.5E-4
39	P1					.2
40	D2					-.8
41	n7	86	.8	10	0.0	3.5
42	D1	86	.8	10	.2	.7
43	D2	86	.8	10	-.8	-.3
44	n7	86	.8	10	3.5	18.0

Walker's model was that the negative strain rate sensitivity correction was not strong enough. This could have been a result of the error mentioned previously in calculating n_5. Steps 1 through 14 recalculated the work hardening parameters to correct for negative strain rate sensitivity. These changes still did not correct the problem and steps 15 through 35 changed the basic strain rate sensitivity of the model and recalculated the work hardening parameters. The high strain work hardening characteristics were set in steps 36 through 37. Thermal recovery was set in step 38. The cyclic response was tuned in steps 39 through 44. Table 11 presents the constants before and after the computer iterations.

Table 11 - Constants for Walker's Exponential Model

Constant	Hand Calculations	Computer Iterations
C	1.132E8	1.000E40
D1	2.794	.7
D2	-8.150	-.3
n2	22,520	33,000
n3	324.9	750.0
n4	-116.7	-250.0
n5	.6567	.6600
n6	-5.081E-4	2.5E-4
n7	1.688	18.00
R0	3.050E-5	3.050E-5

MODEL RESULTS

This chapter will be divided into two sections. The first section will discuss the capabilities of the models to reproduce input data. The second section will cover the predictive abilities of the models. The forms of the models to be covered include Bodner's model without a correction for solute strengthening, Bodner's model with a solute strengthening correction, the model of Krieg, et al. with and without a correction for solute strengthening, Schmidt and Miller's model, and Walker's exponential model. The models were numerically integrated with an Euler forward integration scheme on a Perkin-Elmer 32/10 computer. The time steps used ranged from $5.0X10^{-4}$ sec for test 70 to $5.0X10^{-2}$ sec for test 71.

Reproduction of Test Data

Figure 13 shows the response of the models as compared to test 70 ($\dot{\varepsilon} = 3.151X10^{-3}$ sec^{-1}). The models are all oversquare except for Walker's. Walker's model is showing adverse effects from its dynamic recovery term as the stress is decreasing at higher strain levels. This is more of a problem with the method of constant calculation than the model itself. The iterative portion of the constant calculation process was performed with access to only two points on this curve. Using three points or interactive graphics would have solved this problem.

Figure 14 compares the model outputs to test 71 ($\dot{\varepsilon} = 7.253X10^{-6}$ sec^{-1}). Walker's model is still following the shape of the curve best. The dynamic recovery problem still exists with the Walker

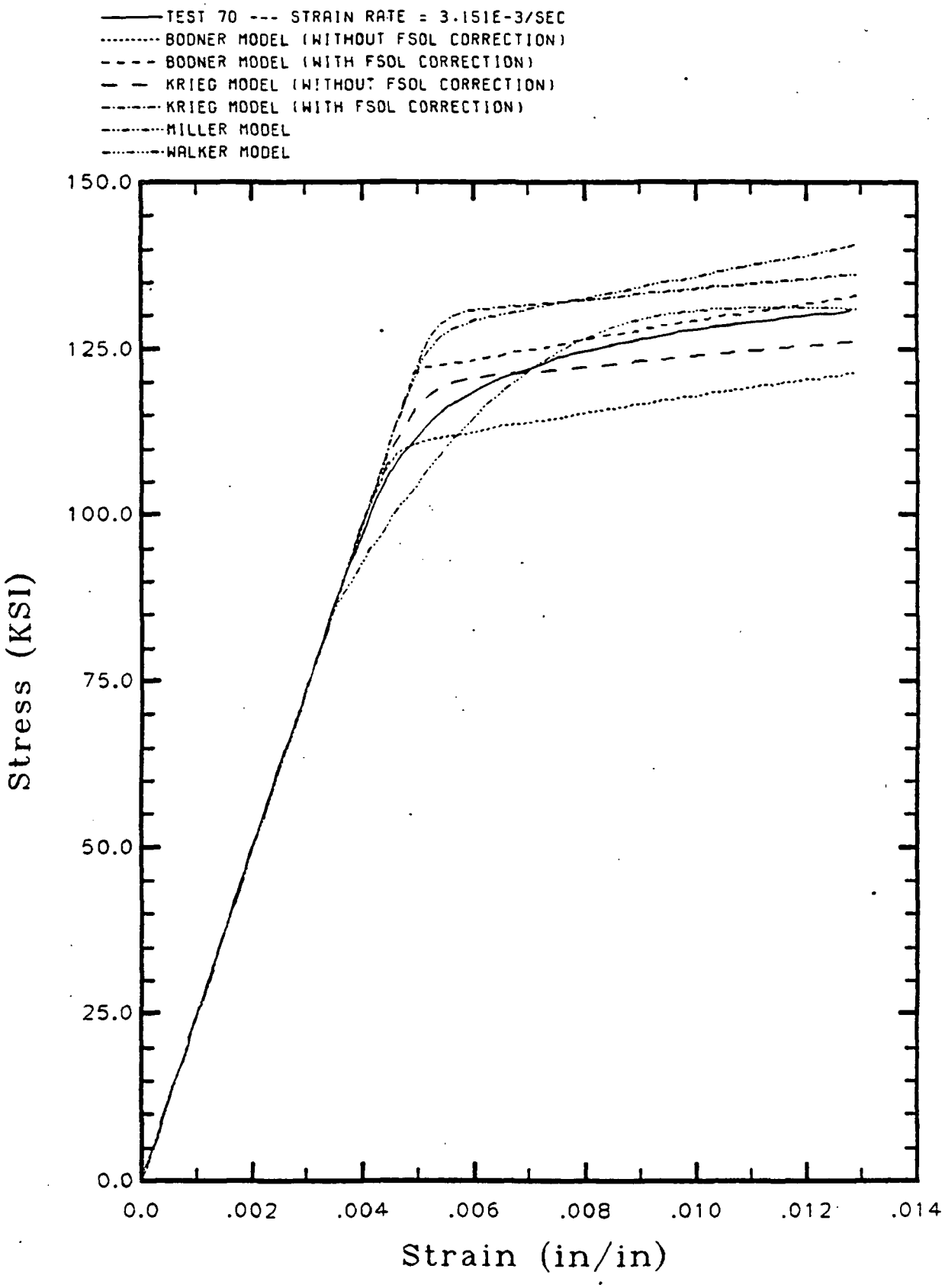

Figure 13 - Model Response as Compared to Test 70

C-2

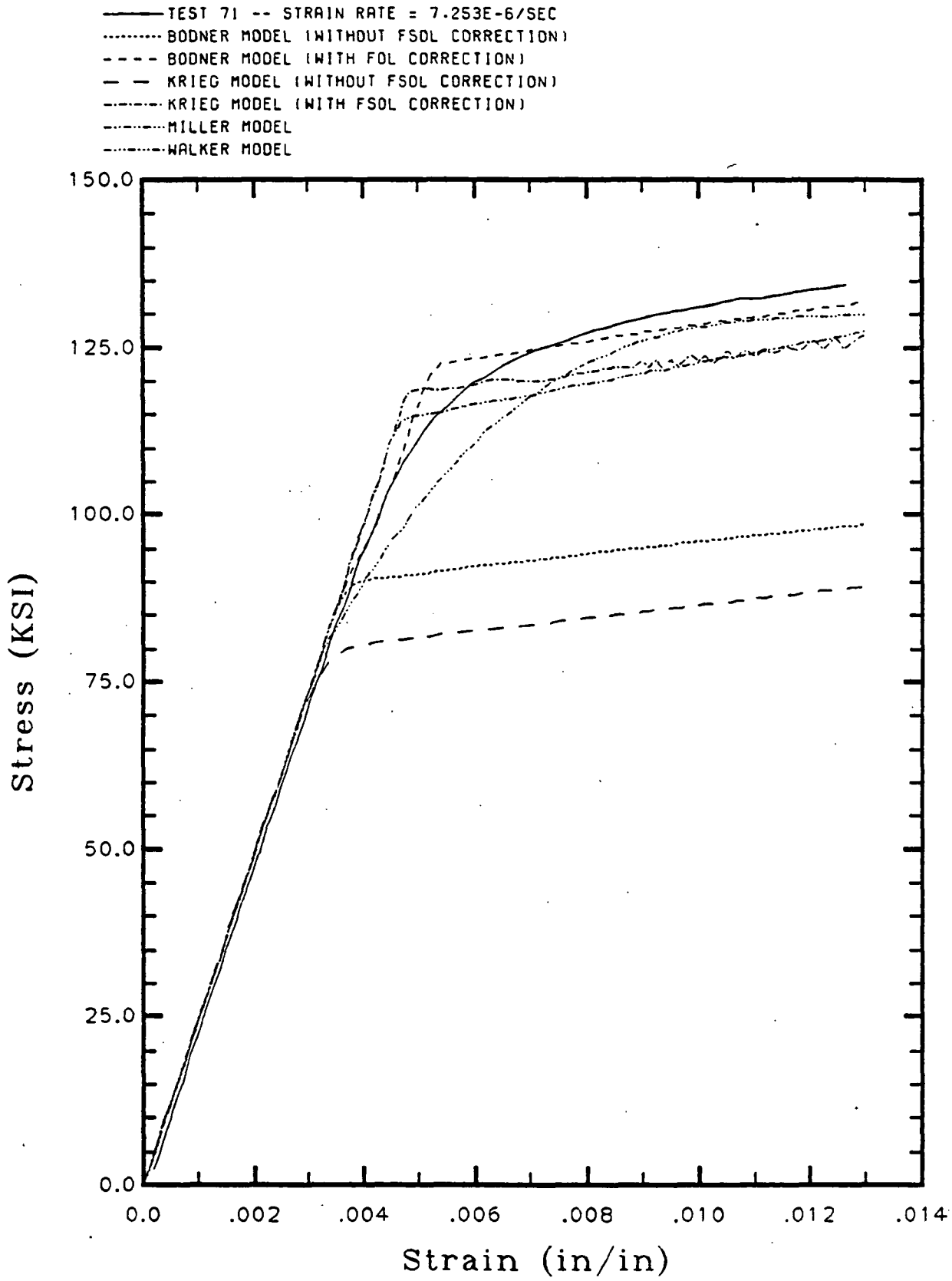

Figure 14 - Model Response as Compared to Test 71

model. The Krieg, et al. model is showing some numerical instability due to the presence of the solute strengthening parameters. The uncorrected versions of Bodner and Krieg, et al. are much lower than the other models. The F_{sol} parameter was simply set to zero in these versions. The other constants remained the same as in the corrected versions. Therefore, the reponse of the uncorrected versions could have been averaged over the strain range better. However, the basic strain rate sensitivity would have remained the same.

Figure 15 interpolates the model response and experimental response between these two strain rates presented above by picking off stress values at .8% total strain for tests of intermediate strain rates and plotting these values versus the log of the applied strain rate. The tests used in Figures 13 and 14 are shown on this figure also. Individual plots of the intermediate strain rate tests are provided in Appendix C. Walker's model is exhibiting negative strain rate sensitivity and the corrected Bodner model is showing no strain rate sensitivity. The other models clearly produce positive strain rate sensitivity. Figure 16 shows these results with greater clarity. Presented in this Figure are the stress values at -.8% for the first compressive cycle.

Figure 17 shows the stress values at +.8% strain for the saturated cycle response. The slowest strain rate provides data from the fourth cycle and the other points are from the 10th cycle. The trend has changed and all the models with correction for solute strengthening are exhibiting negative strain rate sensitivity. This is probably an effect

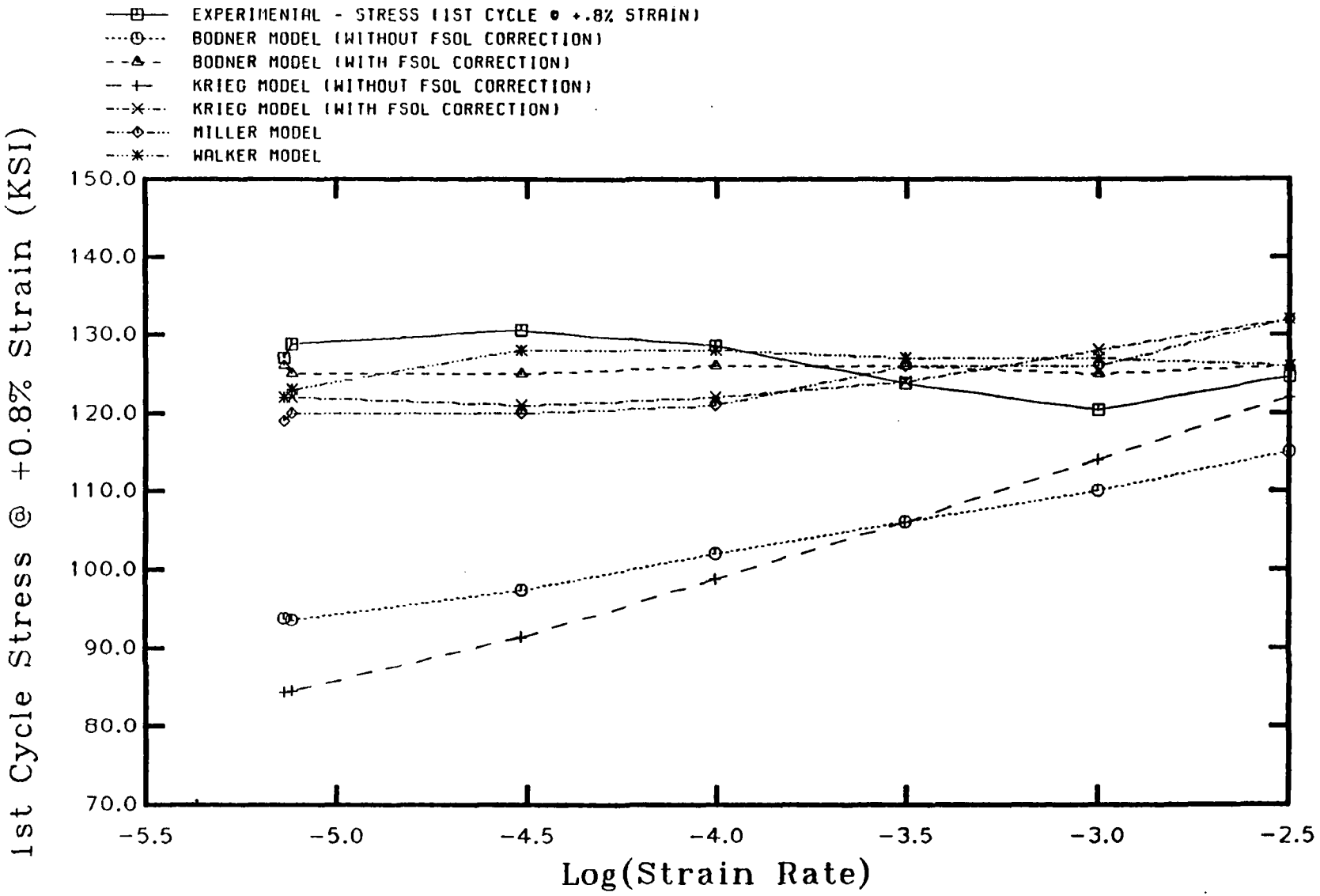

Figure 15 - Stress-Strain Response at +.8% for Cycle 1

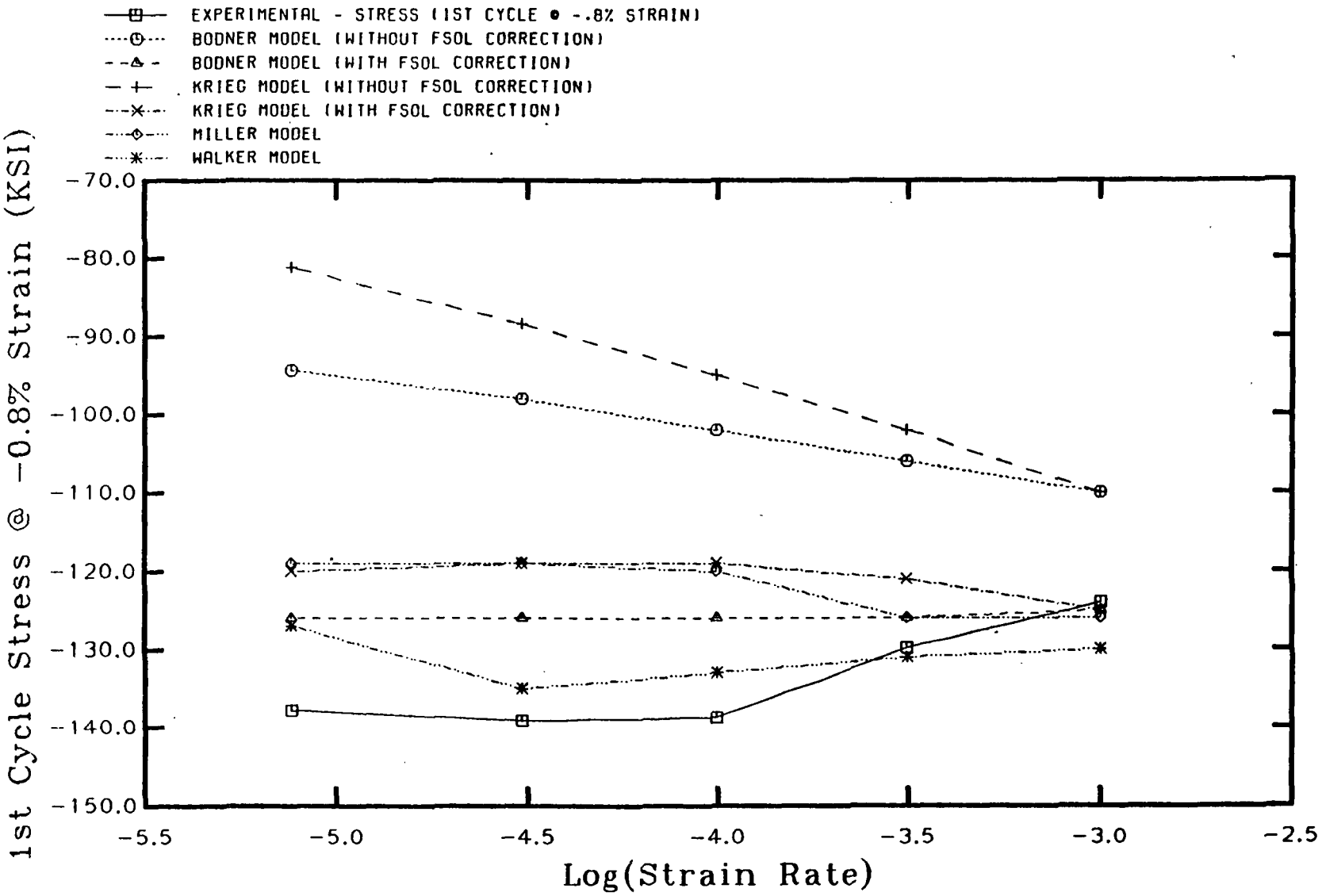

Figure 16 - Stress-Strain Response at -.8% for Cycle 1

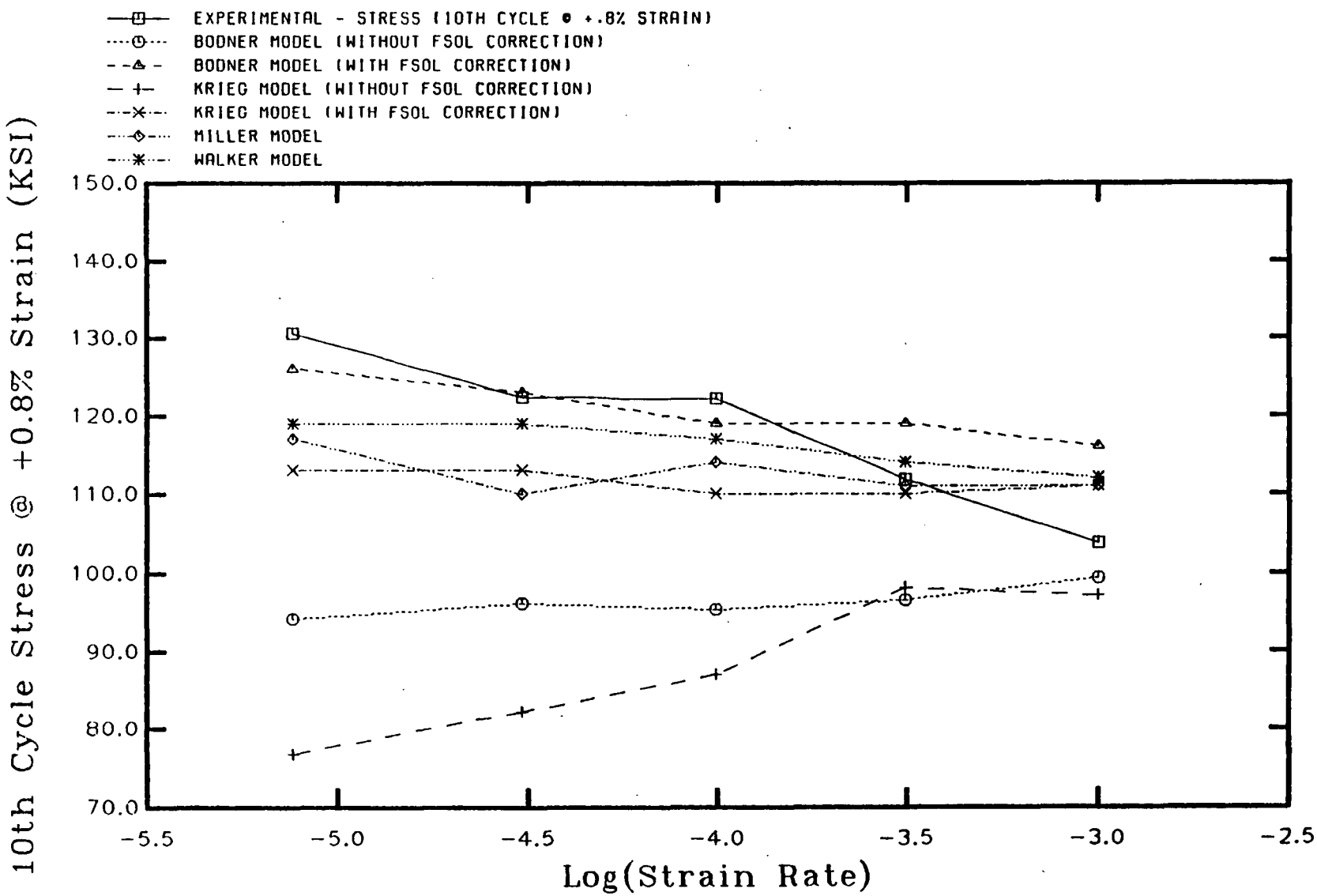

Figure 17 - Stress-Strain Response at +.8% Saturated Cycle

of the drag stress thermal recovery parameters and the cyclic work softening response.

Figure 18 provides the complete 10th cycle hysteresis loops for test 86 ($\dot{\varepsilon} = 1.002X10^{-3}$ sec^{-1}) as compared to the model output. Bodner's model is seen to show some numerical instability due to interaction with the solute strengthening parameter. Figure 19 allows interpolation between the first cycle and the 10th cycle by presenting the values at +.8% strain for each cycle. The corrected Krieg, et al. model and the uncorrected Bodner model reproduce this data closest.

Figure 20 provides the same data for test 80 ($\dot{\varepsilon} = 9.926X10^{-5}$ sec^{-1}). This strain rate shows Walker's model following the experiment the closest. The peak value at the second cycle is reproduced with this model only. Figure 21 presents the cyclic data for test 72 ($\dot{\varepsilon} = 7.626X10^{-6}$ sec^{-1}). The corrected Bodner model is following the data closest. The Walker model is clearly suffering from the lack of a drag stress thermal recovery term. Appendix C contains the cyclic data for the remaining tests as well as the compressive cyclic data.

Figure 22 shows experimental values of back stress compared to the values of back stress compared to the values at the tenth cycle of tests 86 and 65 and the first cycle of test 70 for the models of Walker, Schmidt and Miller, corrected Krieg, et al., and uncorrected Krieg, et al. This figure points to the fact that the constants produced to fit the models' of Krieg, et al. and Schmidt and Miller to the input data do not produce physically realizable results. This can probably be traced to the abnormally high values of the inelastic strain rate equation

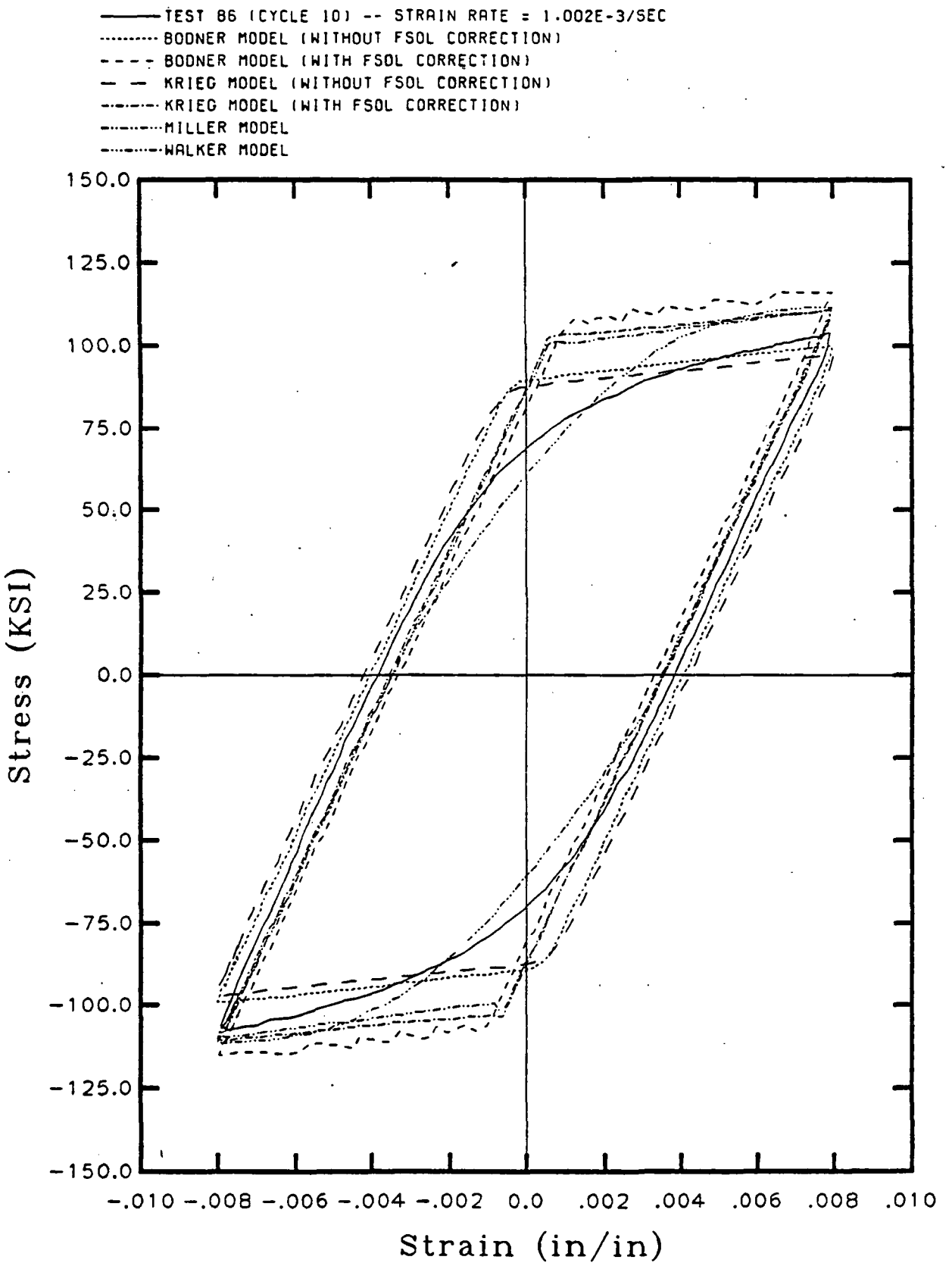

Figure 18 - 10th Cycle Hysteresis Loops Test 86

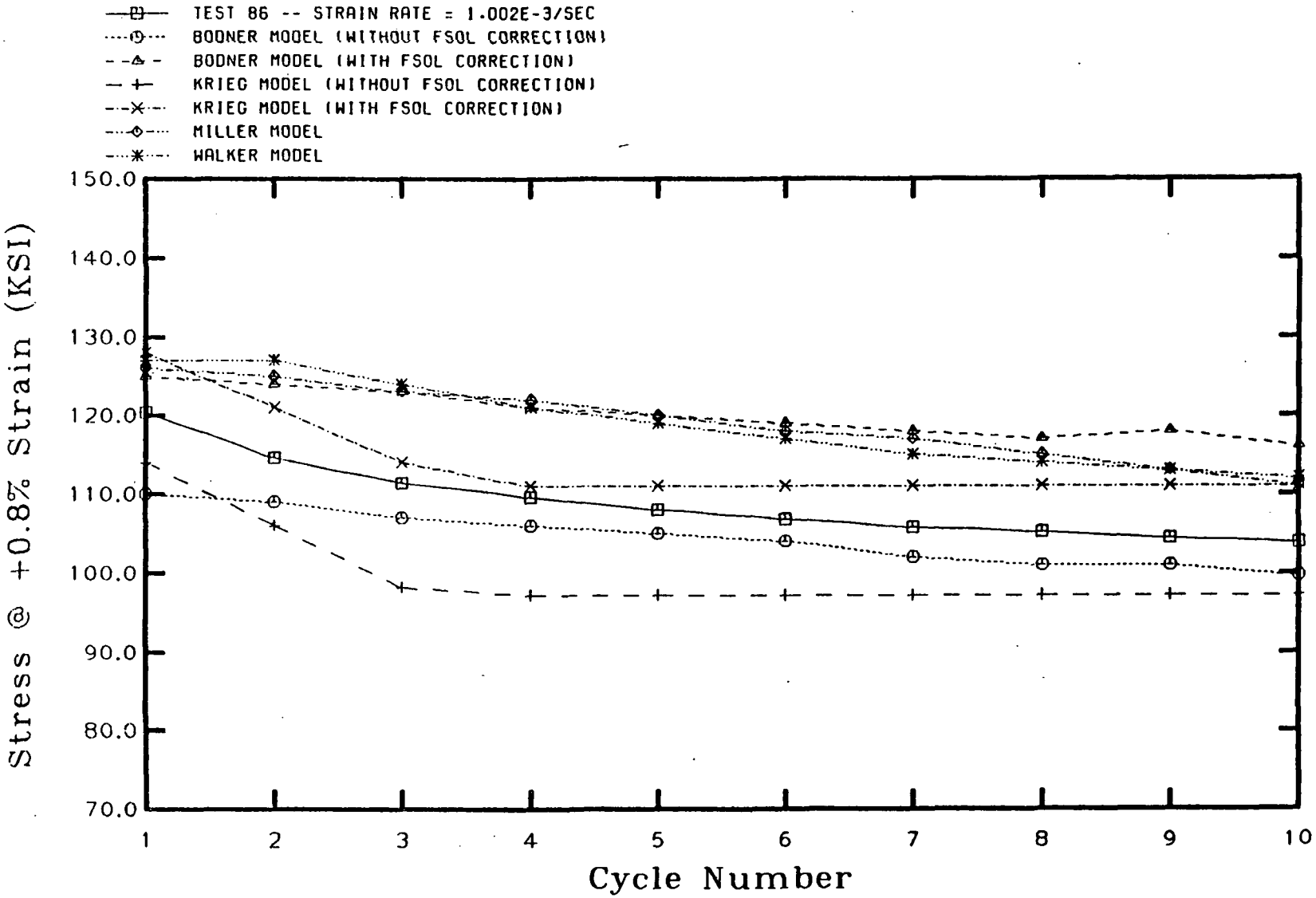

Figure 19 - Test 86 +.8% Response at Each Cycle

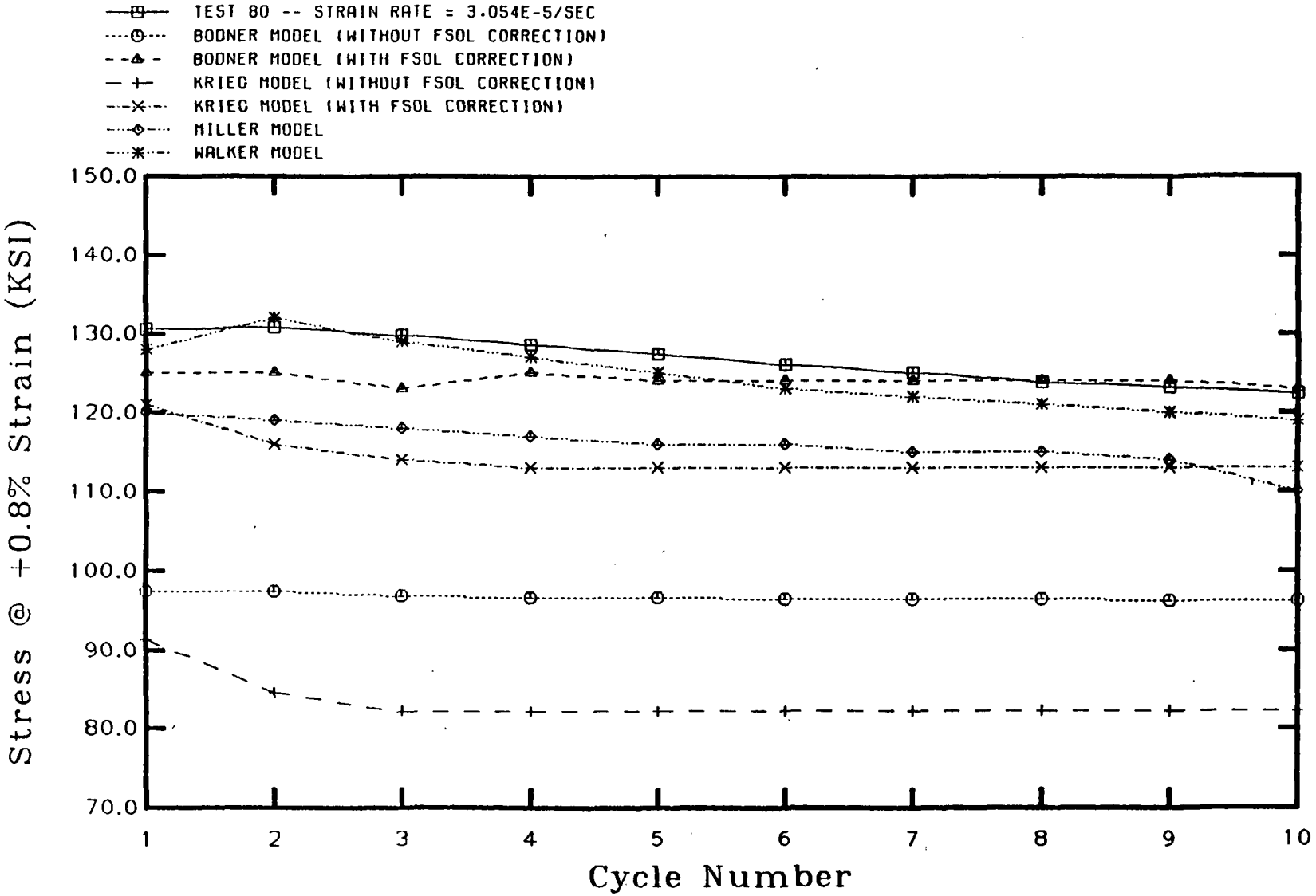

Figure 20 - Test 80 +.8% Response at Each Cycle

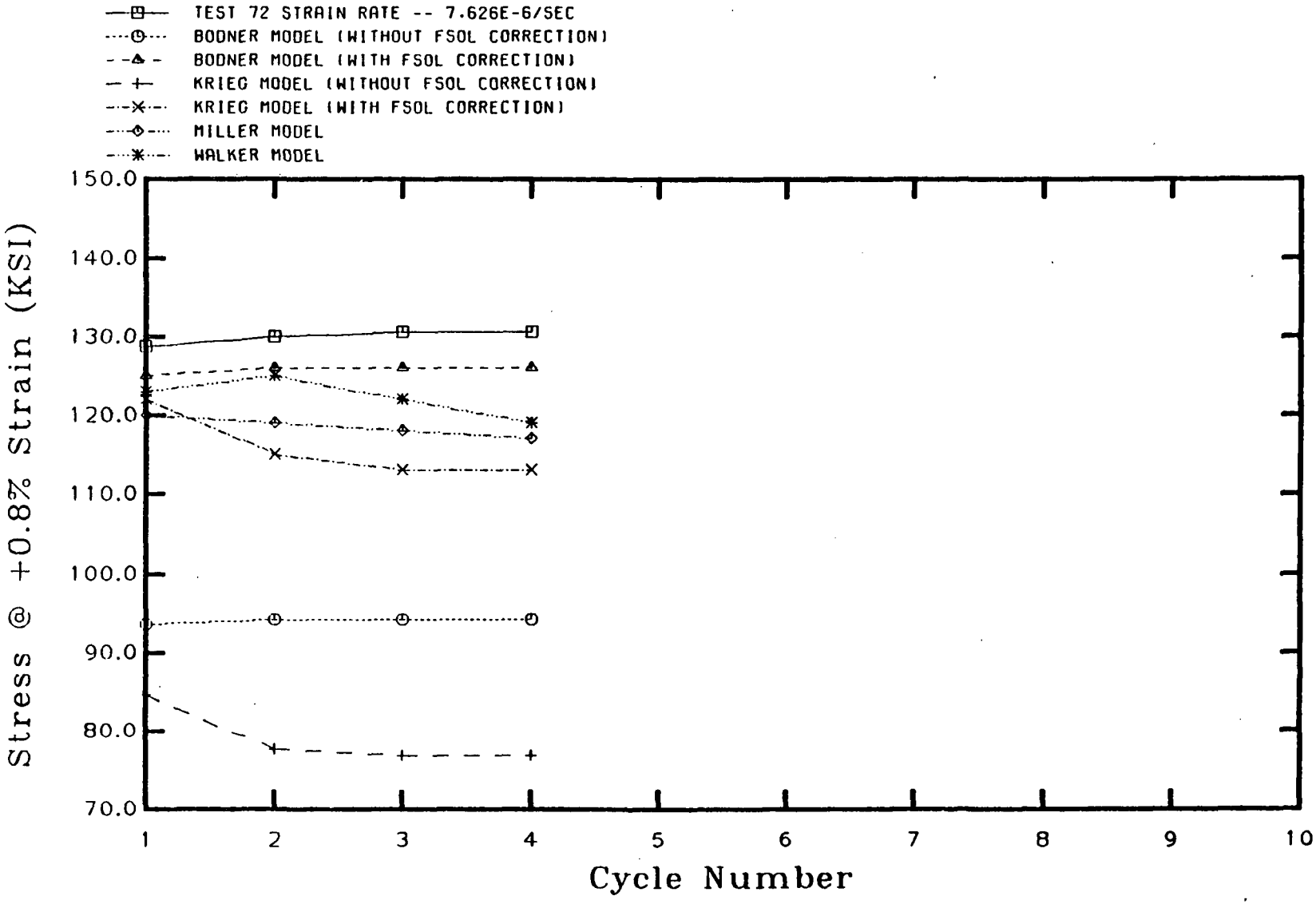

Figure 21 - Test 72 +.8% Response at Each Cycle

"Page missing from available version"

exponent needed to match the strain ageing effects. This may also create the oversquareness of these models.

Predictive Capabilities

The predictive capabilities of the models were explored by the use a complex history test. This experimental test was not used in the calculation of the material constants. Table 12 gives the input history of this test. Figures 23 through 28 show the comparison of the models to this complex history test. The corrected Bodner model in Figure 24 is the least affected by strain rate jumps. Bodner attributes this to the use of plastic work as the measure of work hardening [67]. The interaction of the solute strengthening corrections of all the models may be having an effect on this aspect of all the models. The uncorrected versions in Figures 23 and 25 are very suseptible to these jumps. Yao and Krempl report that the overshoots and undershoots observed during the strain rate jumps are a transient effect of the behavior of a system of coupled nonlinear differential equations [160].

Table 12 - Complex History Test Input

Interval	Beginning Strain	Ending Strain	Strain Rate
1	0.0	.004	9.991E-5
2	.004	.006	4.784E-4
3	.006	.008	9.762E-4
4	.008	0	-5.0E-3
5	0	0	0.0
6	0	-.004	-9.878E-4
7	-.004	-.009	-9.795E-5
8	-.009	.006	9.933E-4
9	.006	008	9.532E-6
10	.008	.01	5.0E-3
11	.01	.01	0
12	.01	.015	4.95E-4
13	.015	0	-1.4925E-3

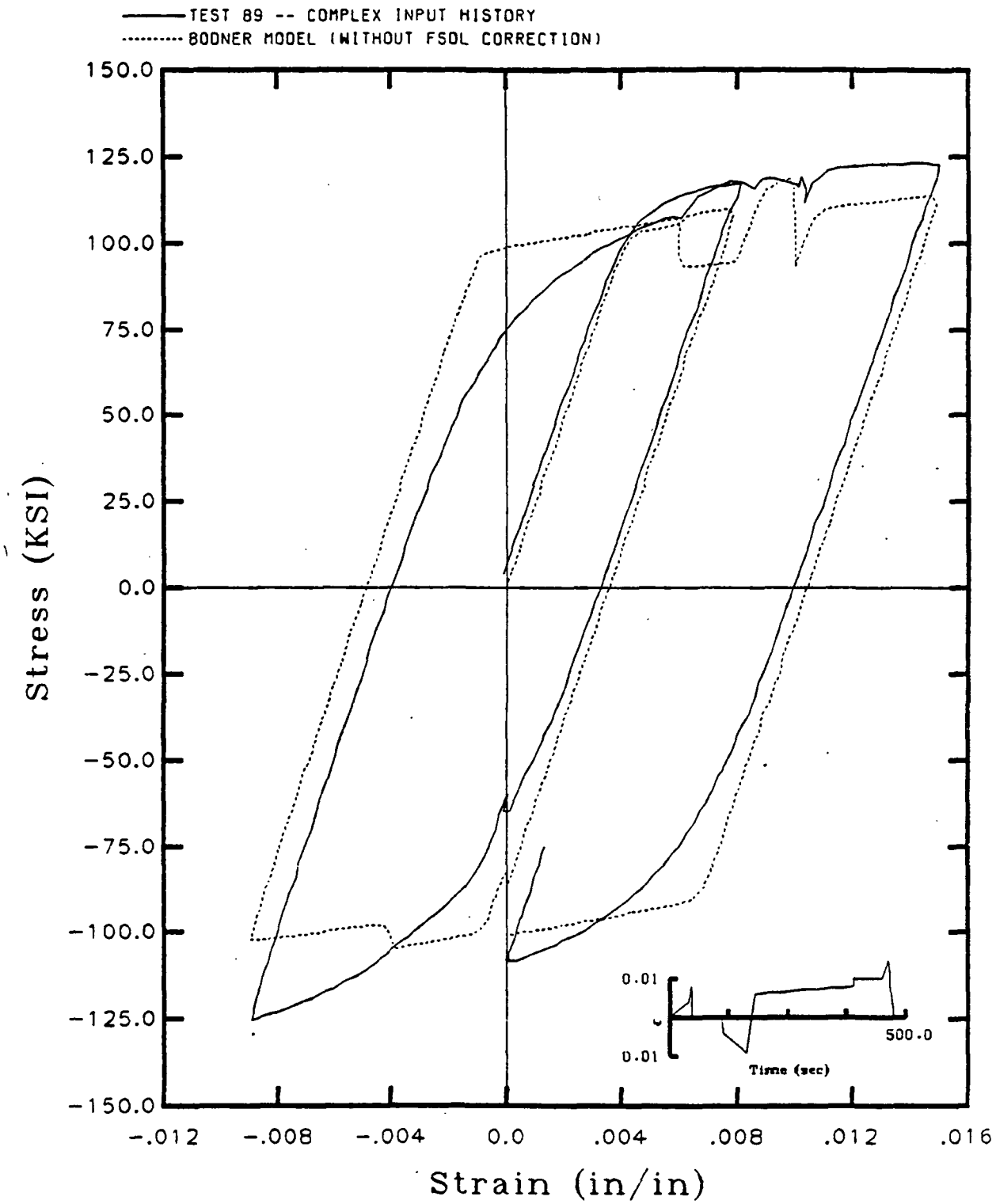

Figure 23 - Complex History - Bodner's Uncorrected Model

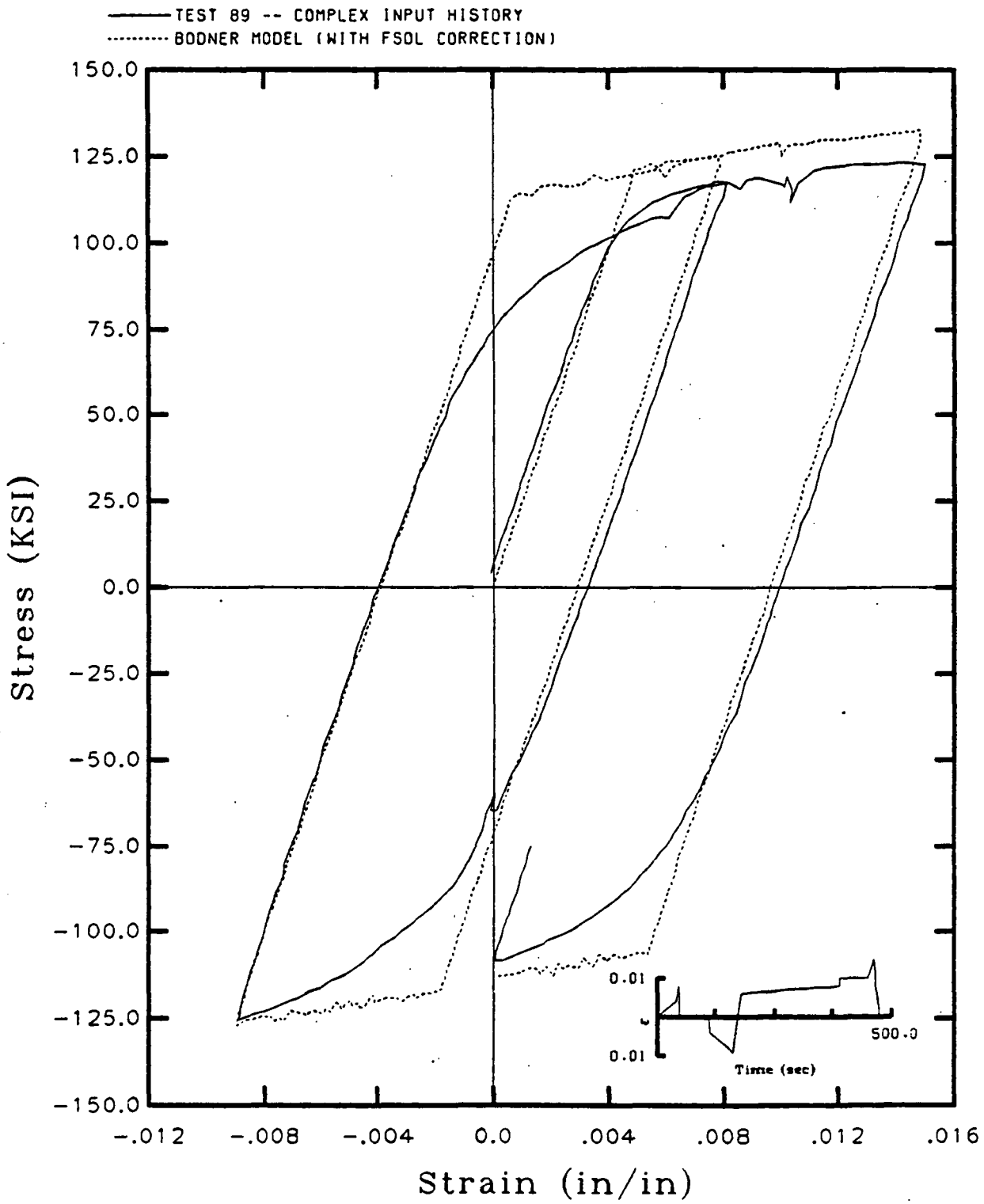

Figure 24 - Complex History - Bodner's Corrected Model

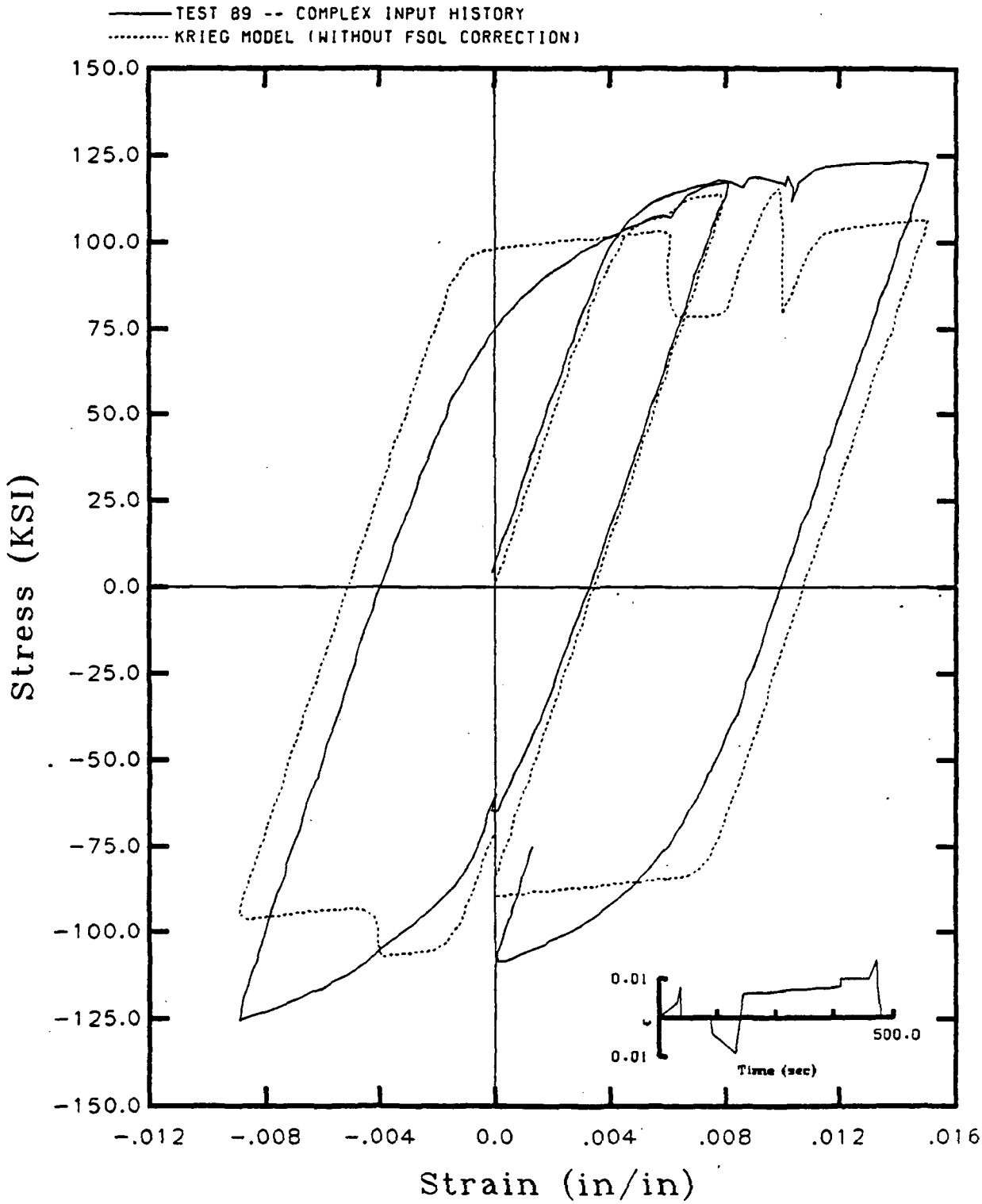

Figure 25 - Complex History - Uncorrected Model of Krieg, et al.

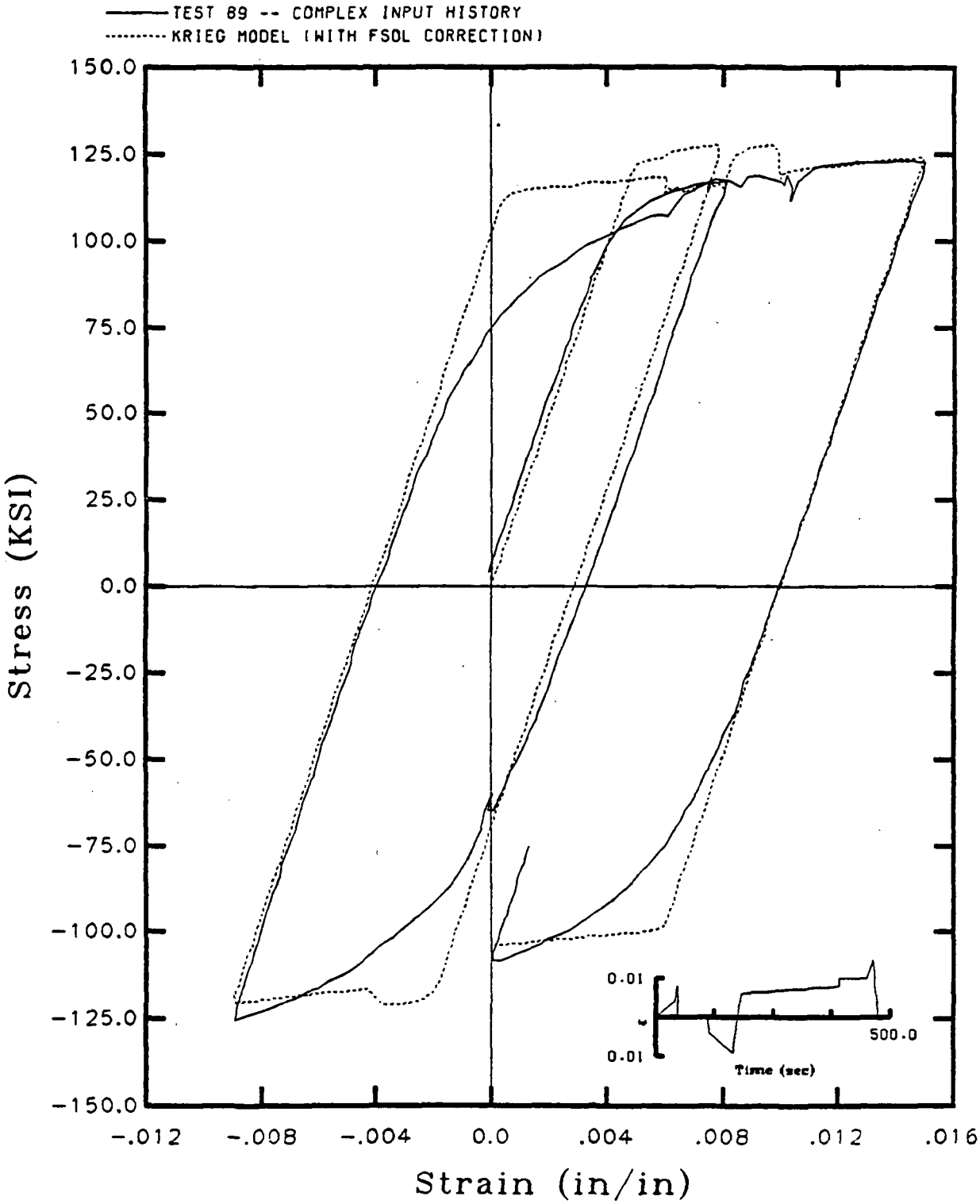

Figure 26 - Corrected Model of Kreig, et al. - Complex History

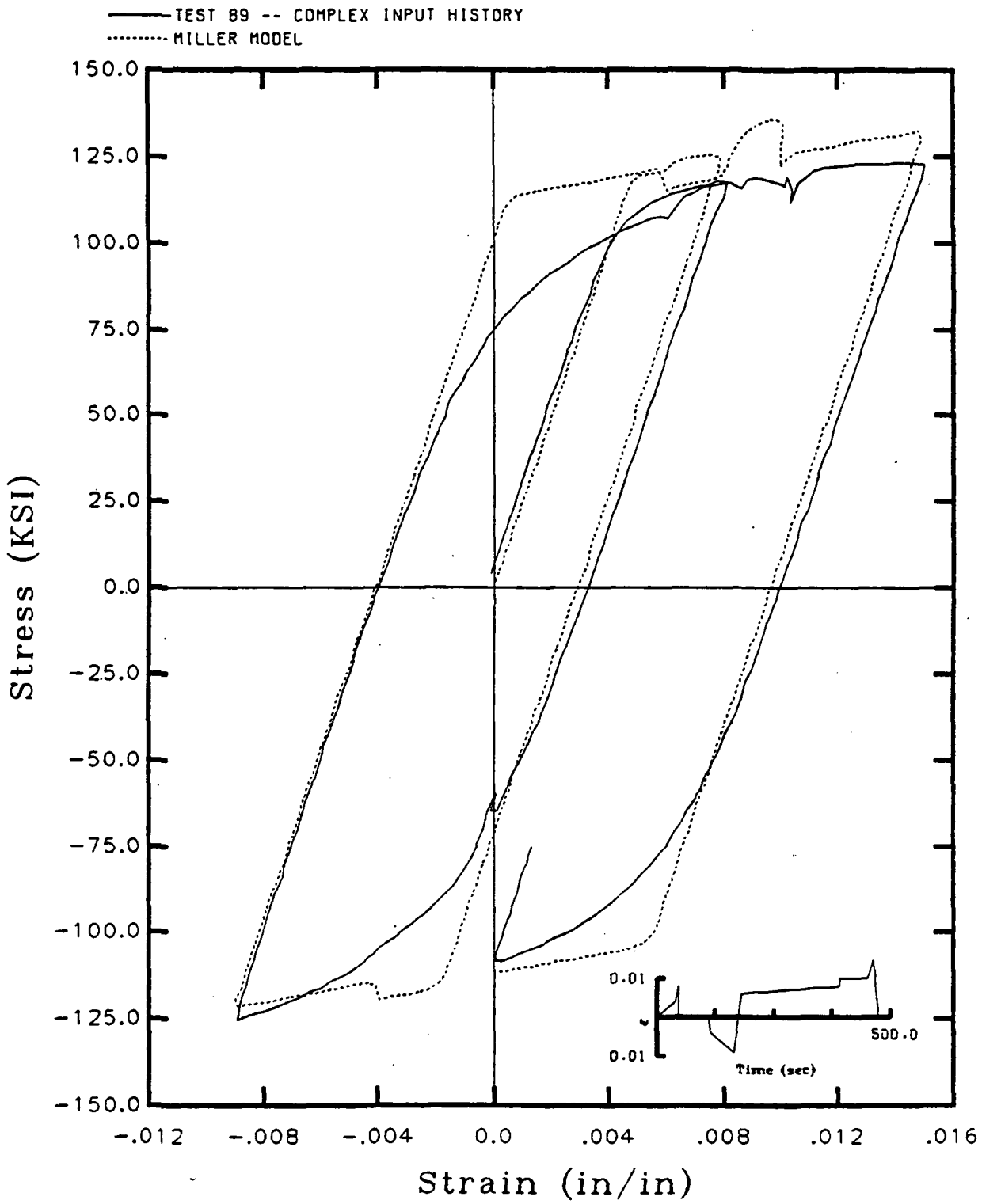

Figure 27 - Complex History - Schmidt and Miller's Model

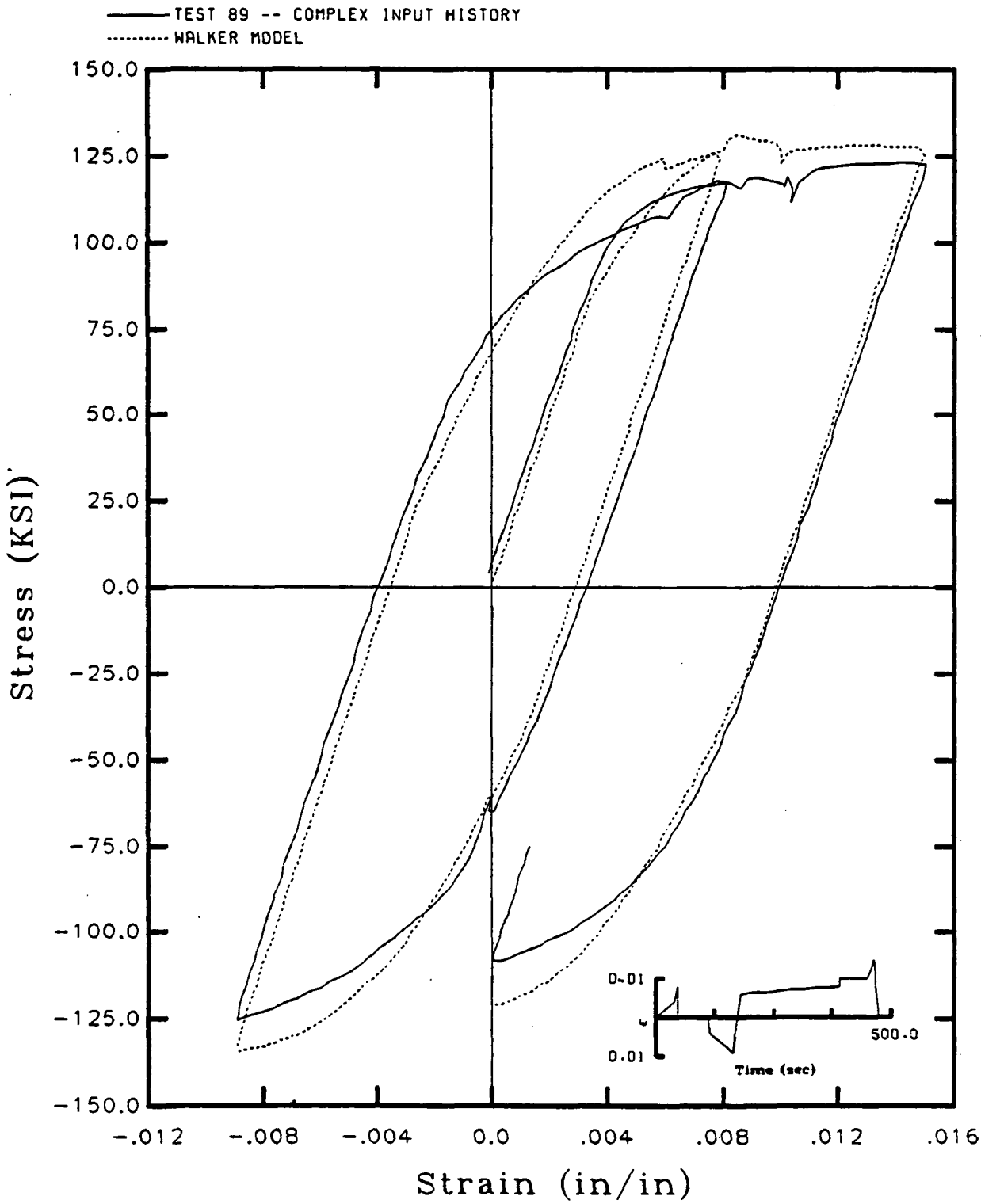

Figure 28 - Complex History - Walker's Model

A comparison of the response of the corrected and uncorrected versions of the Bodner and Krieg, et al. models at the zero strain hold time shows that the F_{sol} correction negates the effects of thermal recovery in such instances. This could be a result of the low value of J or the inelastic strain rate of maximum correction used in these models. The corrected Bodner model had J = $1.0X10^{-6}$ sec^{-1}, the model of Krieg, et al had J = $7.0X10^{-6}$ sec^{-1}, and Schmidt and Miller had J = $1.0X10^{-9}sec^{-1}$. Schmidt and Miller's model showed no thermal recovery at this hold either. The small inelastic strain rates produced by thermal recovery terms would meet increasing hardness if their magnitude was below J. Increasing hardness would tend to drive the stresses up and oppose the action of the thermal recovery terms.

The Walker model follows the shape of the stress strain curve better than the other models. This could be a result of the better modelling of the back stress growth and the lack of an inelastic strain rate exponent. The model of Krieg, et al. had n = 15.0 and Schmidt and Miller had n = 7.0. The constant values of work hardening have also been reported as reasons for this [41,96]. Bodner's model may be suffering from the lack of a back stress or the effects of the plastic work measure of strain hardening. Further study would be required to show this however. The corrected model of Krieg, et al. reproduces the actual stress levels best after initial yield. No explaination can be given for this at this time.

CONCLUSIONS AND RECOMMENDATIONS

This chapter will be divided into three sections. The first section will cover the conclusions and recommendations of this thesis pertaining to the models themselves. The second section will cover the methods of calculating the material constants. The final section will cover the experimental portion of this work. Conclusions reached and recommendations for further study will be presented simultaneously as these topics are very closely related in many cases.

Conclusions and Recommendations based on the Models

The theories of Walker and Bodner with exponentially based inelastic strain rate equations and dynamic recovery terms handle the strain rate sensitivity the best. Bodner's model shows less sensitivity to strain rate jumps possibly due to the plastic work rate measure of strain hardening. The reproduction of the general shape using Walker's model may be aided by better modelling of the back stress term and by the exponentially based inelastic strain rate equation. The drag stress growth law of the Walker model provided the closest fit to data over several cycles at higher strain rates. The second cycle peak seen at the lower strain rates was modelled only by Walker. Bodner's model handled cyclic response best over several cycles at the lower strain rates due to the thermal recovery term. The solute strengthening correction caused numerical instability, negating the effect of thermal recovery during hold times and may have lessened the sensitivity to strain rate jumps.

Future study of these models could take two directions. First a comparison to a material which does not exhibit strain aging effects would be beneficial. The corrections necessary to account for this phenomenon masked some of the information which could have been obtained in this work. An example of this is information about the effect of strain jumps on the predictive capabilities of the models. The thermal recovery capabilities of the models were also adversely affected by the strain ageing corrections. The methods for calculating constants should be checked with a positve strain rate sensitive material.

Second, further study which concentrates on the specific model form should be carried out by the use of extended models. These would be models extended from the existing ones. An example of this would be to replace the inelastic strain measure of work hardening in the model of Krieg, et al. with a measure based on plastic work. The inelastic work measure in Bodner's model could be replaced with an inelastic strain measure. The extended models could then provide true insight into the ramifications of using a measure of plastic work. The effect of using an inelastic strain rate equation based on exponential, power law, and hyperbolic sine functions could be studied. The advantages and disadvantages of providing a model with a back stress term could be studied by providing the Bodner model with one as Moreno and Jordan have done [74].

Conclusions and Recommendations based on the Calculation of Constants

The initial assumptions of back stress being responsible for hardening in monotonic tension and drag stress being responsible for

cyclic hardening/softening appears to be a good assumption for this material system. These assumptions were used for every model in the hand calculations and the computer iterations with success. Krempl, McMahon, and Yao report that a changing drag stress parameter alters the strain rate sensitivity of the model [108]. This effect was not considered in this work and might warrant further study. The initial assumptions of thermal recovery being negligible for rapid tests ($\dot{\varepsilon} > 1.0X10^{-14}$ sec^{-1}), drag stress recovery being dominate in low strain rate cyclic tests, and back stress recovery being dominate in creep tests appear difficult to apply in the presence of solute strengthening effects. This material system requires that a correction for solute strengthening be employed before recovery effects can be calculated. The recovery effects were much smaller than the original hand calculations for the models of Krieg, et al., Bodner, and Walker produced. This observation leads to the conclusion that the recovery effects are largely insignificant for $\dot{\varepsilon} > 1.0X10^{-5}$ sec^{-1}. Miller's model requires the recovery terms to be much more active than the other models. This inflexibility gave some problems in the calculation of Miller's constants.

The solute strengthening effects also masked the true strain rate sensitivity of the material. Information on the strain rate sensitivity needs to be obtained outside the region of solute strengthening effects. The following initial assumptions would have been more appropriate based on these observations:

(1) back stress was assumed responsible for hardening in

monotonic tension;

(2) drag stress was assumed responsible for cyclic softening;

(3) thermal recovery effects were small and masked by solute strengthening effects;

(4) solute strengthening or strain aging effects masked the basic positive strain rate sensitivity of the material.

The model of Krieg et, al. was an easy model to work with since each term in the growth laws could be scaled somewhat seperately of the others. An interesting observation of this model was that the constants of the inelastic strain rate equation could be swept over a broad range but the monotonic hardening stayed relatively constant. There was also a mathematical ambiguity between the constant C and the scaling of the drag stress. The scaling could be transferred from one parameter to the other without any visible change in model response.

Bodner's model "converged" to the final constants with fewer iterations than the other models using the iterative scheme developed in this work. This was probably due to the lack of a back stress parameter. A mathematical ambiguity existed between n and the scaling of the internal state variables when information was not available to calculate n. This is why a value for n can often be picked and still produce a workable model.

Miller's model was highly coupled in that the recovery terms were not were not separated from the hardening terms. The recovery terms can therefore change on the same order of magnitude as the hardening terms. Miller readily admits that this model is designed for materials

which have a very active drag stress parameter [42]. He states that this model may not be applicable for this type of material system. However, a reevaluation of the constants for Miller's model might prove fruitful. A majority of the constants should be calculated outside the region of solute strengthening effects and without artificially seperating the hardening and recovery terms. A solute strengthening parameter would then be added to fit the response to the negative strain rate sensitive region.

Miller's model also maintains control over the saturated states of the internal state variables B and D with the A_1 and A_2 constants. A correction for strain ageing as well as cyclic work softening might be possible by controlling these saturated states. A recommendation for further study based on this model would contain an expanded study of back stress magnitudes over the entire strain rate region considered. A possible method for this will be disscussed in the next section. Suggestions can also be found in Appendix B. The latest form of Miller's model [100] should also be studied as it may be used with material systems similar to this.

Walker's model holds promise for automating the calculation procedure for this type of material. Walker's model has fewer constants, appears to be tailored for this type of material, and can utilize the theta plot concept [90]. The drag stress scaling performs the same strain rate sensivity functions as the n in the power law related models. Expanding knowledge of the back stress values would also be useful for this model.

Conclusions and Recommendations Based on the Experimental Work

The back stress measuring tests both in creep and in cyclic loading were very subjective and uncertain. However, their extreme usefulness and relative success in application with an automated test set-up warrant further study. It appears possible that these tests can be developed into useful inputs to the constant calculation process. More sensitive data acquisition devises with greater resolution and a smaller less massive load frame for more precise control would greatly enhance the usefulness of these tests. The subjectivity could be lessened by using a method such as proposed by Blum and Finkel [150] to analyze the data.

The back stress measuring tests during creep were useful for strain rates less than $1.0X10^{-7}$ sec^{-1}. The cyclic back stress measuring tests were useful for strain rates greater than $1.0X10^{-4}$ sec^{-1}. The region between these two tests could be filled by performing tests during monotonic tension as the stress transient test mentioned by Soloman, Alhquist and Nix [144]. This type of test takes on greater usefulness for a material such as Inconel 718 which exhibits good ductility in tension and high susceptibility to low cycle fatigue.

An automated load frame was invaluable in this work for the complex tests. A smaller load frame might provide more stability during highly sensitive and mode-switching tests. A dead weight load frame would also have worth for the creep and creep-stress drop tests. A more advanced and controllable method of load-up would be a necessity. It would also be useful to utilize the same grips, furnace, extensometer, and data

aquisition equipment as with automated load frame. This would remove some relative errors between the two systems.

REFERENCES

1. H. Tresca, Notes on yield of solid bodies under strong pressure. Comptes Rendus del' Academie des Sciences 59, 754, (1894).
2. M. Levy, Memoire sur les equations generales des mouvements interieurs des corps solides ductiles au dela des limites ou l'elasticite pourrait les ramener a leur premier etat. C. R. Acad. Sci. (Paris) 70, 1323-25 (1870).
3. R. von Mises, Mechanik der festen koerper im plastisch deformablen zustant. Goettinger Nachr., Math.-Phys., Kl, 582-92 (1913).
4. H. Hencky, Zur theorie plastischer deformationen und die hierduch im material hervorgerufenen nach-spannungen. Z. ang. Math. Mech. 4, 323-34, (1924)
5. L. Prandtl, Spannungsvertielurg in plastischen koerpen. Proceedings of the First International Congress on Applied Mechanics, Delft, Technische Boekhandel en Druckerij, Jr. Waltman, Jr., 43-45 (1925).
6. E. Reuss, Bereucksichtigung der elastischen formaenderungen in der plastizitaetstheorie. Zeitschrift fuer Angewandte Mathematic und Mechanik 10, 266-274 (1930).
7. W. Prager, The theory of plasticity: a survey of recent achievements. Proceedings of the Institution of Mechanical Engineers 169, 41-57 (1955).
8. H. Ziegler, A modification of Prager's hardening rule. Q. Appl. Math. 17, 55-65 (1959).
9. D. C. Drucker, A definition of stable inelastic material. J. Appl. Mech. 26, 101-106 (1959.
10. E. C. Bingham, Fluidity and Plasticity, McGraw-Hill, New York, (1922).
11. K. Hohenemser and W. Prager, Uber die ansatze der mechanik isotroper kontinua. ZAMM 12, 216-226 (1932).
12. A. M. Freudenthal, The mathematical theories of the inelastic continuum. Handbuch der Physik, Springer-Verlag, Berlin, (1958).
13. L. E. Malvern, The propagation of longitudinal waves of plastic deformation in a bar of material exhibiting a strain-rate effect. J. Appl. Mech. 18, 203-208 (1951).
14. L. E.Malvern,Plasticwavepropagation in a barof material exhibiting a strain-rate effect. Q. Appl. Math. 8, 405 (1950).
15. J. Lubliner, A generalized theory of strain rate dependent plastic wave propagation in bars. J. Mech. Phys. Solids 12, 59 (1964).
16. P. Perzyna, Fundamental problems in viscoplasticity. Advan. Appl. Mech. 9, 243-377, (1966).
17. P. Perzyna, The constitutive equations for work-hardening and rate-sensitive plastic materials. Proc. Vibr. Probl. 4, 281-290, (1963).

18. P. Perzyna, On the thermodynamic foundations of visco-plasticity. Symposium on the Mechanical Behavior of Materials under Dynamic Loads, San Antonio, Texas, (1967).
19. P. Perzyna and W. Wojno, Thermodynamics of rate sensitive plastic materials. Arch. Mech. Stos. 20, 5, 499, (1968).
20. P. Perzyna, On physical foundations of viscoplasticity. Polska Akademia Nauk, IBPT. Report 28, (1968).
21. N. Cristescu, Dynamic Plasticity, North-Holland, Amsterdam, (1967).
22. P. M. Nagdi and S. A. Murch, On the mechanical behavior of viscoelastic/plastic solids. J. Appl. Mech., 321-328 (1963).
23. O. C. Zienkiewicz and I. C. Cormeau, Visco-plasticity--plasticity and creep in elastic solids--a unified numerical approach. International Journal for Numerical Methods in Engineering 8, 821-845 (1974).
24. S. R. Bodner and Y. Partom, Constitutive equations for elastic-viscoplastic strain-hardening materials. J. Appl. Mech. 42, 385-389 (1975).
25. D. N. Robinson, A unified creep-plasticity model for structural metals at high temperature. TM-5969, ORNL, (1978).
26. D. H. Allen and W. E. Haisler, A theory for analysis of thermoplastic materials. Computers and Structures 13, 124-135 (1981).
27. R. L. Coble, A model for boundry diffusion controlled creep in polycrystalline materials. J. Appl. Phys. 34, 1679-1682, (1963).
28. F. R. N. Nabarro, Report of a conference on the strength of solids. Physical Society of London, 75-79 (1948).
29. C. Herring, Diffusional viscosity of a polycrystalline solid. J. Appl. Phys. 21, 437-445 (1950).
30. O. D. Sherby and J. L. Lytton, Transactions AIME 206, 928 (1956).
31. O. D. Sherby, T. A. Trozera, and J. E. Dorn, Transactions ASM 46, 113 (1954).
32. O. D. Sherby, and P. M. Burke, Mechanical behavior of crystalline solids at elevated temperature. Progress in Materials Science 13, 325-390 (1968).
33. F. Garofalo, Fundamentals of Creep and Creep-rupture in Metals, Macmillan, New York, (1965).
34. J. Weertman, Transactions ASM 61, 681 (1968).
35. T. H. Alden, Transactions ASM 61, 559 (1968).
36. A. K. Mukherjee, J. E. Bird, and J. E. Dorn, Experimental correlations for high-temperature creep. •Transactions ASM 62, 155-179 (1969).
37. G. B. Gibbs, A general dislocation model for high-temperature creep. Philosophical Magazine 25, 771-780 (1972).
38. A. S. Argon, ed., Constitutive Equations in Plasticity, MIT Press, Cambridge, (1975).

39. U. F. Kocks, Laws for work-hardening and low-temperature creep. J. Eng. Mater. Tech. 98, 76-85, (1976).
40. E. W. Hart, Constitutive relations for the nonelastic deformation of metals. J. Eng. Mater. Tech. 98-H, 193 (1976).
41. R. D. Krieg, J. C. Swearengen, and R. W. Rhode, A physically-based internal variable model for rate-dependent plasticity. Proc. ASME/CSME PVP Conference, 15-27 (1978).
42. A. K. Miller, An inelastic constitutive model for monotonic, cyclic, and creep deformation. part I-equations development and analytical procedures, part II-application to type 304 stainless steel. J. Eng. Mat. Tech. 98H, 97-113 (1976).
43. M. A. Biot, Theory of stress-strain relations in anisotropic viscoelasticity and relaxation phenomena. J. Appl. Phys. 25, 1385-1391 (1954).
44. R. A. Schapery, A theory of non-linear viscoelasticity based on irreversible thermodynamics. Proc. 5th U.S. National Congress of Applied Mechanics, ASME, 511-530 (1966).
45. K. C. Valanis, A theory of viscoplasticity without a yield surface part I. general theory. Archives of Mechanics 23, 535-551 (1971).
46. K. C. Valanis, A theory of viscoplasticity without a yield surface part II. application to mechanical behavior of metals. Archives of Mechanics 23, 535-551 (1971).
47. A. E. Green and R. S. Rivlin, The mechanics of non-linear materials with memory-part I. Archives of Rational Mechanics Analysis 1, 1-21 (1957).
48. B. D. Coleman and W. Noll, Foundations of linear viscoelasticity. Review of Modern Physics 33, 239-249 (1961).
49. B. D. Coleman and W. Noll, The thermodynamics of elastic materials with heat conduction and viscosity. Archives of Rational Mechanics Analysis 13, 167 (1963).
50. A. E. Green and P. M. Nagdhi, On continuum thermodynamics. Archives of Rational Mechanics Analysis 48, 352-378 (1972).
51. E. P. Cernocky and E. Krempl, A nonlinear uniaxial integral constitutive equation incorporating rate effects, creep, and relaxation. Int. J. Nonlinear Mech. 14, 183-203 (1979).
52. K. P. Walker, Representation of Hastelloy-X behavior at elevated temperature with a functional theory of viscoplasticity. ASME Pressure Vessels Conference, San Francisco, California, (1980).
53. C. A. Truesdell and R. A. Toupin, The classical field theories. Handbuch der Physik III/1, Springer, Berlin, (1960).
54. I. Muller, The coldness, a universal function in thermoelastic bodies. Archive for Rational Mechanics and

Analysis 41, 319-332 (1971).
55. I. Muller, Entropy, Absolute Temperature and Coldness in Thermodynamics, Springer, Vienna, (1971).
56. A. E. Green and N. Laws, On a global entropy production inequality. Quarterly Journal of Mechanics and Applied Mechanics 25, 1-11 (1972).
57. W. A. Day, The Thermodynamics of Simple Materials with Fading Memory, Springer, New York, (1972).
58. J. Kratochvil and O. W. Dillon, Jr., Thermodynamics of crystalline elastic-visco-plastic materials. J. Appl. Phys. 41, 1470-1479 (1970).
59. J. Kratochvil and O. W. Dillon, Jr., Thermodynamics of elastic-plastic materials as a theory with internal state variables. J. Appl. Phys. 40, 3207-3218 (1969).
60. B. D. Coleman, Thermodynamics of materials with memory. Archive for Rational Mechanics and Analysis 17, 1-46 (1964).
61. B. D. Coleman and M. E. Gurtin, Thermodynamics with internal state variables. J. Chem. Phys. 47, 597-613 (1967).
62. J. Lubliner, On fading memory in materials of evolutionary type. Acta Mech. 8, 75-81 (1969).
63. D. H. Allen, Development of a thermodynamically consistent coupled heat conduction equation for a class of thermovisco-plastic crystalline solids. MM 12415-82-3, Texas A&M University, (1982).
64. R. W. Bailey, Jr., Journal of Institute of Metals 35, 27 (1926).
65. E. Orowan, Journal of West. Scot. Iron and Steel Institute 54, 45 (1946).
66. D. H. Allen, Some comments on inelastic strain in thermo-viscoplastic metals. MM NAG 3-31-83-8, Texas A&M University, (1983).
67. S. R. Bodner, Review of a unified elastic-viscoplastic theory. AFOSR-84-0042, (1984).
68. J. M. Beek, D. H. Allen, and T. M. Milly, A qualitative comparison of current models for nonlinear rate-dependent material behaviour of crystalline solids. MM 4246T-83-14, Texas A&M University, (1983).
69. U. S. Lindholm, K. S. Chan, S. R. Bodner, R. M. Weber, K. P. Walker, and B. N. Cassenti, Constitutive modeling for isotropic materials (HOST). CR-174718, NASA, (1984).
70. P. K. Imbrie, W. E. Haisler, and D. H. Allen, Evaluation of the numerical stability and sensitivity to material parameter variations for several unified constitutive models. MM 4998-85-61, Texas A&M University, (1985).
71. T. M. Milly and D. H. Allen, A comparative study of non-linear rate-dependent mechanical constitutive theories for crystalline solids at elevated temperatures. API-E-5-82, Virginia Polytechnic Institute and State University, (1982).

72. K. P. Walker, Research and development program for nonlinear structural modelling with advanced time-temperature dependent constitutive relationships. CR-165533, NASA, (1981).
73. E. P. Cernocky, An examination of four viscoplastic constitutive theories in uniaxial monotonic loading. Int. J. Solids Structures 18, 989-1005 (1982).
74. V. Moreno, and E. H. Jordan, Prediction of material thermomechanical response with a unified viscoplastic constitutive model. Pro. of the 26th Structures, Structural Dynamics, and Materials Conference, Orlando, Florida, (1985).
75. S. R. Bodner, I. Partom, and Y. Partom, Uniaxial cyclic loading of elastic-viscoplastic materials. J. Appl. Mech. 46, 805 (1979).
76. D. C. Stouffer and S. R. Bodner, A constitutive model for the deformation induced anisotropic plastic flow of materials. Int. J. Eng. Sci. 17, 757-764 (1979).
77. S. R. Bodner and D. C. Stouffer, Comments on anisotropic plastic flow and incompressibility. Int. J. Eng. Sci. 21, 211-215 (1983).
78. S. R. Bodner, Evolution equations for anisotropic hardening and damage of elastic-viscoplastic materials. Plasticity Today: Modelling, Methods, and Applications, Elsevier Applied Science Pub., Barking, England, (1984).
79. S. R. Bodner, A procedure for including damage in constitive equations for elastic-viscoplastic work-hardening materials. Proc. IUTAM Symposium on Physical Nonlinearities in Structural Analysis, Springer-Verlag, Pub., 21-28 (1981).
80. E. T. Onat and F. Fardshisheh, On the state variable representation of mechanical behavior of elastic-plastic solids. Proc. Symposium on Foundations of Plasticity, Noordhoff, Pub., 89-115 (1973).
81. E. T. Onat, Representation of inelastic behavior in the presence of anisotropy and finite deformations. Recent Advances in Creep and Fracture of Engineering Materials and Structures, Pineridge Press, Swansea, U. K., 231-264 (1982).
82. D. H. Allen, A prediction of heat generation in a thermo-viscoplastic uniaxial bar. MM4875-83-10, Texas A&M University, (1983).
83. D. C. Stouffer and S. R. Bodner, A relationship between theory and experiment for a state variable constitutive equation," Mechanical Testing for Deformation Model Development, STP 765, ASTM, 239-250 (1982).
84. D. C. Stouffer, A constitutive representation for In-100. AFWAL-TR-81-4039, Wright-Patterson AFB, (1981).
85. T. Nicholas and M. Boham, Finite element modeling of cracked bodies using the Bodner-Partom flow law. Proceedings of the 2nd Symposium on Nonlinear Constitutive

Relations for High Temperature Applications, Cleveland, Ohio, (1984).
86. L. T. Dame, D. C. Stouffer, and N. Abuelfoutouh, Finite element analysis of notch behavior using a state variable constitutive equation. Proceedings of the 2nd Symposium on Nonlinear Constitutive Relations for High Temperature Applications, Cleveland, Ohio, (1984).
87. R. L. Beaman, Determination of the Bodner material coefficients for IN 718 and their effects on cyclic loading , M. S. Dissertation, Air Force Institute of Technology, (1984).
88. A. M. Merzer, Steady and transient creep behavior based on unified constitutive equations. J. Eng. Mat. Tech., 18-25 (1982).
89. S. R. Bodner, Constitutive equations-directional hardening with incrementally isotropic flow law. Unpublished Research, (1984).
90. U. S. Lindholm, K. S. Chan, S. R. Bodner, R. M. Weber, K. P. Walker, and B. N. Cassenti, Constitutive modelling for isotropic materials (HOST), Second annual contract report, NASA CR-174980 (1985).
91. R. D. Krieg, Numerical integration of some new unified plasticity-creep formulations. 4th International Conference on Structural Mechanics in Reactor Technology, Vol. M, 15-19, (1977).
92. J. Friedel, Dislocations, Addison Wesley, 277-279, (1967).
93. W. B. Jones, R. W. Rhode, and J. C. Swearengen, Deformation modelling and the strain transient dip test. Mechanical Testing for Deformation Model Development, STP 765, ASTM, 102-118 (1982).
94. W. B. Jones and R. W. Rhode, An evaluation of the kinematic variable (back stress) response of metals. 7th International Conference on Structural Mechanics in Reactor Technology, (1983).
95. A. K. Miller and O. D. Sherby, A simplified phenomenological model for non-elastic: predictions of pure aluminum behavior and incorporation of solute strengthening effects. Acta Met. 26, 289-304 (1978).
96. A. K. Miller, Modelling of cyclic plasticity: improvements in simulating normal and anomalous Bauschinger effects. J. Eng. Mat. Tech. 102, 215-220 (1980).
97. C. G. Schmidt, A Unified Phenomenological Model for Solute Hardening, Strain Hardening, and Their Interations in Type 316 Stainless Steel, Ph. D. Dissertation, Stanford University, Department of Materials Science and Engineering, (1979).
98. C. G. Schmidt and A. K. Miller, A unified phenomenological model for non-elastic deformation of type 316 stainless steel-part I: development of the model and calculation of the material constants-part II: fitting and predictive

capabilities. Res Mech. 3, 109-129; 175-193 (1981).
99. H. Kagawa and Y. Asada, Proc. of the ASME International Conference on Advances in Life Prediction Methods, Albany, New York, 33, (1983).
100. T. C. Lowe and A. K. Miller, Improved constitutive equations for modelling strain softening - part 1: conceptual development and part 2: predictions for aluminum, J. Eng. Mat. Tech., 106, 337-348 (1984).
101. O. D. Sherby and A. K. Miller, Combining phenomenology and physics in describing the high temperature mechanical behavior of crystalline solids. J. Eng. Mat. Tech. 101, 387-395 (1979).
102. A. K. Miller and A. A. Ziaai-Moayyed, Some critical experimental tests of the MATMOD constitutive equations with respect to directional hardening and cyclic deformation. Mechanical Testing for Deformation Model Development, STP 765, ASTM, 202-222, (1982).
103. Ruano, A. K. Miller, and O. D. Sherby, The influence of pipe diffusion on the creep of fine-grained materials. Mat. Sci. Eng. 51, 9-16 (1981).
104. C. G. Schmidt and A. K. Miller, The effect of solutes on the strength and strain hardening behavior of alloys. Acta Met. 30, 615-625 (1982).
105. A. K. Miller, Kassner, and Rubin, Verification of a microstructurally-based equation for elevated-temperature transient isotropic hardening. Strength of Metals and Alloys 2, Pergamon Press, 581-587 (1982).
106. A. K. Miller, Kassner, and O. D. Sherby, The seperate roles of subgrains and forest dislocations in the isotropic hardening of type 304 stainless steel. Met. Trans. A 13A (1982).
107. K. P. Walker and D. A. Wilson, Creep crack growth predictions in INCO 718 using a continuum damage model. Pro-ceedings of the 2nd Symposium on Nonlinear Constitutive Relations for High Temperature Applications, Cleveland, Ohio, (1984).
108. E. Krempl, J. J. McMahon, and D. Yao, Viscoplasticity based on overstress with a differential growth law for the equilibrium stress. Proc. of the 2nd Symposium on Nonlinear Constitutive Relations for High Temperature Applications, Cleveland, Ohio, (1984).
109. E. Krempl, The role of servocontrolled testing in the development of the theory of viscoplasticity based on total strain and overstress. Mechanical Testing for Deformation Model Development, STP 765, ASTM, (1982).
110. M. C. M. Liu and E. Krempl, A uniaxial model based on total strain and overstress. J. Mech. Phys. Solids 27 377-391 (1979).
111. M. C. M. Liu, E. Krempl, and D. C. Nairn, An exponential stress-strain law for cyclic plasticity. J. Eng. Mat.

Tech., 322-329 (1976).
112. E. P. Cernocky and E. Krempl, Construction of nonlinear monotonic functions of almost constant or linear behavior. J. Appl. Mech. 45, 781-784 (1978).
113. E. Krempl, An experimental study of room-temperature rate-sensitivity, creep, and relaxation of AISI type 304 stainless steel. J. Mech. Phys. Solids 27, 363-375 (1979).
114. D. N. Robinson and R. W. Swindeman, Unified creep-plasticity constitutive equations for 2-1/4 Cr-1 Mo steel at elevated temperature. TM-8444, (1982).
115. T. J. Delph, A comparative study of two state-variable constitutive theories. •J. Eng. Mat. Tech.• 102, 327-336 (1980).
116. E. T. Onat, Representation of inelastic behavior. Sub-3868/2, ORNL, (1976).
117. J. R. Rice, On the structure of stress-strain relations for time-dependent plastic deformations in metals. J. Appl. Mech. 37E, 728-737 (1970).
118. R. Lagneborg, A modified recovery-creep model and its evaluation. Met. Sci. J. 6, 127-133 (1972).
119. D. N. Robinson, Constitutive relationships for anisotropic high-temperature alloys. TM-83437, NASA, (1983).
120. D. N. Robinson and P. A. Bartolotta, Viscoplastic constitutive relationships with dependence on thermomechanical history, NASA CR-174836 (1985).
121. D. N. Robinson, On thermomechanical testing in support of constitutive equation development for high-temperature alloys, NASA CR-174879 (1985).
122. P. A. Bartolotta, Thermomechanical cyclic hardening behavior of Hastelloy-X, NASA CR-174999 (1985).
123. D. N. Robinson, A candidate creep-recovery model for 2-1/4 Cr-1 Mo steel and its experimental implementation. TM-5110, ORNL (1975).
124. D. N. Robinson, Developments toward refined constitutive for reactor system metals. ORNL-5136, 15-23, (1975).
125. D. N. Robinson, Tests for examining the concept of a flow potential in the stress-strain relations of reactor system metals. ORNL-5235, 23-25, (1976).
126. D. N. Robinson, On the concept of a flow potential and the stress-strain relations of reactor system metals. TM-5571, ORNL, (1976).
127. D. N. Robinson and others, Constitutive equations for describing high-temperature inelastic behavior of structural alloys. Specialists' Meeting on High-temperature Structural Design Technology of LMFBRs, International Atomic Energy Agency, 44-57 (1976).
128. D. N. Robinson, Developments toward refined constitutive laws. ORNL-5281, 30-40 (1976).
129. D. N. Robinson, Developments toward refined constitutive laws. ORNL-5339, 5-16, (1977).

130. D. N. Robinson, Development of a unified constitutive model. ORNL-5374, 8-13 (1977).
131. J. R. Ellis and D. N. Robinson, Some advances in experimentation supporting development of viscoplastic constitutive models. Pro-ceedings of the 2nd Symposium on Nonlinear Constitutive Relations for High Temperature Applications, Cleveland, Ohio, (1984).
132. V. Kumar, S. Huang, S. Mukerjee, and C.-Y. Li, Theoretical and experimental analyses of stresses in reactor components: deformation of type 304 stainless steel. EPRI Final Report for Contract RT697-1, Cornell University, (1979).
133. M. S. Jackson and others, J. Eng. Mat. Tech. 103, 314 (1981).
134. S. Cescotto and F. Leckie, Determination of unified constitutive equations for metals at high temperature. Proc. International Conference on Constitutive Laws for Engineering Materials, 105-111, (1983).
135. E. P. Cernocky and E. Krempl, A theory of viscoplasticity based on infinitesimal total strain. Acta Mech. 36, 263-289 (1980).
136. H. C. Lin and H. C. Wu, Strain-rate effect in the endochronic theory of viscoplasticity. J. Appl. Mech., 43, 92-96 (1976).
137. H. C. Wu and M. C. Yip, Strain rate and strain rate history effects on the dynamic behavior of metallic materials. Int. J. Solids Structures 16, 515-536 (1980).
138. D. H. Allen, Computational aspects of the nonisothermal classical plasticity theory. Computers and Structures, (1982).
139. J. L. Chaboche, Bulletin de L'Academie des Sciences, Serie des Science Techniques 25, 33 (1977).
140. D. Lee and Zaverl, Jr., Acta Met. 26, 385 (1975).
141. A. K. Ghosh, Acta Met. 28, 1443 (1980).
142. J. M. Beek, A comparison of current models for nonlinear rate-dependent material behavior of crystalline solids, M. S. Thesis, Texas A&M University, (1986).
143. D. H. Allen and J. M. Beek, On the use of internal state variables in thermoviscoplastic constitutive equations. MM NAG3-491-84-12, Texas A&M University, (1984).
144 A. A. Soloman, C. N. Ahlquist, and W. D. Nix, The effect of recovery on the measurement of mean internal stresses. Scripta Met., 4, 231, (1970).
145. C. N. Ahlquist and W. D. Nix, A technique for measuring mean internal stress during high temperature creep. Scripta Met. 3, 679-682 (1969).
146. C. N. Ahlquist and W. D. Nix, The measurement of internal stresses during creep of Al and Al-Mg alloys. Acta Met. 19, 373-385 (1971).
147. J. P. Poirier, Microscopic creep models and the interpre-

tation of stress-drop tests during creep. Acta Meta. 25, 913-917 (1977).
148. J. C. Gibeling and W. D. Nix, Observations of anelastic backflow following stress reduction during creep of pure metals. Acta Met. 29, 1769-1784 (1981).
149. W. D. Nix, J. C. Gibeling, and Fuchs, The role of long-range internal back stresses in creep of metals. Mechanical Testing for Deformation Model Development, STP 765, ASTM, 301-321 (1982).
150. W. Blum and A. Finkel, Acta Met. 30, 1705 (1982).
151. F. Garofalo, O. Richmond, and W. F. Damis, Design of apparatus for constant-stress or constant-load creep tests. J. Basic Eng., 84, 285, (1962).
152. Manual on the Use of Thermocouples in Temperature Measurement. ASTM STP 470A, 141-154, (1974).
153. A. B. Thakker and B. A. Cowles, Low strain, long life creep fatigue of AF2-1DA and INCO 718. CR-167989, NASA, (1983).
154. G. E. Korth and G. R. Smolik, Status report of physical and mechanical test data of alloy 718. TREE-1254, DOE, (1978).
155. J. H. Laflen and T. S. Cook, Equivalent damage-a critical assessment. CR-167874, NASA, (1982).
156. T. S. Cook, Cyclic stress-strain behavior of Inconel 718. Mechanical Testing for Deformation Model Development, STP 765, ASTM, 269-282 (1982).
157. C. R. Brinkman and G. E. Korth, Strain fatigue and tensile behavior of Inconel 718 from room temperature to 650^{0}C. JTEVA, 2, 4, 249-259, (1974).
158. D. Fournier and A. Pineau, Low cycle fatigue behavior of Inconel 718 at 298 K and 823 K. Met Trans A, 8A, 1095, (1977).
159. Metals Handbook,9th edition, Volume 4 Heat Treating, American Society for Metals, Metals Park, Ohio.
160. D. Yao and E. Krempl, Viscoplasticity theory based on overstress. The prediction of monotonic and cyclic proportional and nonproportional loading paths of an aluminum alloy, Int. J. of Plasticity, 1/3, (1985), pp. 259-274.
161. P. K. Imbrie, G. H. James, P. S. Hill, W. E. Haisler, and D. H. Allen, An automated procedure for material parameter evaluation for viscoplastic constitutive models, to appear in Pro. of the 3rd Symposium on Nonlinear Constitutive Relations for High Temperature Applications, Akron, Ohio, (1986).
162. S. R. Bodner and A. Rosen, Discontinuous yielding of commercially pure aluminun, J. Mech. Phys. Solids, 15, (1967), pp. 63-77.
163. G. Callelaud and J. L. Chaboche, Macroscopic description of the microstructural changes induced by varying temperature: example of IN100 cyclic behaviour. Pro. of the 3rd International Conference on Mechanical Behaviour of Materials (ICM-3), Cambridge, G. B., (1979).
164. U. S. Lindholm and D. L. Davidson, Low-cycle fatigue with

combined thermal and strain cycling, ASTM STP-520, American Society for Testing and Materials, 473-481, (1973).
165. D. N. Robinson, Thermomechanical Deformation in the presence of metallurgical changes. Pro. of the 2nd Symposium on Nonlinear Constitutive Relations for High Temperature Applications, Cleveland, Ohio, (1984).

APPENDIX A - DATA SET

The major purpose of this appendix is allow the calculations of the chapter IV to be repeated and upgrades to the methods used developed. The data will be presented in tabular form. The average value of Young's modulus for this material was 24,658 ksi.Table A.1 contains data from the initial tensile portion of the cyclic tests and monotonic tensile tests. The first column provides the test number and the second column provides the applied total strain rate. The third column is the stress at which the first visible sign of inelastic flow is seen and the fourth column provides the inelastic strain rate at this stress. The fifth column is the .2% offset value and the sixth column is the stress at .8% total strain.

Table A.2 provides auxiliary information similar to Table A.1. These data were from a second series of material and utilized only when a broader data base was necessary. The material series labeled D2 was the series studied in this work. The material series D8 was presumably from a different lot or heat treatment than the D2 series. Columns one through five contain the same types of information as the respective columns in Table A.1. Column six is the saturated stress from the gamma plot and column seven is the slope of the gamma plot. The gamma plot was described in chapter V under the section covering Bodner's model.

Table A.3 gives data from high strain monotonic tensile tests. This table contains data from both the D2 and D8 series of the

material. Column three provides the value of total strain and column four provides the associated stress value. Column six and seven are the slopes from the gamma and theta plots, respectively. The theta plot was described in chapter V under the section covering Walker's model.

Table A.4 presents the creep data produced in this work. Mixed series data are again presented. Column three contains the applied stress and column four the associated secondary creep rate. The D8 series data were obtained using the dead weight load frame discussed in the previous chapter. The D2 series data were produced on the computer controlled MTS 880 load frame discussed in the previous chapter.

Table A.5 contains the back stress data from this work. The values for back stress are at best estimates of the true value and should be treated as such. Column three of Table A.5 contains the inelastic strain rate and column four contains the stress value associated with the back stress value of column five. Table A.6 contains the creep stress drop data used to arrive at the back stress values in Table A.5. The stress associated with the drop and the associated inelastic strain rate are provided under each test. A linear regression curve fit provided the stress at which a zero strain rate was expected for each test. Table A.7 provides the same data for the cyclic hold time data.

Table A.8 through Table A.13 provide cyclic data from individual tests. The first column provides the half cycle currently being considered. The second column provides the stress value at .8% strain for that half cycle. Columns three, four, and five contain the slope of the gamma plot, saturated stress of the gamma plot, and plastic work

from the gamma plot for each half cycle. Columns six and seven contain the slope and saturated stress from the theta plot for each half cycle.

Table A.1 - First Half Cycle Material Data - D2 Series

Test	$\dot{\varepsilon}^T$ (sec^{-1})	σ_0(ksi)	$\dot{\varepsilon}^I_0$ (sec^{-1})	$\sigma_{.2}$(ksi)	$\sigma_{.8}$(ksi)
70	3.151E-2	97.83	9.144E-4	122.17	124.64
86	1.002E-3	96.68	2.304E-3	117.66	120.19
56	9.966E-3	95.56	2.684E-4	115.17	117.52
65	3.127E-4	97.84	7.599E-5	121.41	123.56
83	9.926E-5	94.56	1.319E-5	123.56	127.52
80	3.054E-5	100.94	7.213E-6	128.86	130.51
72	7.626E-6	101.71	1.550E-6	126.78	128.42
71	7.253E-6	97.67	1.402E-6	124.67	126.95

Table A.2 - Auxilary Tensile Data - D8 Series

Test	$\dot{\varepsilon}^T$ (sec^{-1})	$\sigma_{.2}$ (ksi)	σ_γ (ksi)	γ(ksi)	σ_γ (ksi)	θ
35	9.253E-4	125.29	136.8	2.037	136.3	2.772
37	6.048E-4	125.30	136.3	2.202	137.5	240.9
39	1.793E-4	119.82	130.5	1.772	130.6	206.6
34	7.637E-5	131.36	147.4	1.4004	142.1	319.8
36	5.703E-5	126.82	137.2	2.237	138.5	241.6
42	1.914E-5	127.16	147.2	.6772	137.6	291.8
38	1.410E-5	127.17	144.3	1.2867	140.7	212.4
40	7.029E-6	128.72	137.5	2.917	138.3	328.5

Table A.3 - High Strain Data

Test	Series	ε^T	σ (ksi)	γ (ksi)	θ (ksi)
70	D2	.0128	130.7		287.29
35	D8	.0130	134.43	2.037	
34	D8	.0130	140.38	1.4004	
42	D8	.0129	135.96	.6772	
71	D2	.0126	134.4	2.929	342.25
35	D8	.0399	143.0		
34	D8	.0243	146.08		
42	D8	.0347	144.71		

Table A.4 - Creep Data

Test	Series	σ_a (ksi)	$\dot{\epsilon}^I_s$ (sec^{-1})
60	D2	119.0	1.792E-8
61	D2	124.0	1.012E-7
62	D2	127.0	1.125E-7
63	D2	133.9	2.42E-7
64	D2	138.8	7.117E-7
10	D8	110.0	5.3E-8
12	D8	115.0	9.5E-9
17	D8	120.0	9.55E-8
11	D8	120.0	8.88E-8
19	D8	125.0	3.03E-4

Table A.5 - Back Stress Data - D2 Series

Test	Type	$\dot{\epsilon}^I$ (sec^{-1})	σ (ksi)	B(ksi)
84	Cyclic	2.812E-3	116.48	68.30
88	Cyclic	9.272E-4	100.98	62.47
81	Cyclic	8.635E-4	116.45	64.65
65	Cyclic	2.751E-4	107.84	48.58
63	Creep	2.420E-7	133.91	128.22
61	Creep	1.012E-7	124.00	116.78
60	Creep	1.792E-8	119.04	113.85

Table A.6 - Creep Stress Drop Data

Test	σ (ksi)	$\dot{\varepsilon}^I$
60	117.6	5.616E-8
	115.7	-2.292E-8
	114.2	-1.194E-7
	111.7	0.00
	95.53	-2.753E-7
	85.27	-4.800E-7
	77.96	-8.809E-7
61	121.8	1.635E-7
	119.4	8.545E-8
	117.1	-1.194E-7
	113.9	2.415E-8
	107.4	-3.190E-7
62	126.2	-1.313E-7
	122.3	3.166E-7
	118.8	-2.197E-7
	115.5	1.137E-7
	112.9	-4.288E-8
63	131.5	-3.07E-7
	129.5	.1839E-7
	129.3	.06405E-7
	120.5	-.4958E-7
	117.3	-.3820E-7

Table A.7 - Cyclic Back Stress Hold Data

Test	σ	$\dot{\varepsilon}^I$
65	104.51	2.658E-6
	99.38	1.785E-6
	94.49	1.340E-6
	89.71	9.102E-7
	84.61	3.973E-7
	79.32	2.268E-7
	74.46	7.293E-7
	74.13	5.788E-7
	69.29	4.171E-7
	64.28	3.576E-7
	59.23	1.386E-7
	54.34	3.034E-7
	49.36	7.509E-8
	44.58	-1.784E-7
	39.24	-1.182E-7
81	78.56	3.128E-7
	73.91	-3.852E-7
	73.38	1.535E-7
	68.64	1.616E-7
	68.33	1.201E-7
	58.94	-6.898E-8
	55.85	-3.633E-7
	42.28	-4.009E-7
88	79.03	1.606E-7
	73.61	8.755E-8
	68.71	6.099E-8
	58.37	-2.448E-7
	54.24	-7.279E-8
	38.66	-6.285E-7
84	85.56	1.756E-7
	74.76	3.912E-7
	65.01	-2.256E-7
	56.11	-3.135E-7
	46.28	-3.837E-7

Table A.8 - Cyclic Data - Test 86

Half Cycle	$\sigma_{.8}$ (ksi)	γ (ksi)	σ_{γ} (ksi)	Wp (ksi)	θ (ksi)	σ_{θ} (ksi)
1	120.33			.12852		
2	-124.10	3.620	-128.094	.4643	307.03	-133.47
3	114.49	3.843	116.80	.4560	-307.10	120.93
4	719.05	2.223	-131.73	.4796	295.03	-125.83
5	111.42	3.824	113.00	.4568	-269.30	116.98
6	-115.98	4.068	-115.94	.5016	310.49	-120.93
7	109.47	4.124	109.78	.4873	-306.22	113.91
8	-113.04	4.325	-113.04	.5111	322.62	-117.84
9	108.01	4.079	108.43	.4846	-302.41	112.28
10	-112.42	4.192	-112.04	.5098	310.81	-116.75
11	106.86	4.173	106.91	.4964	-302.19	110.91
12	-111.27	4.318	-110.53	.5196	312.05	-115.45
13	105.91	4.193	106.02	.4947	-303.10	109.84
14	-110.26	4.357	-109.49	.5190	315.07	-114.13
15	105.09	2.363	115.18	.4930	-296.55	109.24
16	-109.44	4.282	-109.00	.5170	308.22	-133.62
17	104.43	4.255	104.36	.5052	-299.03	108.38
18	-108.74	4.234	-108.50	.5166	303.44	-113.10
19	103.88	4.128	104.24	.5044	-288.42	108.36
20	-108.14	4.354	-107.50	.5276	303.96	-112.50
21	103.42	2.426	112.99	.5036	-292.83	107.56
22	-107.65	2.500	-117.50	.5271	298.35	-112.31

Table A.9 - Cyclic Data - Test 56

Half Cycle	$\sigma_{.8}$ (ksi)	γ (ksi)	σ_{γ} (ksi)	Wp (ksi)	θ (ksi)	σ_{θ} (ksi)
1	117.64			.1282		
2	-120.33	3.523	-124.67	.4224	319.63	-127.92
3	111.95	3.863	114.40	.4350	-305.44	118.22
4	-115.33	3.860	-116.89	.4651	298.85	-122.04
5	108.88	4.016	110.14	.4549	-300.78	114.15
6	-112.41	4.013	-112.84	.4729	304.61	-117.71
7	106.87	4.068	107.82	.4640	-299.00	111.74
8	-110.44	4.182	-110.54	.4820	298.64	-115.77
9	105.50	4.073	106.40	.4621	-304.87	109.78
10	-109.00	4.164	-109.23	.4799	297.19	-114.08
11	104.50	4.182	105.01	.4736	-298.61	108.86
12	-107.94	4.163	-108.10	.4923	291.06	-113.18
13	103.59	4.200	104.11	.4711	-269.18	107.96
14	-107.03	4.142	-107.31	.4920	287.98	-112.30
15	102.90	4.263	103.15	.4836	-293.68	107.15
16	-106.25	4.099	-106.83	.4896	283.14	-111.83
17	102.24	4.249	102.61	.4826	-294.02	106.53
18	-105.05	4.149	-105.98	.5010	276.97	-111.54
19	101.71	4.255	102.10	.4814	-294.58	105.90
20	-105.00	4.077	-105.68	.5010	273.76	-111.07
21	101.18	4.297	101.52	.4921	-288.11	105.82
22	-104.59	4.000	-105.50	.4977	264.87	-111.14

Table A.10 - Cyclic Data - Test 65

Half Cycle	$\sigma_{.8}$ (ksi)	γ (ksi)	σ_γ (ksi)	Wp (ksi)	θ (ksi)	σ_θ (ksi)
1	123.91	3.257	130.37	.1064		
2	-129.76	2.599	-140.77	.4727	314.80	-139.93
3	122.55	3.022	129.55	.3921	268.17	134.14
4	-126.17	2.950	-133.43	.4140	261.29	-138.99
5	119.95	2.926	127.15	.3959	243.38	132.85
6	-123.33	2.219	-137.56	.4336	253.43	-136.24
7	117.96	30.43	124.15	.4020	241.85	130.32
8	-121.22					
9	116.38					
10	-119.65					
11	115.12					
12	-118.35	2.954	-124.98	.4116	221.41	-133.19
13	114.15	2.169	127.76	.4081	224.23	124.76
14	-117.32	2.189	-131.27	.4099	223.58	-131.23
15	113.27	2.163	126.76	.4068	229.72	125.08
16	-116.48	2.968	-122.75	.4217	214.72	-131.39
17	112.55	3.398	116.10	.4525	239.09	123.14
18	-115.72	3.148	-120.63	.4540	220.90	-129.41
19	111.94	3.366	115.58	.4514	248.02	121.43
20	-115.12	3.298	-118.99	.4656	217.93	-128.92
21	111.34	3.415	114.80	.4506	247.65	120.78
22	-114.54	3.205	-118.86	.4648	221.88	-127.60

Table A.11 - Cyclic Data - Test 83

Half Cycle	$\sigma_{.8}$ (ksi)	σ (ksi)	σ_γ (ksi)	Wp (ksi)	θ (ksi)	σ_θ (ksi)
1	128.66		134.30	.14978		134.57
2	-138.82	2.912	-148.09	.4249	395.79	-146.84
3	130.07	3.399	135.50	.3829	334.40	138.81
4	-137.35	2.885	-145.28	.40093	299.96	-149.29
5	129.29	3.292	135.20	.3755	319.92	138.81
6	-135.64				320.43	-146.09
7	128.06				285.42	139.79
8	-134.01				290.42	-146.64
9	126.86				290.33	137.94
10	-132.60				280.31	-146.01
11	125.75				267.18	138.76

Table A.12 - Cyclic Data - Test 80

Half Cycle	$\sigma_{.8}$ (ksi)	γ (ksi)	σ_{γ} (ksi)	Wp (ksi)	θ (ksi)	σ_{θ} (ksi)
1	130.59			.06833		
2	-139.24	2.684	-149.25	.3866	368.98	-148.07
3	130.89	3.075	138.46	.3661	310.78	141.82
4	-137.85			.3936	321.97	-149.40
5	129.92	3.140	137.30	.3734	303.02	141.50
6	-136.07				333.99	-146.98
7	128.54				292.52	140.72
8	-134.32				304.11	-147.28
9	127.25				265.97	142.03
10	-132.82				295.35	-146.24
11	126.04				241.28	142.88
12	-131.52				285.46	-145.43
13	124.99				251.77	140.31
14	-130.35				287.86	-143.56
15	123.93				254.05	138.75
16	-129.35				272.44	-143.51
17	123.18				233.61	139.68
18	-128.42				253.32	-144.32
19	122.39				255.53	135.90
20	-127.70				224.54	-146.89
21	121.58				209.09	140.72

Table A.13 - Cyclic Data - Test 72

Half Cycle	$\sigma_{.8}$ (ksi)	γ (ksi)	σ_{γ} (ksi)	Wp (ksi)	θ (ksi)	σ_{θ} (ksi)
1	128.79			.0674		
2	-137.83	2.711	-146.44	.3479	355.88	-146.28
3	130.04	2.713	139.66	.3212	358.55	138.16
4	-138.25	2.818	-147.44	.3396	309.59	-150.57
5	130.66	3.243	137.86	.3185	334.58	140.69
6	-138.10				293.64	-152.15
7	130.69				-375.04	139.38
8	-137.12				341.27	-148.97

APPENDIX B - PROPOSED INITIAL CALCULATION METHODS

The proposed methods will be summarized using a generic viscoplastic modelin the first section of this chapter. This is presented to make the actual calculations more transparent to the reader. The generic model used as an example will be presented first followed by the generic method of initial calculations. Individual sections covering the four models used in this work will follow. The material in Table 1 of the main text and Appendix A should be referred to as needed.

Generic Summary of Constant Calculation Methods

Generic viscoplastic model. The growth laws for the example model are presented below:

$$\dot{\varepsilon}^I = \left(\frac{\sigma - B}{D + F}\right)^n \tag{103}$$

$$\dot{B} = C_1\dot{\varepsilon}^I + C_2 B\,\dot{\varepsilon}^I + C_3 B \tag{104}$$

$$\dot{D} = C_4|\dot{\varepsilon}^I| + C_5 D \tag{105}$$

$$F = F(\dot{\varepsilon}^I) \tag{106}$$

n is a constant measuring strain rate sensitivity. C_1 is a constant measuring back stress hardening. C_2 is handeling back stress dynamic recovery and C_3 measures back stress thermal recovery. C_4 produces drag stress hardening and C_5 models drag stress recovery. F is a parameter

inserted to handle strain aging effects. This parameter can be removed from any model in this appendix and the method still used.

Initial assumptions. The following initial assumptions were made for these methods:

(1) Back stress was assumed responsible for hardening in monotonic tension;

(2) drag stress was assumed responsible for cyclic softening;

(3) thermal recovery effects were small and masked by solute strengthening effects

(4) solute strengthening or strain aging masked the basic positive strain rate sensitivity of the material.

Initial calculations. The first step would be to estimate the constants in the back stress growth law. The back stress growth law is written in the following form to allow the thermal recovery constant C_3 to be included in the calculations:

$$\dot{B} = \left[C_1 + B\left(C_2 + \frac{C_3}{\dot{\varepsilon}^I}\right)\right] \dot{\varepsilon}^I \qquad (107)$$

Differential descriptions of work hardening, experimental estimations of back stress values, relationships between saturated stresses and saturated back stresses, linear regression analysis will all be useful in this step.

The next step was to calculate the strain rate sensitivity constant n and the initial value of drag stress denoted by D_0. The function F

will need to be set to assure a positive value of n. An estimation of n from literature or a region outside of the strain aging region will be helpful. The inelastic strain rate equation is rewritten in the following form:

$$\ln(\sigma - B) = \frac{1}{n} \ln(\dot{\varepsilon}^I) + \ln(D_0 + F) \tag{108}$$

The ability to estimate saturated stresses and back stresses, remove drag stress scaling to another parameter, or place F in the back stress growth law are useful at this stage.

Initial determination of the drag stress parameters C_4 and C_5 can be initiated by rewriting the drag stress growth law in the following form:

$$\dot{D} = \left(C_4 + \frac{C_5}{|\dot{\varepsilon}^I|} D \right) \dot{\varepsilon}^I \tag{109}$$

The constants can be evaluated by repeated application of a differential technique such as the gamma or theta plot at each cycle and/or by monitoring the growth of D versus the cumulative inelastic strain.

Krieg, Swearengen and Rhode's Model

The growth laws for the model of Krieg, et al are repeated below for completeness:

$$\dot{\varepsilon}^I = C\left(\frac{\sigma - B}{D}\right)^n \operatorname{sgn}(\sigma - B) \tag{110}$$

$$\dot{B} = A_1\dot{\varepsilon}^I - A_2B^2[\, e^{(A_3B^2)} - 1\,]\,\mathrm{sgn}(B) \tag{111}$$

$$\dot{D} = A_4|\,\dot{\varepsilon}^I\,| - A_5(D - D_0)^n \tag{112}$$

This method assumes the solute strengthening corrected version of the model is being used. The first step would be to utilize the assumption that saturated back stress is proportional to applied stress as reported by Miller [42]. Tests 84,88,81,and 65 would be used to approximate this proportionality and the results averaged. An equation of the following form would result:

$$B_{lim} = \alpha\,\sigma_{lim} \tag{113}$$

where α is the constant of proportionality.

The constant A_1 will be set by assuming that no thermal recovery is present and B can be written in the following form for saturated conditions:

$$B = A_1\varepsilon^I = \alpha\,\sigma \tag{114}$$

Tests 80,83,65,56,86,70 would be used to produce an average value of A_1 based on ε^I and σ at .8% total strain.

The initial value of D is again set to 1.000 and B is assumed equal to $A_1\varepsilon^I$. The inelastic strain rate equation is written in the following form:

$$\ln\left(\frac{\sigma - A_1\varepsilon^I}{1 + F_{sol}}\right) = \frac{1}{n}\ln(\dot{\varepsilon}^I) - \frac{1}{n}\ln(C) \tag{115}$$

The F_{sol} constants F, β , and J will be set such that a linear fit of test data at .8% total strain will produce a physically realizable n value. The constants β and J could be set as previously mentioned to eliminate some of the "curve-fitting" aspects of this step. The initial value of n = 4.412 from the previous initial calculations could also be used as an estimate of n. Tests with little thermal recovery such as 80,83,65,56,86,and 70 should be used in this step.

The inelastic strain rate equation will then be rewritten in the following form:

$$B = \sigma - (1 + F_{sol})\cdot\left(\frac{\dot{\varepsilon}^I}{C}\right)^{1/n} \tag{116}$$

Values of B will be calculated based on experimental values of σ and $\dot{\varepsilon}^I$ at .8% strain for tests 71,72,80,83. The following approximation for back stress is then made:

$$B = [A_1 - A_2\exp(A_3B^2)(\dot{\varepsilon}^I)^{-1}]\,\varepsilon^I \tag{117}$$

The following linearized equation results:

$$\ln\left[\dot{\varepsilon}^I\left(\frac{B}{\varepsilon^I} - A_1\right)\right] = \ln(A_2) + A_3B^2 \tag{118}$$

A linear least squares fit to the data of tests 71,72,80,and 83 would produce estimations for A_2 and A_3.

Data at .8% total strain from the saturated cyclic loops of tests 72,80,83,65,56,86 would be input into the following equation to produce saturated values of D:

$$D = (\sigma - B) \left(\frac{\dot{\varepsilon}^I}{C}\right)^{-1/n} - F_{sol} \tag{119}$$

The following approximation for drag stress is then made:

$$D = \left[A_4 - A_5 (D - D_0)^n (\dot{\varepsilon}^I)^{-1} \right] R \tag{120}$$

where $R = \Sigma \left|\varepsilon_i^I\right| = \sum_{i=1}^{N} \left| \varepsilon_i^T - \frac{\sigma_i}{E} \right|$

and σ_i, ε_i are the maximum and minimum stress and strain for each half cycle. N is the number of half cycles associated with each current value of D in a cyclic test. The D values and associated $\dot{\varepsilon}^I$ values are those calculated above and $D_0 = 1.0000$. A least squares curve fit could provide estimates of A_4 and A_5.

The constants produced with this proposed procedure should be tuned with a systematic procedure such as described in the computer iteration section. A possible automation of the constant calculation procedure would consist of good initial approximations of the constants which ignores some inherent nonlinearity in the model coupled with a systematic and repeatable iterative method to return the nonlinearity to

the constants.The true test of the above scheme is in its application to a material which responds with positive strain rate sensitivity. The F_{sol} terms could simply be dropped from the above discussionin such a case.

Bodner's Anisotropic Model

The growth laws for Bodner's anisotropic model are repeated below for completeness:

$$\dot{\varepsilon}^I = \frac{2}{\sqrt{3}} D_0 \exp\left[-\left(\frac{Z}{\sigma}\right)^{2n}\right] \operatorname{sgn} \sigma \tag{121}$$

$$Z = Z^I + Z^A = Z^I + B \operatorname{sgn} \sigma \tag{122}$$

$$\dot{Z}^I = m_1 (Z_1 - Z^I) \dot{W}_p - A_1 Z_1 \left(\frac{Z^I - Z_2}{Z_1}\right)^{r_1} \tag{123}$$

$$\dot{B} = m_2 (Z_3 \operatorname{sgn} \sigma - Z^A) \dot{W}_p - A_2 Z_1 \left(\frac{|Z^A|}{Z_1}\right)^{r_2} \operatorname{sgn} Z^A \tag{124}$$

$$W_p = \sigma \varepsilon^I \tag{125}$$

Bodner's model is amenable to a correction for negative strain rate sensitivity similar to Walker's model. The Z_3 variable would be replaced with the following expression:

$$Z_3 = B_1 + B_2 \exp\left(-B_3 \log\left|\frac{\dot{\varepsilon}^I}{\dot{\varepsilon}_0^I}\right|\right) \tag{126}$$

The value of n will be calculated from a region of positive strain

rate sensitive material response as presented earlier. The constants Z_0 and m_2 will also be calculated as before. The following equation will then result for Z_3:

$$Z_3 = B_1 + B_2 \exp(-B_3 \log|\frac{\dot{\varepsilon}^I}{\dot{\varepsilon}_0^I}|) = \sigma[\ 2\ln(\frac{2}{\sqrt{3}} \cdot \frac{D_0}{\dot{\varepsilon}^I})]^{1/2n} - Z_0 \qquad (127)$$

The constants B_3 and $\dot{\varepsilon}_0$ wiould be set in a manner as dscribed in the section discussing Walker's model. The saturated stresses of the gamma plots would be used from tests 71, 72, 80, 83, 65, 56, 86, and 70 to produce least squares estimations of B_1 and B_2. The constants Z_1, m_1, A_1, and r_1 would be calculated in the same manner as before. The approximations commonly used by Bodner of $A_2 = A_1$ and $r_2 = r_1$ could be employed.

Miller's Model

The growth laws for Miller's model are repeated below for completeness:

$$\dot{\varepsilon}^I = B'\{\ \sinh[\ (\frac{\sigma - B}{D})^{1.5}\ ]^n \operatorname{sgn}(\sigma - B) \qquad (128)$$

$$\dot{B} = H_1 \dot{\varepsilon}^I - H_1 B' \sinh(\ A_1|B|\ )^n \operatorname{sgn}(B) \qquad (129)$$

$$\dot{D} = H_2|\ \dot{\varepsilon}^I|(\ C_2 + |B| - \frac{A_2}{A_1} D^3) - H_2 C_2 B' \sinh(\ A_2 D^{1.5})^n \qquad (130)$$

Miller's model is a highly "coupled" model. The back stress recovery and drag stress recovery terms are designed to reproduce specific

saturated states. The recovery terms are not seperated by individual constants from the hardening terms. Instananeous changes on the order of the changes in hardening are possible. A complete calculation of the constants for Miller's model will probably involve iterative procedures since hardening and recovery terms can not be artificially seperated.

Most of the constants for Miller's model should be calculated outside the region of solute strengthening effects. The proposed method brgins by calculating the constants A, B', n, D_0, A_1, A_2, C_1, C_2, and H_1 from tests 42, 38, 40, 34, 80, 72, 71, 60, 61, 62, 63, and 64. The constants A, B', n, and D_0 would be calculated as before. The constants A_1 and A_2 could be calculated using the experimental back stress values of tests 60, 61, and 63. The constant H_2 should be set to an artificially small number to simplify the drag stress hardening term and the calculations.

The constants H_1 and C_2 should be set from the strain controlled tests 42, 38, 34, 80, 72, and 71. These constants must be evaluated iteratively unless a differential method of evaluating the hardening constants such as the gamma plot can be developed. The following equation can be explored as a possible starting point if the same assumtions made for the gamma plot are made and if back stress is the main contributor to monotonic hardening:

$$\theta = \frac{d\sigma}{d\varepsilon}_I = H_1 f \qquad (131)$$

$$f = 1 - \frac{B'}{\dot{\varepsilon}^I}\{ \sinh(A_1[\sigma - \{\sinh^{-1}(\frac{\dot{\varepsilon}^I}{B'})\}^{2/3} D_0])\} \quad (132)$$

A linear curve fit to f versus θ data might give an estimate of H_1 as the slope when monotonic tensile data is used.

Utilizing values of stress and cumulative inelastic strain at .8% total strain from cyclic tests, making the usual gamma plot assumtions and assuming $B = C_1\sigma$ (C_1 is the experimentally determined ratio of saturated stress to back stress) the following equation results:

$$\frac{d\sigma}{d\varepsilon^I} = (1 - C_1)^{-1} H_2 C_2 f_3 \sigma^3 \quad (133)$$

$$f_3 = 1 - \frac{B'}{\dot{\varepsilon}^I}[\sinh (A_2\{ \sigma[1 - C_1][\sinh^{-1}(\frac{\dot{\varepsilon}^I}{B'})]^{-2/3}\}^3)] \quad (134)$$

A linear fit of such an equation may give H_2C_2 as the slope.

The response of the model to the higher strain rates of tests 80, 83, 65, 86, 56, and 70 could be tuned using the F_{sol} parameters. A possible alternative to the F_{sol} correction would be to make the auxiliary constant C_1 dependent on strain rate. C_1 is the constant of proportionality between saturated stress and saturated back stress:

$$B_{ss} = C_1\sigma_{ss} \quad (135)$$

The constants A_1 and A_2 depend on C_1 as follow:

$$A_1 = \frac{A}{C_1} \quad (136)$$

$$A_2 = [\ A\ /\ (1-C_1)\ ]^3 \tag{137}$$

The C_1 value for the creep tests is approximately .99. The C_1 value for cyclic tests is approximately .5. This is somewhat to be expected since stress can not reach full saturation in a cyclic test. The suggestion here is to evaluate each cyclic test in terms of C_1 and produce an appropriate functional form for C_2. It is possible that such a method might handle the negative strain rate sensitivity response, the cyclic work softening response, and produce correct values of saturated back stresses.

Walker's Exponential Model

The growth laws for Walker's model are repeated below for completeness:

$$\dot{\varepsilon}^I = \frac{\exp\left(\frac{\sigma - B}{D}\right) - 1}{C} \tag{138}$$

$$\dot{B} = n_2\dot{\varepsilon}^I - B\ \{\ [\ n_3 + n_4\exp(-n_5|\ \log(\frac{\dot{R}}{\dot{R}_0})\ |)]\ \dot{R} + n_6\} \tag{139}$$

$$D = D_1 + D_2\exp(-n_7 R) \tag{140}$$

$$\dot{R} = |\ \dot{\varepsilon}^I| \tag{141}$$

The constants $\dot{R}_0$ and n_5 would be calculated in the same manner as previously detailed. The negative strain rate sensitivity correction

term could then be calculated for each test using the applied strain rate and the following formula:

$$f_i = \exp(-n_5 \text{abs}\{ \ln[\text{abs}(\frac{\dot{\varepsilon}_i^I}{\dot{R}_0})]\}) \tag{142}$$

where the i index denotes each individual test being considered and abs denotes absolute value.

The constants n_3, n_4, and n_6 will be determined with a linear least squares regression scheme applied to the following equations:

$$n_3 + n_4 f_i + n_6/\dot{\varepsilon}_i^I = N_i$$

where N is the slope of the theta plot and the i index denotes each test considered. The tests considered would be 70, 86, 56, 65, 83, 80, 72, and 71.

The constant n_2 would be estimated by averaging values calculated from the following equation:

$$n_2 = \frac{(n_3 + n_4 \cdot f_i) \cdot \sigma_{1im}}{C_2} \tag{143}$$

where C_2 is the ratio of saturated stress to saturated back stress as estimated from tests 65, 81, 84, and 88. Tests 70, 86, 56, and 65 would be used in this calculation.

The next step would be to calculate C and $D = D_1 + D_2$ from the following equation:

$$\left(\sigma_i - \frac{n_2}{n_3 + n_4 \cdot f_i}\right) = D \cdot \ln\left(\dot{\varepsilon}_i^I\right) + D \cdot \ln\left(C\right) \qquad (144)$$

A linear fit using the saturated stress from the theta plot, f_i, and the applied strain rate for tests 70, 86, 56, 65, 83, and 80 gives D as the slope and allows C to be calculated from the intercept. The constants D_1, D_2, and n_7 would be calculated in the same manner as presented earlier. This method of calculation has been applied by Imbrie, et al. [161].

APPENDIX C - AUXILIARY MODEL RESULTS

This appendix presents model predictions not presented in the text and are included here for completeness. Figure C.1 presents the experimental results for the first half cycle of the cyclic tests and the long term tension tests. Figures C.2 through C.6 present the model predictions of the first half cycle of the cyclic tests 86, 65, 83, 80, and 72. Numerical instabilities can be seen which result from the Fsol parameters.

Figure C.7 provides the experimental hystenesis loops. Figure C.8 through C.11 compare the model results to tests 65, 83, 80, and 72. The values at -.8% strain for each test and the associated model predictions are shown in Figure C.12.

The values at +.8% of each cycle are shown for test 65 and 83 in Figure C.13 and C.14 respectively. The values at -.8% for tests 86, 65, 83, 80, and 72 are shown in Figures C.15 through C.19.

The model's predictions are shown compared to a complex history test of the same input and material series as the test 89 mentioned in Chapter VII in Figures C.20 through C.26. A region of discontinuous yielding or the Portvin - Le Chatelier effect can be seen in the region between .005 and .014 strain. Bodner and Rosen discuss this phenomena in reference [162].

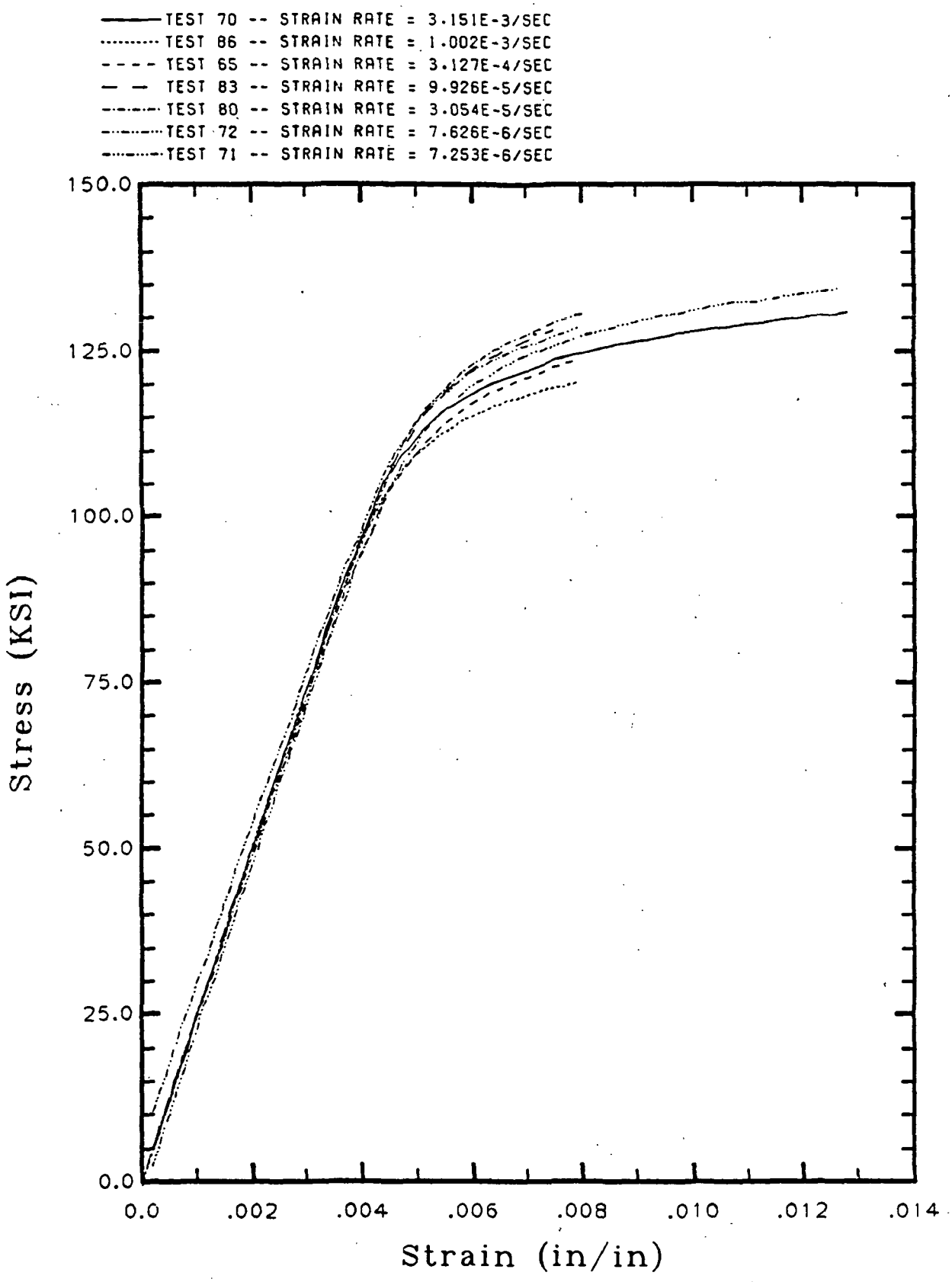

Figure C.1 - Experimental Monotonic Tests

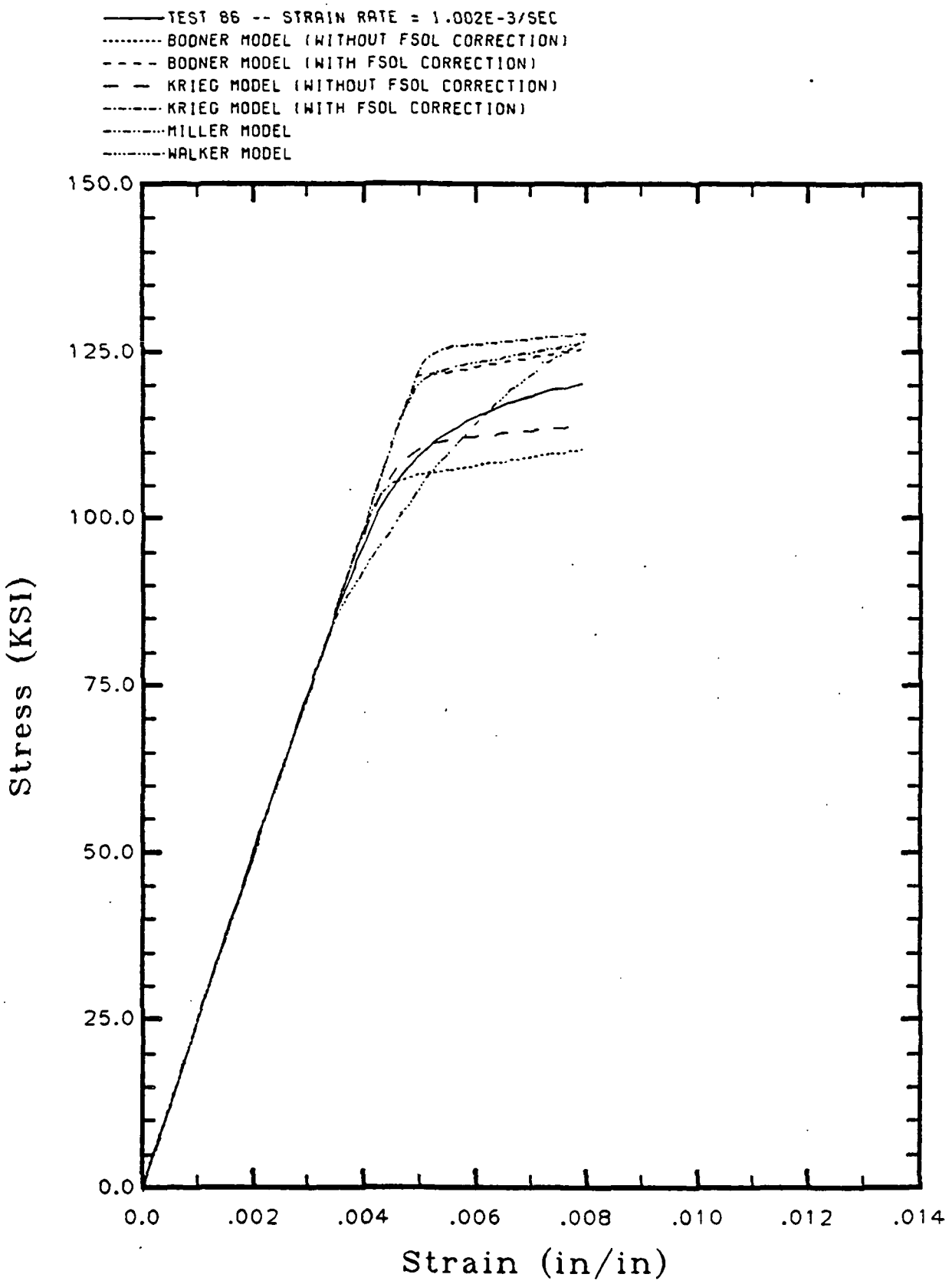

Figure C.2 - Model Response As Compared to Test 86

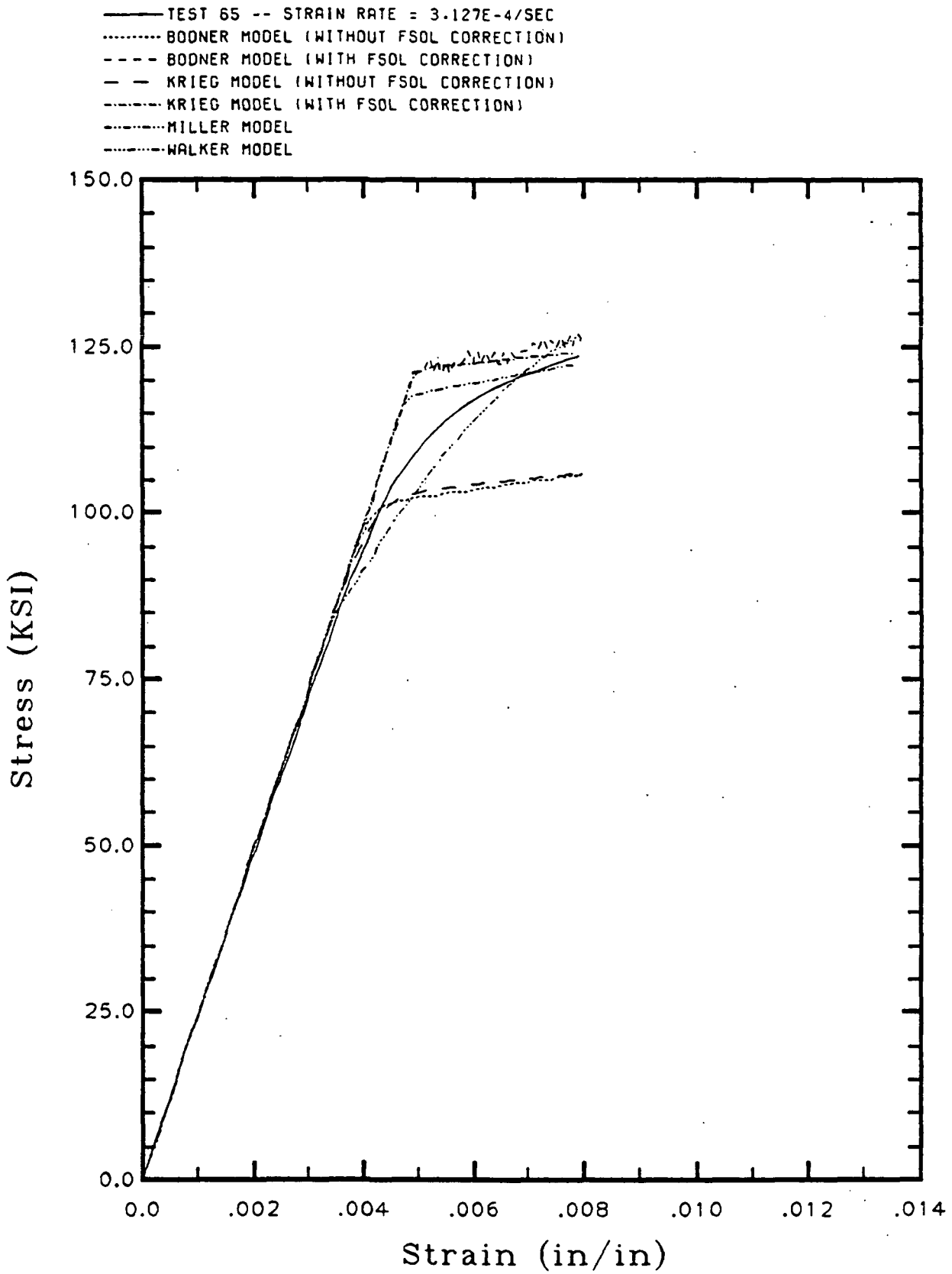

Figure C.3 - Model Response as Compared to Test 65

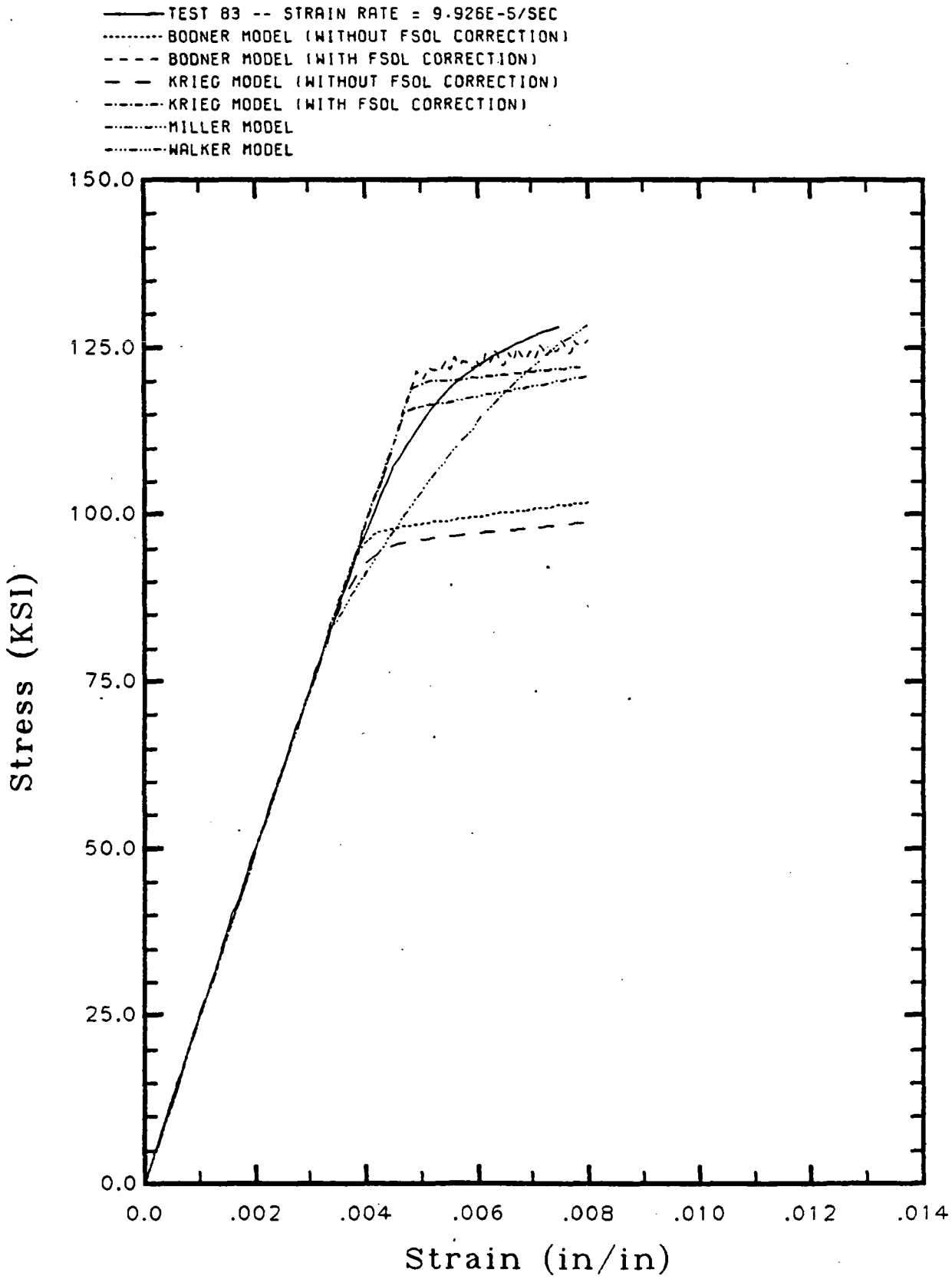

Figure C.4 - Model Response as Compared to Test 83

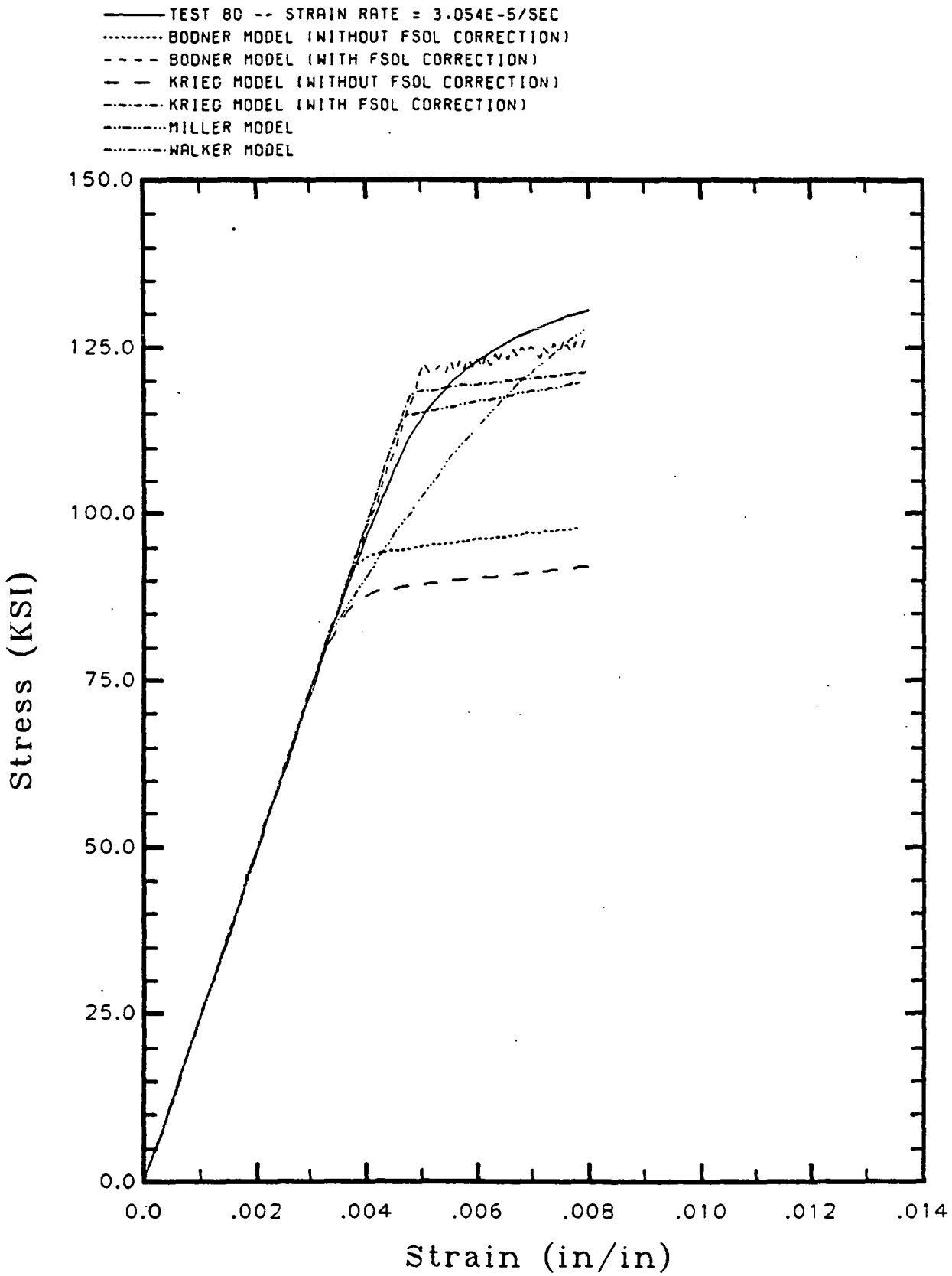

Figure C.5 - Model Response as Compared to Test 80

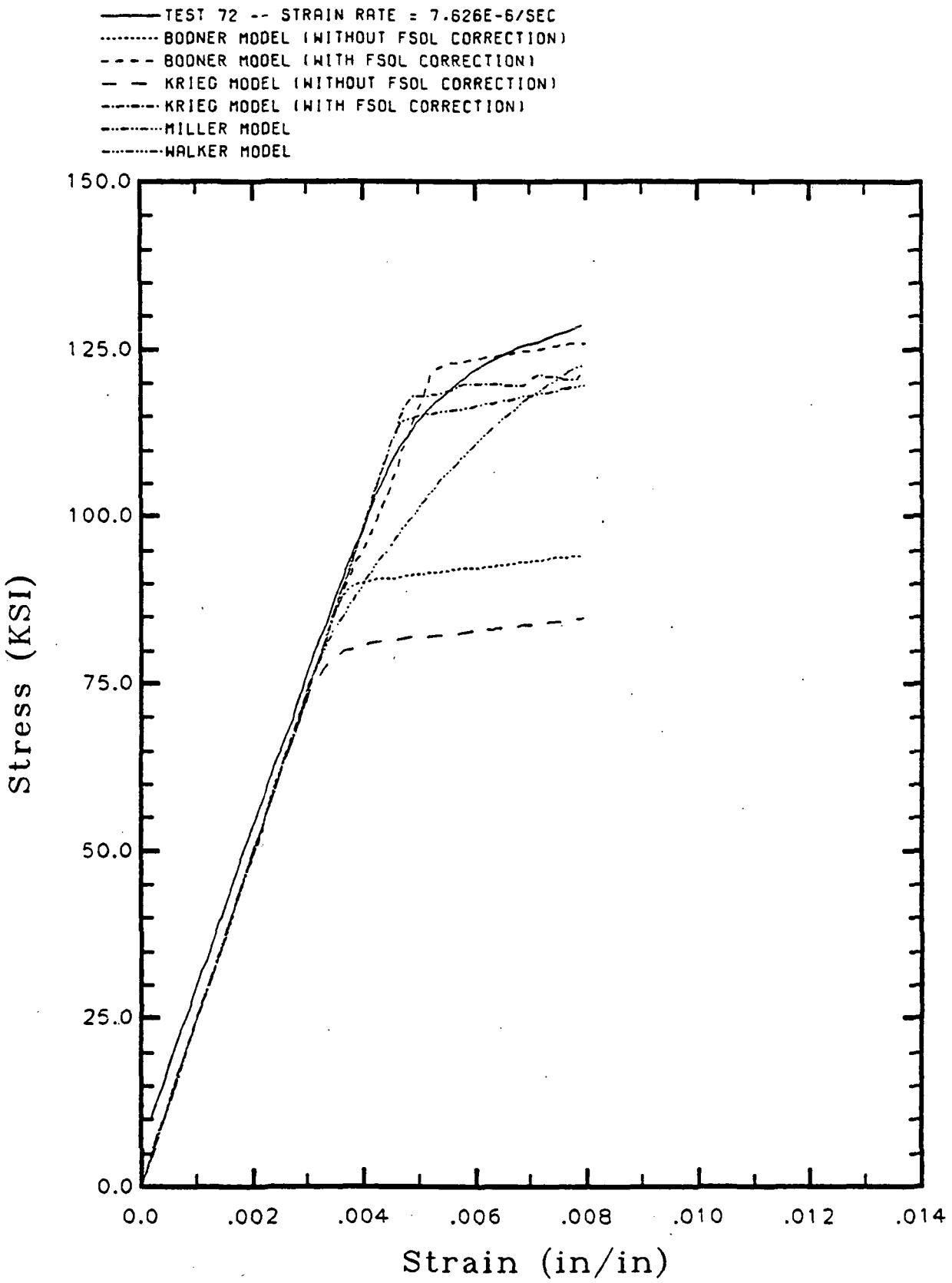

Figure C.6 - Model Response as Compared to Test 72

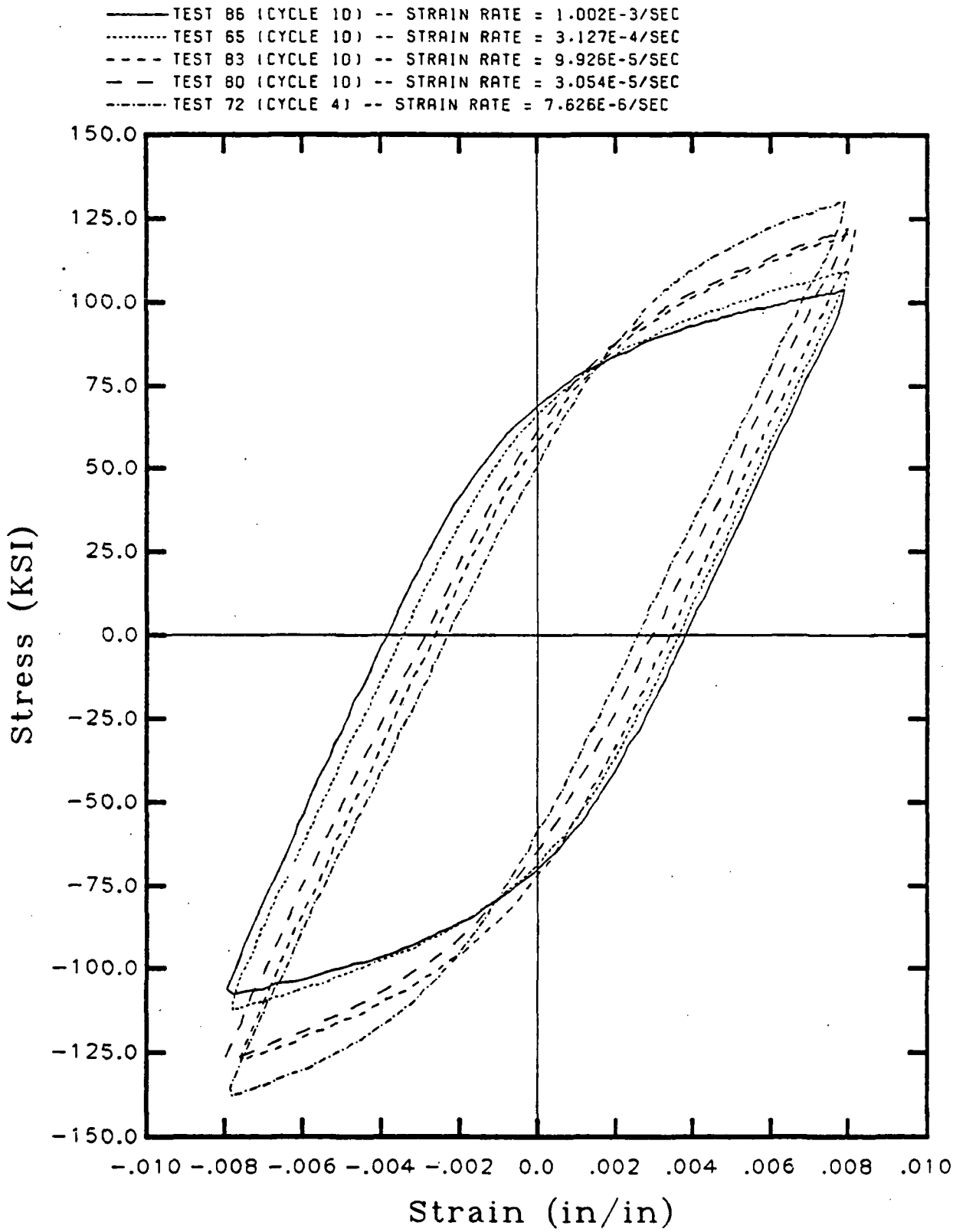

Figure C.7 - Experimental Hysteresis Loops

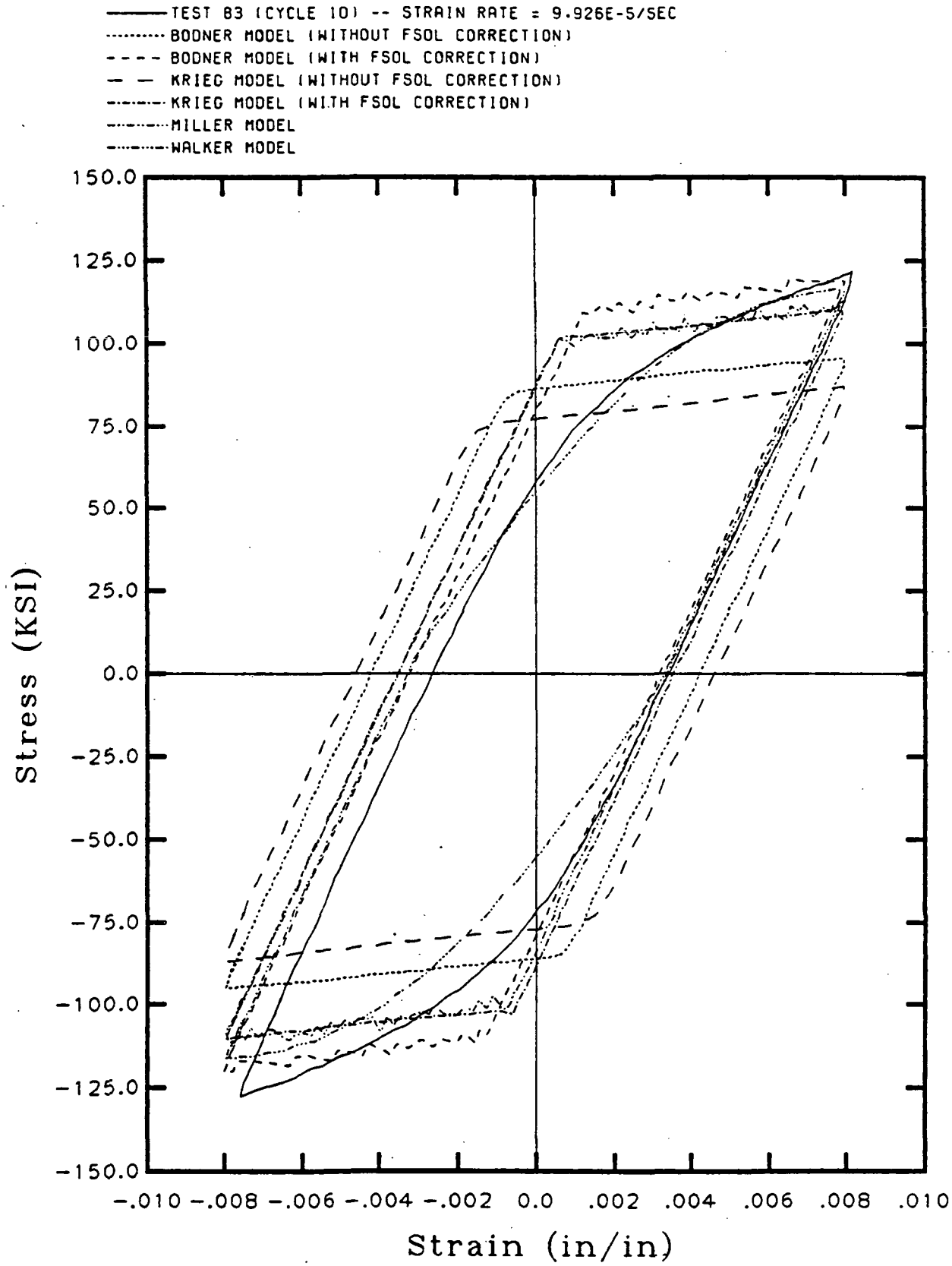

Figure C.9 - 10th Cycle Hysteresis Loops for Test 83

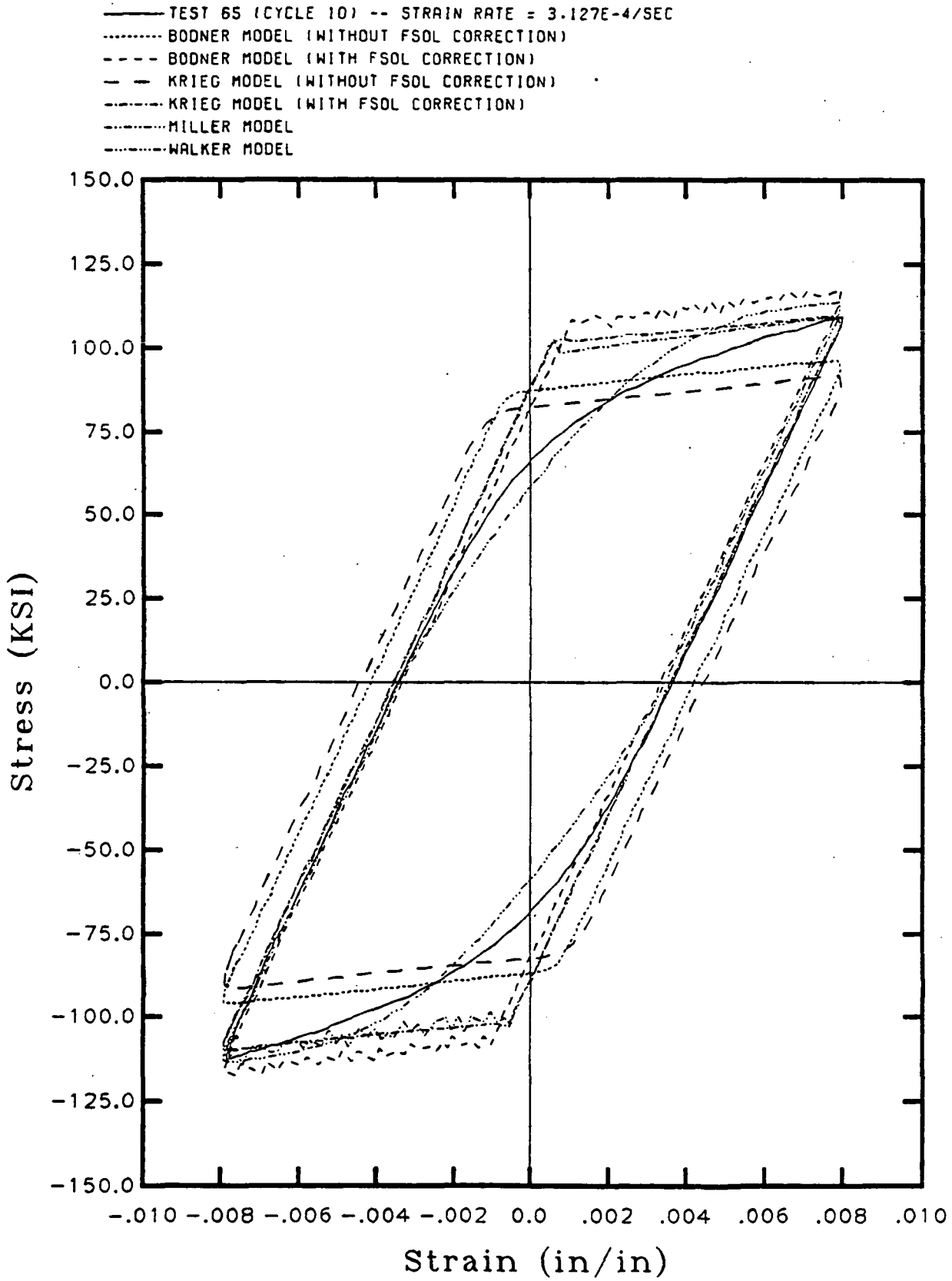

Figure C.8 10th Cycle Hysteresis Loops for Test 65

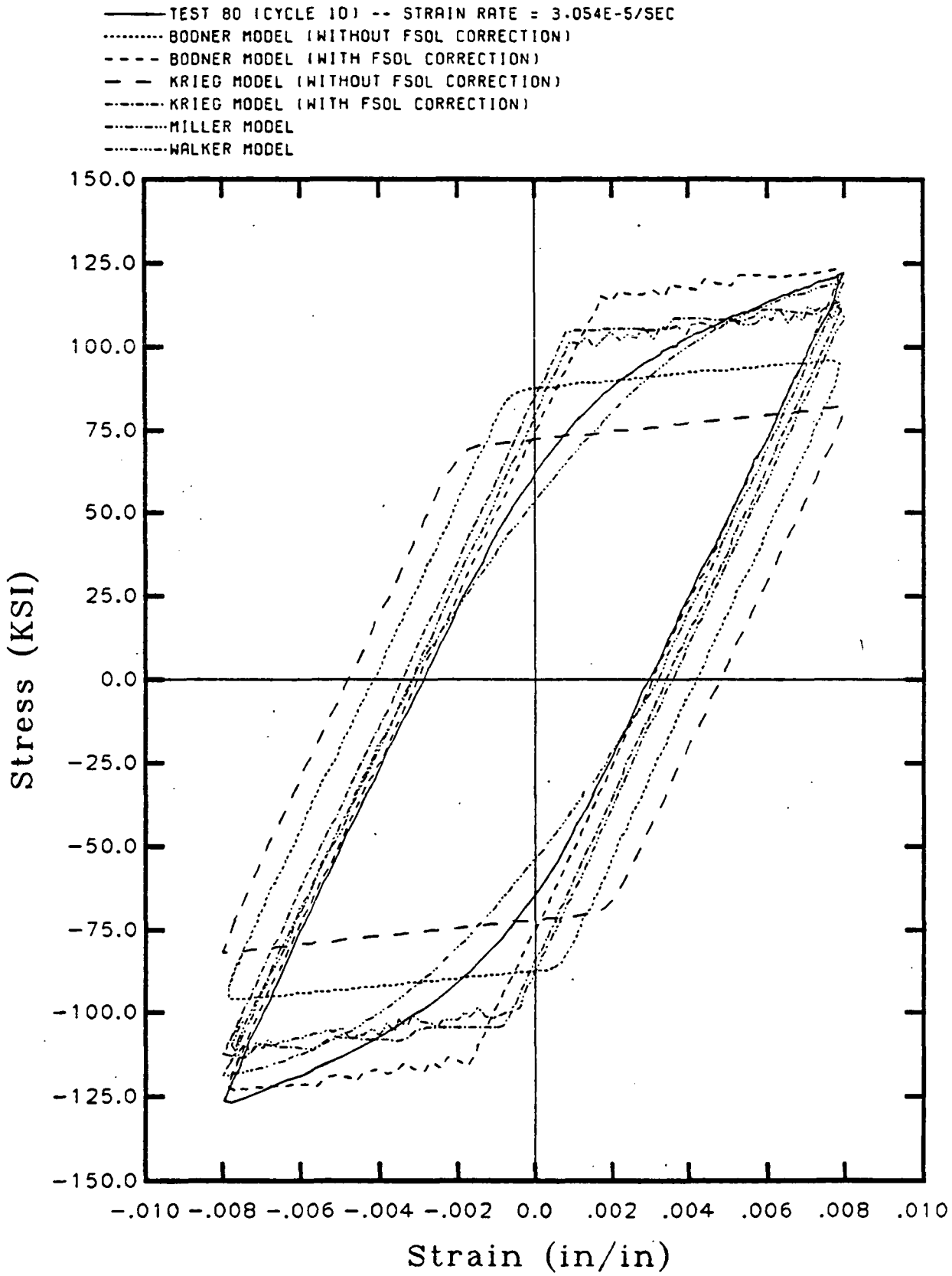

Figure C.10 - 10th Cycle Hysteresis Loops for Test 80

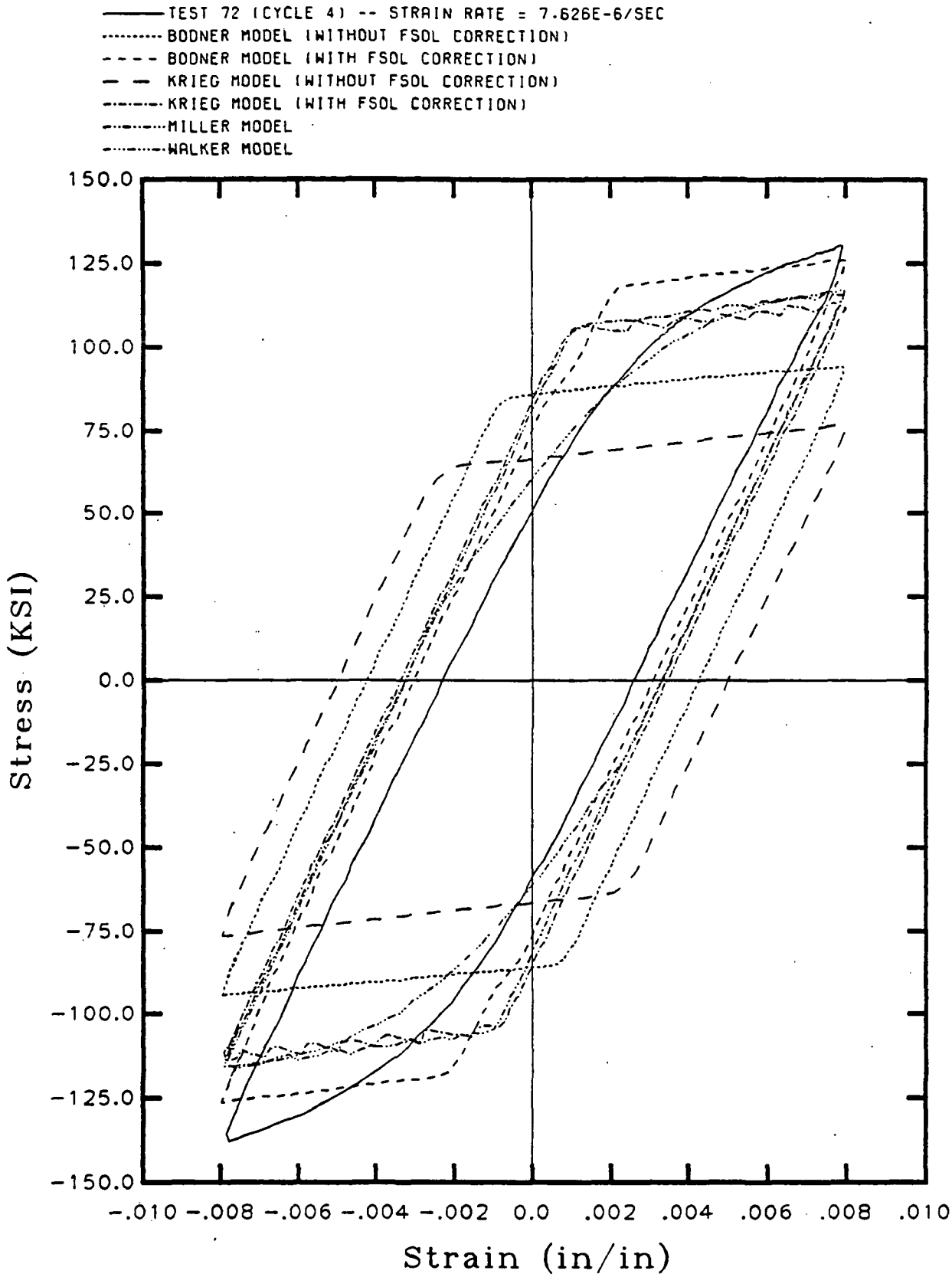

Figure C.11 - 4th Cycle Hyeteresis Loops for Test 72

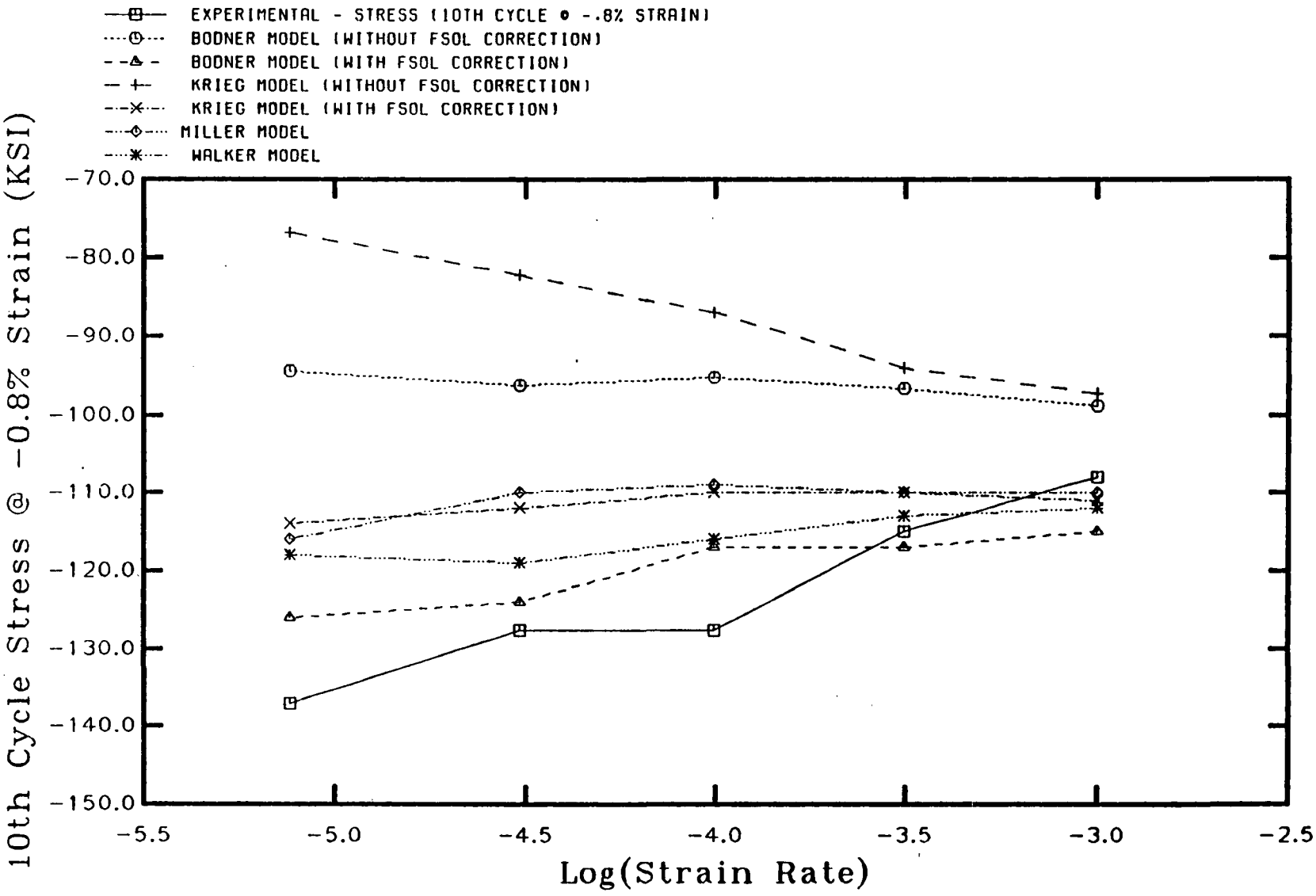

Figure C.12 - Stress-Strain Response at -.8% Saturated Cycle

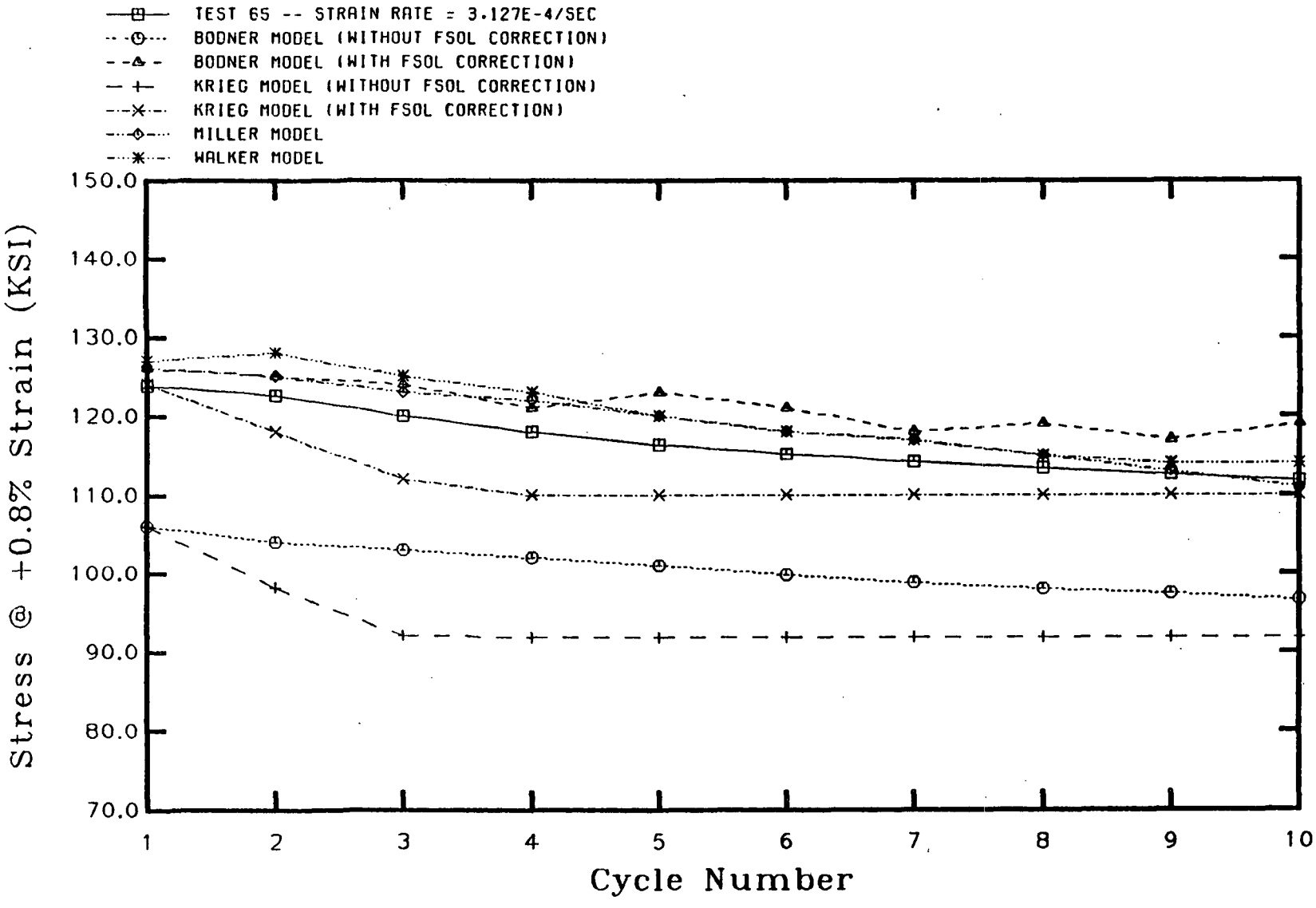

Figure C.13 - Test 65 +.8% Response at Each Cycle

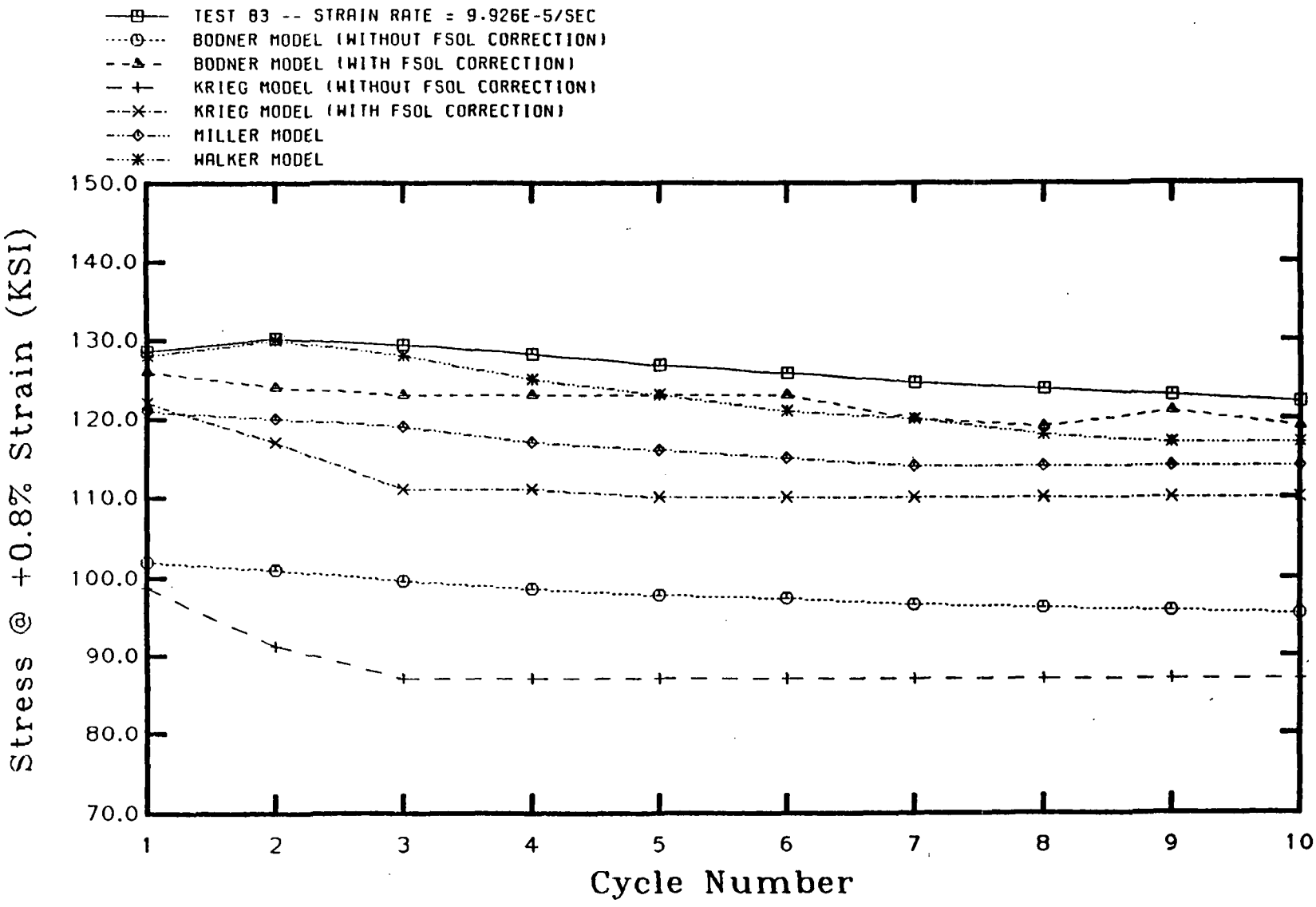

Figure C.14 - Test 83 +.8% Response at Each Cycle

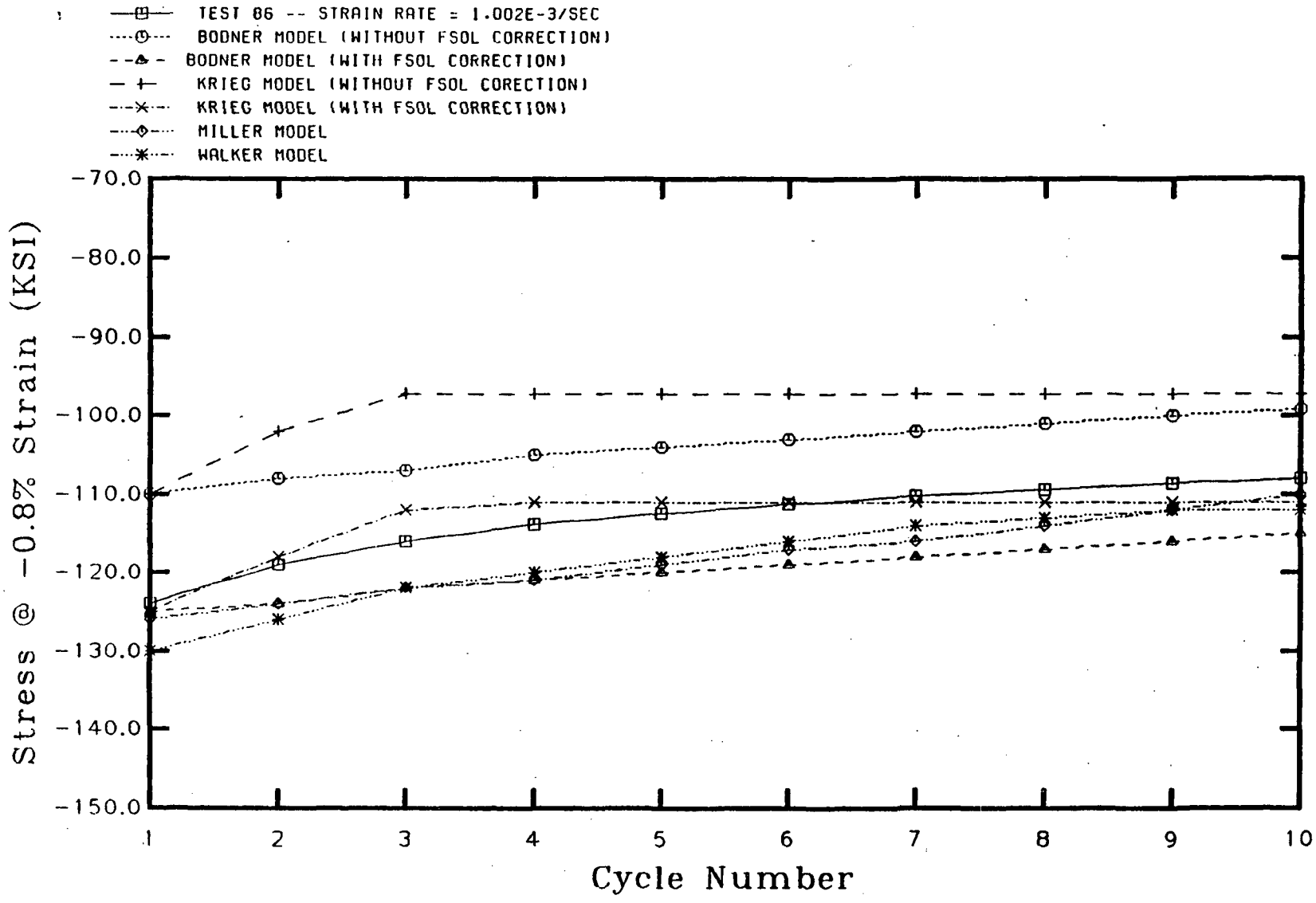

Figure C.15 - Test 86 -.8% Response at Each Cycle

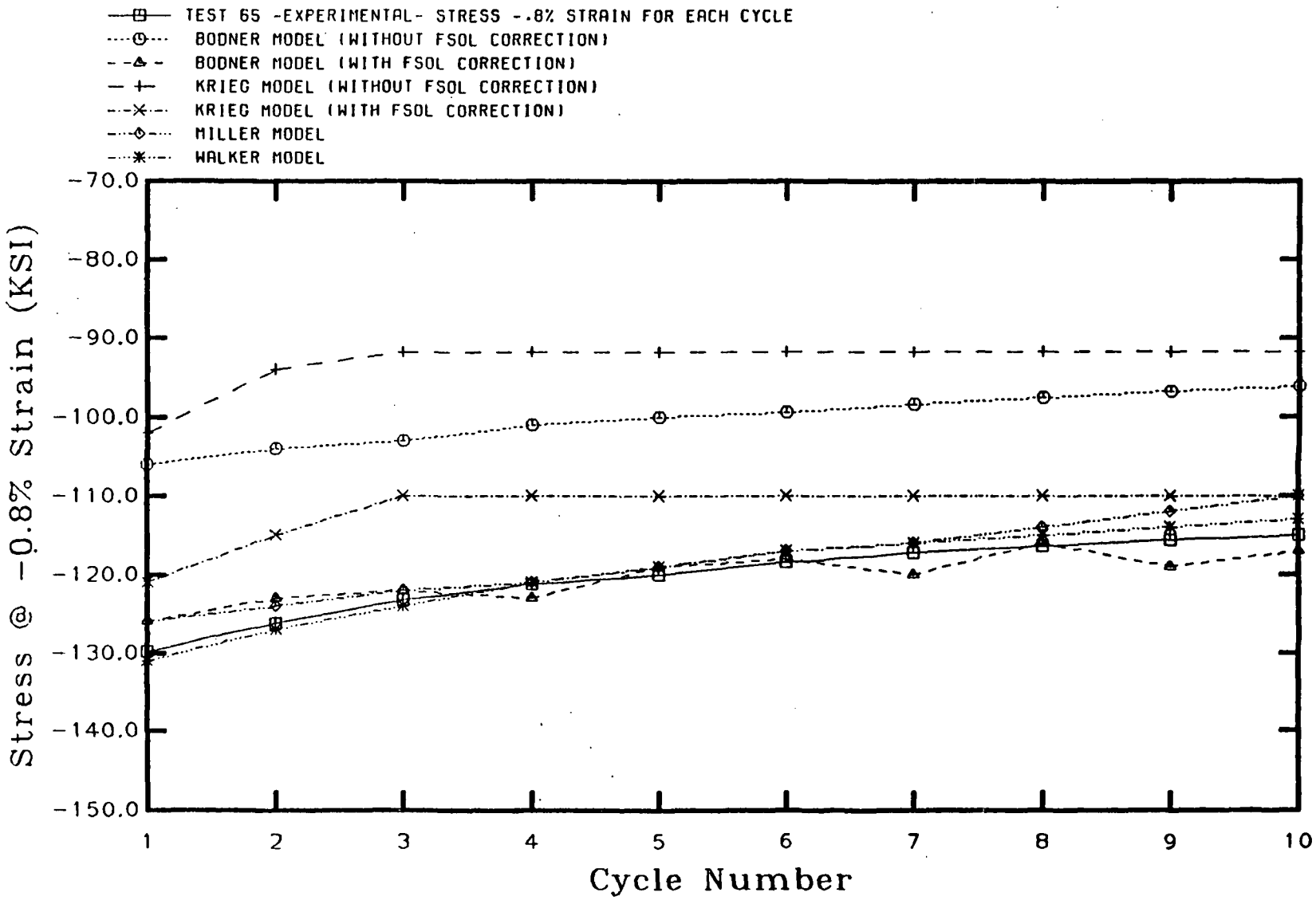

Figure C.16 - Test 65 -.8% Response at Each Cycle

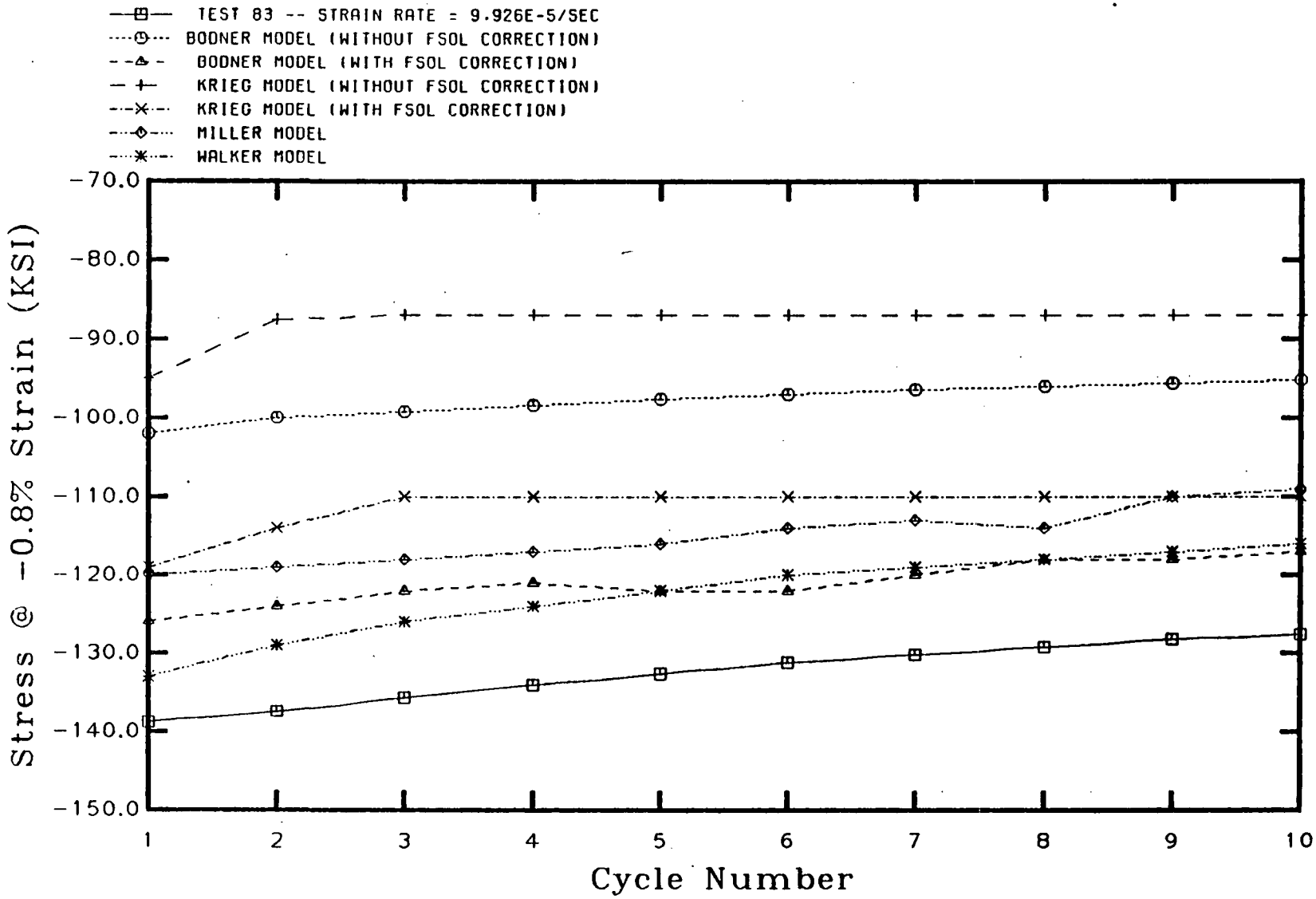

Figure C.17 - Test 83 -.8% Response at Each Cycle

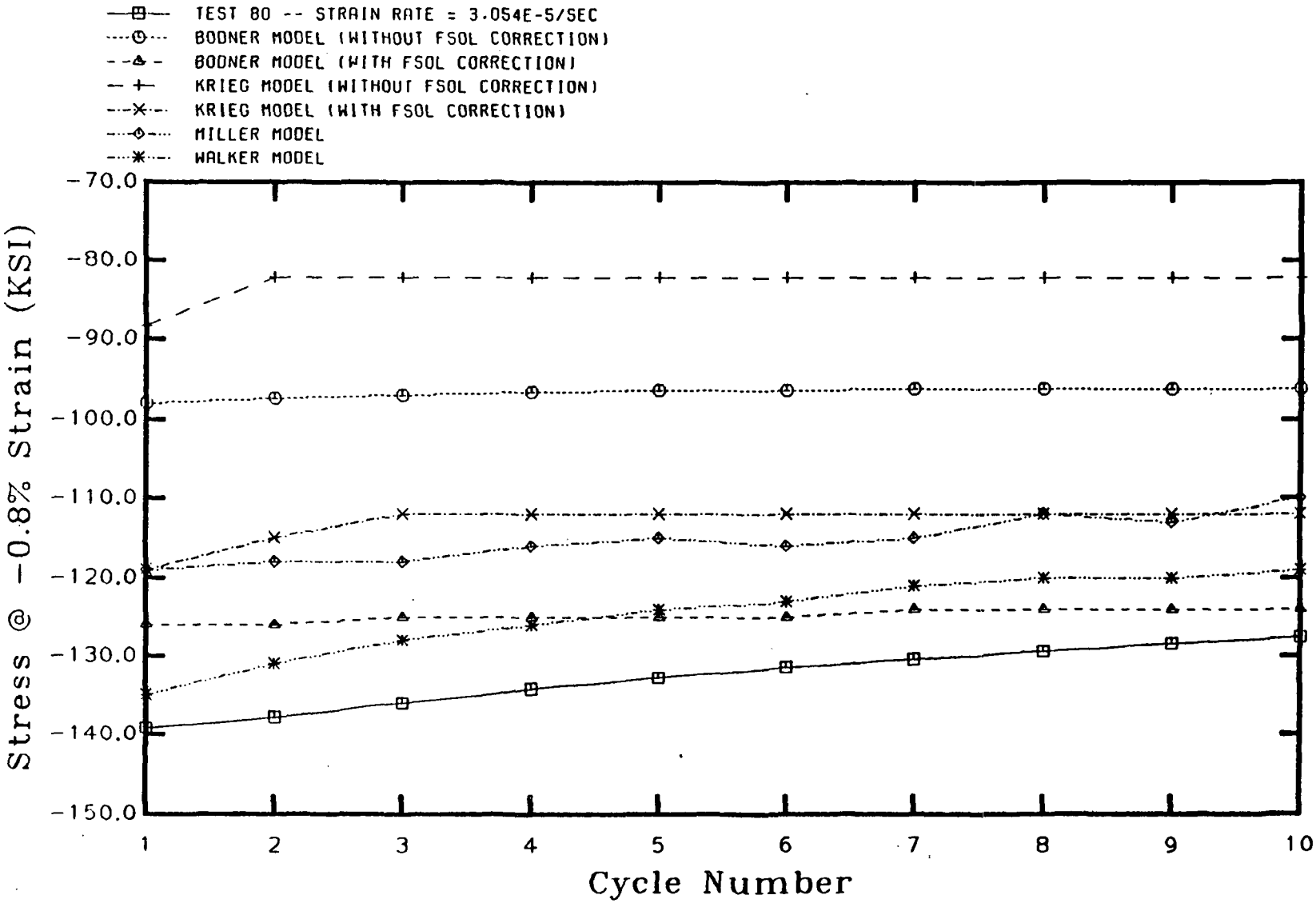

Figure C.18 - Test 80 -.8% Response at Each Cycle

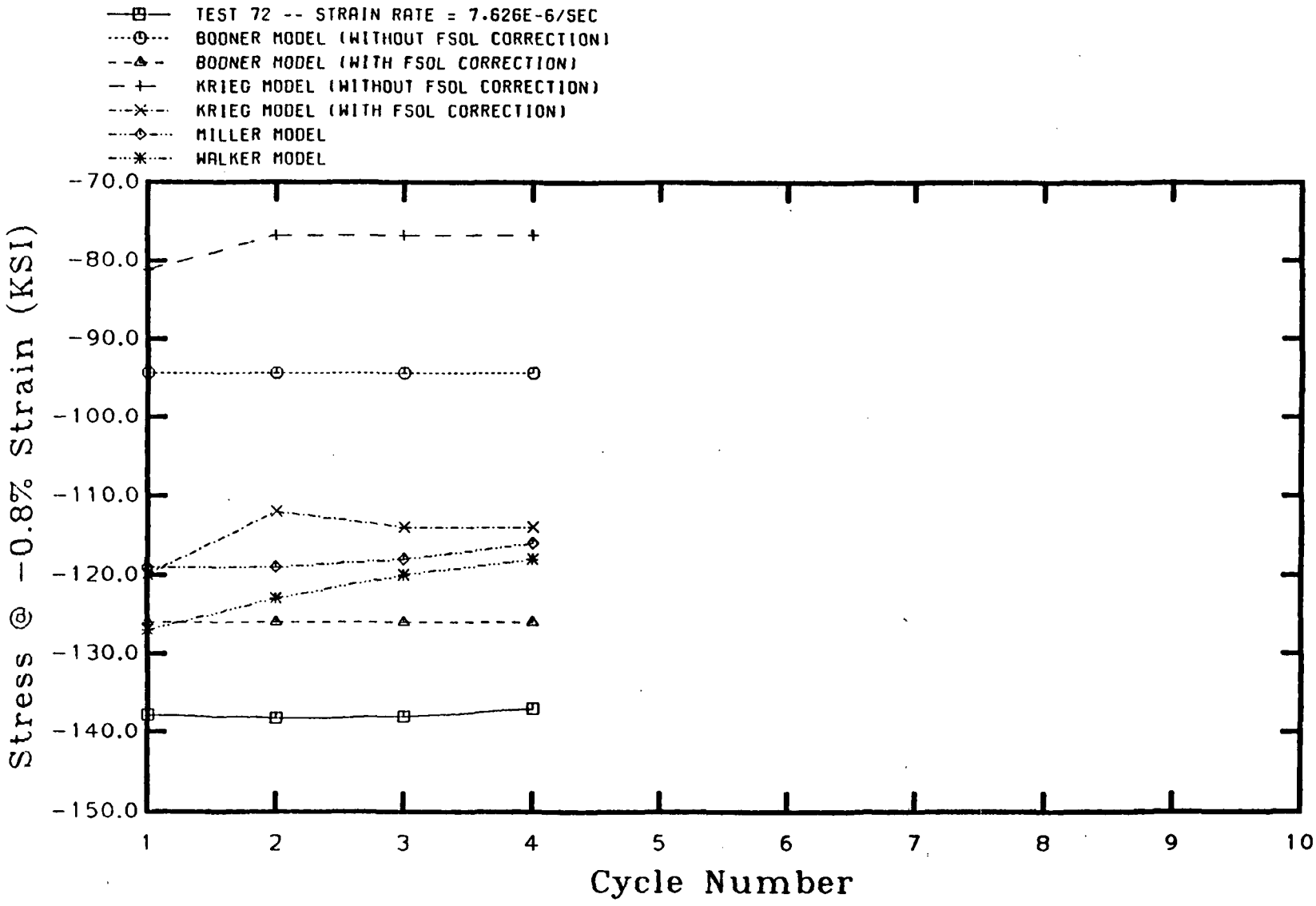

Figure C.19 - Test 72 -.8% Response at Each Cycle

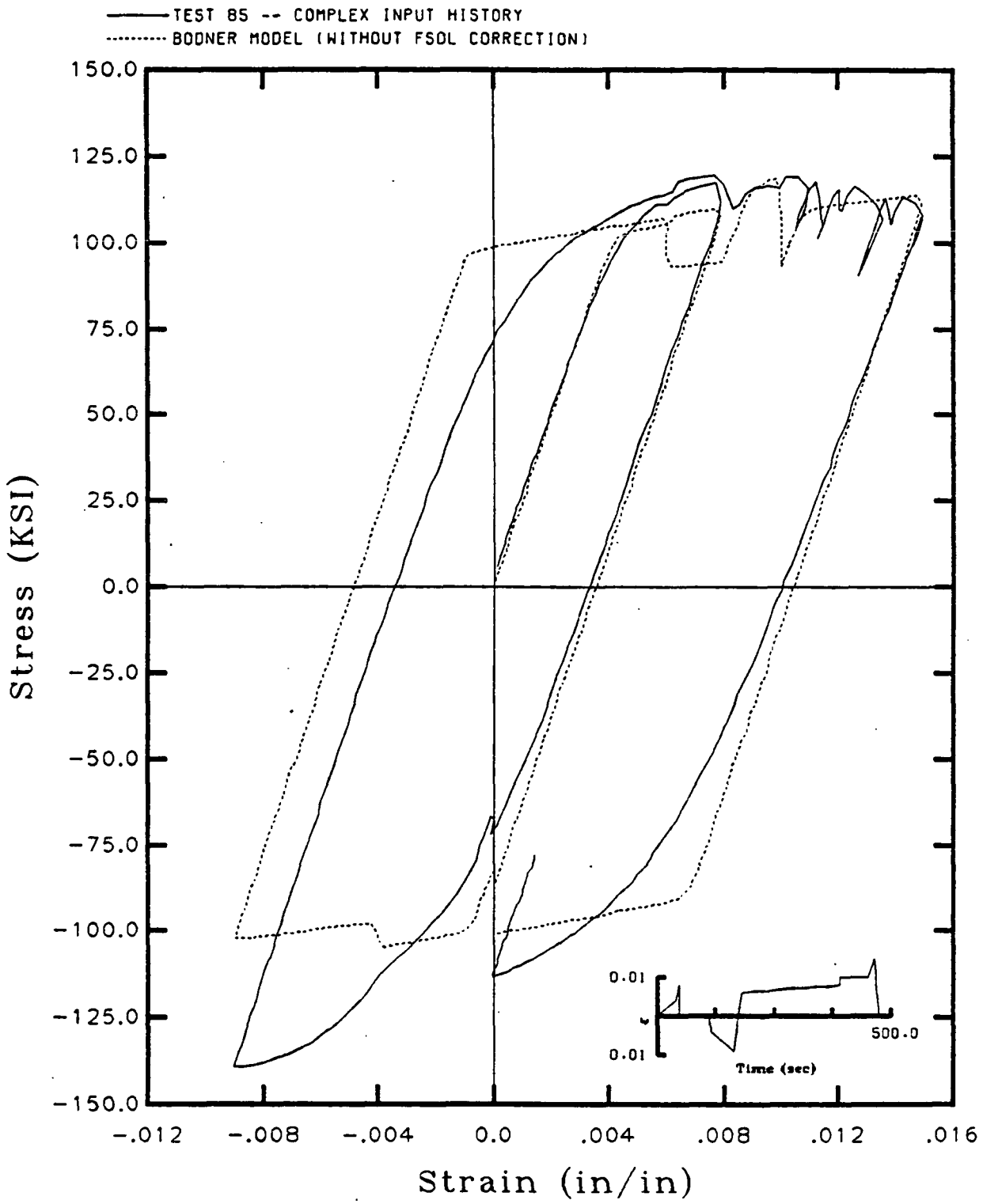

Figure C.20 - Test 85 Bodner's Uncorrected Model

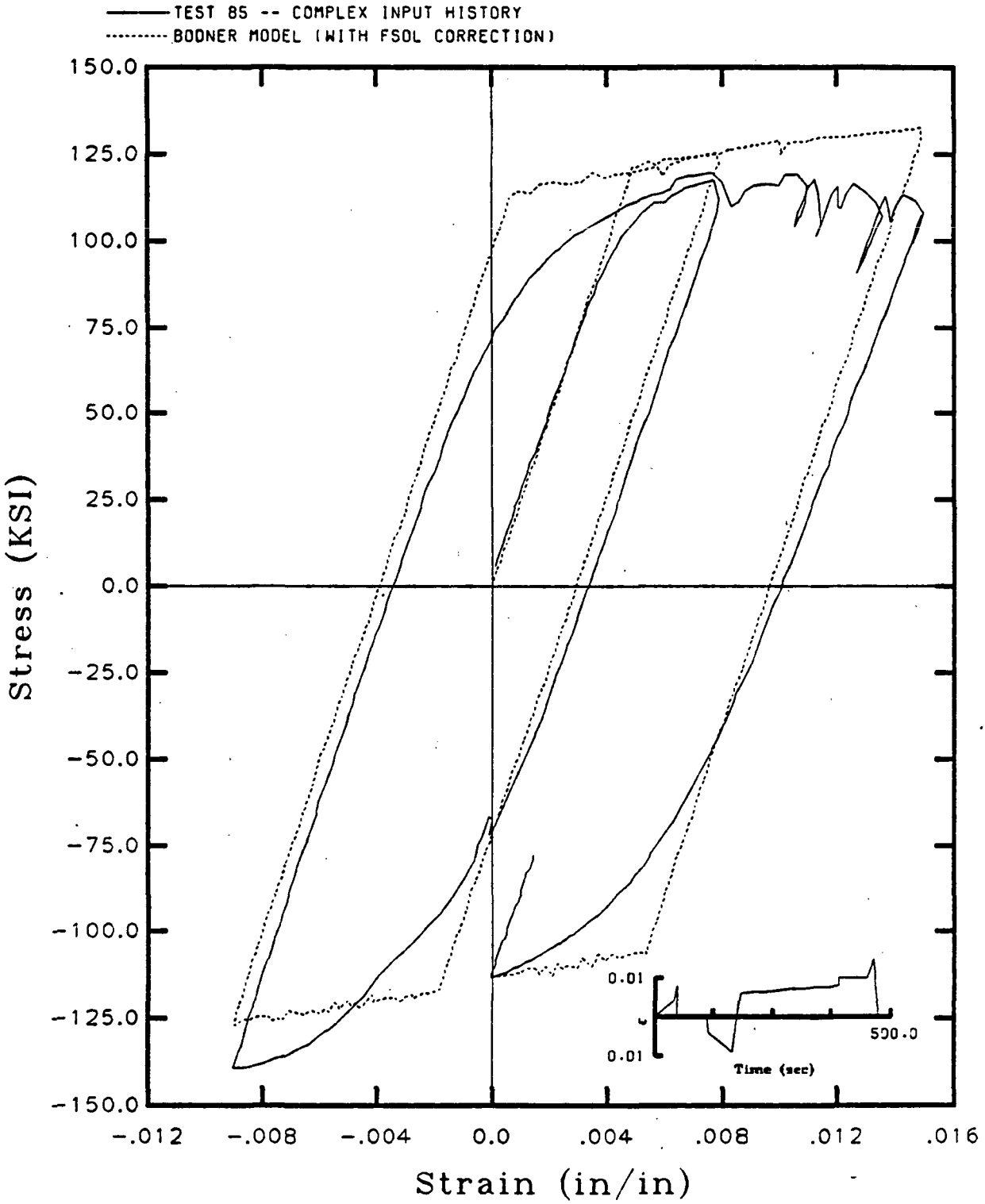

Figure C. 21 - Test 85 Bodner's Corrected Model

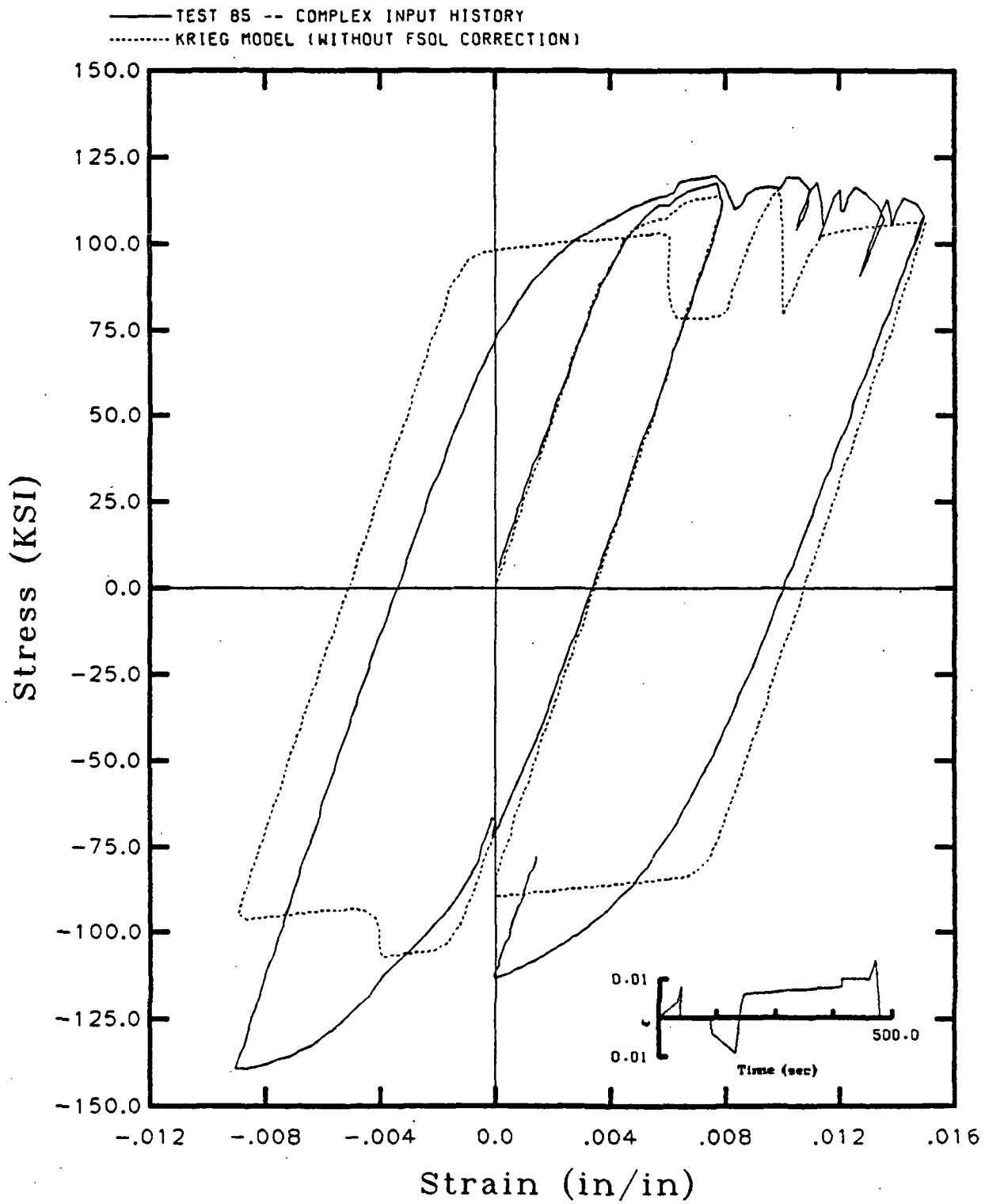

Figure C.22 - Test 85 Uncorrected Model of Krieg, et al.

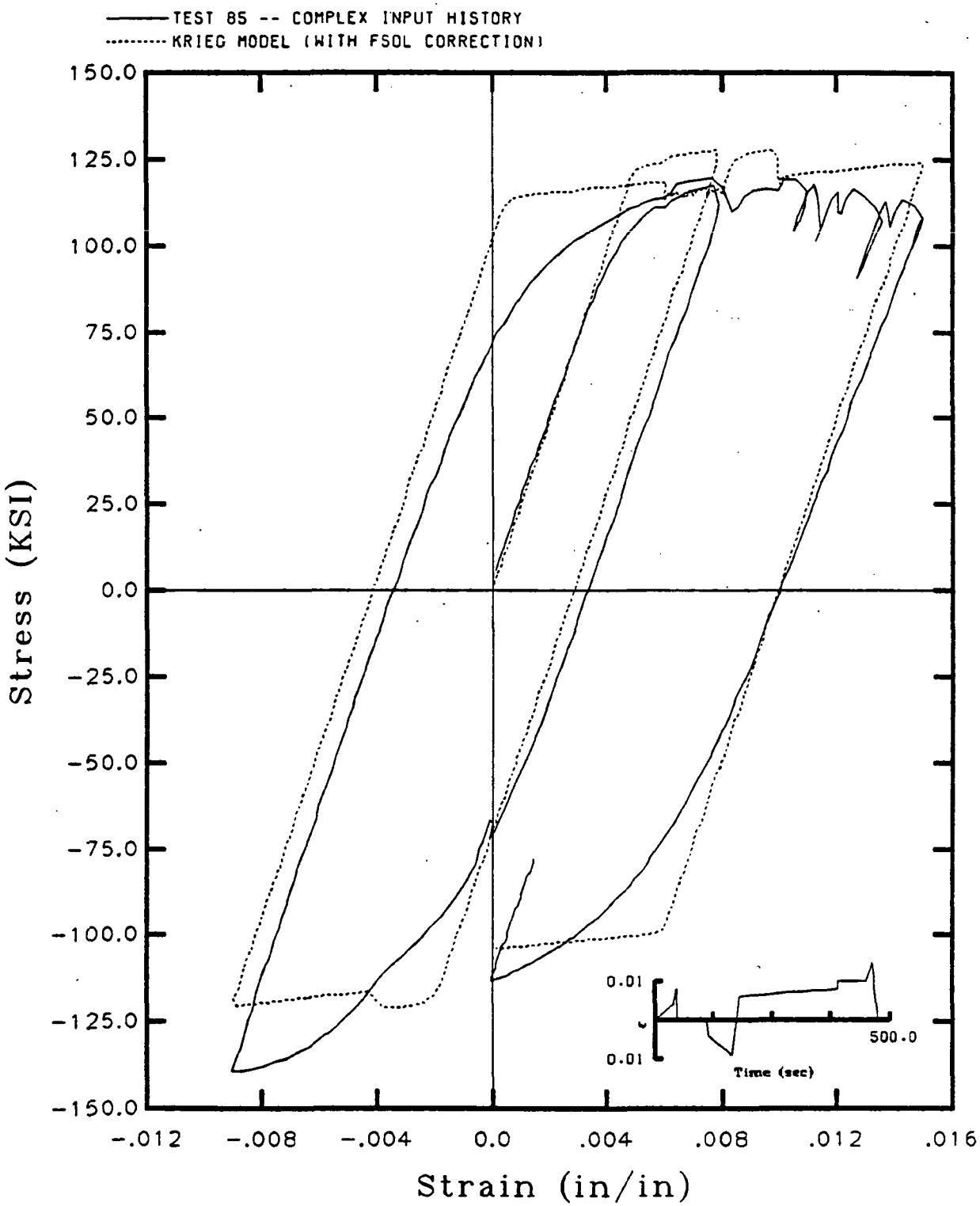

Figure C.23 - Test 85 Corrected Model of Krieg, et al.

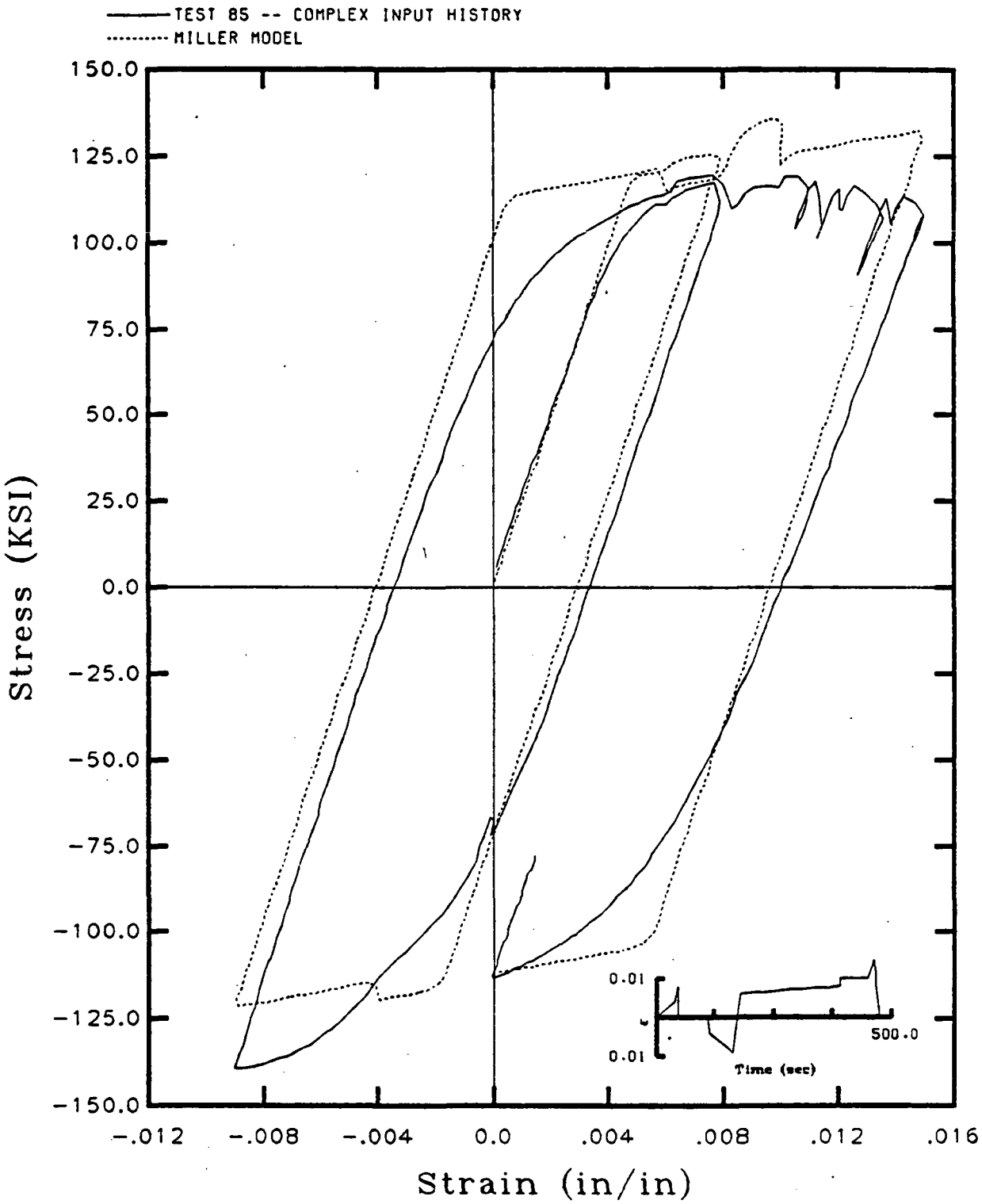

Figure C.24 - Test 85 Miller's Model

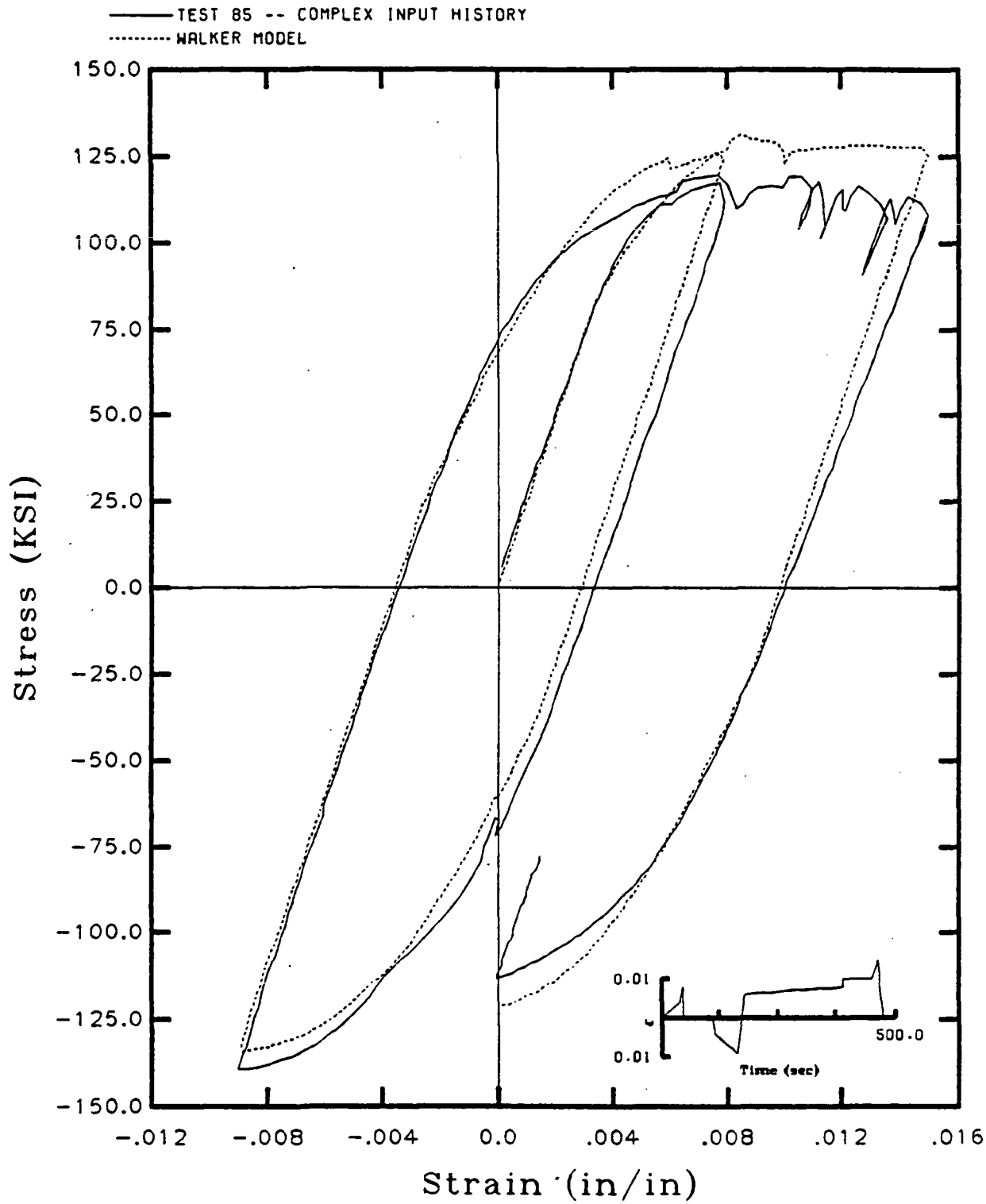

Figure C.25 - Test 85 Walker's Model

APPENDIX D - EXPERIMENTAL COMPUTER PROGRAMS

The appendix presents the test software developed for this work which would be necessary to repeat or expand on this work. All programs are written in MTS Basic. Program VCYC6 allows the user to run cyclic tests, monotonic tension tests, and cyclic tests with creep hold times. The test parameters can be changed on the fly. Data acquisition for both the cyclic test and the hold times as provided for. All data is stored in binary form on floppy diskettes. The program CRP3 performs creep tests and creep stress drop tests. The program BACK2 allows the user to analyze cyclic creep hold time data on creep stress drop data. The program does a linear regression curve fit through the data. The number of points used for the curve fit is chosen by the user for each step.

GMPLT8 analyzes each test with the gamma plot. The stress inelastic strain history is calculated and a stress-inelastic strain polynomial curve fit performed. This curve fit is differentiated at each data point and divided by the value of stress at that point to create a $\frac{d\sigma}{dW_p}$ versus σ plot. Linear regression curve fits for the upper and lower slopes are performed based on the mumber of points input by the user. This version is configured to automatically step through a cyclic test and produce gamma plot for each half cycle. The program WALK2 performs the same functions with the theta plot.

VCYC6

```
1 REM CYCLIC TEST - STRAIN CONTROL
8 CLRTXWIN
10 REM WRITTEN BY GEORGE JAMES AND PAUL SEAN HILL - JUNE 1985
20 PRINT 'THIS PROGRAM PERFORMS A CYCLIC STRAIN CONTROLLED TEST WHICH
IS'
24 PRINT 'IS CAPABLE OF SWITCHING STRAIN LIMITS DURING THE TEST.'
28 PRINT
30 PRINT 'THE PROGRAM SWITCHES FROM LOAD TO STRAIN CONTROL AND IT IS IM-
'
40 PRINT 'PORTANT THAT THE DISPLAY #2 SHOWS A POSITIVE VALUE FOR THIS'
45 PRINT 'SWITCH.'
47 PRINT
70 PRINT 'THE TEST DATA IS STORED ON 5.25" FLEXIBLE DISC ON DU1: IN
BINARY'
100 PRINT 'FORM.  RELAXATION DATA IS STORED IN HARD COPY FORM ONLY.' \
PRINT
110 PRINT 'THE CAPABILITY TO PRINT AND PLOT THE DATA IS PROVIDED FOR
THE'
120 PRINT 'CURRENT TEST OR FOR EXISTING FILES.'
125 PRINT  \ PRINT
126 PRINT  \ PRINT
130 DIM A(64,3),B(64,3),M(2,2),M0(2,2),M1(2,2),M2(2,2)
140 REM ----------------
150 REM PRINT ONLY INPUT
160 REM ----------------
170 PRINT
180 PRINT 'TYPE'; \ TXTBOLD \ PRINT ' TEST';
182 TXTNORMAL \ PRINT ' IF YOU WANT TO RUN A NEW TEST'
184 PRINT  \ PRINT '                    OR'
186 PRINT
190 PRINT 'TYPE'; \ TXTBOLD \ PRINT ' PRINT'; \ TXTNORMAL
195 PRINT ' IF YOU WANT TO PRINT EXISTING FILES'
196 PRINT
200 INPUT R$
210 IF R$='TEST' THEN GO TO 330
220 IF R$='PRINT' THEN GO TO 240
225 TXTINVERS
230 PRINT 'INVALID ENTRY, TYPE TEST OR PRINT' \ TXTNORMAL \ GO TO 170
240 PRINT 'ENTER FILE NAME (<=5 CHARACTERS)'; \ INPUT F$
250 IF LEN(F$)<=5 THEN GO TO 270
255 TXTINVERS
260 PRINT 'INVALID FILE NAME' \ TXTNORMAL \ GO TO 240
270 F1$='DU1:'+F$+'C.DAT'
280 F2$='DU1:'+F$+'.DAT'
285 P0=0
290 GO TO 6900
300 REM ----------
310 REM TEST INPUT
320 REM ----------
```

```
330 GO TO 350
340 CLOSE #1,2,3
350 PRINT
360 PRINT 'ENTER FILE NAME (<=5 CHARACTERS)'; \ INPUT F$
370 IF LEN(F$)<=5 THEN GO TO 390
375 TXTINVERS
380 PRINT 'INVALID FILE NAME ' \ TXTNORMAL \ GO TO 350
390 F1$='DU1:'+F$+'C.DAT'
400 F2$='DU1:'+F$+'.DAT'
410 OPEN F1$ FOR OUTPUT AS FILE 1, FILESIZE 2
420 OPEN F2$ FOR OUTPUT AS FILE 2, FILESIZE 30
430 OPEN 'LP:' FOR OUTPUT AS FILE 3
431 PRINT 'ENTER THE SAMPLE NUMBER'; \ INPUT B$
432 PRINT 'ENTER THE SAMPLE TEMPERATURE IN DEGREES CELSIUS'; \ INPUT A$
440 PRINT 'ENTER LOAD CALIBRATION (LBS/VOLT)'; \ INPUT LO
460 PRINT 'ENTER EXTENSOMETER CALIBRATION (IN/VOLT)'; \ INPUT XO
470 PRINT 'ENTER GAUGE LENGTH (IN)'; \ INPUT GO
480 PRINT 'ENTER GAUGE AREA (IN*IN)'; \ INPUT AO
490 PRINT 'ENTER STRAIN RATE (IN/IN/SEC)'; \ INPUT RO
500 R1=(RO*GO)/(XO*10)
510 PRINT 'ENTER MAXIMUM STRAIN (IN/IN)'; \ INPUT SO
520 S1=(SO*GO)/(XO*10)
530 PRINT 'ENTER MINIMUM STRAIN (IN/IN)'; \ INPUT S2
540 S3=(S2*GO)/(XO*10)
550 PRINT 'ENTER TIME/POINT (SEC)'; \ INPUT TO
560 PRINT 'ENTER LENGTH OF DATA ACQUISITION (CYCLES)'; \ INPUT CO
570 C1=2*CO
580 T1=((2*CO)*((SO-S2)/(RO*TO)))
590 PRINT 'NUMBER OF POINTS EXPECTED    ';T1
620 PRINT 'ENTER LOAD RANGE DURING HOLD TIMES (1,2,3, OR 4)'; \ INPUT L1
625 PRINT 'ENTER LOAD CALIBRATION FOR HOLD TIMES (LBS/VOLT)'; \ INPUT L2
630 PRINT 'ENTER TIME/POINT DURING HOLD TIMES (MIN)'; \ INPUT T2
632 CLRTXWIN
633 PRINT 'SAMPLE NUMBER                    ';B$
634 PRINT 'SAMPLE TEMPERATURE (DEG C)       ';A$
635 PRINT 'LOAD CALIBRATION   (LBS/VOLT)    ';LO
640 PRINT 'EXTENSOMETER CAL.  (IN/VOLT)     ';XO
650 PRINT 'GAUGE LENGTH       (IN)          ';GO
660 PRINT 'GAUGE AREA         (IN*IN)       ';AO
680 PRINT 'STRAIN RATE        (IN/IN/SEC)   ';RO
690 PRINT 'MAXIMUM STRAIN     (IN/IN)       ';SO
700 PRINT 'MINIMUM STRAIN     (IN/IN)       ';S2
710 PRINT 'TIME/POINT         (SEC)         ';TO
720 PRINT 'LENGTH OF D.A.     (CYCLES)      ';CO
730 PRINT 'NUMBER OF POINTS                 ';T1
735 PRINT 'HOLD-LOAD RANGE                  ';L1
740 PRINT 'HOLD-LOAD CAL.     (LBS/VOLT)    ';L2
745 PRINT 'HOLD-TIME/POINT    (MIN)         ';T2
750 PRINT  \ PRINT 'ARE ALL PARAMETERS OK ';
752 TXTBOLD \ PRINT '(Y/N)'; \ TXTNORMAL \ INPUT R$
```

```
760 IF R$='N' THEN GO TO 340
780 PRINT #1,LO;',';XO;',';GO;',';AO;',';RO;',';R1;',';SO;',';S1
790 PRINT #1,S2;',';S3;',';TO;',';CO;',';T1;',';L1;',';L2;',';T2
800 REM -------------------------
810 REM DATA ACQUISITION FUNCTIONS
820 REM -------------------------
830 CLINIT
880 CKSTOP
890 CKTIME(1,.01,K)
900 I1=INT(TO/K)
910 ADTIMED(1,A,B,1,I1)
920 ADSLAVE(1,2,6)
940 ADRMAX(3,M,1)
950 ADRMIN(3,MO,1)
960 ADRMAX(3,M1,2)
970 ADRMIN(3,M2,2)
980 REM -------------------
990 REM REAL TIME PLOT INPUT
1000 REM -------------------
1010 PRINT  \ PRINT 'DO YOU WANT A REAL TIME PLOT?'; \ TXTBOLD
1015 PRINT ' (Y/N)'; \ TXTNORMAL \ INPUT R$
1030 IF R$='N' THEN GO TO 1060
1050 G=1 \ GO TO 1070
1060 G=0 \ GO TO 1209
1070 X$='IN/IN'
1080 PRINT  \ PRINT 'REAL TIME PLOT PARAMETERS' \ PRINT
1090 PRINT 'ENTER MAXIMUM STRAIN'; \ INPUT X2
1100 PRINT 'ENTER MINIMUM STRAIN'; \ INPUT X1
1110 PRINT 'ENTER STRAIN STEP SIZE'; \ INPUT X3
1120 Y$='PSI' \ PRINT
1130 PRINT 'ENTER MAXIMUM STRESS'; \ INPUT Y2
1140 PRINT 'ENTER MINIMUM STRESS'; \ INPUT Y1
1150 PRINT 'ENTER STRESS STEP SIZE'; \ INPUT Y3
1160 PRINT 'ARE THESE PARAMETERS OK?'; \ TXTBOLD \ PRINT '(Y/N)';
1165 TXTNORMAL \ INPUT R$
1180 IF R$='N' THEN GO TO 1090
1200 REM --------------
1203 REM TEST FUNCTIONS
1206 REM --------------
1209 CLRTXWIN
1212 TXTNORMAL \ PRINT  \ TXTINVERS \ TXTSPOS(1,5,10)
1215 PRINT 'KEY INTERUPT SUMMARY' \ TXTNORMAL
1218 TXTSPOS(1,8,1) \ PRINT '<ESC>E - END TEST'
1221 PRINT '<ESC>H - HOLD TEST FOR RELAXATION'
1224 PRINT '<ESC>R - RESUME TEST AFTER HOLD'
1227 PRINT '<ESC>P - CHANGE CYCLE PARAMETERS'
1228 PRINT '<ESC>A - HALT DATA ACQUISITION AND CONTINUE TEST'
1230 PRINT  \ TXTFLASH \ PRINT  \ PRINT  \ PRINT
1232 PRINT 'BRING UP THE HYDRAULIC PRESSURE.....'
1233 PRINT 'ZERO LOAD WITH SET POINT CONTROL AND STRAIN WITH ZERO
```

```
ADJUST'
1234 PRINT 'PLACE PRINTER ON SWITCH "A" '
1235 TXTNORMAL \ PRINT  \ PRINT
1236 PRINT 'HIT RETURN TO SWITCH TO STRAIN CONTROL.'
1240 INPUT R$
1242 PRINT 'ZERO STRAIN AGAIN WITH SET POINT CONTROLLER' \ TXTNORMAL
1245 KBINT('E',3, LINE 4600 )
1248 KBINT('H',4, LINE 1266 )
1251 KBINT('R',4, LINE 1269 )
1254 KBINT('P',5, LINE 12000 )
1255 KBINT('A',3, LINE 13000 )
1257 KBENB
1260 G1=0
1263 GO TO 1272
1266 G1=1 \ RETURN
1269 G1=2 \ RETURN
1272 ADINIT
1275 CLRANGESENSE(1,2,X5)
1300 IF X5=4 THEN X5=10
1310 IF X5=3 THEN X5=5
1320 ADIMMED(2,S4)
1330 S4=-(S4/X5)
1340 CLSWITCH(1,2,,S4)
1341 PRINT  \ PRINT  \ TXTFLASH
1345 PRINT  \ PRINT 'HIT RETURN TO START TEST.' \ INPUT R$
1346 GTIME(Z3,Z2,Z1) \ GDATE(Z6,Z5,Z4)
1350 IF G=0 THEN GO TO 1420
1360 TEKMODE(1,1)
1370 PHYL(1,10,85,10,85)
1380 SCALE(1,0,X1,X2,Y1,Y2)
1390 AXES(1,0,0)
1400 LABEL(1,X$,Y$,X3,Y3,1)
1410 INVEC
1425 T6=0
1430 ADGO \ ETIME
1500 FGGO
1505 B0=0 \ F1=0
1550 FGREPT(1,'SINE', RATE R1,C1,S1,S3)
1600 FGSTATUS(1,H1)
1605 IF G=0 THEN GO TO 1635
1610 ADIMMED(2,X4)
1615 ADIMMED(1,Y4)
1620 X4=(X4*((10*X0)/G0))
1625 Y4=(Y4*((10*L0)/A0))
1630 PLOT(1,X4,Y4)
1635 IF H1=0 THEN GO TO 4650
1640 CLHYDSENSE(1,H2)
1645 IF H2=0 THEN GO TO 5100
1650 IF G1=1 THEN GO TO 2200
1653 IF A1=1 THEN GO TO 1600
```

```
1655 IF A=64 THEN B=0
1660 IF A<64 THEN GO TO 1600 \ A=-1
1665 F1=1
1670 AOUT(#2,A(1,0),64*4,B0,E)
1675 P=INT(E/4) \ P0=P0+P
1680 B0=B0+1
1685 FGSTATUS(1,H1)
1690 IF G=0 THEN GO TO 1710
1695 ADIMMED(2,X4) \ ADIMMED(1,Y4)
1700 X4=(X4*((10*X0)/G0)) \ Y4=(Y4*((10*L0)/A0))
1705 PLOT(1,X4,Y4)
1710 IF H1=0 THEN GO TO 4650
1715 CLHYDSENSE(1,H2)
1720 IF H2=0 THEN GO TO 5100
1725 IF G1=1 THEN GO TO 2200
1730 IF B=64 THEN A=0
1735 IF B<64 THEN GO TO 1685 \ B=-1
1740 F1=0
1745 AOUT(#2,B(1,0),64*4,B0,E)
1750 P=INT(E/4) \ P0=P0+P
1755 B0=B0+1
1760 GO TO 1600
2100 REM -------------
2150 REM HOLD FUNCTIONS
2200 REM -------------
2300 IF G=0 THEN GO TO 2450
2350 HOME
2400 VTMODE(1,0)
2450 ADIMMED(2,X5)
2500 ADIMMED(1,L6)
2505 IF S8=0 THEN GO TO 2525
2510 X9=L6*L2*10/A0
2515 IF X9<=S9 THEN GO TO 2525
2520 GO TO 2450
2525 FGHOLD \ ADHOLD(1)
2550 PRINT 'HOLD AT';((X5*X0*10)/G0);'(IN/IN)' \ PRINT
2600 PRINT 'INITIAL STRESS =';((L6*L2*10)/A0);' PSI' \ PRINT
2650 PRINT #3,'HOLD AT';((X5*X0*10)/G0);'(IN/IN)' \ PRINT #3
2700 PRINT #3,'INITIAL STRESS =';((L6*L2*10)/A0);' PSI'
2750 PRINT #3
2800 PRINT #3,'STRESS (PSI)';TAB(30)'TIME (MIN)'
2850 ETIME(T3)
2900 CLOFFSENSE(1,1,L3,F)
2950 CLRANGESENSE(1,1,L4)
3000 ADIMMED(1,L5)
3050 IF L4=4 THEN L5=-(L5/10)
3100 IF L4=3 THEN L5=-(L5/5)
3150 IF L4=2 THEN L5=-(L5/2)
3200 IF L4=1 THEN L5=-L5
3250 CLRANGESWITCH(1,1,L1,L5)
```

```
3300 ADIMMED(1,L5) \ ETIME(T4)
3350 SLEEP(T4+(T2*60))
3400 L5=((L5*L2*10)/A0)
3450 ETIME(T4) \ T4=((T4-T3)/60)
3500 PRINT 'STRESS =';L5;'(PSI)';TAB(30)'TIME =';T4;'(MIN)' \ PRINT
3550 PRINT #3,L5;TAB(30)T4
3560 CLHYDSENSE(1,H2)
3570 IF H2=0 THEN GO TO 5100
3600 IF G1=2 THEN GO TO 3850
3650 GO TO 3300
3700 REM ---------------
3750 REM RESUME FUNCTIONS
3800 REM ---------------
3850 PRINT
3855 PRINT 'DO YOU WANT TO SPECIFY THE INITIAL STRESS FOR THE NEXT
HOLD';
3857 TXTBOLD \ PRINT '(Y/N)'; \ TXTNORMAL
3860 INPUT R$ \ IF R$='N' THEN GO TO 3875
3865 PRINT  \ PRINT 'WHAT INITIAL STRESS DO YOU WANT TO HOLD AT NEXT'; \
INPUT S9
3870 S8=1 \ GO TO 3899
3875 S8=0
3899 CLRANGESWITCH(1,1,L4,L3)
3900 ETIME(T5) \ T5=T5-T3 \ T6=T6+T5
3950 FGRESUME \ ADRESUME(1)
4000 IF G=0 THEN GO TO 4400
4050 TEKMODE(1,1)
4100 PHYL(1,10,85,10,85)
4150 SCALE(1,0,X1,X2,Y1,Y2)
4200 AXES(1,0,0)
4250 LABEL(1,X$,Y$,X3,Y3,1)
4300 INVEC
4350 G1=0
4400 IF F1=0 THEN GO TO 1655
4410 IF F1=1 THEN GO TO 1730
4450 ------------------------
4500 REM END OF TEST FUNCTIONS
4550 ------------------------
4600 FGREMOVE(1,1)
4650 CLSWITCH(1,1,,0)
4700 FGGO
4750 FGARB(1,'RAMP', TIME 5,0)
4800 IF G=1 THEN GO TO 4900
4850 PRINT 'SWITCHING TO LOAD CONTROL AND RAMPING DOWN...'
4900 FGSTATUS(1,H1)
4950 IF H1=0 THEN GO TO 5350
5000 GO TO 4900
5100 FGREMOVE(1)
5150 CLSWITCH(1,1,,0)
5250 IF G=1 THEN GO TO 5350
```

```
5300 PRINT 'HYDRAULIC SHUT-DOWN DETECTED'
5350 FGTOTALSEG(1,C2)
5400 FGSTOP \ ADSTOP
5450 ETIME(T7) \ T7=T7-T6
5500 IF G=0 THEN GO TO 5700
5550 INVEC
5600 HOME
5650 VTMODE(1,0)
5700 PRINT 'END OF TEST' \ PRINT
5750 CLRANGESWITCH(1,2,,0)
5800 REM ------------------
5850 REM STORING DATA POINTS
5900 REM ------------------
5950 IF F1=1 THEN GO TO 5970
5960 N=A \ AOUT(#2,A(1,0),N*4,B0,E) \ GO TO 5980
5970 N=B \ AOUT(#2,B(1,0),N*4,B0,E)
5980 B0=B0+1
5990 P=INT(E/4)
6000 P0=P0+P
6500 PRINT 'TOTAL POINTS TRANSFERRED = ';P0
6550 C2=C2/2
6600 M3=((ELEVEL(M(1,1))*L0*10)/A0)
6650 M4=((ELEVEL(M0(1,1))*L0*10)/A0)
6700 M5=((ELEVEL(M1(1,1))*X0*10)/G0)
6750 M6=((ELEVEL(M2(1,1))*X0*10)/G0)
6800 PRINT #1,C2;',';M3;',';M4;',';M5;',';M6;',';T7;',';P0
6810 PRINT #1,Z1;',';Z2;',';Z3;',';Z4;',';Z5;',';Z6
6811 PRINT #1,A$
6812 PRINT #1,B$
6850 CLOSE #1,2,3
6900 PRINT  \ PRINT 'DO YOU WANT TO PRINT THE RESULTS? ';
6905 TXTBOLD \ PRINT '(Y/N)'; \ TXTNORMAL \ INPUT R$
7000 IF R$='N' THEN GO TO 7250
7100 PRINT 'PLACE PRINTER SWITCH TO POSITION "A" '
7150 PRINT 'HIT RETURN TO CONTINUE' \ INPUT R$
7200 GOSUB 7450
7205 IF Z9=1 THEN GO TO 7270
7250 PRINT 'DO YOU WANT TO PLOT THE RESULTS (DEFAULT ANS. IS NO THIS
TIME)';
7252 TXTBOLD \ PRINT '(Y/N)'; \ TXTNORMAL \ INPUT R$
7260 IF R$='Y' THEN Z9=1
7265 IF R$='Y' THEN GO TO 7100
7270 CLRTXWIN \ STOP
7300 REM ----------------------------
7350 REM SUBROUTINE FOR PRINTING RESULTS
7400 REM ----------------------------
7450 OPEN F1$ FOR INPUT AS FILE 1
7500 OPEN F2$ FOR INPUT AS FILE 2
7550 OPEN 'LP:' FOR OUTPUT AS FILE 3
7600 INPUT #1,L0,X0,G0,A0,R0,R1,S0,S1,S2,S4,T0,C0,T1,L1,L2,T2
```

```
7650 INPUT #1,C2,M3,M4,M5,M6,T7,P0
7755 INPUT #1,Z1,Z2,Z3,Z4,Z5,Z6
7760 INPUT #1,A$
7765 INPUT #1,B$
7700 PRINT #3
7750 Z$='FILENAME                          <####'
7800 PRINT #3,USING Z$,F$
7810 PRINT #3
7811 PRINT #3,'DATE: ';Z5;'-';Z4;'-';Z6;'                              ';
7812 PRINT #3,'TIME: ';Z1;':';Z2;':';Z3
7850 PRINT #3
7855 PRINT #3,'SAMPLE NUMBER                    ';B$
7860 PRINT #3,'SAMPLE TEMPERATURE (DEG C)       ';A$
7900 PRINT #3,'LOAD CALIBRATION   (LBS/VOLT)    ';L0
7950 PRINT #3,'EXTENSOMETER CAL.  (IN/VOLT)     ';X0
8000 PRINT #3,'GAUGE LENGTH       (IN)          ';G0
8050 PRINT #3,'GAUGE AREA         (IN*IN)       ';A0
8100 PRINT #3,'STRAIN RATE        (IN/IN/SEC)   ';R0
8150 PRINT #3,'CYCLES COMPLETED                 ';C2
8200 PRINT #3,'MAXIMUM STRESS     (PSI)         ';M3
8250 PRINT #3,'MINIMUM STRESS     (PSI)         ';M4
8300 PRINT #3,'MAXIMUM STRAIN     (IN/IN)       ';M5
8350 PRINT #3,'MINIMUM STRAIN     (IN/IN)       ';M6
8400 PRINT #3,'POINTS TAKEN                     ';P0
8450 PRINT #3,'TIME/POINT         (SEC)         ';T0
8500 PRINT #3,'HOLD-LOAD RANGE                  ';L1
8550 PRINT #3,'HOLD-LOAD CAL.     (LBS/SEC)     ';L2
8600 PRINT #3,'HOLD-TIME/POINT    (SEC)         ';T2
8610 IF Z9=1 THEN GO TO 10100
8650 REM ------------------
8700 REM READING STORED DATA
8750 REM ------------------
8800 PRINT #3,'TIME (SEC)';TAB(20)'STRESS (PSI)';TAB(40)'STRAIN (IN/IN)'
8805 A(0,0)=0 \ A(0,1)=(A(0,1)*L0)/A0
8810 A(0,2)=(A(0,2)*L0)/G0
8815 PRINT #3,A(0,0);TAB(20)A(0,1);TAB(40)A(0,2)
8850 B0=0 \ N1=P0 \ T=0
8900 N1=N1-64 \ N2=64 \ IF N1<=0 THEN N2=N1+64
8950 AINP(#2,A(1,0),N2*4,B0,P)
9050 IF N1<=0 THEN GO TO 9200
9100 B0=B0+1
9200 ELEVAR(A,1,2,10)
9300 FOR J=1 TO N2
9350 T=T+T0 \ A(J,0)=T
9400 A(J,1)=(A(J,1)*L0)/A0
9450 A(J,2)=(A(J,2)*X0)/G0
9500 PRINT #3,A(J,0);TAB(20)A(J,1);TAB(40)A(J,2)
9550 NEXT J
9552 IF N1<=0 THEN GO TO 9600
9554 GO TO 8900
```

```
9600 PRINT  \ PRINT 'DO YOU WANT TO PLOT THE RESULTS? ';
9605 TXTBOLD \ PRINT '(Y/N)'; \ TXTNORMAL \ INPUT R$
9700 IF R$='N' THEN GO TO 9850
9800 GOSUB 10100
9850 CLOSE #1,2,3
9900 RETURN
9950 REM ----------------------
10000 REM SUBROUTINE TO PLOT DATA
10050 REM ----------------------
10100 PRINT 'PLACE PRINTER SWITCH IN POSITION "B" '
10150 PRINT 'HIT RETURN TO CONTINUE'; \ INPUT R$ \ PRINT  \ PRINT
10200 PRINT 'MAXIMUM STRAIN (IN/IN)       ';M5
10250 PRINT 'MIMIMUM STRAIN (IN/IN)       ';M6
10300 X$='IN/IN'
10350 PRINT 'ENTER MAXIMUM STRAIN'; \ INPUT X2
10400 PRINT 'ENTER MINIMUM STRAIN'; \ INPUT X1
10450 PRINT 'ENTER STRAIN STEP SIZE'; \ INPUT X3
10500 PRINT 'MAXIMUM STRESS (PSI)         ';M3
10550 PRINT 'MINIMUM STRESS (PSI)         ';M4
10600 Y$='PSI'
10650 PRINT 'ENTER MAXIMUM STRESS'; \ INPUT Y2
10700 PRINT 'ENTER MINIMUM STRESS'; \ INPUT Y1
10750 PRINT 'ENTER STRESS STEP SIZE'; \ INPUT Y3
10800 PRINT #3 \ PRINT #3 \ PRINT #3
10850 PRINT 'ARE THESE PARAMETERS OK? ';
10860 TXTBOLD \ PRINT '(Y/N)'; \ TXTNORMAL \ INPUT R$
10950 IF R$='N' THEN GO TO 10200
11050 REM -----------------
11100 REM GRAPHICS FUNCTIONS
11150 REM -----------------
11200 TEKMODE(1,1) \ Z9=1
11250 PHYL(1,10,85,10,85)
11300 SCALE(1,0,X1,X2,Y1,Y2)
11350 AXES(1,0,0)
11400 LABEL(1,X$,Y$,X3,Y3,1)
11450 INVEC
11451 BO=0 \ N1=PO \ T=0
11452 N1=N1-64 \ N2=64 \ IF N1<=0 THEN N2=N1+64
11453 AINP(#2,A(1,0),N2*4,BO,P)
11454 IF N1<=0 THEN GO TO 11456
11455 BO=BO+1
11456 ELEVAR(A,1,2,10)
11457 FOR J=1 TO N2
11458 T=T+TO \ A(J,0)=T
11459 A(J,1)=(A(J,1)*LO)/AO
11460 A(J,2)=(A(J,2)*XO)/GO
11461 X4=A(J,2)
11462 Y4=A(J,1)
11463 PLOT(1,X4,Y4)
11464 NEXT J
```

```
11465 IF N1<=0 THEN GO TO 11750
11466 GO TO 11452
11750 INVEC
11800 HOME
11850 COPY
11900 VTMODE(1,0)
11950 RETURN
11960 REM -------------------------
11970 REM PARAMETER CHANGE FUNCTIONS
11980 REM -------------------------
12000 VTMODE \ CLRTXWIN
12050 PRINT 'WHAT IS THE NEW MAXIMUM STRAIN';
12100 INPUT S0
12150 PRINT 'WHAT IS THE NEW MINIMUM STRAIN';
12200 INPUT S2
12205 PRINT 'DO YOU WANT TO CHANGE THE STRAIN RATE';
12206 TXTBOLD \ PRINT '(Y/N)'; \ TXTNORMAL \ INPUT R$
12210 IF R$='N' THEN GO TO 12230
12220 PRINT 'WHAT IS THE NEW STRAIN RATE (IN/IN/SEC)'; \ INPUT R0
12225 R1=(R0*G0)/(X0*10)
12230 PRINT 'DO YOU WANT TO CHANGE THE NUMBER OF TOTAL CYCLES';
12232 TXTBOLD \ PRINT '(Y/N)'; \ TXTNORMAL \ INPUT R$
12235 IF R$='N' THEN GO TO 12250
12245 PRINT 'WHAT IS THE NEW TOTAL NUMBER OF CYCLES'; \ INPUT C0 \
C1=C0*2
12250 S1=(S0*G0)/(X0*10)
12300 S3=(S2*G0)/(X0*10)
12350 FGREMOVE(1,1)
12400 FGTOTALSEG(1,C2)
12450 C1=C1-C2
12500 FGREPT(1,'SINE', RATE R1,C1,S1,S3)
12505 IF G=0 THEN GO TO 12550
12510 TEKMODE(1,1)
12515 PHYL(1,10,85,10,85)
12520 SCALE(1,0,X1,X2,Y1,Y2)
12525 AXES(1,0,0)
12530 LABEL(1,X$,Y$,X3,Y3,1)
12535 INVEC
12550 RETURN
13000 REM SET FLAGS TO HALT DATA ACQUISTION
13010 A1=1
13020 ADREMOVE(1)
13500 RETURN


1 REM CREEP/STRESS DROP - LOAD CONTROL
8 CLRTXWIN
9 U=SYS(7)
10 REM WRITTEN BY GEORGE JAMES AND PAUL SEAN HILL - JULY 1985
20 PRINT 'THIS PROGRAM PERFORMS A CREEP TEST AND IS LOADED AT A'
```

```
24 PRINT 'CONSTANT LOAD RATE.'
28 PRINT
30 PRINT 'THE PROGRAM ALLOWS A SPECIFIED STRESS INCREMENT TO BE'
40 PRINT 'INSTANTANEOUSLY REMOVED AND THEN REPLACED ON COMMAND.'
45 PRINT 'AFTER A PERIOD OF CREEP, THE LOAD CAN BE RAMPED UP AGAIN,'
46 PRINT 'OR THE TEST CAN BE ENDED BY KEYBOARD INTERUPTS.'
47 PRINT
70 PRINT 'THE TEST DATA IS STORED ON 5.25" FLEXIBLE DISC ON DU1: IN
BINARY'
100 PRINT 'FORM.  STRESS DROP DATA IS ALSO STORED ON 5.25" DISC.' \
PRINT
110 PRINT 'THE CAPABILITY TO PRINT AND PLOT THE DATA IS PROVIDED FOR
THE'
120 PRINT 'CURRENT TEST OR FOR EXISTING FILES.'
125 PRINT  \ PRINT
126 PRINT  \ PRINT
130 DIM A(64,3),B(64,3),M(2,2),MO(2,2),M1(2,2),M2(2,2)
140 REM ---------------
150 REM PRINT ONLY INPUT
160 REM ---------------
170 PRINT
180 PRINT 'TYPE'; \ TXTBOLD \ PRINT ' TEST';
182 TXTNORMAL \ PRINT ' IF YOU WANT TO RUN A NEW TEST'
184 PRINT  \ PRINT '                    OR'
186 PRINT
190 PRINT 'TYPE'; \ TXTBOLD \ PRINT ' PRINT'; \ TXTNORMAL
195 PRINT ' IF YOU WANT TO PRINT EXISTING FILES'
196 PRINT
200 INPUT R$
210 IF R$='TEST' THEN GO TO 330
220 IF R$='PRINT' THEN GO TO 240
225 TXTINVERS
230 PRINT 'INVALID ENTRY, TYPE TEST OR PRINT' \ TXTNORMAL \ GO TO 170
240 PRINT 'ENTER FILE NAME (<=5 CHARACTERS)'; \ INPUT F$
250 IF LEN(F$)<=5 THEN GO TO 270
255 TXTINVERS
260 PRINT 'INVALID FILE NAME' \ TXTNORMAL \ GO TO 240
270 F1$='DU1:'+F$+'C.DAT'
280 F2$='DU1:'+F$+'.DAT'
285 PO=0
290 GO TO 6900
300 REM ----------
310 REM TEST INPUT
320 REM ----------
330 GO TO 350
340 CLOSE #1,2,3
350 PRINT
360 PRINT 'ENTER FILE NAME (<=5 CHARACTERS)'; \ INPUT F$
370 IF LEN(F$)<=5 THEN GO TO 390
375 TXTINVERS
```

```
380 PRINT 'INVALID FILE NAME ' \ TXTNORMAL \ GO TO 350
390 F1$='DU1:'+F$+'C.DAT'
400 F2$='DU1:'+F$+'.DAT'
410 OPEN F1$ FOR OUTPUT AS FILE 1, FILESIZE 1
420 OPEN F2$ FOR OUTPUT AS FILE 2, FILESIZE 30
430 OPEN 'LP:' FOR OUTPUT AS FILE 3
431 PRINT 'ENTER THE SAMPLE NUMBER'; \ INPUT B$
435 PRINT 'ENTER THE SAMPLE TEMPERATURE IN DEGREES CELSIUS'; \ INPUT A$
440 PRINT 'ENTER LOAD CALIBRATION (LBS/VOLT)'; \ INPUT LO
460 PRINT 'ENTER EXTENSOMETER CALIBRATION (IN/VOLT)'; \ INPUT XO
470 PRINT 'ENTER GAUGE LENGTH (IN)'; \ INPUT GO
480 PRINT 'ENTER GAUGE AREA (IN*IN)'; \ INPUT AO
490 PRINT 'ENTER LOAD RATE (PSI/SEC)'; \ INPUT RO
500 R1=(RO*LO)/(XO*10)*AO
510 PRINT 'BEGIN CREEP AT WHAT STRESS (PSI)'; \ INPUT SO
520 S1=(SO*LO)/(XO*10)*AO
525 T1=S1/R1
550 PRINT 'ENTER TIME/POINT FOR DATA ACQUISITION (SEC)'; \ INPUT TO
560 T3=T1/TO
620 PRINT 'ENTER LOAD RANGE DURING STRESS DROP (1,2,3, OR 4)'; \ INPUT
L1
625 PRINT 'ENTER LOAD CALIBRATION FOR STRESS DROP (LBS/VOLT)'; \ INPUT
L2
630 PRINT 'ENTER TIME/POINT DURING STRESS DROP (MIN)'; \ INPUT T2
632 CLRTXWIN
633 PRINT 'SAMPLE NUMBER                    ';B$
635 PRINT 'SAMPLE TEMPERATURE     (DEG C)   ';A$
636 PRINT 'LOAD CALIBRATION       (LBS/VOLT)';LO
640 PRINT 'EXTENSOMETER CAL.      (IN/VOLT) ';XO
650 PRINT 'GAUGE LENGTH           (IN)      ';GO
660 PRINT 'GAUGE AREA             (IN*IN)   ';AO
680 PRINT 'LOAD RATE              (PSI/SEC) ';RO
690 PRINT 'INIT. CREEP STRESS     (PSI)     ';SO
710 PRINT 'TIME/POINT             (SEC)     ';TO
715 PRINT 'TOT. POINTS IN RAMP UP (SEC)     ';T3
735 PRINT 'STRESS DROP RANGE                ';L1
740 PRINT 'STR DROP LOAD CAL      (LBS/VOLT)';L2
745 PRINT 'DROP-TIME/POINT        (MIN)     ';T2
750 PRINT  \ PRINT 'ARE ALL PARAMETERS OK ';
752 TXTBOLD \ PRINT '(Y/N)'; \ TXTNORMAL \ INPUT R$
760 IF R$='N' THEN GO TO 340
780 PRINT #1,LO;',';XO;',';GO;',';AO;',';RO;',';R1;',';SO;',';S1
790 PRINT #1,TO;',';L1;',';L2;',';T2;',';T3
800 REM -------------------------
810 REM DATA ACQUISITION FUNCTIONS
820 REM -------------------------
830 CLINIT
880 CKSTOP
890 CKTIME(1,.01,K)
900 I1=INT(TO/K)
```

```
910 ADTIMED(1,A,B,1,I1)
920 ADSLAVE(1,2,6)
940 ADRMAX(3,M,1)
950 ADRMIN(3,M0,1)
960 ADRMAX(3,M1,2)
970 ADRMIN(3,M2,2)
980 REM ------------------
990 REM REAL TIME PLOT INPUT
1000 REM ------------------
1010 PRINT  \ PRINT 'DO YOU WANT A REAL TIME PLOT?'; \ TXTBOLD
1015 PRINT ' (Y/N)'; \ TXTNORMAL \ INPUT R$
1030 IF R$='N' THEN GO TO 1060
1050 G=1 \ GO TO 1070
1060 G=0 \ GO TO 1209
1070 X$='IN/IN'
1080 PRINT  \ PRINT 'REAL TIME PLOT PARAMETERS' \ PRINT
1090 PRINT 'ENTER MAXIMUM STRAIN'; \ INPUT X2
1100 PRINT 'ENTER MINIMUM STRAIN'; \ INPUT X1
1110 PRINT 'ENTER STRAIN STEP SIZE'; \ INPUT X3
1120 Y$='PSI' \ PRINT
1130 PRINT 'ENTER MAXIMUM STRESS'; \ INPUT Y2
1140 PRINT 'ENTER MINIMUM STRESS'; \ INPUT Y1
1150 PRINT 'ENTER STRESS STEP SIZE'; \ INPUT Y3
1160 PRINT 'ARE THESE PARAMETERS OK?'; \ TXTBOLD \ PRINT '(Y/N)';
1165 TXTNORMAL \ INPUT R$
1180 IF R$='N' THEN GO TO 1090
1200 REM -------------
1203 REM TEST FUNCTIONS
1206 REM -------------
1209 CLRTXWIN
1212 TXTNORMAL \ PRINT  \ TXTINVERS \ TXTSPOS(1,5,10)
1215 PRINT 'KEY INTERUPT SUMMARY' \ TXTNORMAL
1218 TXTSPOS(1,8,1) \ PRINT '<ESC>E - END TEST'
1221 PRINT '<ESC>D - DROP STRESS INCREMENT FOR STRESS DROP TEST'
1222 PRINT '<ESC>S - STEP UP TO ORIGINAL LOAD.'
1224 PRINT '<ESC>R - RAMP UP TO ANOTHER STRESS LEVEL.'
1227 PRINT '<ESC>E - END TEST, RAMP TO ZERO LOAD.'
1228 PRINT '<ESC>A - HALT DATA ACQUISITION AND CONTINUE TEST'
1229 ETIME(T3) \ SLEEP(T3+5)
1230 PRINT  \ TXTFLASH \ PRINT  \ PRINT  \ PRINT
1232 PRINT 'BRING UP THE HYDRAULIC PRESSURE.....'
1233 PRINT 'ZERO LOAD WITH SET POINT CONTROL AND STRAIN WITH ZERO
ADJUST'
1234 ETIME(T3) \ SLEEP(T3+3) \ PRINT  \ PRINT 'PLACE PRINTER ON SWITCH
"A" '
1235 PRINT  \ PRINT
1240 ETIME(T3) \ SLEEP(T3+3)
1245 KBINT('E',3, LINE 4500 )
1248 KBINT('D',4, LINE 1266 )
1251 KBINT('R',4, LINE 1270 )
```

```
1255 KBINT('A',3, LINE 13000 )
1256 KBINT('S',4, LINE 1269 )
1257 KBENB
1260 G1=0
1263 GO TO 1272
1266 G1=1 \ RETURN
1269 G1=2 \ RETURN
1270 G1=3\RETURN
1272 ADINIT
1275 CLRANGESENSE(1,2,X5)
1300 IF X5=4 THEN X5=10
1310 IF X5=3 THEN X5=5
1341 PRINT  \ PRINT
1345 PRINT  \ PRINT 'HIT RETURN TO START TEST.' \ INPUT R$ \ TXTNORMAL
1346 GTIME(Z3,Z2,Z1) \ GDATE(Z6,Z5,Z4)
1350 IF G=0 THEN GO TO 1420
1360 TEKMODE(1,1)
1370 PHYL(1,10,85,10,85)
1380 SCALE(1,0,X1,X2,Y1,Y2)
1390 AXES(1,0,0)
1400 LABEL(1,X$,Y$,X3,Y3,1)
1410 INVEC
1420 REM
1425 T6=0
1430 ADGO \ ETIME
1500 FGGO
1505 B0=0 \ F1=0
1550 FGRAMP(1,T1,S1)
1600 REM
1605 IF G=0 THEN GO TO 1640
1610 ADIMMED(2,X4)
1615 ADIMMED(1,Y4)
1620 X4=(X4*((10*X0)/G0))
1625 Y4=(Y4*((10*L0)/A0))
1630 PLOT(1,X4,Y4)
1640 CLHYDSENSE(1,H2)
1645 IF H2=0 THEN GO TO 5100
1650 IF G1=1 THEN GO TO 2200
1652 IF G1=3 THEN GOTO 3700
1655 IF A=64 THEN B=0
1660 IF A<64 THEN GO TO 1600 \ A=-1
1665 F1=1
1670 AOUT(#2,A(1,0),64*4,B0,E)
1675 P=INT(E/4) \ P0=P0+P
1680 B0=B0+1
1685 REM
1690 IF G=0 THEN GO TO 1710
1695 ADIMMED(2,X4) \ ADIMMED(1,Y4)
1700 X4=(X4*((10*X0)/G0)) \ Y4=(Y4*((10*L0)/A0))
1705 PLOT(1,X4,Y4)
```

```
1715 CLHYDSENSE(1,H2)
1720 IF H2=0 THEN GO TO 5100
1725 IF G1=1 THEN GO TO 2200
1727 IF G1=3 THEN GOTO 3700
1730 IF B=64 THEN A=0
1735 IF B<64 THEN GO TO 1685 \ B=-1
1740 F1=0
1745 AOUT(#2,B(1,0),64*4,B0,E)
1750 P=INT(E/4) \ P0=P0+P
1755 B0=B0+1
1760 GO TO 1600
2100 REM --------------
2150 REM DROP FUNCTIONS
2200 REM --------------
2300 IF G=0 THEN GO TO 2450
2350 HOME
2400 VTMODE(1,0)
2450 ADIMMED(2,X5)
2500 ADIMMED(1,L6)
2525 ADHOLD(1)
2550 PRINT 'HOW MUCH STRESS DO YOU WANT TO DROP'; \ INPUT D0
2555 D1=(S0-D0)*L0*A0/X0/10
2560 FGSTEP(1,D1)
2850 ETIME(T3)
3300 ADIMMED(1,L5) \ ETIME(T4)
3350 SLEEP(T4+(T2*60))
3400 L5=((L5*L2*10)/A0)
3450 ETIME(T4) \ T4=((T4-T3)/60)
3560 CLHYDSENSE(1,H2)
3570 IF H2=0 THEN GO TO 5100
3600 IF G1=2 THEN GO TO 12000
3650 GO TO 3300
3700 REM ---------------
3750 REM RAMP UP FUNCTIONS
3800 REM ---------------
3850 PRINT
3855 PRINT 'ENTER LOAD RATE (PSI/SEC)'; \ INPUT R0
3860 R1=(R0*L0)/(X0*10)*A0
3865 PRINT 'BEGIN NEXT CREEP AT WHAT STRESS (PSI)'; \ INPUT S0
3870 S1=(S0*L0)/(X0*10)*A0
3871 ADIMMED(1,S5)
3875 T1=(S1-S5)/R1
3899 CLRANGESWITCH(1,1,L4,L3)
4000 IF G=0 THEN GO TO 4400
4050 TEKMODE(1,1)
4100 PHYL(1,10,85,10,85)
4150 SCALE(1,0,X1,X2,Y1,Y2)
4200 AXES(1,0,0)
4250 LABEL(1,X$,Y$,X3,Y3,1)
4300 INVEC
```

```
4310 FGRAMP(1,T1,S1)
4350 G1=0
4400 IF F1=0 THEN GO TO 1655
4410 GO TO 1730
4450 ------------------------
4500 REM END OF TEST FUNCTIONS
4550 ------------------------
4700 FGGO
4750 FGRAMP(1,5,0)
4800 IF G=1 THEN GO TO 4900
4850 PRINT 'TEST OVER, RAMPING DOWN...'
4900 FGSTATUS(1,H1)
4950 IF H1=0 THEN GO TO 5350
5000 GO TO 4900
5100 REM
5250 IF G=1 THEN GO TO 5400
5300 PRINT 'HYDRAULIC SHUT-DOWN DETECTED'
5400 FGSTOP \ ADSTOP
5450 ETIME(T7) \ T7=T7-T6
5500 IF G=0 THEN GO TO 5700
5550 INVEC
5600 HOME
5650 VTMODE(1,0)
5700 PRINT 'END OF TEST' \ PRINT
5750 CLRANGESWITCH(1,2,,0)
5800 REM ------------------
5850 REM STORING DATA POINTS
5900 REM ------------------
5950 IF F1=1 THEN GO TO 5970
5960 N=A \ AOUT(#2,A(1,0),N*4,B0,E) \ GO TO 5980
5970 N=B \ AOUT(#2,B(1,0),N*4,B0,E)
5980 B0=B0+1
5990 P=INT(E/4)
6000 P0=P0+P
6500 PRINT 'TOTAL POINTS TRANSFERRED = ';P0
6550 C2=C2/2
6600 M3=((ELEVEL(M(1,1))*L0*10)/A0)
6650 M4=((ELEVEL(M0(1,1))*L0*10)/A0)
6700 M5=((ELEVEL(M1(1,1))*X0*10)/G0)
6750 M6=((ELEVEL(M2(1,1))*X0*10)/G0)
6800 PRINT #1,C2;',';M3;',';M4;',';M5;',';M6;',';T7;',';P0
6810 PRINT #1,Z1;',';Z2;',';Z3;',';Z4;',';Z5;',';Z6
6811 PRINT #1,A$
6812 PRINT #1,B$
6850 CLOSE #1,2,3
6900 PRINT  \ PRINT 'DO YOU WANT TO PRINT THE RESULTS? ';
6905 TXTBOLD \ PRINT '(Y/N)'; \ TXTNORMAL \ INPUT R$
7000 IF R$='N' THEN GO TO 7250
7100 PRINT 'PLACE PRINTER SWITCH TO POSITION "A" '
7150 PRINT 'HIT RETURN TO CONTINUE' \ INPUT R$
```

```
7200 GOSUB 7450
7205 IF Z9=1 THEN GO TO 7270
7250 PRINT 'DO YOU WANT TO PLOT THE RESULTS (DEFAULT ANS. IS NO THIS
TIME)';
7252 TXTBOLD \ PRINT '(Y/N)'; \ TXTNORMAL \ INPUT R$
7260 IF R$='Y' THEN Z9=1
7265 IF R$='Y' THEN GO TO 7100
7270 CLRTXWIN \ STOP
7300 REM ------------------------------
7350 REM SUBROUTINE FOR PRINTING RESULTS
7400 REM ------------------------------
7450 OPEN F1$ FOR INPUT AS FILE 1
7500 OPEN F2$ FOR INPUT AS FILE 2
7550 OPEN 'LP:' FOR OUTPUT AS FILE 3
7600 INPUT #1,L0,X0,G0,A0,R0,R1,S0,S1,S2,S4,T0,C0,T1,L1,L2,T2
7650 INPUT #1,C2,M3,M4,M5,M6,T7,P0
7655 INPUT #1,Z1,Z2,Z3,Z4,Z5,Z6
7660 INPUT #1,A$
7665 INPUT #1,B$
7700 PRINT #3
7750 Z$='FILENAME                          <####'
7800 PRINT #3,USING Z$,F$
7810 PRINT #3
7811 PRINT #3,'DATE: ';Z5;'-';Z4;'-';Z6;'                          ';
7812 PRINT #3,'TIME: ';Z1;':';Z2;':';Z3
7850 PRINT #3
7855 PRINT #3,'SAMPLE NUMBER                    ';B$
7860 PRINT #3,'SAMPLE TEMPERATURE (DEG C)       ';A$
7900 PRINT #3,'LOAD CALIBRATION   (LBS/VOLT)    ';L0
7950 PRINT #3,'EXTENSOMETER CAL.  (IN/VOLT)     ';X0
8000 PRINT #3,'GAUGE LENGTH       (IN)          ';G0
8050 PRINT #3,'GAUGE AREA         (IN*IN)       ';A0
8100 PRINT #3,'STRAIN RATE        (IN/IN/SEC)   ';R0
8150 PRINT #3,'CYCLES COMPLETED                 ';C2
8200 PRINT #3,'MAXIMUM STRESS     (PSI)         ';M3
8250 PRINT #3,'MINIMUM STRESS     (PSI)         ';M4
8300 PRINT #3,'MAXIMUM STRAIN     (IN/IN)       ';M5
8350 PRINT #3,'MINIMUM STRAIN     (IN/IN)       ';M6
8400 PRINT #3,'POINTS TAKEN                     ';P0
8450 PRINT #3,'TIME/POINT         (SEC)         ';T0
8500 PRINT #3,'HOLD-LOAD RANGE                  ';L1
8550 PRINT #3,'HOLD-LOAD CAL.     (LBS/SEC)     ';L2
8600 PRINT #3,'HOLD-TIME/POINT    (SEC)         ';T2
8610 IF Z9=1 THEN GO TO 10100
8650 REM ------------------
8700 REM READING STORED DATA
8750 REM ------------------
8800 PRINT #3,'TIME (SEC)';TAB(20)'STRESS (PSI)';TAB(40)'STRAIN (IN/IN)'
8805 A(0,0)=0 \ A(0,1)=(A(0,1)*L0)/A0
8810 A(0,2)=(A(0,2)*L0)/G0
```

```
8815 PRINT #3,A(0,0);TAB(20)A(0,1);TAB(40)A(0,2)
8850 BO=0 \ N1=PO \ T=0
8900 N1=N1-64 \ N2=64 \ IF N1<=0 THEN N2=N1+64
8950 AINP(#2,A(1,0),N2*4,BO,P)
9050 IF N1<=0 THEN GO TO 9200
9100 BO=BO+1
9200 ELEVAR(A,1,2,10)
9300 FOR J=1 TO N2
9350 T=T+TO \ A(J,0)=T
9400 A(J,1)=(A(J,1)*LO)/AO
9450 A(J,2)=(A(J,2)*XO)/GO
9500 PRINT #3,A(J,0);TAB(20)A(J,1);TAB(40)A(J,2)
9550 NEXT J
9552 IF N1<=0 THEN GO TO 9600
9554 GO TO 8900
9600 PRINT  \ PRINT 'DO YOU WANT TO PLOT THE RESULTS? ';
9605 TXTBOLD \ PRINT '(Y/N)'; \ TXTNORMAL \ INPUT R$
9700 IF R$='N' THEN GO TO 9850
9800 GOSUB 10100
9850 CLOSE #1,2,3
9900 RETURN
9950 REM ----------------------
10000 REM SUBROUTINE TO PLOT DATA
10050 REM ----------------------
10100 PRINT 'PLACE PRINTER SWITCH IN POSITION "B" '
10150 PRINT 'HIT RETURN TO CONTINUE'; \ INPUT R$ \ PRINT  \ PRINT
10200 PRINT 'MAXIMUM STRAIN (IN/IN)       ';M5
10250 PRINT 'MIMIMUM STRAIN (IN/IN)       ';M6
10300 X$='IN/IN'
10350 PRINT 'ENTER MAXIMUM STRAIN'; \ INPUT X2
10400 PRINT 'ENTER MINIMUM STRAIN'; \ INPUT X1
10450 PRINT 'ENTER STRAIN STEP SIZE'; \ INPUT X3
10500 PRINT 'MAXIMUM STRESS (PSI)         ';M3
10550 PRINT 'MINIMUM STRESS (PSI)         ';M4
10600 Y$='PSI'
10650 PRINT 'ENTER MAXIMUM STRESS'; \ INPUT Y2
10700 PRINT 'ENTER MINIMUM STRESS'; \ INPUT Y1
10750 PRINT 'ENTER STRESS STEP SIZE'; \ INPUT Y3
10800 PRINT #3 \ PRINT #3 \ PRINT #3
10850 PRINT 'ARE THESE PARAMETERS OK? ';
10860 TXTBOLD \ PRINT '(Y/N)'; \ TXTNORMAL \ INPUT R$
10950 IF R$='N' THEN GO TO 10200
11050 REM -----------------
11100 REM GRAPHICS FUNCTIONS
11150 REM -----------------
11200 TEKMODE(1,1) \ Z9=1
11250 PHYL(1,10,85,10,85)
11300 SCALE(1,0,X1,X2,Y1,Y2)
11350 AXES(1,0,0)
11400 LABEL(1,X$,Y$,X3,Y3,1)
```

```
11450 INVEC
11451 BO=0 \ N1=PO \ T=0
11452 N1=N1-64 \ N2=64 \ IF N1<=0 THEN N2=N1+64
11453 AINP(#2,A(1,0),N2*4,BO,P)
11454 IF N1<=0 THEN GO TO 11456
11455 BO=BO+1
11456 ELEVAR(A,1,2,10)
11457 FOR J=1 TO N2
11458 T=T+TO \ A(J,0)=T
11459 A(J,1)=(A(J,1)*LO)/AO
11460 A(J,2)=(A(J,2)*XO)/GO
11461 X4=A(J,2)
11462 Y4=A(J,1)
11463 PLOT(1,X4,Y4)
11464 NEXT J
11465 IF N1<=0 THEN GO TO 11750
11466 GO TO 11452
11750 INVEC
11800 HOME
11850 COPY
11900 VTMODE(1,0)
11950 RETURN
12000 REM --------------------------------
12010 REM STEP BACK UP AFTER A STRESS DROP
12020 REM --------------------------------
12030 FGSTEP(1,S1)
12040 IF G=0 THEN GO TO 4400
12050 TEKMODE(1,1)
12060 PHYL(1,10,85,10,85)
12070 SCALE(1,0,X1,X2,Y1,Y2)
12080 AXES(1,0,0)
12090 LABEL(1,X$,Y$,X3,Y3,1)
12100 INVEC
12110 ADRESUME(1)
12550 IF F1=0 THEN GOTO 1655
12560 GOTO 1730
12900 REM --------------------------------
13000 REM SET FLAGS TO HALT DATA ACQUISTION
13001 REM --------------------------------
13020 ADREMOVE(1)
13500 RETURN
```

BACK2

```
1 REM THIS PROGRAM FITS A LINEAR CURVE TO DATA TAKEN FROM
2 REM HOLD TIME FROM DATA STORED IN BINARY FORM STORED
3 REM ON DISK DU1
```

```
4 REM WRITTEN BY GEORGE JAMES & EVA SMITH, AUGUST 3, 1984
20 DIM C1(321,3),D(32,3),D1(50,6),D2(2,2),D3(2,2),D4(2,2),D5(2,2)
25 DIM N(321,3),X(321),Y(321),C(10),A(10,11),X1(321),B(10,11),A1(32,2)
30 PRINT 'ENTER FILE NAME (<=5 CHARACTERS)'; \ INPUT F$
40 IF LEN(F$)<=5 THEN GO TO 70
50 TXTINVERS
60 PRINT 'INVALID FILE NAME' \ TXTNORMAL \ GO TO 30
70 F1$='DU1:'+F$+'C.DAT'
80 F2$='DU1:'+F$+'.DAT'
90 K1=1
100 REM ---------------------------------
110 REM SUBROUTINE TO PRINT RELAXATION DATA
120 REM ---------------------------------
125 PRINT  \ PRINT 'SWITCH PRINTER TO "A" AND HIT RETURN';
126 INPUT R$
127 PRINT
130 OPEN 'LP:' FOR OUTPUT AS FILE 3
140 F4$='DU1:'+F$+'S.DAT'
150 OPEN F4$ FOR INPUT AS FILE #4
160 INPUT #4,DO,T2,L2,A0,X0,GO
170 PRINT #3,'HOLD #';TAB(30)'STRESS(PSI)';TAB(60)'# OF POINTS'
180 FOR I=1 TO DO
190 INPUT #4,D1(I,1),D1(I,2),D1(I,3),D1(I,4),D1(I,5),D1(I,6)
200 PRINT #3,I;TAB(30)D1(I,1);TAB(60)D1(I,2)
210 NEXT I
220 CLOSE #4
230 PRINT 'INPUT # OF HOLD TIME DESIRED'; \ INPUT DO
240 P4=D1(DO,2)
250 F5$='DU1:'+F$+'S.D'+STR$(DO)
260 OPEN F5$ FOR INPUT AS FILE 5
270 B1=0 \ N1=D1(DO,2) \ T=0 \ N3=1
280 N1=N1-32 \ N2=32 \ IF N1<=0 THEN N2=N1+32
290 FINP(#5,C1(N3,0),N2*4,B1,P3)
300 B1=B1+1 \ N3=N3+32
320 IF N1<=0 THEN GO TO 335
330 GO TO 280
335 ELEVAR(C1,1,2,10)
340 CLOSE #5
342 PRINT ,'INPUT LENGTH OF TIME DESIRED FOR CURVE FIT (SEC)';
344 INPUT T4
346 P1=T4/T2
348 PRINT  \ PRINT 'NUMBER OF POINTS USED =';P1
360 REM --------------------CALCULATING E-----------------------
370 REM ---------------
380 REM FORMING A MATRIX
390 REM ---------------
395 T=-T2
400 FOR J=1 TO P1
405 T=T+T2
410 X(J)=T
```

```
420 Y(J)=(C1(J,2)*X0)/G0
430 X1(J)=1
440 NEXT J
450 FOR J=1 TO 2
460 A(J,1)=0
470 A(J,3)=0
480 FOR K=1 TO P1
490 A(J,1)=A(J,1)+X1(K)
500 A(J,3)=A(J,3)+Y(K)*X1(K)
510 X1(K)=X1(K)*X(K)
520 NEXT K
530 NEXT J
540 A(2,2)=0
550 FOR J=1 TO P1
560 A(2,2)=A(2,2)+X1(J)
570 X1(J)=X1(J)*X(J)
580 NEXT J
590 A(1,2)=A(2,1)
600 PRINT #3,'A MATRIX' \ PRINT #3
610 PRINT #3,A(1,1);A(1,2);A(1,3)
620 PRINT #3,A(2,1);A(2,2);A(2,3)
630 PRINT #3
640 REM ----------------
650 REM LU DECOMPOSITION
660 REM ----------------
670 FOR I=1 TO 2
680 FOR J=2 TO 2
690 S5=0
700 IF J>I THEN GO TO 770
710 J1=J-1
720 FOR K=1 TO J1
730 S5=S5+A(I,K)*A(K,J)
740 NEXT K
750 A(I,J)=A(I,J)-S5
760 GO TO 870
770 I1=I-1
780 IF I=0 THEN GO TO 820
790 FOR K=1 TO I1
800 S5=S5+A(I,K)*A(K,J)
810 NEXT K
820 IF ABS(A(I,I))<1.00000E-10 THEN GO TO 840
830 GO TO 860
840 PRINT 'SMALL VALUE ON DIAGONAL DETECTED'
850 STOP
860 A(I,J)=(A(I,J)-S5)/A(I,I)
870 NEXT J
880 NEXT I
890 PRINT #3 \ PRINT #3,'LU DECOMPOSITION OF A MATRIX'
900 PRINT #3
910 PRINT #3,A(1,1);A(1,2);A(1,3)
```

```
920 PRINT #3,A(2,1);A(2,2);A(2,3)
930 PRINT #3
940 REM ----------------------
950 REM SOLVING MATRIX EQUATIONS
960 REM ----------------------
970 C(1)=A(1,3)/A(1,1)
980 C(2)=(A(2,3)-A(2,1)*C(1))/A(2,2)
990 C(1)=C(1)-A(1,2)*C(2)
1000 PRINT #3
1010 PRINT #3,'COEFFFICIENTS OF LEAST SQUARES FIT'
1020 PRINT #3,C(1);C(2)
1030 PRINT #3
1040 B1=0
1050 FOR I=1 TO P1
1060 S5=C(2)*X(I)+C(1)
1070 B1=B1+(Y(I)-S5)^2
1080 NEXT I
1090 B1=B1/(P1-1)
1100 PRINT #3 \ PRINT #3,'E=';C(2)
1110 PRINT #3,'BETA=';B1
1120 PRINT #3,'T2=';T2
1130 PRINT #3,'FILENAME=';F$
1140 PRINT #3,'HOLD NUMBER=';D0
1142 PRINT
#3,'************************************************************'
1145 PRINT #3 \ PRINT #3 \ PRINT #3 \ PRINT #3
1150 Q1=0 \ Q2=P1*T2
1160 Q3=Q2/10
1170 Q$='TIME(SEC)'
1180 Y1=((C1(1,2)*X0)/G0)-1.00000E-04 \ Y2=Y1+2.00000E-04
1190 Y3=(Y2-Y1)/10
1200 Y$='IN/IN'
1420 REM ------------------
1430 REM GRAPHICS FUNCTIONS
1440 REM ------------------
1445 PRINT  \ PRINT 'SWITCH PRINTER TO "B" & HIT RETURN'
1446 PRINT 'WHEN PROMPTED HIT RETURN AGAIN'; \ INPUT R$
1450 TEKMODE(1,1)
1460 PHYL(1,10,85,10,85)
1470 SCALE(1,0,Q1,Q2,Y1,Y2)
1480 AXES(1,0,0)
1490 LABEL(1,Q$,Y$,Q3,Y3,1)
1505 T=-T2
1510 FOR I=1 TO P1
1515 T=T+T2
1520 Q4=T
1530 Y4=(C1(I,2)*X0)/G0
1550 MARK(1,4,Q4,Y4)
1570 NEXT I
1575 INVEC
```

```
1580 T=-T2
1590 FOR I=1 TO P1
1600 T=T+T2
1610 Q4=T
1620 W4=(T*C(2))+C(1)
1630 PLOT(1,Q4,W4)
1640 NEXT I
1650 INVEC
1660 HOME
1665 INPUT R$
1670 COPY
1680 VTMODE(1,0)
1685 A1(K1,2)=C(2) \ A1(K1,1)=DO \ K1=K1+1
1690 PRINT  \ PRINT 'DO YOU WISH TO RUN ANOTHER HOLD TIME (Y/N)';
1700 INPUT R$
1710 IF R$='N' THEN GO TO 1750
1720 PRINT  \ PRINT 'SWITCH PRINTER TO "A" & HIT RETURN'; \ INPUT R$
1730 PRINT
1740 GO TO 230
1750 PRINT  \ PRINT 'DO YOU WANT TO FIT THE RATE VALUES (Y/N)'; \ INPUT
R$
1760 IF R$='N' THEN GO TO 12008
1770 FOR I=1 TO K1-1
1775 PRINT
1780 PRINT 'FOR HOLD TIME #';A1(I,1);' DO YOU WANT TO USE THIS RATE
(Y/N)';
1790 PRINT A1(I,2) \ INPUT R$
1800 IF R$='N' THEN GO TO 1830
1810 PRINT  \ PRINT 'INPUT THE ASSOCIATED STRESS VALUE' \ INPUT A1(I,0)
1820 GO TO 1840 \ PRINT
1830 A1(I,0)=0
1840 NEXT I
1850 PRINT \ PRINT 'SWITCH PRINTER TO "A" AND HIT RETURN'; \ INPUT R$
2652 REM ---------RATE CURVE FIT-------------------------
2654 REM ---------------
2655 REM FORMING A MATRIX
2656 REM ---------------
2658 J=0 \ PRINT  \ PRINT #3
2660 FOR J1=1 TO K1-1
2665 IF A1(J,0)=0 THEN GO TO 2700 \ J=J+1
2670 X(J)=A1(J1,0)
2680 Y(J)=A1(J1,2)*1.00000E+06
2690 X1(J)=1
2692 PRINT 'HOLD TIME=';A1(J1,1) \ PRINT #3,'HOLD TIME=';A1(J1,1)
2694 PRINT 'STRAIN RATE=';A1(J1,2) \ PRINT #3,'STRAIN RATE=';A1(J1,2)
2696 PRINT 'STRESS=';A1(J1,0) \ PRINT #3,'STRESS=';A1(J1,0)
2698 PRINT  \ PRINT #3
2700 NEXT J1
2702 P2=J
2704 PRINT 'ARE THESE VALUES OK (Y/N)'; \ INPUT R$
```

```
2706 IF R$='N' THEN GO TO 1775
2708 PRINT
2710 FOR J=1 TO 9
2720 A(J,1)=0
2730 A(J,11)=0
2740 FOR K=1 TO P2
2750 A(J,1)=A(J,1)+X1(K)
2760 A(J,11)=A(J,11)+Y(K)*X1(K)
2770 X1(K)=X1(K)*X(K)
2780 NEXT K
2790 NEXT J
2795 FOR I=2 TO 10
2800 A(10,I)=0
2810 FOR J=1 TO P2
2820 A(10,I)=A(10,I)+X1(J)
2830 X1(J)=X1(J)*X(J)
2840 NEXT J
2845 NEXT I
2847 FOR J=2 TO 10
2849 FOR I=1 TO 9
2850 A(I,J)=A(I+1,J-1)
2855 PRINT #3,'A(';I;',';J;')= ';A(I,J)
2857 NEXT I
2859 NEXT J
2860 PRINT #3
2900 REM ----------------
2910 REM LU DECOMPOSITION
2920 REM ----------------
2930 FOR I=1 TO 10
2940 FOR J=2 TO 10
2950 S5=0
2960 IF J>I THEN GO TO 3006
2970 J1=J-1
2980 FOR K=1 TO J1
2990 S5=S5+A(I,K)*A(K,J)
3000 NEXT K
3002 A(I,J)=A(I,J)-S5
3004 GO TO 3060
3006 I1=I-1
3008 IF I=0 THEN GO TO 3016
3010 FOR K=1 TO I1
3012 S5=S5+A(I,K)*A(K,J)
3014 NEXT K
3016 IF ABS(A(I,I))<1.00000E-10 THEN GO TO 3030
3020 GO TO 3050
3030 PRINT 'SMALL VALUE ON DIAGONAL DETECTED FOR REDUCTION #';I
3040 STOP
3050 A(I,J)=(A(I,J)-S5)/A(I,I)
3060 NEXT J
3070 NEXT I
```

```
3130 REM ----------------------
3140 REM SOLVING MATRIX EQUATIONS
3150 REM ----------------------
3155 FOR I=2 TO 10
3160 FOR J=1 TO I
3165 C(J)=A(J,11)
3170 NEXT J
3175 GOSUB 4000
3180 I1=I-1
3190 PRINT #3
3200 PRINT #3,'COEFFFICIENTS OF LEAST SQUARES FIT OF DEGREE';I1
3210 FOR J=1 TO I
3220 PRINT #3,C(J)
3230 NEXT J
3235 B1=0
3240 FOR I2=1 TO P2
3245 S5=0
3250 FOR I3=2 TO I
3255 J3=I-I3+2
3260 S5=(S5+C(J3))*X(I2)
3265 NEXT I3
3267 S5=S5+C(1)
3270 B1=B1+(Y(I2)-S5)^2
3280 NEXT I2
3290 B1=B1/(P2-1)
3300 PRINT #3
3400 PRINT #3,'BETA=';B1
3405 B(I,0)=B1
3410 FOR J=1 TO I
3420 B(I,J)=C(J)
3430 NEXT J
3440 NEXT I
3450 PRINT #3
12000 PRINT  \ PRINT 'DO YOU WANT TO DO ANOTHER RATE FIT (Y/N)';
12002 INPUT R$
12004 IF R$='N' THEN GO TO 12008
12006 GO TO 1690
12008 STOP
12010 END
```

GMPLT8

```
10 REM PLOT WORK RATE VS STRESS
20 X$='*                          *                          *'
30 X=SYS(7)
40 CLRTXWIN
50 REM
60 REM This program was written by Paul Sean Hill and George
```

```
65 REM James Nov 1985 in
70 REM order to calculate the inelastic work rate vs stress
80 REM for use with the Bodner constant code in determining
85 REM saturation stresses for various cases.
90 REM
100 DIM N(250,4),X(250),Y(250),C(10),A(10,11),X1(250),B(10,11)
110 DIM S(10,5),E(10,5),Y1(250),E1(250,3),M(2)
120 PRINT 'What is Youngs modulus for this test'; \ INPUT C(2) \ PRINT
130 C9=C(2)
135 PRINT  \ PRINT ,'Input block number to start with'; \ INPUT B0
140 PRINT  \ PRINT ,'Input point to start with'; \ INPUT P1
145 PRINT  \ PRINT ,'Input point to end with'; \ INPUT P3
150 PRINT  \ PRINT ,'input beginning half cycle'; \ INPUT F
210 PRINT
270 PRINT 'Enter the file name for experimental data (<=5 CHARACTERS)';
280 INPUT F$
290 IF LEN(F$)<=5 THEN GO TO 305
300 PRINT 'INVALID FILE NAME' \ GO TO 270
305 OPEN 'LP:' FOR OUTPUT AS FILE 3
310 F2$='DU1:'+F$+'.DAT'
320 F1$='DU1:'+F$+'C.DAT'
330 REM ------------------------------FILE INPUT----------------------
340 OPEN F2$ FOR INPUT AS FILE 2
350 OPEN F1$ FOR INPUT AS FILE 1
370 Z$='FILENAME                              <####'
380 INPUT #1,L0,X0,G0,A0,U1,U2,U3,U4,T0,U5,U6,U7,U8,P0
390 PRINT #3,USING Z$,F$
400 PRINT #3
410 PRINT #3,'BLOCK NUMBER = ';B0
420 PRINT #3,'STARTING POINT = ';P1
430 PRINT #3,'ENDING POINT = ';P3
440 PRINT #3,'HALF CYCLE = ';F
480 P0=P3
500 P2=P3
510 REM ------------------
520 REM READING STORED DATA
530 REM ------------------
540 N4=P3 \ N3=1 \ T=0-T0
550 N4=N4-64 \ N2=64 \ IF N4<=0 THEN N2=N4+64
560 AINP(#2,E1(N3,0),N2*4,B0,P)
570 IF N4<=0 THEN GO TO 600
580 B0=B0+1 \ N3=N3+64
590 GO TO 550
600 ELEVAR(E1,1,2,10)
610 FOR J=P1 TO P3
620 T=T+T0 \ N(J,0)=T
630 N(J,1)=E1(J,2)*L0/A0/1000
640 N(J,2)=E1(J,1)*X0/G0
650 NEXT J
660 CLOSE #1,2
```

```
970 PRINT #3 \ PRINT #3 \ PRINT #3,'For Youngs modulus = ';C9;
1370 REM ----CALCULATING PLASTIC STRAINS AND RATE OF PLASTIC WORK-------
1375 N(P1,3)=0
1380 FOR I=P1+1 TO P3
1390 N(I,3)=N(I-1,3)+(N(I,2)-N(I-1,2))-((N(I,1)-N(I-1,1))/C9)
1410 NEXT I
1412 P6=P1
1420 IF ABS(N(P6,3))<2.00000E-03 THEN GO TO 1424
1422 GO TO 1430
1424 P6=P6+1
1426 GO TO 1420
1430 P4=P3-1
1440 P5=P6+1
1450 P2=P3-P6+1
1480 REM ---------RATE CURVE FIT-------------------------
1490 REM ----------------
1500 REM FORMING A MATRIX
1510 REM ----------------
1520 FOR J1=P6 TO P3
1530 J=J1-P6+1
1540 X(J)=N(J1,3)
1550 Y(J)=N(J1,1)
1560 X1(J)=1
1570 NEXT J1
1580 FOR J=1 TO 9
1590 A(J,1)=0
1600 A(J,11)=0
1610 FOR K=1 TO P2
1620 A(J,1)=A(J,1)+X1(K)
1630 A(J,11)=A(J,11)+Y(K)*X1(K)
1640 X1(K)=X1(K)*X(K)
1650 NEXT K
1660 NEXT J
1670 FOR I=2 TO 10
1680 A(10,I)=0
1690 FOR J=1 TO P2
1700 A(10,I)=A(10,I)+X1(J)
1710 X1(J)=X1(J)*X(J)
1720 NEXT J
1730 NEXT I
1740 FOR J=2 TO 10
1750 FOR I=1 TO 9
1760 A(I,J)=A(I+1,J-1)
1770 NEXT I
1780 NEXT J
1790 REM ----------------
1800 REM LU DECOMPOSITION
1810 REM ----------------
1820 FOR I=1 TO 10
1830 FOR J=2 TO 10
```

```
1840 S5=0
1850 IF J>I THEN GO TO 1920
1860 J1=J-1
1870 FOR K=1 TO J1
1880 S5=S5+A(I,K)*A(K,J)
1890 NEXT K
1900 A(I,J)=A(I,J)-S5
1910 GO TO 2020
1920 I1=I-1
1930 IF I=0 THEN GO TO 1970
1940 FOR K=1 TO I1
1950 S5=S5+A(I,K)*A(K,J)
1960 NEXT K
1970 IF ABS(A(I,I))<1.00000E-20 THEN GO TO 1990
1980 GO TO 2010
1990 PRINT 'SMALL VALUE ON DIAGONAL DETECTED FOR REDUCTION #';I
2010 A(I,J)=(A(I,J)-S5)/A(I,I)
2020 NEXT J
2030 NEXT I
2040 REM ------------------------
2050 REM SOLVING MATRIX EQUATIONS
2060 REM ------------------------
2070 FOR I=2 TO 10
2080 FOR J=1 TO I
2090 C(J)=A(J,11)
2100 NEXT J
2110 GOSUB 2590
2120 I1=I-1
2130 PRINT #3
2140 PRINT #3,'COEFFFICIENTS OF LEAST SQUARES FIT OF DEGREE';I1
2150 FOR J=1 TO I
2160 PRINT #3,C(J)
2170 NEXT J
2180 B1=0
2190 FOR I2=1 TO P2
2200 S5=0
2210 FOR I3=2 TO I
2220 J3=I-I3+2
2230 S5=(S5+C(J3))*X(I2)
2240 NEXT I3
2250 S5=S5+C(1)
2260 B1=B1+(Y(I2)-S5)^2
2270 NEXT I2
2280 B1=B1/(P2-1)
2290 PRINT #3,'BETA=';B1
2300 B(I,0)=B1
2310 FOR J=1 TO I
2320 B(I,J)=C(J)
2330 NEXT J
2340 NEXT I
```

```
2350 PRINT #3
2360 PRINT ,'INPUT DEGREE OF POLYNOMIAL DESIRED'; \ INPUT I
2370 I9=I
2380 FOR J=P6 TO P3
2390 N(J,2)=0
2400 N(J,4)=0
2405 N(J,0)=0
2410 FOR K=1 TO I9+1
2420 N(J,4)=N(J,4)+B(I,K)*N(J,3)^(K-1)
2430 IF K<2 THEN GO TO 2445
2440 N(J,2)=N(J,2)+B(I,K)*(K-1)*(N(J,3)^(K-2))
2445 N(J,0)=N(J,0)+(B(I,K)/K)*(N(J,3)^K)
2450 NEXT K
2455 N(J,2)=N(J,2)/N(J,1)
2460 NEXT J
2470 FOR J=1 TO P6-1
2480 N(J,2)=0
2490 N(J,4)=0
2500 NEXT J
2502 W1=N(P3,0)-N(P6,0)
2504 PRINT #3 \ PRINT #3,'PLASTIC WORK =';W1
2510 PRINT #3,'STRESS(KSI)'TAB(15)'INEL STRN';
2520 PRINT #3,TAB(30)'STRESS-FIT';TAB(45)'dS/dWP-FIT'
2540 FOR I=P6 TO P3
2550 PRINT #3,N(I,1);TAB(15)N(I,3);TAB(30)N(I,4);TAB(45)N(I,2)
2570 NEXT I
2580 GO TO 2790
2590 C(1)=C(1)/A(1,1)
2600 FOR I2=2 TO I
2610 I1=I2-1
2620 S5=0
2630 FOR K=1 TO I1
2640 S5=S5+A(I2,K)*C(K)
2650 NEXT K
2660 C(I2)=(C(I2)-S5)/A(I2,I2)
2670 NEXT I2
2680 FOR J=2 TO I
2690 N2=I-J+2
2700 N1=I-J+1
2710 S5=0
2720 FOR K=N2 TO I
2730 S5=S5+A(N1,K)*C(K)
2740 NEXT K
2750 C(N1)=C(N1)-S5
2760 NEXT J
2770 RETURN
2780 REM ----------PLOT DATA----------
2790 PRINT 'PLACE PRINTER SWITCH IN POSITION "B" '
2800 PRINT 'HIT RETURN TO CONTINUE'; \ INPUT R$ \ PRINT  \ PRINT
2810 Y$='STRESS (KSI)'
```

```
2820 PRINT 'ENTER MAXIMUM, MINIMUM STRESS'; \ INPUT Y2,Y1
2830 PRINT 'ENTER STRESS STEP SIZE'; \ INPUT Y3
2840 X$='INEL STRAIN'
2850 PRINT 'ENTER MAXIMUM, MINIMUM INELASTIC WORK'; \ INPUT X2,X1
2860 PRINT 'ENTER INELASTIC WORK STEP SIZE'; \ INPUT X3
2870 PRINT #3 \ PRINT #3 \ PRINT #3
2880 PRINT #3,Y$,I9;'th ORDER'
2890 PRINT #3,'*                                        *'
2900 PRINT #3,'*                                        *'
2910 PRINT 'ARE THESE PARAMETERS OK? ';
2920 INPUT R$
2930 IF R$='N' THEN GO TO 2820
2940 TEKMODE(1,1)
2950 PHYL(1,10,85,10,85)
2960 SCALE(1,0,X1,X2,Y1,Y2)
2970 AXES(1,0,0)
2980 LABEL(1,X$,Y$,X3,Y3,1)
2990 INVEC
3000 FOR I=P5 TO P4
3010 X4=N(I,3)
3020 Y4=N(I,1)
3030 MARK(1,4,X4,Y4)
3040 INVEC
3050 NEXT I
3060 FOR I=P5 TO P4
3070 X4=N(I,3)
3080 Y4=N(I,4)
3090 PLOT(1,X4,Y4)
3100 NEXT I
3110 HOME
3120 COPY
3130 VTMODE(1,0)
3140 PRINT 'Is this fit close enough'; \ INPUT A$
3150 PRINT  \ PRINT
3160 IF A$='N' THEN GO TO 2360
3170 PRINT 'Do you wish to continue the calculations'; \ INPUT A$
3180 IF A$='N' THEN GO TO 4580
3185 X$=Y$ \ X1=Y1 \ X2=Y2 \ X3=Y3 \ X4=Y4
3190 Y$='INEL WORK RATE'
3200 PRINT 'ENTER MAXIMUM RATE'; \ INPUT Y2
3210 PRINT 'ENTER MINIMUM RATE'; \ INPUT Y1
3220 PRINT 'ENTER RATE STEP SIZE'; \ INPUT Y3
3230 PRINT #3 \ PRINT #3 \ PRINT #3
3240 PRINT 'ARE THESE PARAMETERS OK? ';
3250 TXTBOLD \ PRINT '(Y/N)'; \ TXTNORMAL \ INPUT R$
3260 IF R$='N' THEN GO TO 3200
3270 TEKMODE(1,1)
3280 PHYL(1,10,85,10,85)
3290 SCALE(1,0,X1,X2,Y1,Y2)
3300 AXES(1,0,0)
```

```
3310 LABEL(1,X$,Y$,X3,Y3,1)
3320 INVEC
3330 FOR I=P5 TO P4
3340 X4=N(I,1)
3350 Y4=N(I,2)
3360 MARK(1,4,X4,Y4)
3370 INVEC
3380 NEXT I
3440 HOME
3510 PRINT 'How many points do you want for the lower portion';
3520 INPUT T2
3530 PRINT 'How many points do you want for the upper portion';
3540 INPUT T1
3545 INPUT R$
3560 P7=P6+T1
3565 P=T1 \ I1=1
3566 FOR I=P6 TO P7
3567 X(I1)=N(I,1)
3568 Y(I1)=N(I,2) \ PRINT #3,X(I1),Y(I1) \ I1=I1+1
3569 NEXT I
3570 GOSUB 15000
3580 M2=C2
3590 M4=C1
3595 M5=-M4/M2
3600 P7=P3
3601 P=T2 \ I1=1
3602 P8=P7-T2
3603 FOR I=P8 TO P7
3604 X(I1)=N(I,1) \ Y(I1)=N(I,2) \ PRINT #3,X(I1),Y(I1) \ I1=I1+1
3605 NEXT I
3607 GOSUB 15000
3608 M1=C2
3609 M6=C1
3610 M7=-M6/M1
3670 FOR I=P5 TO P4
3680 E1(I,1)=M1*N(I,1)+M6
3690 E1(I,2)=M2*N(I,1)+M4
3710 NEXT I
3720 PRINT #3 \ PRINT #3
3730 PRINT #3,'M2 = ';M2
3740 PRINT #3,'UPPER Y INTERCEPT = ';M4
3750 PRINT #3,'BACK STRESS = ';M5
3752 PRINT #3,'M1 = ';M1
3754 PRINT #3,'LOWER Y INTERCEPT = ';M6
3755 PRINT #3,'SATURATED STRESS = ';M7
3760 PRINT #3 \ PRINT #3
3790 PRINT #3
3800 PRINT #3 \ PRINT #3,Y$
3900 INVEC
3940 FOR I=P6 TO P3
```

```
3950 X4=N(I,1)
3960 Y4=E1(I,1)
3970 PLOT(1,X4,Y4)
3980 NEXT I
3990 INVEC
4000 INVEC
4100 FOR I=P6 TO P3
4110 X4=N(I,1)
4120 Y4=E1(I,2)
4130 PLOT(1,X4,Y4)
4140 NEXT I
4145 INVEC
4150 HOME
4160 COPY
4170 VTMODE(1,1)
4180 PRINT ,'DO YOU WANT TO CONTINUE'; \ INPUT R$
4190 IF R$='N' THEN GO TO 4580
4200 P1=P3-INT(P3/64)*64
4210 P3=P1+79
4220 F=F+1
4230 PRINT #3,'-------------------------------------------------'
4240 GO TO 340
4580 CLOSE (#3)
4585 STOP
4590 END
15000 REM S1= SUM OF X(J)
15010 REM S2 = SUM OF X(J)^^2
15020 REM S3 = SUM OF Y(J)
15030 REM S4 = SUM OF X(J) * Y(J)
15040 S1=0 \ S2=0 \ S3=0 \ S4=0
15050 FOR J=1 TO P
15060 S1=S1+X(J) \ S2=S2+X(J)^2 \ S3=S3+Y(J) \ S4=S4+(X(J)*Y(J))
15070 NEXT J
15080 C1=(S3*S2-S1*S4)/(P*S2-S1*S1)
15090 C2=(P*S4-S1*S3)/(P*S2-S1*S1)
15100 RETURN
15110 END
15200 REM FOR J=1 TO P
15210 REM X(J)=LOG(X(J))
15220 REM Y(J)=LOG(Y(J))
15230 REM NEXT J
15250 REM C1=EXP(C1)
15300 REMFOR J=1 TO P
15400 REM Y(J)=LOG(Y(J))
15410 REM NEXT J
15500 REM C1=EXP(C1)
```

WALK2

```
10 REM PLOT WORK RATE VS STRESS
20 X$='*                              *                              *'
30 X=SYS(7)
40 CLRTXWIN
50 REM
60 REM This program was written by Paul Sean Hill and George
65 REM James Nov 1985 in
70 REM order to calculate the inelastic strain rate vs stress
80 REM for use in determining
85 REM saturation stresses for the calculation of Walker's model.
90 REM
100 DIM N(250,4),X(250),Y(250),C(10),A(10,11),X1(250),B(10,11)
110 DIM S(10,5),E(10,5),Y1(250),E1(250,3),M(2)
120 PRINT 'What is Youngs modulus for this test'; \ INPUT C(2) \ PRINT
130 C9=C(2)
135 PRINT  \ PRINT ,'Input block number to start with'; \ INPUT BO
140 PRINT  \ PRINT ,'Input point to start with'; \ INPUT P1
145 PRINT  \ PRINT ,'Input point to end with'; \ INPUT P3
150 PRINT  \ PRINT ,'input beginning half cycle'; \ INPUT F
210 PRINT
270 PRINT 'Enter the file name for experimental data (<=5 CHARACTERS)';
280 INPUT F$
290 IF LEN(F$)<=5 THEN GO TO 305
300 PRINT 'INVALID FILE NAME' \ GO TO 270
305 OPEN 'LP:' FOR OUTPUT AS FILE 3
310 F2$='DU1:'+F$+'.DAT'
320 F1$='DU1:'+F$+'C.DAT'
330 REM ------------------------------FILE INPUT----------------------
340 OPEN F2$ FOR INPUT AS FILE 2
350 OPEN F1$ FOR INPUT AS FILE 1
370 Z$='FILENAME                              <####'
380 INPUT #1,LO,XO,GO,AO,U1,U2,U3,U4,TO,U5,U6,U7,U8,PO
390 PRINT #3,USING Z$,F$
400 PRINT #3
410 PRINT #3,'BLOCK NUMBER = ';BO
420 PRINT #3,'STARTING POINT = ';P1
430 PRINT #3,'ENDING POINT = ';P3
440 PRINT #3,'HALF CYCLE = ';F
480 PO=P3
500 P2=P3
510 REM -------------------
520 REM READING STORED DATA
530 REM -------------------
540 N4=P3 \ N3=1 \ T=0-TO
550 N4=N4-64 \ N2=64 \ IF N4<=0 THEN N2=N4+64
560 AINP(#2,E1(N3,0),N2*4,BO,P)
570 IF N4<=0 THEN GO TO 600
```

```
580 BO=BO+1 \ N3=N3+64
590 GO TO 550
600 ELEVAR(E1,1,2,10)
610 FOR J=P1 TO P3
620 T=T+TO \ N(J,0)=T
630 N(J,1)=E1(J,2)*LO/AO/1000
640 N(J,2)=E1(J,1)*XO/GO
650 NEXT J
660 CLOSE #1,2
970 REM PRINT #3  \ PRINT #3 \ PRINT #3,'For Youngs modulus = ';C9;
1370 REM ----CALCULATING PLASTIC STRAINS AND RATE OF PLASTIC WORK-------
1375 N(P1,3)=0
1380 FOR I=P1+1 TO P3
1390 N(I,3)=N(I-1,3)+(N(I,2)-N(I-1,2))-((N(I,1)-N(I-1,1))/C9)
1410 NEXT I
1412 P6=P1
1420 IF ABS(N(P6,3))<2.00000E-03 THEN GO TO 1424
1422 GO TO 1430
1424 P6=P6+1
1426 GO TO 1420
1430 P4=P3-1
1440 P5=P6+1
1450 P2=P3-P6+1
1480 REM ---------RATE CURVE FIT-------------------------
1490 REM ----------------
1500 REM FORMING A MATRIX
1510 REM ----------------
1520 FOR J1=P6 TO P3
1530 J=J1-P6+1
1540 X(J)=N(J1,3)
1550 Y(J)=N(J1,1)
1560 X1(J)=1
1570 NEXT J1
1580 FOR J=1 TO 9
1590 A(J,1)=0
1600 A(J,11)=0
1610 FOR K=1 TO P2
1620 A(J,1)=A(J,1)+X1(K)
1630 A(J,11)=A(J,11)+Y(K)*X1(K)
1640 X1(K)=X1(K)*X(K)
1650 NEXT K
1660 NEXT J
1670 FOR I=2 TO 10
1680 A(10,I)=0
1690 FOR J=1 TO P2
1700 A(10,I)=A(10,I)+X1(J)
1710 X1(J)=X1(J)*X(J)
1720 NEXT J
1730 NEXT I
1740 FOR J=2 TO 10
```

```
1750 FOR I=1 TO 9
1760 A(I,J)=A(I+1,J-1)
1770 NEXT I
1780 NEXT J
1790 REM ---------------
1800 REM LU DECOMPOSITION
1810 REM ---------------
1820 FOR I=1 TO 10
1830 FOR J=2 TO 10
1840 S5=0
1850 IF J>I THEN GO TO 1920
1860 J1=J-1
1870 FOR K=1 TO J1
1880 S5=S5+A(I,K)*A(K,J)
1890 NEXT K
1900 A(I,J)=A(I,J)-S5
1910 GO TO 2020
1920 I1=I-1
1930 IF I=0 THEN GO TO 1970
1940 FOR K=1 TO I1
1950 S5=S5+A(I,K)*A(K,J)
1960 NEXT K
1970 IF ABS(A(I,I))<1.00000E-20 THEN GO TO 1990
1980 GO TO 2010
1990 PRINT 'SMALL VALUE ON DIAGONAL DETECTED FOR REDUCTION #';I
2010 A(I,J)=(A(I,J)-S5)/A(I,I)
2020 NEXT J
2030 NEXT I
2040 REM ------------------------
2050 REM SOLVING MATRIX EQUATIONS
2060 REM ------------------------
2070 FOR I=2 TO 10
2080 FOR J=1 TO I
2090 C(J)=A(J,11)
2100 NEXT J
2110 GOSUB 2590
2120 I1=I-1
2130 PRINT
2140 PRINT ,'COEFFFICIENTS OF LEAST SQUARES FIT OF DEGREE';I1
2150 FOR J=1 TO I
2160 REM PRINT ,C(J)
2170 NEXT J
2180 B1=0
2190 FOR I2=1 TO P2
2200 S5=0
2210 FOR I3=2 TO I
2220 J3=I-I3+2
2230 S5=(S5+C(J3))*X(I2)
2240 NEXT I3
2250 S5=S5+C(1)
```

```
2260 B1=B1+(Y(I2)-S5)^2
2270 NEXT I2
2280 B1=B1/(P2-1)
2290 PRINT ,'BETA=';B1
2300 B(I,0)=B1
2310 FOR J=1 TO I
2320 B(I,J)=C(J)
2330 NEXT J
2340 NEXT I
2350 PRINT
2360 PRINT ,'INPUT DEGREE OF POLYNOMIAL DESIRED'; \ I=4
2370 I9=I
2380 FOR J=P6 TO P3
2390 N(J,2)=0
2400 N(J,4)=0
2405 N(J,0)=0
2410 FOR K=1 TO I9+1
2420 N(J,4)=N(J,4)+B(I,K)*N(J,3)^(K-1)
2430 IF K<2 THEN GO TO 2445
2440 N(J,2)=N(J,2)+B(I,K)*(K-1)*(N(J,3)^(K-2))
2445 N(J,0)=N(J,0)+(B(I,K)/K)*(N(J,3)^K)
2450 NEXT K
2460 NEXT J
2470 FOR J=1 TO P6-1
2490 N(J,4)=0
2500 NEXT J
2502 W1=N(P3,0)-N(P6,0)
2504 PRINT #3 \ PRINT #3,'PLASTIC STRAIN =';W1
2510 REM PRINT #3,'STRESS(KSI)'TAB(15)'INEL STRN';
2520 REM PRINT #3,TAB(30)'STRESS-FIT';TAB(45)'dS/dEP-FIT'
2540 FOR I=P6 TO P3
2550 REM PRINT #3,N(I,1);TAB(15)N(I,3);TAB(30)N(I,4);TAB(45)N(I,2)
2570 NEXT I
2580 GO TO 3510
2590 C(1)=C(1)/A(1,1)
2600 FOR I2=2 TO I
2610 I1=I2-1
2620 S5=0
2630 FOR K=1 TO I1
2640 S5=S5+A(I2,K)*C(K)
2650 NEXT K
2660 C(I2)=(C(I2)-S5)/A(I2,I2)
2670 NEXT I2
2680 FOR J=2 TO I
2690 N2=I-J+2
2700 N1=I-J+1
2710 S5=0
2720 FOR K=N2 TO I
2730 S5=S5+A(N1,K)*C(K)
2740 NEXT K
```

```
2750 C(N1)=C(N1)-S5
2760 NEXT J
2770 RETURN
2780 REM ----------------------PLOT DATA--------------------------------
2790 PRINT 'PLACE PRINTER SWITCH IN POSITION "B" '
2800 PRINT 'HIT RETURN TO CONTINUE'; \ INPUT R$ \ PRINT  \ PRINT
2810 Y$='STRESS (KSI)'
2820 PRINT 'ENTER MAXIMUM, MINIMUM STRESS'; \ INPUT Y2,Y1
2830 PRINT 'ENTER STRESS STEP SIZE'; \ INPUT Y3
2840 X$='INEL STRAIN'
2850 PRINT 'ENTER MAXIMUM, MINIMUM INELASTIC STRAIN'; \ INPUT X2,X1
2860 PRINT 'ENTER INELASTIC STRAIN STEP SIZE'; \ INPUT X3
2870 PRINT #3 \ PRINT #3 \ PRINT #3
2880 PRINT #3,Y$,I9;'th ORDER'
2890 PRINT #3,'*                                        *'
2900 PRINT #3,'*                                        *'
2910 PRINT 'ARE THESE PARAMETERS OK? ';
2920 INPUT R$
2930 IF R$='N' THEN GO TO 2820
2940 TEKMODE(1,1)
2950 PHYL(1,10,85,10,85)
2960 SCALE(1,0,X1,X2,Y1,Y2)
2970 AXES(1,0,0)
2980 LABEL(1,X$,Y$,X3,Y3,1)
2990 INVEC
3000 FOR I=P5 TO P4
3010 X4=N(I,3)
3020 Y4=N(I,1)
3030 MARK(1,4,X4,Y4)
3040 INVEC
3050 NEXT I
3060 FOR I=P5 TO P4
3070 X4=N(I,3)
3080 Y4=N(I,4)
3090 PLOT(1,X4,Y4)
3100 NEXT I
3110 HOME
3120 COPY
3130 VTMODE(1,0)
3140 PRINT 'Is this fit close enough'; \ INPUT A$
3150 PRINT  \ PRINT
3160 IF A$='N' THEN GO TO 2360
3170 PRINT 'Do you wish to continue the calculations'; \ INPUT A$
3180 IF A$='N' THEN GO TO 4580
3185 X$=Y$ \ X1=Y1 \ X2=Y2 \ X3=Y3 \ X4=Y4
3190 Y$='INEL WORK RATE'
3200 PRINT 'ENTER MAXIMUM RATE'; \ INPUT Y2
3210 PRINT 'ENTER MINIMUM RATE'; \ INPUT Y1
3220 PRINT 'ENTER RATE STEP SIZE'; \ INPUT Y3
3230 PRINT #3 \ PRINT #3 \ PRINT #3
```

```
3240 PRINT 'ARE THESE PARAMETERS OK? ';
3250 TXTBOLD \ PRINT '(Y/N)'; \ TXTNORMAL \ INPUT R$
3260 IF R$='N' THEN GO TO 3200
3270 TEKMODE(1,1)
3280 PHYL(1,10,85,10,85)
3290 SCALE(1,0,X1,X2,Y1,Y2)
3300 AXES(1,0,0)
3310 LABEL(1,X$,Y$,X3,Y3,1)
3320 INVEC
3330 FOR I=P5 TO P4
3340 X4=N(I,1)
3350 Y4=N(I,2)
3360 MARK(1,4,X4,Y4)
3370 INVEC
3380 NEXT I
3440 HOME
3510 PRINT 'How many points do you want for the lower portion';
3520 T2=5
3530 PRINT 'How many points do you want for the upper portion';
3540 T1=10
3545 REM INPUT R$
3560 P7=P6+T1
3565 P=T1 \ I1=1
3566 FOR I=P6 TO P7
3567 X(I1)=N(I,1)
3568 Y(I1)=N(I,2) \ PRINT #3,X(I1),Y(I1) \ I1=I1+1
3569 NEXT I
3570 GOSUB 15000
3580 M2=C2
3590 M4=C1
3595 M5=-M4/M2
3600 P7=P3
3601 P=T2 \ I1=1
3602 P8=P7-T2
3603 FOR I=P8 TO P7
3604 X(I1)=N(I,1) \ Y(I1)=N(I,2) \ PRINT #3,X(I1),Y(I1) \ I1=I1+1
3605 NEXT I
3607 GOSUB 15000
3608 M1=C2
3609 M6=C1
3610 M7=-M6/M1
3670 FOR I=P5 TO P4
3680 E1(I,1)=M1*N(I,1)+M6
3690 E1(I,2)=M2*N(I,1)+M4
3710 NEXT I
3720 PRINT #3 \ PRINT #3
3730 PRINT #3,'M2 = ';M2
3740 PRINT #3,'UPPER Y INTERCEPT = ';M4
3750 PRINT #3,'BACK STRESS = ';M5
3752 PRINT #3,'M1 = ';M1
```

```
3754 PRINT #3,'LOWER Y INTERCEPT = ';M6
3755 PRINT #3,'SATURATED STRESS = ';M7
3760 PRINT #3 \ PRINT #3
3790 PRINT #3
3800 PRINT #3 \ PRINT #3,Y$
3810 GO TO 4200
3900 INVEC
3940 FOR I=P6 TO P3
3950 X4=N(I,1)
3960 Y4=E1(I,1)
3970 PLOT(1,X4,Y4)
3980 NEXT I
3990 INVEC
4000 INVEC
4100 FOR I=P6 TO P3
4110 X4=N(I,1)
4120 Y4=E1(I,2)
4130 PLOT(1,X4,Y4)
4140 NEXT I
4145 INVEC
4150 HOME
4160 COPY
4170 VTMODE(1,1)
4180 PRINT ,'DO YOU WANT TO CONTINUE'; \ INPUT R$
4190 IF R$='N' THEN GO TO 4580
4200 P1=P3-INT(P3/64)*64
4210 P3=P1+80
4220 F=F+1
4230 PRINT #3,'-------------------------------------------------'
4240 GO TO 340
4580 CLOSE (#3)
4585 STOP
4590 END
15000 REM S1= SUM OF X(J)
15010 REM S2 = SUM OF X(J)^^2
15020 REM S3 = SUM OF Y(J)
15030 REM S4 = SUM OF X(J) * Y(J)
15040 S1=0 \ S2=0 \ S3=0 \ S4=0
15050 FOR J=1 TO P
15060 S1=S1+X(J) \ S2=S2+X(J)^2 \ S3=S3+Y(J) \ S4=S4+(X(J)*Y(J))
15070 NEXT J
15080 C1=(S3*S2-S1*S4)/(P*S2-S1*S1)
15090 C2=(P*S4-S1*S3)/(P*S2-S1*S1)
15100 RETURN
15110 END
15200 REM FOR J=1 TO P
15210 REM X(J)=LOG(X(J))
15220 REM Y(J)=LOG(Y(J))
15230 REM NEXT J
15250 REM C1=EXP(C1)
```

```
15300 REMFOR J=1 TO P
15400 REM Y(J)=LOG(Y(J))
15410 REM NEXT J
15500 REM C1=EXP(C1)
```